

# Functional polypeptides obtained by living ring opening polymerizations of N-carboxyanhydrides

**Citation for published version (APA):**

Habraken, G. J. M. (2011). *Functional polypeptides obtained by living ring opening polymerizations of N-carboxyanhydrides*. [Phd Thesis 1 (Research TU/e / Graduation TU/e), Chemical Engineering and Chemistry]. Technische Universiteit Eindhoven. <https://doi.org/10.6100/IR712652>

**DOI:**

[10.6100/IR712652](https://doi.org/10.6100/IR712652)

**Document status and date:**

Published: 01/01/2011

**Document Version:**

Publisher's PDF, also known as Version of Record (includes final page, issue and volume numbers)

**Please check the document version of this publication:**

- A submitted manuscript is the version of the article upon submission and before peer-review. There can be important differences between the submitted version and the official published version of record. People interested in the research are advised to contact the author for the final version of the publication, or visit the DOI to the publisher's website.
- The final author version and the galley proof are versions of the publication after peer review.
- The final published version features the final layout of the paper including the volume, issue and page numbers.

[Link to publication](#)

**General rights**

Copyright and moral rights for the publications made accessible in the public portal are retained by the authors and/or other copyright owners and it is a condition of accessing publications that users recognise and abide by the legal requirements associated with these rights.

- Users may download and print one copy of any publication from the public portal for the purpose of private study or research.
- You may not further distribute the material or use it for any profit-making activity or commercial gain
- You may freely distribute the URL identifying the publication in the public portal.

If the publication is distributed under the terms of Article 25fa of the Dutch Copyright Act, indicated by the "Taverne" license above, please follow below link for the End User Agreement:

[www.tue.nl/taverne](http://www.tue.nl/taverne)

**Take down policy**

If you believe that this document breaches copyright please contact us at:

[openaccess@tue.nl](mailto:openaccess@tue.nl)

providing details and we will investigate your claim.

# Functional Polypeptides Obtained by Living Ring Opening Polymerizations of N-Carboxyanhydrides

PROEFSCHRIFT

ter verkrijging van de graad van doctor aan de  
Technische Universiteit Eindhoven, op gezag van de  
rector magnificus, prof.dr.ir. C.J. van Duijn, voor een  
commissie aangewezen door het College voor  
Promoties in het openbaar te verdedigen  
op dinsdag 24 mei 2011 om 16.00 uur

door

Gijsbrecht Jacobus Maria Habraken

geboren te Boxtel

Dit proefschrift is goedgekeurd door de promotor:

prof.dr. C.E. Koning

Copromotor:

Dr. A. Heise

Habraken, G.J.M.

A catalogue record is available from the Library Eindhoven University of Technology.

ISBN: 978-90-8891-269-6

Copyright © 2011 by G.J.M. Habraken

The results described in this thesis formed part of the research program of the Dutch Polymer Institute (DPI), DPI project #610.

Cover Design: G.J.M. Habraken & Proefschriftmaken.nl || [printyourthesis.com](http://printyourthesis.com)

Printed at Proefschriftmaken.nl || [printyourthesis.com](http://printyourthesis.com)

# Contents

|  |           |
|--|-----------|
| <b>List of abbreviations</b>   | <b>7</b>  |
| <b>Summary</b>   | <b>9</b>  |
| <b>Chapter 1: Introduction</b>   | <b>11</b> |
| 1.1 Peptides   | 12        |
| 1.2 N-Carboxyanhydride Ring Opening Polymerization (NCA ROP)             | 12        |
| 1.2.1 NAM vs AMM and side reactions                                      | 13        |
| 1.2.2 Living NCA ROP   | 14        |
| 1.2.3 Polymer architectures by NCA ROP                                   | 15        |
| 1.3 Biohybrid block copolymers   | 17        |
| 1.3.1 Combination with (an)ionic polymerization                          | 17        |
| 1.3.2 Combinations with living radical polymerizations                   | 18        |
| 1.3.3 Combinations with other ROPs                                       | 20        |
| 1.3.4 Combinations by convergent approaches: thiol-ene / click reactions | 20        |
| 1.4 Applications   | 21        |
| 1.4.1 Enzymatic degradation  | 21        |
| 1.4.2 Bio(medical) applications  | 21        |
| 1.4.3 Biomimetic crystallization   | 22        |
| 1.4.4 NCA ROP prepared block copolymers: self-assembled structures       | 22        |
| 1.5 Aim and outline of this thesis                                       | 24        |
| <b>Chapter 2: NCA Monomer Synthesis and Living NCA ROP through NAM</b>   | <b>31</b> |
| 2.1 Introduction   | 32        |
| 2.2 Experimental   | 34        |
| 2.3 Results & discussion   | 38        |
| 2.3.1 Monomer synthesis  | 38        |
| 2.3.2 Effect of temperature on polypeptide structure                     | 39        |
| 2.3.3. Effect of temperature and pressure on NCA ROP: monomer conversion | 43        |
| 2.3.4 Polypeptide structure analysis: temperature & pressure             | 49        |
| 2.4 Conclusions  | 52        |

---

|   |            |
|---|------------|
| <b>Chapter 3: Random Copolypeptides, Graft Copolypeptides and Block Copolypeptides by NCA ROP</b>   | <b>55</b>  |
| 3.1 Introduction  | 56         |
| 3.2 Experimental  | 57         |
| 3.3 Results & discussion  | 60         |
| 3.3.1 Copolymerization  | 60         |
| 3.3.2 Graft copolymerization  | 62         |
| 3.3.3 Block copolymerization  | 64         |
| 3.3.4 Polypeptide organogels  | 68         |
| 3.4 Conclusions   | 69         |
| <br>  |            |
| <b>Chapter 4: Thiol Chemistry on Well-Defined Synthetic Polypeptides</b>  | <b>73</b>  |
| 4.1 Introduction  | 74         |
| 4.2 Experimental  | 76         |
| 4.3 Results & discussion  | 79         |
| 4.4 Conclusions   | 85         |
| <br>  |            |
| <b>Chapter 5: Biomimetic CaCO<sub>3</sub> Crystallization with Fluorescent Polypeptides Prepared by N-Carboxyanhydride Ring Opening Polymerization.</b> | <b>87</b>  |
| 5.1 Introduction  | 88         |
| 5.1.1 Calcium carbonate crystallization   | 88         |
| 5.1.2 Polymer additives   | 88         |
| 5.2 Experimental  | 92         |
| 5.3 Results & discussion  | 95         |
| 5.3.1 Polypeptide preparation   | 95         |
| 5.3.2 Crystallization experiments   | 98         |
| 5.3.3 Determination of the location of fluorescent polypeptide  | 102        |
| 5.4 Conclusions   | 106        |
| <br>  |            |
| <b>Chapter 6: Peptide Block Copolymers by N-Carboxyanhydride Ring Opening Polymerization and Atom Transfer Radical Polymerization</b>                   | <b>109</b> |
| 6.1 Introduction  | 110        |
| 6.2 Experimental  | 111        |
| 6.3 Results & discussion  | 113        |
| 6.3.1 NCA polymerizations   | 113        |

---

|  |            |
|--|------------|
| 6.3.2 ATRP macroinitiation   | 115        |
| 6.4 Conclusions  | 121        |
| <b>Chapter 7: Selective Enzymatic Degradation of Biohybrid Block Copolymers Particles</b>                              | <b>125</b> |
| 7.1 Introduction   | 126        |
| 7.2 Experimental   | 127        |
| 7.3 Results & discussion   | 132        |
| 7.3.1 Synthesis of polypeptide-based NMRP macroinitiators  | 132        |
| 7.3.2 NMRP reactions and deprotection  | 134        |
| 7.3.3 Particle formation in phosphate buffer solution  | 137        |
| 7.3.4 Enzymatic degradation  | 139        |
| 7.4 Conclusions  | 143        |
| <b>Chapter 8: Enzymatically Degradable Polypeptide Vesicles with the Potential for Selective Delivery Applications</b> | <b>147</b> |
| 8.1 Introduction   | 148        |
| 8.2 Experimental   | 149        |
| 8.3 Results & discussion   | 151        |
| 8.3.1 Synthesis and vesicle formation  | 151        |
| 8.3.2 Enzymatic degradation of polypeptide vesicles  | 154        |
| 8.3.3 Functionalities for cell-membrane recognition  | 157        |
| 8.4 Conclusions  | 159        |
| <b>Curriculum Vitae</b>  | <b>161</b> |
| <b>List of Publications</b>  | <b>162</b> |
| <b>Acknowledgements</b>  | <b>163</b> |



# List of Abbreviations

|              |   |
|--------------|---|
| ACC          | amorphous calcium carbonate   |
| Ala          | alanine   |
| AMM          | activated monomer mechanism   |
| Arg          | arginine  |
| Asp          | aspartic acid   |
| ATRP         | atomic transfer radical polymerization  |
| <i>t</i> Boc | <i>tert</i> -butyloxycarbonyl   |
| CE           | capillary electrophoresis   |
| Cryo-TEM     | cryogenic transmission electron microscopy  |
| CSLM         | confocal scanning laser microscopy  |
| Cys          | cysteine  |
| DLS          | dynamic light scattering  |
| DMAc         | N,N-dimethylacetamide   |
| DMF          | N,N-dimethylformamide   |
| DMSO         | dimethylsulfoxide   |
| DOPA         | 3,4-dihydroxyphenyl-L-alanine   |
| DP           | degree of polymerization  |
| Fmoc         | 9-fluorenylmethoxycarbonyl  |
| FTIR         | fourier transform - infrared  |
| Gln          | glutamine   |
| Glu          | glutamic acid   |
| GPEC         | gradient polymer elution chromatography   |
| HFIP         | 1,1,1,3,3,3-hexafluoroisopropanol   |
| HMTETA       | 1,1,4,7,10,10-hexamethyl triethylenetetramine                                       |
| HV           | high vacuum   |
| Leu          | leucine   |
| Lys          | lysine  |
| MALDI-ToF-MS | matrix assisted laser desorption / ionitiation - time of flight - mass spectroscopy |
| $M_n$        | number average molecular weight   |
| $M_w$        | weight average molecular weight   |
| NAM          | normal amine mechanism  |
| NCA          | N-carboxyanhydride  |
| NMP          | N-methylpyrrolidone   |
| NMR          | nuclear magnetic resonance  |
| NMRP         | nitroxide mediated radical polymerization   |
| PBA          | poly( <i>n</i> -butylacrylate)  |
| PBLA         | poly( $\beta$ -benzyl-L-aspartate)  |



---

|                        |   |
|------------------------|---|
| PBLC                   | poly(S-benzyl-L-cysteine)   |
| PBLG                   | poly( $\gamma$ -benzyl-L-glutamate)                                       |
| PBLS                   | poly(O-benzyl-L-serine)   |
| PBLT                   | poly(O-benzyl-L-threonine)  |
| PBMA                   | poly( <i>tert</i> -butylmethacrylate)                                     |
| PtBMLC                 | poly(S- <i>tert</i> -butylmercapto-L-cysteine)                            |
| PtBOCLL                | poly(N $\epsilon$ - <i>tert</i> -Boc-L-lysine)                            |
| PCL                    | polycaprolactone  |
| PDMEAMA                | poly(2-dimethylaminoethyl methacrylate)                                   |
| PDI                    | polydispersity index  |
| PEG                    | polyethylene glycol   |
| P(EG <sub>2</sub> Lys) | N $\epsilon$ -2-[2-(2-methoxyethoxy)ethoxy]acetyl-L-lysine                |
| P( $\alpha$ -gal Lys)  | poly( $\alpha$ -D-galactose-L-lysine)                                     |
| Phe                    | phenylalanine   |
| PILP                   | polymer induced liquid precursor  |
| P( $\alpha$ -man Lys)  | poly( $\alpha$ -D-mannose-L-lysine)                                       |
| PMDETA                 | 1,1,4,7,7-pentamethyldiethylenetriamine                                   |
| PMeLG                  | poly( $\gamma$ -methyl-L-glutamate)                                       |
| PMMA                   | polymethylmethacrylate  |
| PNIPAM                 | poly(N-isopropylacrylamide)   |
| PS                     | polystyrene   |
| PTLL                   | poly(N $\epsilon$ -trifluoroacetyl-L-lysine)                              |
| PZLL                   | poly(N $\epsilon$ -benzyloxycarbonyl-L-lysine)                            |
| RAFT                   | reversible addition-fragmentation chain transfer                          |
| RGD                    | arginine-glycine-aspartic acid  |
| ROP                    | ring opening polymerization   |
| RT                     | room temperature  |
| SEC                    | size exclusion chromatography   |
| SEM                    | scanning electron microscope  |
| Ser                    | serine  |
| SG-1                   | N- <i>tert</i> -butyl-N-(1-diethylphosphono-2,2-dimethylpropyl) nitroxide |
| $T_g$                  | glass transition temperature  |
| TIPNO                  | 2,2,5-trimethyl-4-phenyl-3-azahexane-3-nitroxide                          |
| TFA                    | trifluoroacetic acid  |
| Tyr                    | tyrosine  |
| Val                    | valine  |

# Summary

## Functional Polypeptides Obtained by Living Ring Opening Polymerizations of N-Carboxyanhydrides

N-Carboxyanhydride ring opening polymerization (NCA ROP) is a method to prepare polypeptides with a high degree of polymerization in large quantities. The living polymerization technique of NCA ROP gave the opportunity to synthesize many polymer architectures with well-defined blocks and copolymers with a well-controllable composition. By combining other polymerization techniques, biohybrid polymers have been prepared. Although the polypeptides prepared by NCA ROP have a random amino acid order and a polydispersity, which is uncommon for natural peptides and proteins, they still can be considered as natural polymers and still have some of the features of natural peptides. For example, they can form secondary structures and can be degraded enzymatically. This provides opportunities for biomedical applications such as drug-delivery and hydrogels for the polypeptides and the hybrid polymers prepared by NCA ROP. The goals of this thesis were to study the living ROP of the NCAs and to make use of the versatility of the polymerization technique to obtain polypeptide and hybrid polymer architectures. Finally, the functionality of the polypeptide products was investigated for biomimetic crystallization, self-organization and enzymatic degradation.

In the field of NCA ROP there are several methods known for living polymerizations. These can be classified as methods where the mechanism is altered to ensure that no side reactions can occur at the reactive polypeptide chain end and methods in which the reaction conditions are optimized to obtain living polymerizations. A lower temperature and a decreased pressure have both been claimed by separate groups to give the best results. In a systematic study for several different NCA monomers the monomer conversion, molecular weight distribution and chain composition were studied for reactions performed at different temperatures and different pressures. Depending on the monomer species, different side reactions were identified; these were found to be temperature dependent. Monomer conversion studies identified two groups of monomer. The first group of the NCA monomers ( $\gamma$ -benzyl-L-glutamate, N<sub>ε</sub>-benzyloxycarbonyl-L-lysine and L-alanine) showed fast monomer conversion and responded to the low pressure, showing an increase in the speed of propagation at room temperature. The number of side reactions was low, so the optimal reaction conditions for this group of monomers is under high vacuum and at room temperature. The second group ( $\beta$ -benzyl-L-aspartate, O-benzyl-L-serine and O-benzyl-L-threonine) showed a lower rate of monomer conversion and no beneficial effect was observed at low pressures. For this second group of monomers, the number of side reactions was also much higher. The best results for a living polymerization of this group of NCAs were obtained at 0 °C under atmospheric pressure.

Using the previously mentioned living ring opening polymerization techniques, different polypeptide architectures have been synthesized. Copolypeptides, graft copolypeptides and block copolypeptides have been synthesized. Although NCA ROP is known as a living polymerization the solubility and the formation of secondary structures can decrease the solubility of the reaction products, resulting in less well-defined block copolypeptides upon macroinitiation. Therefore, the block copolypeptides have been intensively studied to identify the optimal block order synthesis. Improved and quicker reaction conditions were found for tetrablock copolypeptides by combining the optimal solubility and reaction conditions.

Biohybrid block and graft copolymers were synthesized by combining radical polymerizations with NCA ROP. Grafted structures were obtained from the free radical chain transfer reaction or thiol-ene reaction with the thiols of poly( $\gamma$ -benzyl-L-glutamate-co-L-cysteine). Biohybrid block copolymers were obtained by using amine-functionalized bifunctional initiators for atomic transfer radical polymerization (ATRP) and nitroxide mediated radical polymerization (NMRP).

The functionality of the copolypeptides was investigated for the biomimetic crystallization of calcium carbonate. Due to the random distribution of amino acids in copolypeptides, this enabled a facile understanding of the function of amino acid species in natural peptides in biomineralization. Fluorescein-labeled copolypeptides of L-glutamic acid, L-aspartic acid and L-alanine were prepared and used in the crystallization of calcium carbonate. The crystal morphology was highly altered by the addition of the independent copolypeptides. An elongated crystal was found for the crystallization in the presence of poly(L-aspartic acid-co-L-alanine) and a crystal with round features was found for the crystallization with poly(L-glutamic acid-co-L-alanine). The fluorescent-labeled polypeptides were incorporated in the crystals.

The enzymatic degradation of the polypeptides and biohybrid block copolymers containing L-glutamic acid and L-alanine was also studied. The enzymes elastase and thermolysin were used for this study, since these are known to be selective towards L-alanine-containing peptide bonds. First, biohybrid block copolymers were prepared by using NMRP in combination with NCA ROP. In the hydrophilic polypeptide block the quantity of the L-alanine was altered to direct enzymatic degradation. The hydrophobic block was either polystyrene with a  $T_g$  of 100 °C or poly(*n*-butylacrylate) with a  $T_g$  of -49 °C. In phosphate buffer solutions these biohybrid block copolymers formed micelles and vesicles. Upon addition of the enzymes, the poly(*n*-butylacrylate)-containing polymers with a 50% L-alanine content in the hydrophilic block did give an enzymatic response, manifesting itself as an increased particle size and precipitation. For the polystyrene biohybrid block copolymers no response was found for the same polypeptide composition, due to the stability of the high  $T_g$  core or membrane material.

Block copolypeptides of L-glutamic acid and L-alanine were prepared by living NCA ROP and were found to self-assemble into vesicles in water. A first attempt was made to make vesicles with cell-membrane recognition combined with an enzymatic release trigger for targeted delivery.

# Chapter 1

## Introduction

## 1.1 Peptides

Peptides and proteins play an important role in everyday life. They can help in the recognition of biological substrates, function as catalysts (enzymes) and have advanced structural properties (e.g. elastine and collagen) in organisms.<sup>1</sup> Proteins and peptides also play a significant role in the formation of biological calcium phosphate and calcium carbonate structures, such as bones and mother of pearl. Viruses have a shell of self-organized peptide building blocks, protecting the RNA or DNA. Peptides are a natural product and can be degraded under the right conditions with the help of enzymes. The natural process of peptide synthesis is by transcription from DNA and translation from RNA to the protein end product. By this process a high number of amino acids (up to 27,000 for the muscle protein connectin) are put in the right order for every natural peptide.<sup>2</sup> The difference between proteins and peptides is the number of amino acids. Below a number of 50 repeating units the name is 'peptide.' When a peptide has a higher number of amino acids in a specific sequence this is referred to as a 'protein.'<sup>3</sup> The order of the amino acids in a peptide will dictate the secondary structure of the peptide. Some amino acids favor structures such as  $\alpha$ -helices, a  $\beta$ -sheets or turns. In one protein molecule this can lead to different secondary structures stabilizing the protein and giving it an overall three-dimensional conformation, the tertiary structure.

Synthetic approaches to produce peptides and proteins are various, but all have their advantages and limitations. The process closest to nature is the manipulation of DNA of bacteria or other organisms for the production of a specific peptide. Bacteria can produce the peptide under the right conditions in a reactor (biotechnology). Purification of the product then depends on whether it is excreted by the bacteria into the solution or stored inside the cell.<sup>4</sup> Other organisms, such as goats and cows excrete the product, for example, in milk.<sup>5,6</sup> This then can be further purified. Using this procedure, similar complex peptides as found in nature can be obtained.

Synthesis of peptides with a well-defined amino acid sequence and structure can be achieved on laboratory scale by a one-by-one amino acid addition on a solid support (Merrifield synthesis). However, this is only possible up to limited molecular weights and in low quantities. The purification to remove the products with an incomplete sequence is intensive.<sup>7,8</sup> If peptides without a specific amino acid sequence are needed, the ring opening polymerization (ROP) of N-carboxyanhydrides (NCA) of amino acids is a useful alternative. The term used for these polymerized amino acid products is synthetic polypeptides, indicating that it is a number of repeating peptide bonds in a molecule.

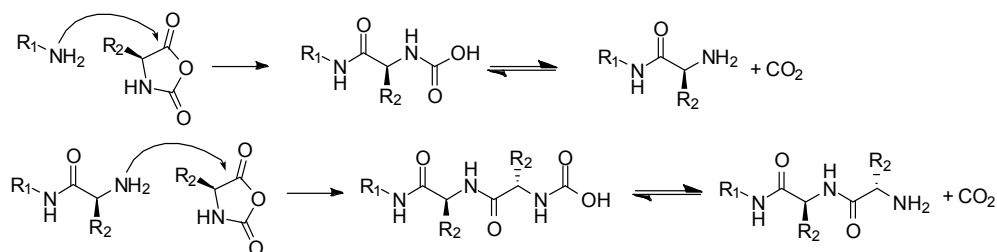
### 1.2 N-Carboxyanhydride ring opening polymerization (NCA ROP)

NCA ROP is a polymerization method used to produce polypeptides efficiently without controlling the sequence of the amino acids. Therefore even above a degree of polymerization of 50 the products of NCA ROP cannot be called proteins. NCA monomers of amino acids are readily accessible and can mostly be produced using techniques involving the phosgenation of protected amino acids or by alternatives methods.<sup>9-12</sup> By combining different NCA monomers simultaneously in one reaction a

copolypeptide can be prepared, but as with most copolymerizations (except for perfect alternating copolymers, e.g. the copolymer of styrene and maleic anhydride) the order of the monomers in the product can vary.<sup>13</sup> The produced polypeptides are inhomogeneous with respect to their (inter and intra chain) composition and degree of polymerization (polydispersity). The advantages of this NCA ROP technique are the high yields of polypeptides and the wide range of achievable molecular weights. The invention of the living NCA ROP methods has even allowed architectures such as multiblock copolypeptides to be synthesized.<sup>14-18</sup> When utilizing the properties of different amino acids, such as the tendency for the organization into certain secondary structures or their hydrophobicity and hydrophilicity, the produced polypeptides can be used for self-organized systems.<sup>19,20</sup>

### 1.2.1 NAM vs AMM and side reactions

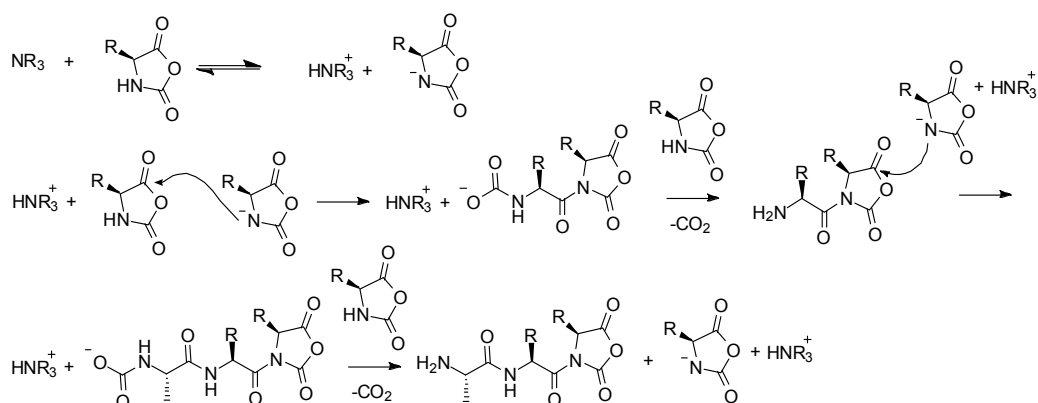
NCA ROP can be initiated by a nucleophile or a base, each following a different mechanism. Nucleophiles can be water, alcohols or primary amines.<sup>21,22</sup> Unhindered primary amines seem to have the fastest initiation rate. In a nucleophilic attack on the carbonyl of the NCA, the ring is opened and carbamic acid is formed with the transfer of the proton (Scheme 1.1). The proton can also be transferred to a base resulting in a more stable carbamic ion. The carbamic acid is converted to a primary amine with the elimination of CO<sub>2</sub>. The conversion of the carbamic ion to the primary amine and CO<sub>2</sub> consists of two reversible reactions.<sup>23</sup> The formed primary amine then can continue the propagation. This method is called the normal amine mechanism (NAM).



**Scheme 1.1.** Normal amine mechanism (NAM) of NCA ROP.

In the case of initiation with a base the proton on the NCA nitrogen is abstracted and forms an anion (Scheme 1.2). This then attacks at the 5-CO position and propagates. During this polymerization, called the activated monomer mechanism (AMM), an equivalent of the NCA anion will remain in the reaction. Both polymerization methods have drawbacks due to side reactions. The polymerizations have to be carried out under dry conditions, since water can initiate the polymerization. Side reactions that affect the end group can result in terminations, but the formation of cyclic structures has been identified as well.<sup>24,25</sup> Another problem is the limited solubility of the polypeptides and the formation of secondary structures during the polymerization, which hinders propagation. Judging simply from the reaction

mechanism this ring-opening polymerization seems straightforward, however only recently breakthroughs have resulted in truly living polymerizations.



**Scheme 1.2.** Activated Monomer Mechanism (AMM) for NCA ROP.

### 1.2.2 Living NCA ROP

In the last ten years, with the introduction of controlled and living NCA ROP methods, the interest in NCA ROP has increased tremendously. A living polymerization is a chain polymerization where transfer and termination reactions do not occur. The rate of initiation is faster than propagation, resulting in an equal chain length among the chains. In this case, the molecular weight increase during the polymerization is controlled. Using the new living NCA ROP methods, block copolypeptides with different block sizes and compositions have been prepared with interesting self-assembly properties.<sup>26</sup> Three of the proposed methods have different mechanisms compared to the NAM. The catalytic cobalt or nickel-mediated NCA ROP coordinates the NCA monomer to the chain end, where it then protects the end group against side reactions.<sup>14</sup> Block copolypeptides prepared using this method are synthesized by adding a second batch of monomer to the polymerization mixture after complete conversion of the first monomer. For the silazane method, the end group is protected with trimethylsilyl carbamate which coordinates the monomer for insertion.<sup>15</sup> The ammonium halide initiators, proposed by Dimitrov et al., allow the polymerization to propagate following the NAM, but the polypeptides have a protected end group in the dormant state.<sup>16</sup> The other two methods, exploit low temperature and high vacuum to optimize the conditions needed for living polymerization. The carbamic groups and CO<sub>2</sub> are removed more quickly from the solution under high vacuum. This shifts the equilibrium resulting in more primary amines and as a result this should yield a higher polymerization rate.<sup>17</sup> In the case of the low temperature method, the frequency of the most common side reactions, such as chain end terminations, is decreased. The higher activation energy of the side reaction gives a greater decrease in the rate of reaction by decreasing the temperature. Side reactions, such as the formation of the formyl end group were shown to decrease dramatically.<sup>18</sup>

### 1.2.3 Polymer architectures by NCA ROP

From a wide variety of amino acids, all having their own characteristics and functionalities, a diversity of polymer architectures has been made (Figure 1.1).<sup>21,22</sup> The most straightforward is the synthesis of copolypeptides made by dissolving the NCA monomers at the same time before adding the initiator. The reactivity of the different amino acids can vary resulting in a different monomer residue sequence distribution, such as alternating, random or gradient containing chains. The reactivity ratios of the NCA monomers have been determined with different methods.<sup>27-32</sup>

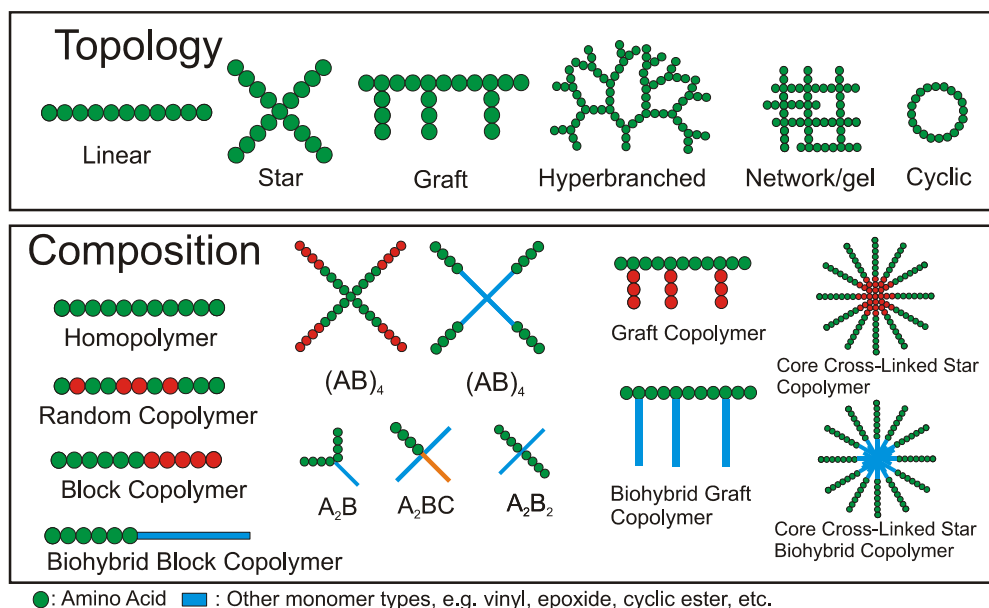


**Figure 1.1.** Examples of polymer architectures obtained by NCA ROP in combination with other polymerization techniques.

As mentioned before, living NCA ROP techniques have been used to prepare block copolypeptides. In the synthesis of block copolypeptides the order of addition is of importance and usually a more soluble polypeptide block is prepared first. The synthesis of block copolypeptides from a bifunctional initiator results in a triblock copolypeptide with the sequential addition of a second monomer. Table 1.1 gives an overview of block copolypeptides reported in literature.

As shown in Table 1.1 the versatility of NCA ROP block copolymerizations is high, but has some limitations. The number of species used for the first block is limited since solubility plays an important role. The second block can have a less soluble composition, such as with leucine, alanine and phenylalanine amino acid residues. Between the different available living methods, the method using



the nickel and cobalt catalysts are reported to allow the greatest variability for monomer species and to be able to give the highest number of blocks in a NCA ROP sequence. The high vacuum technique also seems to be quite successful.

**Table 1.1.** Block copolypeptides prepared by NCA ROP reported in literature.<sup>a</sup>

| 1st block              | 2nd <sup>b</sup>       | 3rd  | 4th  | 5th  | Method     | References | Comments       |
|------------------------|------------------------|------|------|------|------------|------------|----------------|
| PBLG                   | PAla                   |      |      |      | HV         | 33         |                |
|                        | PZLL                   |      |      |      | HV, Ni-Cat | 14,17      |                |
|                        | PfBocLL                |      |      |      | HV         | 34         |                |
|                        | PGly                   |      |      |      | HV         | 17         |                |
|                        | PTyr                   |      |      |      | HV         | 17         |                |
|                        | PLEu                   |      |      |      | HV, Ni-Cat | 14,17      |                |
|                        | PPro                   |      |      |      | Ni-Cat     | 14         |                |
|                        | PCys(Z)                |      |      |      | Ni-Cat     | 35         |                |
| PMeLG                  | PLEu                   |      |      |      | RT         | 36         |                |
| PZLL                   | PBLG                   |      |      |      | HV, Ni-Cat | 14,17      |                |
|                        | PGln                   |      |      |      | Ni-Cat     | 35         |                |
|                        | PLEu                   |      |      |      | Ni-Cat     | 14         |                |
|                        | PLEu                   | PZLL |      |      | Co-Cat     | 37         |                |
|                        | PLEu                   | PZLL | PLEu | PZLL | Co-Cat     | 38         |                |
|                        | PDOPA(Z <sub>2</sub> ) |      |      |      | Co-Cat     | 39         |                |
|                        | PAla                   |      |      |      | Ni-Cat     | 35         |                |
|                        | PTyr                   |      |      |      | Ni-Cat     | 35         |                |
|                        | PSer                   |      |      |      | Ni-Cat     | 35         |                |
|                        | PCys(Z)                |      |      |      | Ni-Cat     | 35         |                |
|                        | PCystine               |      |      |      | Silazane   | 40         |                |
|                        | PPhe                   |      |      |      | 30 °C      | 41         |                |
|                        | P(α-man Lys)           |      |      |      | Co-Cat     | 42         |                |
| P(EG <sub>2</sub> Lys) | PBLA                   |      |      |      | Ni-Cat     | 43         |                |
|                        | PBLG                   |      |      |      | Ni-Cat     | 44         |                |
|                        | PZLL                   |      |      |      | Ni-Cat     | 44         |                |
| P(α-man Lys)           | PZLL                   |      |      |      | Co-Cat     | 42         |                |
|                        | P(α-gal Lys)           |      |      |      | Co-Cat     | 42         |                |
| PTLL                   | PLEu                   |      |      |      | 0 °C       | 45         |                |
| PArg(Z <sub>2</sub> )  | PLEu                   |      |      |      | Co-Cat     | 46         |                |
| PBLT                   | PBLG                   |      |      |      | 35 °C      | 47         | PDI high       |
|                        | PfBocLL                |      |      |      | 35 °C      | 47         | PDI high       |
| PPhe                   | PBLG                   |      |      |      | RT         | 48         | From dendrimer |

Some of the methods are mentioned as HV: high vacuum method, Co- / Ni-Cat: catalytic cobalt- / nickel-mediated method. A temperature represents the polymerization reaction temperature. (a) This does not include claims in patents.<sup>49,50</sup> (b) In the case of a multifunctional initiator the number of sequentially polymerized blocks is mentioned.

Non-linear polypeptides have been prepared by NCA ROP in combination with functionalization or selective deprotection methods. In the case of grafted copolypeptides of PGlu-g-PBLG the benzyl esters of PBLG were substituted by amidation of an excess of 1,2-diaminoethane and used for the

initiation of the NCA ROP of the PBLG grafts. An example of dendritic-graft and branched copolypeptides by living NCA ROP used lysine NCA monomers with different protective groups.<sup>51,52</sup> The dendritic-grafted polypeptides were prepared using a copolypeptide of  $N_\epsilon$ -benzyloxycarbonyl-L-lysine (ZLL) and  $N_\epsilon$ -*tert*-butyloxycarbonyl-L-lysine (*t*BocLL), where the *t*-Boc groups were removed selectively, followed by the polymerization of the grafts from the free amines. The branched polypeptides were prepared by an end group functionalization of a linear lysine block with  $N_\alpha, N_\epsilon$ -diFmoc-L-lys, which gave two primary amines after a selective deprotection with piperidine for the initiation of new polypeptide branches.

Covalently bonded networks can be formed by using a difunctional monomer or with a postpolymerization step. An interesting diNCA monomer can be made from L-cystine, which can be found in wool. In cystine two cysteine molecules are connected together by a sulfur-sulfur bond. After polymerization this disulfide bond can be reduced to form thiols and degrade the cross-links in the material.<sup>40,53</sup> There are several methods for forming a network after the polymerization, for example the oxidation of the free thiols. Another method involves the use of 3,4-dihydroxyphenyl-L-alanine (DOPA).<sup>54</sup> This amino acid can be cross-linked by oxidation, where it forms quinone side groups which can be cross-linked by a radical process. For most of these cross-linking reactions the local concentration of reactive groups needs to be high, which can be achieved in self-organized structures.<sup>39</sup>

### 1.3 Biohybrid block copolymers

By the combination of natural and synthetic polymers advanced materials can be obtained. In the case of proteins one of the most important examples is the PEGylation of proteins for the protection against degradation. For this targeted application different methods have been developed for connecting a functionalized polymer to a specific amino acid site or end group. By reacting the amine groups with, for example *N*-hydroxysuccinimidyl esters or aldehydes a bioconjugate can be formed. The free thiol groups of cysteine maleimide- or disulfide-functionalized polymers can also be used.<sup>55</sup> All of these methodologies use a preproduced natural substance, whereas with NCA-prepared polypeptides the polymerization order can be switched around.

Most of the polymerization techniques that are combined with NCA ROP need specific functional end groups for coupling. This can be done by end group modification or by initiation from a bifunctional initiator with the capability of introducing a second polymer type. Living polymerization techniques combined with NCA ROP are anionic polymerization, living radical polymerization and several ring opening polymerization.

#### 1.3.1 Combination with (an)ionic polymerization

Anionic polymerizations are known to be mostly initiated by alkali metals where the negative ion reacts by addition. The polymer can be functionalized by reacting its active end group with a chain stopper with a specific functionality.<sup>56</sup> In the case of NCA ROP, a primary amine is the preferred group for the

initiation of a following polymerization step. Polyethylene glycol is prepared by anionic ring-opening polymerization and functionalized with a primary amine. This PEG-NH<sub>2</sub> has been used for the initiation of the NCA ROP of  $\gamma$ -benzyl-L-glutamate (BLG) and  $\beta$ -benzyl-L-aspartate (BLA).<sup>57</sup> By a comparable method, using amine functionalized PMMA, Bamfort et al. were able to prepare the biohybrid block copolymer PMMA-*b*-PBLG.<sup>58</sup> Later the same approach was used by the group of Schlaad to prepare PS-*b*-PBLG, PS-*b*-P(S-PBLG)<sub>8</sub> and the same structures with PZLL as polypeptide.<sup>59,60</sup> Another polymer prepared by the same group was polybutadiene-*b*-poly( $\gamma$ -benzyl-L-glutamate).<sup>61</sup> The use of 1,1-diphenylethylene (DPE) has allowed several anionically polymerized polymers to be combined and functionalized with amines for NCA ROP. DPE end-capped polymers were functionalized for attaching other anionic prepared polymers or for the initiation of NCA ROP. This method allowed the synthesis of star-shaped biohybrid polymers, such as (PS)<sub>2</sub>-PBLG, (PS)<sub>2</sub>-(PBLG)<sub>2</sub> or (PS)<sub>2</sub>-(PMeS)-PBLG.<sup>34</sup> All the block copolymers prepared by the combination of these techniques were based on a macroinitiator prepared by anionic polymerization.

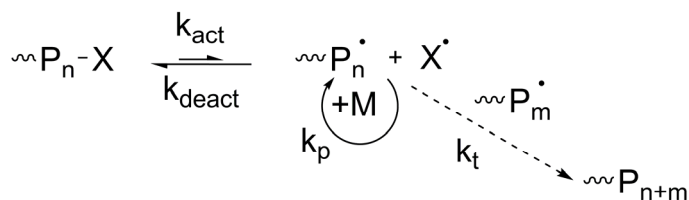
### 1.3.2 Combinations with living radical polymerizations

The introduction of controlled living radical techniques have provided more opportunities for combining NCA ROP with other polymers. Although the polymerizations are called living, some termination reactions can still occur. Living radical polymerizations, such as nitroxide mediated radical polymerization (NMRP), atomic transfer radical polymerization (ATRP) and reversible addition-fragmentation chain transfer (RAFT) polymerization have been combined with NCA ROP.

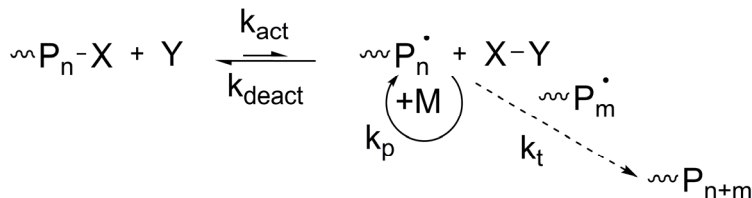
NMRP is based on the cleavage of an oxygen-carbon bond in the nitroxide initiator at higher temperatures (Scheme 1.3). The dissociated molecule forms a stable nitroxide radical that acts as a radical scavenger, while the other formed radical is reactive for initiation of the monomer. The propagation step of the polymerization is controlled by the reversibility of the nitroxide radical by coupling to the radical at the chain end. This equilibrium keeps the concentration of reactive radicals low during the polymerization, thereby decreasing the chance of termination. Depending on the addition of free nitroxide, better control can be achieved throughout the polymerization. The monomer species that can be polymerized by this method are limited to styrenes, acrylates, acrylamides and butadiene.<sup>62</sup> The polymerization of methacrylates only seems to be successful when copolymerized with at least 10 mol% styrene.<sup>63</sup>

Functionalized NMRP initiators were synthesized by Bosman et.al. opening up the possibility to combine NMRP with other polymerization techniques.<sup>64</sup> Examples of the combination of a SPPS prepared peptide with a nitroxide initiator have been shown for TIPNO and SG-1 nitroxides.<sup>65,66</sup> An amine-functionalized TIPNO initiator was used for the tandem polymerization of PBLG and polystyrene.<sup>67</sup> Further functionalization of this bifunctional initiator yielded the initiator for the nickel-catalyzed NCA polymerization.<sup>68</sup>

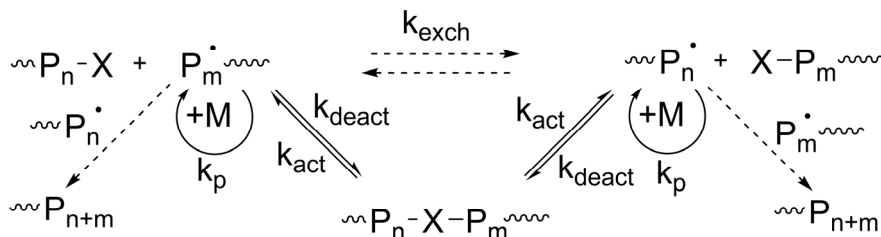
## Nitroxide Mediated Radical Polymerization (NMRP)



## Atom Transfer Radical Polymerization (ATRP)



## Reversible Addition-Fragmentation Chain Transfer (RAFT)



**Scheme 1.3.** Reaction mechanisms of living radical polymerizations: NMRP, ATRP, RAFT.

Another controlled radical polymerization technique is ATRP.<sup>69</sup> The ATRP principle rests on the catalytic cycle of a transition metal complex that increases in oxidation state by extracting a halide from the polymer chain end, thereby forming an active radical.<sup>69</sup> This transition is reversible and an equilibrium between dormant and active chains is achieved. There is a wide variety of initiating groups, but esters are used mostly as initiating species.<sup>70,71</sup> The initiators can be functionalized, but also the halide chain end can easily be transformed into any desired group. A wide variety of catalysts has been tested showing different reactivities.<sup>72</sup>

An example is the synthesis of PMMA-*b*-PBLG, where first MMA was polymerized by ATRP and subsequently the bromine end group was converted into an amine. This end group was then functionalized with a nickel complex and finally, a controlled living NCA ROP was carried out.<sup>73</sup> A similar approach was used for the polymerization of PNIPAM-*b*-PZLL.<sup>74</sup> PMMA-*b*-PBLG was synthesized by the combination of the catalytic nickel-mediated NCA polymerization followed by ATRP from an ester bromide.<sup>75</sup> SPPS prepared peptide macroinitiators with a primary halogen initiator were shown by Rettig

et al. to be capable of initiation of an ATRP reaction.<sup>76</sup> Also a secondary halogen initiator was used with a copper chloride catalyst.<sup>77</sup>

The least common combination is that of NCA ROP with RAFT polymerization. Here, a generated radical is transferred by a RAFT agent. In this case the RAFT agent was functionalized with a primary amine. In RAFT the presence of a free amine leads to aminolysis of the RAFT agent (thioester), resulting in reduced control over the polymerization and a high polydispersity (1.65). If the RAFT polymerization is done first in the presence of the *t*-Boc protected amine followed by NCA ROP after deprotection, lower polydispersities were obtained (1.19).<sup>78</sup>

### 1.3.3 Combinations with other ROPs

Block copolymers of polypeptides with poly(caprolactone) and poly(L-lactide) have been prepared. The ring opening polymerizations of the cyclic esters is performed first with the use of a bifunctional molecule. This carries an alcohol function for the initiation of the ROP of lactones or lactides, but also a group that can be transformed into an amine. Protected amines have been used, but also groups that are converted into primary amines after the polymerization, such as halogens or nitril groups. The formed primary amines were then used for the initiation of NCA ROP to prepare the second polypeptide block. Hybrid block copolymers such as PCys-*b*-PLLA and polypeptide-*b*-PCL were synthesized.<sup>79,80</sup>

### 1.3.4 Combinations by convergent approaches: thiol-ene / click reactions

All the previously discussed reactions covered divergent synthesis methods, where one polymer block is used as a macroinitiator. Other methods applying a convergent approach have also been shown to be very successful for the synthesis of block copolymers. Here two specific functionalized chain ends react with one another to form a block copolymer.

The use of the azide-alkyne Huisgen cycloaddition has been shown to be successful for the synthesis of block copolymers of PBLG-*b*-PDMEAMA and dextran-*b*-PBLG.<sup>81,82</sup> One polymer chain end is functionalized with an alkyne, while the other chain end carries an azide. The use of a copper(I) catalyst allows the formation of a triazole ring. Apart from reactive chain ends, the polymer can also contain functional groups as side groups originating from the monomer. For non-linear polymer architectures an amine initiator with difunctional alkyne functionality was synthesized to make AB<sub>2</sub> star polymers.<sup>83</sup> Recently, much effort has been made to make polypeptides by NCA ROP with alkyne side groups.<sup>84-86</sup> By reacting these alkyne side groups with azide-functionalized PEG chains, grafted polymer structures can be formed. Also small functional molecules can be added, as in the case of carbohydrates for specific targeting of cell membranes.

Another method to obtain these grafted structures is applying thiol-ene chemistry.<sup>87</sup> Here a free thiol reacts with a double carbon-carbon bond. This can occur either by a Michael addition type reaction or by radical chain transfer. The reactivity of the vinyl depends on the side group and many side reactions

can occur, such as polymerization and termination by coupling. Thiol-ene chemistry showed to be not too reliable for block copolymer synthesis by reacting the two preformed polymers.<sup>88</sup>

## 1.4 Applications

NCA ROP prepared polypeptides are very versatile, due to the different available side groups and the biological aspect of these polymers. With the use of the living NCA ROP and the biohybrid architectures new structures can be formed which can be further used for delivery and recognition applications.

### 1.4.1 Enzymatic degradation

Peptidase or protease enzymes are known to degrade peptides and proteins. Several types have been classified according to their reactive site. A catalytic triad of aspartic acid, histidine and serine was identified for the enzymes chymotrypsin, trypsin and elastase. By exchanging the existing amino acids in the enzymes' reactive site, the accessibility or the charge stabilization is altered, favoring the degradation of specific amino acids. Other types of enzymes have reactive centers consisting of cystein-histidine, aspartic acid-aspartic acid or a bound metal ion (typically zinc).<sup>1</sup>

Many different copolypeptides have been prepared by NCA ROP and tested for different enzymes. One of the earliest interests was in the enzymatic cleavage of short aliphatic amino acids (Val, Phe, Leu, Ala) in combination with soluble monomers, such as L-glutamic acid and L-lysine. Enzymes such as the endopeptidases papain, trypsin, chymotrypsins, elastase, ficin, pepsin, and subtilisin were tested for this application.<sup>89-91</sup> Over time the high molecular weights of the polypeptides decreased after the addition of the enzymes, resulting in lower viscosities. By screening of the enzymatic cleavage of amino acid dimers, the selectivity towards certain amino acid sequences was shown.<sup>92,93</sup>

### 1.4.2 Bio(medical) applications

Although polypeptides prepared by NCA ROP do not have the well-defined amino acid order required for certain biological processes, such as cell-ligation and catalysis (enzymes), there are still suitable applications for these materials. An interesting application is an anti-bacterial polypeptide solution. Most anti-bacterial materials are prepared from synthetic polymers, which can remain toxic when introduced to the environment. Polypeptides are susceptible to enzymatic degradation and are therefore more environmentally friendly. An optimization study of an anti-bacterial copolypeptide showed that when a combination of the cationic L-lysine and hydrophobic amino acids, such as L-alanine, L-phenylalanine and L-leucine was used, an optimal material was found. The L-lysine disrupts the cell membrane, while the hydrophobic monomers give it a better access to the hydrophobic cell membrane.<sup>94</sup> In this specific case the order of the amino acids did not have an effect, but for processes such as cell-ligation the order of the amino acids is of high importance. A well-studied sequence is the arginine-glycine-aspartic acid sequence (RGD) for cell-recognition.<sup>95</sup> The order of this sequence is of great importance, since any other order is inactive (GRD or DGR). Attempts have been made to prepare a copolypeptide or a

sequence with NCA monomers, but unfortunately this has not been successful.<sup>96,97</sup> Other materials that can be used for cell recognition are glycopeptides. Here a single carbohydrate unit interacts with a specific lectin protein on a cell membrane.<sup>98</sup> These glycans are connected to amines or alcohols on the side chains. In a few cases the synthesis of a sugar-substituted NCA and the polymerization thereof has been reported.<sup>42,99</sup> Other synthetic methods use a post polymerization step to functionalize the polypeptides by coupling the sugar to the amines of poly(L-lysine).<sup>100</sup> Also other methods such as thiol-ene and the azide-alkyne Huisgen cycloaddition have been used recently for the functionalization of polypeptides.<sup>85,86,101</sup> It was shown that these materials interact with specific lectins. One NCA ROP copolypeptide product has been proven to be useful for the therapeutic application against multiple sclerosis (MS) and possibly rheumatoid arthritis.<sup>102,103</sup> The copolypeptide of L-tyrosine, L-glutamic acid, L-lysine and L-alanine have been shown to improve the neurologic functions of MS patients.

### 1.4.3 Biomimetic crystallization

Natural hybrid materials of inorganic and organic materials can be found in mammalian and invertebrate organisms. In mammalian bone a matrix of collagen defines the orientation of the hydroxyapatite.<sup>104</sup> In marine organisms different inorganic materials can be found. For example, silicon oxide is found in diatoms, while calcium carbonate is found in sea shells, sponges and coral.<sup>105,106</sup> The ability of these organisms to utilize these inorganic materials to obtain advanced structures originates from the use of organic molecules that control the crystallization. In most cases peptides play a role in the crystallization speed or inhibition, in the formed crystal polymorph and crystal shape. The identified natural peptides and proteins that influence the biomineralization contain many amino acids and different hydrophobic and hydrophilic regions.<sup>107-109</sup> Several NCA prepared polypeptides have been used to determine their effects in biomineralization. Poly(L-aspartic acid) has been studied very well, since it is known that it can stabilize amorphous calcium carbonate early in the crystallization process.<sup>105</sup> The same process was seen for poly(L-glutamic acid), while poly(L-lysine) seems to increase the crystallization speed.<sup>110</sup> The homopolypeptide poly(L-lysine) did also give twin-sphere calcite crystal structures.<sup>111</sup> Block copolymers of poly(ethylene glycol) and poly(L-glutamic acid) or poly(L-aspartic acid) were used as additive in CaCO<sub>3</sub> crystallization, resulting in vaterite spheres.<sup>112</sup> Copolypeptides of aspartic acid and O-phospho-L-threonine were prepared and compared with well-ordered copolypeptides of aspartic acid and O-phospho-L-threonine of the same composition for biomineralization. The same crystal shapes could be acquired with the same compositions, but under different conditions. This indicates that the order in which the amino acids are placed has some effect on the crystal end products.<sup>113</sup>

### 1.4.4 NCA ROP prepared block copolymers: self-assembled structures

In the solid state, some block copolymers have been reported which have interesting self-assembly properties, where the self-organized  $\alpha$ -helices play an important role: PBLG-*b*-PS, PBLG-*b*-PAIa.<sup>33,114</sup> However, most research has been done on structures in water with possible delivery purposes. Here

hybrid structures of the combination of hydrophobic polymer with a polyelectrolyte, such as poly(L-lysine) and poly(L-glutamic acid) have been reported.<sup>59,60,115</sup> Variations of this combination have been reported, for example for stabilized emulsion particles by PS-*b*-PLLys or PS-*b*-(PS-*g*-PLLys) and cross-linked polystyrene nanoparticles stabilized by a poly(L-glutamic acid) corona. Non-linear micelles were reported for PS-*b*-PLys with short polystyrene chains.<sup>115</sup> Polybutadiene-*b*-poly(L-glutamic acid) have been shown to form vesicles.<sup>61</sup> Combinations of polyethylene glycol and poly(L-glutamic acid) and poly(L-aspartic acid) use the PEG block for solubility, while the carboxylic acids can be used to complex metal ions or to covalently bind anti-tumor molecules for drug delivery.<sup>116</sup> Zwitterionic Lys-*co*-Glu polypeptide blocks were combined with the soluble PNIPAM to study a micelle structure that is both pH and temperature dependent.<sup>117</sup>

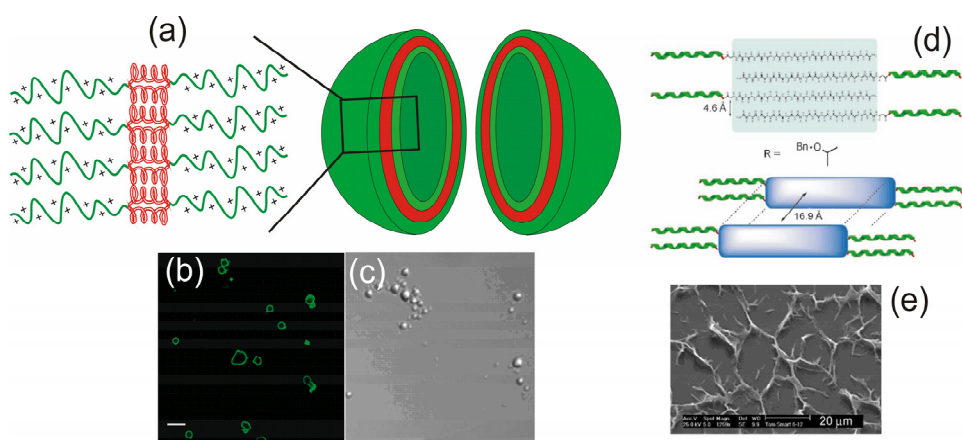


**Figure 1.2.** Examples of self-organized block copolypeptides. Polypeptide vesicles of PLys-*b*-PLeu (a), CSLM of fluorescein functionalized PLys-*b*-PLeu (b) and DIC optical microscopy of PLys-*b*-PLeu (c).<sup>118</sup> Tapes from the organogel of PBLT<sub>26</sub>-*b*-PBLG<sub>22</sub> in chloroform and the SEM of the dried organogel (e).<sup>19</sup>

Block copolypeptides have been studied intensively. Here, the formation of a secondary structure plays an important role in forming the shape of the self-organized structure. An example where both  $\alpha$ -helices and  $\beta$ -sheets play an important role is the self-organization in chloroform of poly(O-benzyl-L-threonine) containing block copolypeptides into tapes (Figure 1.2d, e). When the threonine is organized into anti-parallel  $\beta$ -sheets the  $\alpha$ -helical blocks of poly( $\gamma$ -benzyl-L-glutamate) or poly( $N_\epsilon$ -*t*-BOC-L-lysine) are directed outwards. This self-organization results in organogels with a 3 wt% polypeptide content.<sup>19</sup> Most self-assembled structures are based on a polyelectrolyte and a hydrophobic  $\alpha$ -helical system. The formation of vesicles (Figure 1.2a, b, c) and aggregates from poly(L-lysine)-*b*-poly(L-leucine) have been reported by Nowak et al. in 2005, the formation of tapes from the same block combination was already reported in 2002.<sup>119,118</sup> For this block copolypeptide system the chain length was important to determine whether a tape or a vesicle was formed. Alterations on both systems have been made by the same



research group. Increased mechanical properties, such as a higher storage modulus and lower polypeptide concentrations of the hydrogels, have been achieved by using pentablock copolypeptides with the L-leucine blocks as the second and fourth block.<sup>38</sup> The long middle block of poly(L-lysine) enabled the growth of longer crystal-like L-leucine membranes. The hydrogels showed good compatibility with tissue in the nerve system, which should enable the polypeptides to be used as a scaffold.<sup>120</sup> For the polypeptide vesicles, the L-lysine block was substituted for L-arginine, which can be transported through a cell membrane and therefore is useful for intracellular delivery.<sup>46,121</sup> Better stability of the vesicles was achieved by cross-linking of the incorporated DOPA.<sup>39</sup> Similar vesicle systems have been reported for PGLu-*b*-PPhe, with short poly(L-phenylalanine) chains.<sup>41</sup> Triblock copolypeptides of PLys-*b*-PBLG-*b*-PLys also have been reported to form vesicles.<sup>122</sup> The long hydrophobic PBLG central core forms two hydrophobic  $\alpha$ -helices that form a membrane. Short, fully-deprotected poly(L-lysine)-*b*-poly(L-glutamic acid) has been shown to form vesicles depending on the pH of the solvent. In the pH region between 4.0 and 10.0 the block copolypeptide chains were fully dissolved, but below and above these values vesicles were formed due to the removal of the charge from one of the blocks.<sup>123</sup>

### 1.5 Aim and outline of this thesis

The aim of this thesis is to optimize the NCA ROP process and the synthesis of NCA-based polymer architectures. The versatility of the prepared polypeptides will be shown in biomimicking processes, such as mineralization, degradation and self-organization. These processes demonstrate the varying functionalities of synthetic polypeptides.

Chapter 2 discusses the synthesis of the NCA monomers from their amino acid precursors. These are polymerized under different reaction conditions to allow the optimization of the NCA ROP by NAM. A study has been carried out by MALDI-ToF-MS on the side reactions that occur at different temperatures. The monomer conversion was measured over time at different temperatures and different pressures. After analyzing the homopolypeptides thoroughly the optimal conditions were determined for each NCA monomer species. In Chapter 3 this information is used further for the synthesis of copolypeptides, grafted copolypeptides and block copolypeptides. For the copolypeptides, a new methodology is presented for analysis using MALDI-ToF-MS. The formation of organogels by certain block copolypeptides during the polymerization is also investigated.

The synthesis of hybrid polymers using NCA prepared polypeptides is described in Chapters 4, 6 and 7. In Chapter 4 the focus is on the synthesis of copolymers with *S-tert*-butylmercapto-L-cysteine and the subsequent reactions of the selectively deprotected free thiols. The thiols can be used for thiol-ene reactions, radical chain transfer reactions as well as cross-linking by oxidation. In Chapters 6 and 7 the synthesis of linear hybrid block copolymers is described using NCA ROP in combination with living radical polymerization techniques.

Applications of the prepared polymers can be found in Chapters 5, 7 and 8. In Chapter 5 copolypeptides are used for the biomimetic crystallization of calcium carbonate. An intensive study on the role of the polypeptide during the crystallization and the effect on the crystal structure is discussed. In Chapter 7 hybrid block copolymer micelles are used for a selective enzymatic degradation. Chapter 8 describes the synthesis of functional polypeptide vesicles for drug delivery purposes. In particular, the enzymatic degradation and recognition properties are studied.

## References

- <sup>1</sup> J.M. Berg, J.L. Tymoczko, L. Stryer, *Biochemistry* **2002**, fifth edition, W.H. Freeman and company, New York
- <sup>2</sup> K. Maruyama, *Trends Biochem. Sci.* **2002**, 27, 264-266
- <sup>3</sup> *Pure & Appli. Chem.* **1984**, 56, 595-624
- <sup>4</sup> G. Georgiou and L. Segatori, *Curr. Opin. Biotechnol.* **2005**, 16, 538-545
- <sup>5</sup> H. Baldassarre D.K. Hockley, M. Doré, E. Brochu, B. Hakier, X. Zhao and V. Bordignon *Transgenic Res.* **2008**, 17, 73-84
- <sup>6</sup> D. Salamone, L. Barãnao, C. Santos, L. Bussmannnd, J. Artuso, C. Werning, A. Prync, C. Carbonetto, S. Dabsys, C. Munarf, R. Salaberry, G. Berra, I. Berra, N. Fernández, M. Papouchado, M. Foti, N. Judewicz, I. Mujica, L. Muñoz, S. Fenández Alvarez, E. González, J. Zimmermann, M. Criscuolo and C. Melo, *J. Biotechnol.* **2006**, 124, 469-472
- <sup>7</sup> M. Amblard, J.-A. Fehrentz, J. Martinez, and G. Subra, *Mol. Biotechnol.* **2006**, 33, 239-254
- <sup>8</sup> M. Verlander, *Int. J. Pept. Res. Ther.* **2007**, 13, 75-82
- <sup>9</sup> N.M.B. Smeets, P.L.J. van der Weide, J. Meuldijk, J.A.J.M. Vekemans and L.A. Hulshof, *Org. Process Res. Dev.* **2005**, 9, 757-763
- <sup>10</sup> F. Corneille, J.-L. Copier, J.-P. Senet, Y. Robin, EP 1201659, **2002**
- <sup>11</sup> W. Vayaboury, O. Giani, H. Collet, A. Commeyras, F. Schué, *Amino Acids* **2004**, 27, 161-167
- <sup>12</sup> Y. Fujita, K. Koga, H.-K. Kim, X.-S. Wang, A. Sudo, H. Nishida and T. Endo, *J. Polym. Sci. Part A: Polym. Chem.* **2007**, 45, 5365-5370.
- <sup>13</sup> B. Klumperman, *Polym. Chem.* **2010**, 1, 558-562
- <sup>14</sup> T.J. Deming, *Nature* **1997**, 390, 386-389
- <sup>15</sup> H. Lu and J.J. Cheng, *J. Am. Chem. Soc.* **2007**, 129, 14114-14115
- <sup>16</sup> I. Dimitrov and H. Schlaad, *Chem. Commun.* **2003**, 2944-2945
- <sup>17</sup> T. Aliferis, H. Iatrou, N. Hadjichristidis, *Biomacromolecules* **2004**, 5, 1653-1656.
- <sup>18</sup> W. Vayaboury, O. Giani, H. Cottet, A. Deratani and F. Schué, *Macromol. Rapid Commun.* **2004**, 25, 1221-1224.
- <sup>19</sup> M.I. Gibson and N. Cameron, *Angew. Chem. Int. Ed.* **2008**, 47, 5160-5162, Copyright Wiley-VCH Verlag GmbH & Co. KGaA. Reproduced with permission.
- <sup>20</sup> T.J. Deming, *Prog. Polym. Sci.* **2007**, 32, 858-875
- <sup>21</sup> N. Hadjichristidis, H. Iatrou, M. Pitskalis and G. Sakellariou, *Chem. Rev.* **2009**, 109, 5528-5578
- <sup>22</sup> H.R. Kricheldorf, *Angew. Chem. Int. Ed.* **2006**, 45, 572-5784
- <sup>23</sup> G. Puxty, R. Rowland, A. Allport, Q. Yang, M. Bown, R. Burns, M. Maeder and M. Attalla, *Environ. Sci. Technol.* **2009**, 43, 6427-6433
- <sup>24</sup> H.R. Kricheldorf, C. v. Lossow, and G. Schwarz, *Macromolecules* **2005**, 38, 5513-5518
- <sup>25</sup> H.R. Kricheldorf, C. v. Lossow and G. Schwarz, *Macromol. Chem. Phys.* **2005**, 206, 282-290
- <sup>26</sup> H. Schlaad, *Adv. Polym. Sci.* **2006**, 202, 53-73
- <sup>27</sup> R.E. Nylund and W.G. Miller, *J. Am. Chem. Soc.* **1965**, 87, 3537-3542
- <sup>28</sup> M. Atreyi, M.V.R. Rao and S. Kumar, *Biopolymers* **1983**, 22, 747-753
- <sup>29</sup> K. Ishiwari, T. hayashi and A. Nakajima, *Bull. Inst. Chem. Res., Kyoto Univ.* **1977**, 55, 366-375
- <sup>30</sup> A. Wamsley, J. Bhaskara, P. Phiasivongsa and X. Li, *J. Polym. Sci. Part A: Polym. Chem.* **2004**, 42, 317-325
- <sup>31</sup> H.R. Kricheldorf and G. Schillig, *Makromol. Chem.* **1978**, 179, 1175-1191
- <sup>32</sup> H.R. Kricheldorf, *Makromol. Chem.* **1979**, 180, 147-159

- <sup>33</sup> A. Gitsas, G. Floudas, M. Mondeshki, H.W. Spiess, T. Aliferis, H. Iatrou, and N. Hadjichristidis, *Macromolecules* **2008**, 41, 8072-8080
- <sup>34</sup> A. Karatzas, H. Iatrou, N. Hadjichristidis, K. Inoue, K. Sugiyama, and A. Hirao, *Biomacromolecules* **2008**, 9, 2072-2080
- <sup>35</sup> J.N. Cha, G.D. Stucky, D.E. Morse and T.J. Deming, *Nature* **2000**, 403, 289-292
- <sup>36</sup> V. Goury, D. Jhurry, A. Bhaw-Luximon, B.M. Novak and J. Bellene, *Biomacromolecules* **2005**, 6, 1987-1991
- <sup>37</sup> A.P. Nowak, J. Sato, V. Breedveld and T.J. Deming, *Supramol. Chem.* **2006**, 18, 423-427
- <sup>38</sup> Z. Li and T.J. Deming, *Soft Matter* **2010**, 6, 2546-2551
- <sup>39</sup> E.P. Holowka and T.J. Deming, *Macromol. Biosci.* **2010**, 10, 496-502
- <sup>40</sup> A. Sulistio, A. Widjaya, A. Blencowe, X. Zhang and G. Qiao, *Polym. Prepr. (Am. Chem. Soc., Div. Polym. Chem.)* **2010**, 51, 121-122
- <sup>41</sup> J. Sun, X. Chen, C. Deng, H. Yu, Z. Xie and X. Jing, *Langmuir* **2007**, 23, 8308-8315
- <sup>42</sup> J.R. Kramer and T.J. Deming, *J. Am. Chem. Soc.* **2010**, 132, 15068-15071
- <sup>43</sup> L.E. Euliss, S.G. Grancharov, S. O'Brien, T.J. Deming, G.D. Stucky, C. B. Murray and G. A. Held, *Nano Lett.* **2003**, 3, 1489-1493
- <sup>44</sup> M. Yu, A.P. Nowak and T.J. Deming, *J. Am. Chem. Soc.* **1999**, 121, 12210-12211
- <sup>45</sup> W. Vayaboury, O. Giani, H. Cottet, S. Bonaric and F. Schué, *Macromol. Chem. Phys.* **2008**, 209, 1628-1637
- <sup>46</sup> E.P. Holowka, V.Z. Sun, D.T. Kamei and T.J. Deming, *Nature Mat.* **2007**, 6, 52-57
- <sup>47</sup> M.I. Gibson and N.R. Cameron, *J. Polym. Sci. Part A: Polym. Chem.* **2009**, 47, 2882-2891
- <sup>48</sup> W. Zhuang, L. Liao, H. Chen, J. Wang, Y. Pan, L. Zhang, D. Liu, *Macromol. Rapid Commun.* **2009**, 30, 920-924
- <sup>49</sup> T.J. Deming, M. Yu, S.A. Curtin, J. Hwang, M.D. Wyrsta, A. Nowak and S.W. Seidel, *US 20020032309*, **2002**
- <sup>50</sup> C. Scholz and V. Vayaboury, *WO 2009058291* **2009**
- <sup>51</sup> H.-A. Klok and J. Rodríguez-Hernández, *Macromolecules* **2002**, 35, 8718-8723
- <sup>52</sup> J. Rodríguez-Hernández, M. Gatti, H.-A. Klok, *Biomacromolecules* **2003**, 4, 249-258
- <sup>53</sup> H.W. Jones and H.P. Lundgren, *J. Am. Chem. Soc.* **1951**, 73, 5465-5466
- <sup>54</sup> M. Yu and T.J. Deming, *Macromolecules* **1998**, 31, 4739-4745
- <sup>55</sup> K.L. Heredia and H.D. Maynard, *Org. Biomol. Chem.* **2007**, 5, 45-53
- <sup>56</sup> A. Douy and B. Gallot, *Polymer* **1982**, 1039-1044
- <sup>57</sup> N. Nishiyama and K. Kataoka, *Adv. Polym. Sci.* **2006**, 193, 67-101
- <sup>58</sup> M. Tanaka, A. Mori, Y. Imanishi and C.H. Bamford, *Int. J. Biol. Macromol.* **1985**, 7, 173-181
- <sup>59</sup> H. Kukula, H. Schlaad and K. Tauer, *Macromolecules* **2002**, 35, 2538-2544
- <sup>60</sup> H. Schlaad, H. Kukula, B. Smarsly, M. Antonietti and T. Pakula, *Polymer* **2002**, 43, 5321-5328
- <sup>61</sup> H. Kukula, H. Schlaad, M. Antonietti and S. Förster, *J. Am. Chem. Soc.* **2002**, 124, 1658-1663
- <sup>62</sup> C.J. Hawker, A.W. Bosman and E. Harth, *Chem. Rev.* **2001**, 101, 3661-3688
- <sup>63</sup> D. Benoit, V. Chaplinski, R. Braslau and C.J. Hawker, *J. Am. Chem. Soc.* **1999**, 121, 3904-3920
- <sup>64</sup> A.W. Bosman, R. Vestberg, A. Heumann, J.M.J. Fréchet and C.J. Hawker, *J. Am. Chem. Soc.* **2003**, 125, 715-728
- <sup>65</sup> T. Trimaille, K. Mabrouk, V. Monnier, L. Charles, D. Bertin and D. Gigmes, *Macromolecules*, **2010**, 43, 4864-4870
- <sup>66</sup> M.L. Becker, J. Liu and K.L. Wooley, *Chem. Commun.* **2003**, 180-181
- <sup>67</sup> R.J.I. Knoop, G.J.M. Habaken, N. Gogibus, S. Steig, H. Menzel, C.E. Koning and A. Heise, *J. Polym. Sci. Part A: Polym. Chem.* **2008**, 46, 3068-3077

- <sup>68</sup> S. Steig, F. Cornelius, A. Heise, R. J. I. Knoop, G. J. M. Habraken, C. E. Koning and H. Menzel, *Macromol. Symp.* **2007**, 248, 199-206
- <sup>69</sup> K. Matyjaszewski and J. Xia, *Chem. Rev.* **2001**, 101, 2921-2990
- <sup>70</sup> V. Coessens, T. Pintauer and K. Matyjaszewski, *Prog. Polym. Sci.* **2001**, 26, 337-377
- <sup>71</sup> W.A. Braunecker and K. Matyjaszewski, *Prog. Polym. Sci.* **2007**, 32, 93-146
- <sup>72</sup> N.V. Tsarevsky and K. Matyjaszewski *Chem. Rev.* **2007**, 107, 2270-2299
- <sup>73</sup> K.R. Brzezinska and T.J. Deming, *Macromol. Biosci.* **2004**, 4, 566-569
- <sup>74</sup> C.-J. Huang and F.-C. Chang, *Macromolecules* **2008**, 41, 7041-7052
- <sup>75</sup> S. Steig, F. Cornelius, P. Witte, B.B.P. Staal, C.E. Koning, A. Heise and H. Menzel, *Chem. Commun.* **2005**, 5420-5422
- <sup>76</sup> H. Rettig, E. Krause and H.G. Börner, *Macromol. Rapid. Commun.* **2004**, 13, 1251-1256
- <sup>77</sup> Y. Mei, K.L. Beers, H.C.M. Byrd, D.L. VanderHart and N.R. Washburn, *J. Am. Chem. Soc.* **2004**, 126, 3472-3476
- <sup>78</sup> X. Zhang, J. Li, W. Li and A. Zhang, *Biomacromolecules* **2007**, 8, 3557-3567
- <sup>79</sup> J. Sun, X. Chen, T. Lu, S. Liu, H. Tian, Z. Guo and X. Jing, *Langmuir* **2008**, 24, 10099-10106
- <sup>80</sup> H.R. Kricheldorf and K. Hauser, *Biomacromolecules* **2001**, 2, 1110-1115
- <sup>81</sup> W. Agut, D. Taton and S. Lecommandoux, *Macromolecules* **2007**, 40, 5653-5661
- <sup>82</sup> C. Schatz, S. Louguet, J.-F. Le Meins, and S. Lecommandoux, *Angew. Chem. Int. Ed.* **2009**, 48, 2572 -2575
- <sup>83</sup> J. Rao, Y. Zhang, J. Zhang, and S. Liu *Biomacromolecules* **2008**, 9, 2586-2593
- <sup>84</sup> A.C. Engler, H.-I. Lee, and P.T. Hammond, *Angew. Chem. Int. Ed.* **2009**, 48, 9334 -9338
- <sup>85</sup> H. Tang and D. Zhang, *Biomacromolecules* **2010**, 11, 1585-1592
- <sup>86</sup> J. Huang, G.J.M. Habraken, F. Audouin and A. Heise, *Macromolecules* **2010**, 43, 6050-6057
- <sup>87</sup> C.E. Hoyle, T. Y. Lee and T. Roper, *J. Polym. Sci. A; Polym. Chem.* **2004**, 42, 5301-5338
- <sup>88</sup> S.P.S. Koo, M.M. Stamenovic, R.A. Prasath, A.J. Inglis, F.E. Du Prez, C. Barner-Kowollik, W. Van Camp and T. Junkers, *J. Polym. Sci. Part A: Polym. Chem.* **2010**, 48, 1699-1713
- <sup>89</sup> W.G. Miller, *J. Am. Chem. Soc.* **1964**, 86, 3913-3918
- <sup>90</sup> T. Hayashi, Y. Tabata and A. Nakajima, *Polym. J.* **1985**, 17, 463-471
- <sup>91</sup> H. Sugiyama and H. Noda, *Biopolymers* **1970**, 9, 459-469
- <sup>92</sup> R.H.P. Doezé, B.A. Maltman, C.L. Egan, R.V. Ulijn and S.L. Flitsch, *Angew. Chem. Int. Ed.* **2004**, 43, 3138 -3141
- <sup>93</sup> P.D. Thornton, R.J. Mart and R.V. Ulijn, *Adv. Mater.* **2007**, 19, 1252-1256
- <sup>94</sup> C. Zhou, X. Qi, P. Li, W.N. Chen, L. Mouad, M.W. Chang, S. Su Jan Leong and M.B. Chan-Park, *Biomacromolecules* **2010**, 11, 60-68
- <sup>95</sup> A. Hautanen, J. Gailit, D.M. Mann and E. Ruoslahti, *J. Biol. Chem.* **1989**, 264, 1437-1442
- <sup>96</sup> L. van Kralingen, *Controlled polymerization of amino acid derivatives* **2008**, thesis Stellenbosch University
- <sup>97</sup> R.-Z. Hou, Y.-J. Liu, N. Zhang, Y.-B. Huang, H. Wang, Y. Yang, L. Xu and X.-Z. Zhang, *Prep. Biochem. Biotechnol.* **2006**, 36, 243-252
- <sup>98</sup> H.-J. Gabius, H.-C. Siebert, S. Andry, J. Jiménez-Barbero and H. Rüdiger, *ChemBioChem* **2004**, 5, 740-764
- <sup>99</sup> K. Aoi, K. Tsutsumiuchi and M. Okada, *Macromolecules* **1994**, 27, 875-877
- <sup>100</sup> Z. Tian, M. Wang, A.-Y. Zhang and Z.-G. Feng, *Polymer* **2008**, 49, 446-454
- <sup>101</sup> J. Sun and H. Schlaad, *Macromolecules* **2010**, 43, 4445-4448
- <sup>102</sup> M.B. Bornstein, A.I. Miller, D. Teitelbaum, R. Arnon, M. Sela, *Ann. Neurol.* **1982**, 11, 317-319
- <sup>103</sup> M. Fridkis-Hareli, E.F. Rosloniec, L. Fugger and J.L. Strominger, *Proc. Natl. Acad. Sci. U. S. A.* **1998**, 95, 12528-12531

- <sup>104</sup> F. Nudelman, K. Pieterse, A. George, P.H.H. Bomans, H. Friedrich, L.J. Brylka, P.A.J. Hilbers, G. de With and N.A.J.M. Sommerdijk, *Nature Mat.* **2010**, 9, 1004-1009
- <sup>105</sup> L.B. Gower, *Chem. Rev.* **2008**, 108, 4551-4627
- <sup>106</sup> M.B. Dickerson, K.H. Sandhage and R.R. Naik, *Chem. Rev.* **2008**, 108, 4935-4978
- <sup>107</sup> B.-A. Gotliv, N. Kessler, J.L. Sumerel, D.E. Morse, N. Tuross, L. Addadi and S. Weiner, *ChemBioChem* **2005**, 6, 304-314
- <sup>108</sup> G. Fu, S.R. Qui, C.A. Orme, D.E. Morse and J.J. De Yoreo, *Adv. Mater.* **2005**, 17, 2678-2683
- <sup>109</sup> D.B. Deoliveira and R.A. Laursen, *J. Am. Chem. Soc.* **1997**, 119, 10627-10631
- <sup>110</sup> B. Njegic-Dzakula, L. Brecevic, G. Falini and D. Kralj, *Crys. Growth Des.* **2009**, 9, 2425-2434
- <sup>111</sup> Y. Yao, W. Dong, S. Zhu, X. Yu and D. Yan, *Langmuir* **2009**, 25, 13238-13243
- <sup>112</sup> P. Kašparová, M. Antonietti and H. Cölfen, *Colloid. Surf. A* **2004**, 250, 153-162
- <sup>113</sup> S. Hayashi, K. Ohkawa and H. Yamamoto, *Macromol. Biosci.* **2006**, 6, 228-240
- <sup>114</sup> H.-A. Klok and S. Lecommandoux, *Adv. Polym. Sci.* **2006**, 202, 75-111
- <sup>115</sup> A. Lübbert, V. Castelletto, I.W. Hamley, H. Nuhn, M. Scholl, L. Bourdillon, C. Wandrey and H.-A. Klok, *Langmuir* **2005**, 21, 6582-6589
- <sup>116</sup> K. Osada and K. Kataoka, *Adv. Polym. Sci.* **2006**, 202, 113-153
- <sup>117</sup> J. Li, T. Wang, D. Wu, X. Zhang, J. Yan, S. Du, Y. Guo, J. Wang, and A. Zhang *Biomacromolecules* **2008**, 9, 2670-2676
- <sup>118</sup> Reprint adapted with permission from E.P. Holowka, D.J. Pochan, and T.J. Deming, *J. Am. Chem. Soc.* **2005**, 127, 12423-12428. Copyright 2011 American Chemical Society.
- <sup>119</sup> A.P. Nowak, V. Breedveld, L. Pakstis, B. Ozbas, D.J. Pine, D. Pochan and T.J. Deming, *Nature* **2002**, 417, 424-428
- <sup>120</sup> C.-Y. Yang, B. Song, Y. Aob, A.P. Nowak, R.B. Abelowitz, R.A. Korsak, L.A. Havton, T.J. Deming and M.V. Sofroniew, *Biomaterials* **2009**, 30, 2881-2898
- <sup>121</sup> V. Sun, Z. Li, T.J. Deming and D.T. Kamei, *Biomacromolecules* **2011**, ASAP: DOI: 10.1021/bm101036f
- <sup>122</sup> H. Iatrou, H. Frielinghaus, S. Hanski, N. Federigos, J. Ruokolainen, O. Ikkala, D. Richter, J. Mays and N. Hadjichristidis, *Biomacromolecules* **2007**, 8, 2173-2181
- <sup>123</sup> J. Rodríguez-Hernández and S. Lecommandoux, *J. Am. Chem. Soc.* **2005**, 127, 2026-2027



# Chapter 2

## NCA Monomer Synthesis and Living NCA ROP through NAM

### Abstract

*The living ring opening polymerizations of N-carboxyanhydride (NCA ROP) has been a very active field the last 13 years. Many new methods for the living NCA ROP have been established since then, both altering the mechanism and optimizing the normal amine mechanism. In this chapter we want to investigate the optimal conditions for the normal amine mechanism (NAM) for the NCA ROP of several NCA monomers choosing or combining the high vacuum method and the low temperature approach. The polymerizations were followed by FTIR in combination with SEC and analyzed by MALDI-ToF-MS to determine the chain composition. We found that for the polymerizations of PZLL, PAla the high vacuum method at 20 °C should be used. For PBLG high vacuum at both higher and lower temperatures could be used. For the other monomers the vacuum did not affect the polymerizations, but at a higher temperature more side reactions were found. Therefore these polymerizations should be performed at 0 °C. The results show that both techniques should be combined for a successful NCA ring opening polymerization. This work gives a new insight into the discussion of the most optimal living NCA ROP technique.*

This chapter is partially based on G.J.M. Habraken, M. Peeters, C.H.J.T. Dietz C.E. Koning and A. Heise, *Polym. Chem.* **2010**, 1, 514-524 and G.J.M. Habraken, C.H.R.M. Wilsens, C.E. Koning and A. Heise, *Polym. Chem.* Accepted



## 2.1 Introduction

The interest in well-defined synthetic polypeptide architectures derived from the ring opening polymerization of N-carboxyanhydrides (NCA) has increased significantly in the last ten years.<sup>1</sup> This can be ascribed to the enormous potential arising from the combination of synthetic peptide segments and with either synthetic or natural building blocks. For example, numerous reports have been published on the synthesis and self-organization of polypeptide block copolymers and polypeptide conjugates into vesicles, micelles and nanoparticles. The increased attention that these materials receive was clearly facilitated by the development of synthetic methods, which allow for the control of the ring opening polymerization of NCAs.<sup>2-15</sup>

Amino acid NCA monomers are readily accessible, mostly using techniques involving phosgenation of protected amino acids or by alternatives methods.<sup>16-19</sup> While the polymerization of NCAs is generally straightforward, for example fast polymerization can be achieved by the addition of a base or nucleophilic initiator, it is by no means trivial to control the polymerization and the molecular weight of polymers.<sup>20-22</sup>

Generally, nucleophiles like primary amines initiator can initiate the NCA polymerization and produce polypeptides with a molecular weight determined by the amine to NCA ratio (normal amine mechanism, NAM). Mechanistically, the first step in the NAM is the attack of a primary (nucleophilic) amine on the C-2 position of the NCA causing the ring to open. This is followed by the transformation of the carbamic ion and decomposition of the carbamic acid under liberation of CO<sub>2</sub> (Scheme 2.1). The newly formed primary amine then propagates the polymerization. As stated in the literature the carbamic acid is only stable at lower temperatures, while the carbamic ion is a more stable form depending on the solvent.<sup>22,23</sup> However, prone to side-reactions with solvents, end-group termination and competing polymerization mechanisms, the reactions often lack the level of control to synthesize more complex polymer architectures like block copolymers. Side reactions frequently occur involving the more basic amines, which easily abstract the proton from an NCA monomer resulting in initiation by the anion to the NCA monomer (activated monomer mechanism, AMM). Water contaminants can also initiate the NCA as a nucleophile, making it crucial to work under dry conditions. Another issue is the low solubility of some polypeptides, resulting in partial precipitation of polymer chains during the polymerization. The reactive polymer chain ends are then not accessible anymore for propagation, whilst the well-dissolved chains continue to grow resulting in a broad polydispersity. Moreover, solvent-induced reactions have been shown to occur for certain monomers with DMF and NMP, resulting in cyclic structures.<sup>24-26</sup>

Generally two different approaches were taken to prevent chain termination in NCA polymerization. When compared to NAM, the first approach builds on different reaction mechanisms by end-group protection and the formation of dormant chain ends. For example, the nickel mediated NCA ROP coordinates the NCA monomer to the chain end, where it then protects the end-group from side reactions.<sup>27</sup> In the silazane method the end-group is protected by a trimethylsilyl carbamate and

coordinates the monomer for insertion, while releasing CO<sub>2</sub>.<sup>28</sup> The ammonium halide initiators proposed by Schlaad propagate following the NAM, but have a protected end group in the dormant state.<sup>29</sup>

While all three methods rely on the addition of a regulating agent, control of the NCA polymerization can also be achieved by optimizing the NAM conditions themselves, for example by lowering the reaction temperature or applying a high vacuum. For the efficiency of the high vacuum technique several reasons have been mentioned. The first one is the acceleration of the reaction by efficient removal of the CO<sub>2</sub> (Scheme 2.1).<sup>22</sup> Secondly, with the removal of CO<sub>2</sub> a side reaction involving DMF resulting in formaldehyde and dimethylamine is suppressed.<sup>32</sup> In the key-publication on the high vacuum technique the high control of the polymerization was shown for  $\gamma$ -benzyl-L-glutamate (BLG) NCA and evident from the linear increase of the molecular weight and the low polydispersity.<sup>33</sup> However, expansion to other NCAs or an investigation on the chain composition, such as the end groups was not carried out. Recently, the synthesis of poly(O-benzyl-L-tyrosine) with diamino-hexane under vacuum conditions was compared to glove-box conditions. The reaction products obtained after 24 hours were investigated by NALDI-ToF-MS and the formation of formamide end-groups by reaction of the peptide with the solvent DMF was found even for the high vacuum technique.<sup>34</sup> For the reaction performed in the glove-box many more side reactions were found, such as the ureido acid terminated product and polymers from the activated monomer mechanism.

The effect of decreased reaction temperature on the reduction of side reactions in NCA polymerization was also shown recently. Capillary electrophoresis (CE) was used to determine the chain compositions of poly(N-*tert*-butyloxycarbonyl-L-lysine) after 48 hours.<sup>35,36</sup> At 0 °C the polypeptide end-groups had retained their primary amines compared to the reactions performed at room temperature, where formyl and ureido-acid end groups were found. Unfortunately, the effect of the lower temperature only has been investigated for this single polypeptide species.

While the low temperature NCA polymerization thus provides an advantage in terms of structural control, a drawback of the polymerization at 0 °C is the long reaction times. On the other hand, the application of vacuum at higher temperatures seems to increase the reaction kinetics but the literature suggests that some side reactions still occur.<sup>36</sup> However, a comparison cannot be made easily because different analytical methods (SEC, CE, MALDI-ToF-MS) were used to prove the degree of control of the polymerizations. In addition, different NCA monomers were studied, which makes comparison harder due to different side reactions occurring for different monomers, different polymerization kinetics and chain conformations in the reaction solution.

The goal of this work was to optimize the NAM by performing NCA ROPs for several NCA monomers by combining the low temperature NCA polymerization with the high vacuum technique. First the effect of the temperature was established on the polypeptide structure for several polypeptide species. Reactions were then carried out varying the temperature from 0 °C and 20 °C a nitrogen flow at atmospheric pressure and a high vacuum of  $1 \times 10^{-5}$  bar. The results were used to give a recommendation of the most ideal reaction conditions for individual NCAs.

## 2.2 Experimental

### Materials

Benzylamine 99.5% purified by redistillation, *S*-*tert*-butylmercapto-L-cysteine, *S*-benzyl-L-cysteine, glycine, L-alanine, L-lysine,  $\alpha$ -pinene 98%, bis(trichloromethyl) carbonate (triphosgene) 99%, MgSO<sub>4</sub>, KHSO<sub>4</sub>, NaOH, dicyclohexylamine and *t*-BOC anhydride were purchased from Aldrich. L-Glutamic acid,  $\gamma$ -benzyl ester, L-aspartic acid,  $\beta$ -benzyl ester, O-benzyl-L-serine, O-benzyl-L-threonine.HCl, N<sub>ε</sub>-benzyloxycarbonyl-L-lysine, N<sub>ε</sub>-9-fluorenylmethoxycarbonyl-L-lysine and N<sub>δ</sub>-trityl-L-glutamine were supplied by Bachem. DMF (extra dry), ethylacetate, *tert*-butanol, *n*-heptane, *n*-pentane and diethylether were purchased from Biosolve. All chemicals were used without any purification unless mentioned. DMF and ethylacetate were used directly from the bottle or stored under an inert, dry atmosphere.

### Methods

FTIR measurements were performed on a PerkinElmer SpectrumOne FTIR Spectrometer, using a universal ATR sampling accessory (resolution 1 cm<sup>-1</sup>). Samples for the IR spectroscopy were taken from the reaction mixtures and analyzed without any further modification.

1,1,1,3,3,3-Hexafluoroisopropanol size exclusion chromatography (HFIP SEC) was performed on a system equipped with a Waters 1515 Isocratic HPLC pump, a Waters 2414 refractive index detector (40 °C), a Waters 2707 autosampler, a PSS PFG guard column followed by 2 PFG-linear-XL (7  $\mu$ m, 8\*300 mm) columns in series at 40°C. HFIP (Apollo Scientific Limited) with potassium trifluoro acetate (3 g/L) was used as eluent at a flow rate of 0.8 mL min<sup>-1</sup>. The molecular weights were calculated against polymethyl methacrylate standards (Polymer Laboratories, M<sub>p</sub> = 580 Da up to M<sub>p</sub> = 7.1\*10<sup>6</sup> Da).

For the SEC analysis using DMF (Biosolve) as eluent measurements were done on a Waters Alliance system equipped with a Waters 2695 separation module, a Waters 2414 refractive index detector (40 °C), a Waters 486 UV detector, a PSS GRAM guard column followed by 2 PSS GRAM columns in series of 100 Å (10  $\mu$ m particles) and 3000 Å (10  $\mu$ m particles) respectively at 60°C. DMF was used as eluent at a flow rate of 1 mL min<sup>-1</sup>. The molecular weights were calculated using polystyrene standards. Before SEC analysis is performed, the samples were filtered through a 0.2  $\mu$ m PTFE filter (13mm, PP housing, Alltech)

<sup>1</sup>H-NMR analyses were performed on a Mercury 400. For the monomers deuterated chloroform was used. For the polymers DMSO-d<sub>6</sub> and deuterated TFA were used.

Matrix Assisted Laser Desorption / Ionization - Time of Flight - Mass Spectroscopy (MALDI-ToF-MS) analysis was carried out on a Voyager DE-STR from Applied Biosystems (laser frequency 20 Hz, 337nm and a voltage of 25kV). The matrix material used was T-2-(3-(4-*t*-Butyl-phenyl)-2-methyl-2-propenylidene)malononitrile (DCTB) (40 mg/ml). Potassium trifluoroacetic acid (KTFA) was added as cationic ionization agent (5 mg/ml). The polymer sample was dissolved in HFIP (1 mg/ml), to which the

matrix material and the ionization agent were added (5:1:5), and the mixture was placed on the target plate. Samples were precipitated from the reaction medium in diethylether, filtered and placed in a freezer before measuring.

## Synthesis

**Synthesis of NCA of  $\gamma$ -benzyl-L-glutamate.** L-Glutamic acid,  $\gamma$ -benzyl ester ( 25.18 g, 106 mmol) and  $\alpha$ -pinene (30.1 g, 221 mmol) were dissolved in 240 ml ethylacetate. Triphosgene (13.96 g, 47.04 mmol) was dissolved in 60 ml ethylacetate and added slowly once the reaction was refluxed. The solution became clear and all solids disappeared after 3 hours. 2/3 of the ethylacetate was removed by distillation. 200ml *n*-heptane was added and the solution was heated to recrystallize. The NCA was recrystallized twice and subsequently washed with *n*-heptane, dried under vacuum and stored in a refrigerator under P<sub>2</sub>O<sub>5</sub>. Yield: 23.01 g, 87.4 mmol, 88 %. <sup>1</sup>H-NMR (400MHz, CDCl<sub>3</sub>,  $\delta$ , ppm): 2.20 (m, 2H, CH<sub>2</sub>), 2.59 (t, 2H, CH<sub>2</sub>, J=6.8 Hz), 4.37 (t, H, CH<sub>2</sub>O, J=6.1 Hz), 5.14 (s, 2H, CH<sub>2</sub>O) 6.57 (s, 1H, NH) 7.36 (m, 5H, ArH), <sup>13</sup>C-NMR (400MHz, CDCl<sub>3</sub>,  $\delta$ , ppm ): 26.77 (CH<sub>2</sub>CH), 29.57 (CH<sub>2</sub>CO), 56.81 (CH) 67.03 (CH<sub>2</sub>O), 128.29 (ArH), 128.53(ArH), 128.68(ArH), 135.27(ArH), 152.30 (NHC(O)O), 169.56 (CH<sub>2</sub>CO(O)), 172.36 (CHC(O)O), Meltingpoint: 94 °C

**Synthesis of NCA of O-benzyl-L-serine.** The same procedure as for the synthesis of the NCA of  $\gamma$ -benzyl-L-glutamate was applied. Yield: 22.3 g (100.8 mmol); 79.1%. <sup>1</sup>H-NMR (400 MHz, CDCl<sub>3</sub>,  $\delta$ , ppm): 3.72 (m, 2H, (CH<sub>2</sub>)), 4.39 (t, 1H, (CH)), 4.53 (s, 2H, (CH<sub>2</sub>Ar)), 6.75 (s, 1H, (NH)), 7.27 (m, 5H, (ArH)), <sup>13</sup>C-NMR (400 MHz, CDCl<sub>3</sub>,  $\delta$ , ppm ): 58.49 (CH), 67.67 (CH<sub>2</sub>CH), 73.67 (CH<sub>2</sub>Ar), 127.78 (Ar), 128.22 (Ar), 128.62 (Ar), 136.64 (Ar), 152.86 (C(O)ONH), 167.86 (OC(O)CH).

**Synthesis of NCA of S-benzyl-L-cysteine.** The same procedure as for the synthesis of the NCA of  $\gamma$ -benzyl-L-glutamate was applied. Yield: 5.08 g (21.4 mmol); 89.5 %. <sup>1</sup>H-NMR (400 MHz, CDCl<sub>3</sub>,  $\delta$ , ppm): 2.80 (m, 2H, CH<sub>2</sub>), 3.77 (s, 2H, CH<sub>2</sub>Ar), 4.33 (q, 1H, CH, J=3.7 Hz), 6.44 (s, 1H, NH) 7.317 (m, 5H, ArH), <sup>13</sup>C-NMR (400 MHz, CDCl<sub>3</sub>,  $\delta$ , ppm ): 32.62 (CH<sub>2</sub>CH), 37.04 (CH<sub>2</sub>Ar), 57.70 (CH), 127.73 (ArH), 128.92 (ArH), 137.09 (ArH), 152.12 (NHC(O)O), 168.14 (C(O)OCH<sub>2</sub>).

**Synthesis of NCA of S-tert-butylmercapto-L-cysteine.** The same procedure as for the synthesis of the NCA of  $\gamma$ -benzyl-L-glutamate was applied. Yield: 4.90 g, 20.8 mmol, 88 %. <sup>1</sup>H-NMR (400MHz, CDCl<sub>3</sub>,  $\delta$ , ppm): 1.36 (d, 9H, ((CH<sub>3</sub>)<sub>3</sub>C)), J=1.0), 2.8 (m, 1H, (CH<sub>2</sub>)), 3.23 (m, 1H, (CH<sub>2</sub>)), 4.71 (dd, 1H, CH, J=3.3 Hz, J=9.1 Hz) 6.57 (s, 1H, NH), <sup>13</sup>C-NMR (400MHz, CDCl<sub>3</sub>,  $\delta$ , ppm ): 29.82 ((CH<sub>3</sub>)<sub>3</sub>C)), 40.71 (CH<sub>2</sub>), 49.13 (C(CH<sub>3</sub>)<sub>3</sub>), 57.24 (CH), 151.50 (O(CO)NH), 168.23 (O(CO)CH), Meltingpoint: 107 °C

**Synthesis of NCA of N-benzyloxycarbonyl-L-lysine.** The same procedure as for the synthesis of the NCA of  $\gamma$ -benzyl-L-glutamate was applied. Yield: 4.66 g (15.2 mmol); 85.5%. <sup>1</sup>H-NMR (400 MHz,

DMSO,  $\delta$ , ppm): 1.32 (m, 4H, CH<sub>2</sub>CH<sub>2</sub>), 1.64 (m, 2H, CH<sub>2</sub>), 2.97 (q, 2H, CH<sub>2</sub>, J=6.4 Hz), 4.40 (t, 1H, CH, J= 5.1), 4.99 (s, 2H, CH<sub>2</sub>O), 7.23 (s, 1H, NH), 7.32 (m, 5H, ArH), 9.06 (s, 1H, NH), <sup>13</sup>C-NMR (400 MHz, DMSO,  $\delta$ , ppm ): 22.04 (CH<sub>2</sub>CH<sub>2</sub>CH), 29.21 (CH<sub>2</sub>CH<sub>2</sub>NH), 31.08 (CH<sub>2</sub>CH), 40.35 (CH<sub>2</sub>NH), 57.45 (CH), 65.58 (CH<sub>2</sub>Ar), 128.15 (Ar), 128.18 (Ar), 128.78 (Ar), 137.69 (Ar), 152.41 (C(O)NHCH), 156.54 (C(O)NHCH<sub>2</sub>), 172.09 (C(O)CH).

**NCA of N $\epsilon$ -9-fluorenylmethoxycarbonyl-L-lysine.** The same procedure as for the synthesis of the NCA of  $\gamma$ -benzyl-L-glutamate was applied. Yield: 4.20 g, 10.7 mmol, 78.5%, <sup>1</sup>H-NMR (400 MHz, CDCl<sub>3</sub>,  $\delta$ , ppm): 7.77 (d, 2H, ArH, J= 7.5 Hz), 7.59 (d, 2H, ArH, J= 7.5 Hz), 7.40 (t, 2H, ArH, J= 7.2), 7.31 (t, 2H, ArH, J = 7.2), 6.68 (s, 1H, NH), 4.85 (s, 1H, NH), 4.44 (t, 2H, OCH<sub>2</sub>CH, J = 6.0), 4.29 (t, 1H, CHC(O), J = 5.4 Hz), 4.21 (t, 1H, CHCH<sub>2</sub>O, J = 6.5 Hz), 3.18 (m, 2H, CH<sub>2</sub>NH), 1.96 (m, 2H, CH<sub>2</sub>CH), 1.53 (m, 2H, CH<sub>2</sub>), 1.42 (m, 2H, CH<sub>2</sub>) <sup>13</sup>C-NMR: 169.9 (OC(O)CH), 153.8 (C(O)NH), 152.5 ((CO)NH), 143.8 (Ar), 141.3 (Ar), 127.7 (Ar), 127.1 (Ar), 125.0 (Ar), 120.0 (Ar), 66.7 (CH<sub>2</sub>O), 57.4 (CH), 47.2 (CH), 40.0 (CH<sub>2</sub>), 30.8 (CH<sub>2</sub>), 21.3 (CH<sub>2</sub>).

**NCA of glycine.** The same procedure as for the synthesis of the NCA of  $\gamma$ -benzyl-L-glutamate was applied. Yield: 3.86 g, 38.2 mmol, 28%, <sup>1</sup>H-NMR (400 MHz, d-TFA) ppm: 4.7 (2H, s, NH-CH<sub>2</sub>-CO), 11.60 (1H, s, NH). <sup>13</sup>C-NMR (400 MHz, d, TFA-d) ppm; 46.9 (NHCH<sub>2</sub>), 156.9 (C(O)N), 168.8 (C(O)O).

**NCA of L-alanine.** The same procedure as for the synthesis of the NCA of  $\gamma$ -benzyl-L-glutamate was applied with the addition that the L-alanine was grounded to a fine powder before use. Yield: 9.67 g, 84.0 mmol, 74.4% <sup>1</sup>H-NMR (400 MHz, d<sub>6</sub>-DMSO,  $\delta$ , ppm): 8.96 (s, 1H, NH), 4.46 (q, 1H, CH, J= 7.0 Hz), 1.31 (d, 3H, CH<sub>3</sub>, J= 7.0Hz) <sup>13</sup>C-NMR (400 MHz, DMSO-d<sub>6</sub>,  $\delta$ , ppm): 172.8 (CHC(O)O), 152.1 (NHC(O)O), 53.3 (CH), 17.2 (CH<sub>3</sub>).

**NCA of  $\beta$ -benzyl-L-aspartate.** The same procedure as for the synthesis of the NCA of  $\gamma$ -benzyl-L-glutamate was applied. Yield: 20.5 g, 82.3 mmol, 73.8% <sup>1</sup>H-NMR( 200 MHz, CDCl<sub>3</sub>,  $\delta$ , ppm): 7.37 (m, 5H, ArH), 6.25 (s, 1H, NH), 5.19 (s, 2H, CH<sub>2</sub>O), 4.59 (t, 1H, CH), 3.08 (m, 2H, CH<sub>2</sub>) <sup>13</sup>C-NMR ( 200 MHz, CDCl<sub>3</sub>,  $\delta$ , ppm ): 171.6 (OC(O)CH), 169.8 (OC(O)CH<sub>2</sub>), 155.7 (C(O)NH), 133.5 (Ar), 128.9 (Ar), 128.5 (Ar), 128.3 (Ar) 69.3 (CH<sub>2</sub>Ar), 54.3 (CH), 34.86 (CH<sub>2</sub>CH).

**Synthesis of NCA of N $\delta$ -trityl-L-glutamine.** N $\delta$ -Trityl-L-glutamine (4.99 g, 12.8 mmol) and  $\alpha$ -pinene (4.69 g, 34.4 mmol) were dissolved in 40 ml ethylacetate. To this a solution of triphosgene (1.76 g, 5.93 mmol) in 20 ml ethylacetate was added dropwise under reflux. After 1 hour the solution was clear with some precipitated solids. After decantation the solution was concentrated. Yield: 4.40 g, 10.6 mmol, 82.5% <sup>1</sup>H-NMR( 400 MHz, DMSO,  $\delta$ , ppm): 9.04 (s, 1H, NH) 8.67 (s, 1H, NH), 7.28-7.15 (m, 15H, ArH), 4.33 (t, 1H, CH, J= 6.0), 2.42 (m, 2H, CH<sub>2</sub>), 1.87 (m, 2H, CH<sub>2</sub>) <sup>13</sup>C-NMR ( 400 MHz, DMSO,  $\delta$ , ppm ):

171.8 (OC(O)CH), 171.0 (C(O)NH), 152.3 (C(O)NH), 145.2 (Ar), 128.9 (Ar), 127.9 (Ar), 126.8 (Ar) 69.7 (C(Ar)<sub>3</sub>), 56.9 (CH), 31.2 (CH<sub>2</sub>), 27.3 (CH<sub>2</sub>).

**NCA of O-benzyl-L-threonine synthesis from HCl salt.** O-benzyl-L-threonine.HCl (5.00 g, 23.9 mmol) and  $\alpha$ -pinene (8.3 g, 60 mmol) were added to 40 ml ethyl acetate in a 100 ml round bottom flask. To this a solution of triphosgene (2.8 g, 9.47 mmol) in 20 ml ethyl acetate was added dropwise under reflux. After 2.5 hours the solution was clear. Two third of the ethyl acetate was removed by rotary evaporation and the product was recrystallized from a *n*-heptane/ethyl acetate solution 3 times. Yield: 3.385 g, 14.4 mmol, 60.2%. <sup>1</sup>H NMR (400 MHz, CDCl<sub>3</sub>) ppm; 1.25 (3H, d, J = 6.5 Hz, CH<sub>3</sub>), 3.85 (1H, q, J = 6.4 Hz, CHCH<sub>3</sub>), 4.12 (1H, d, J = 4.3 Hz, NHCH), 4.36 (1H, d, J = 11.5 Hz, CH<sub>2</sub>b), 4.52 (1H, d, J = 11.50 Hz CH<sub>2</sub>a), 6.96 (1H, NH), 7.18–7.28 (5H, aryl CH). <sup>13</sup>C NMR (400 MHz, d, CDCl<sub>3</sub>) ppm; 15.9 (CH<sub>3</sub>), 62.9 (NHCH), 71.3 (CH<sub>2</sub>), 73.0 (CHCH<sub>3</sub>), 127.8, 128.0, 128.5, 136.9 (aryl C), 152.9 (C(O)N), 167.8 (C(O)O).

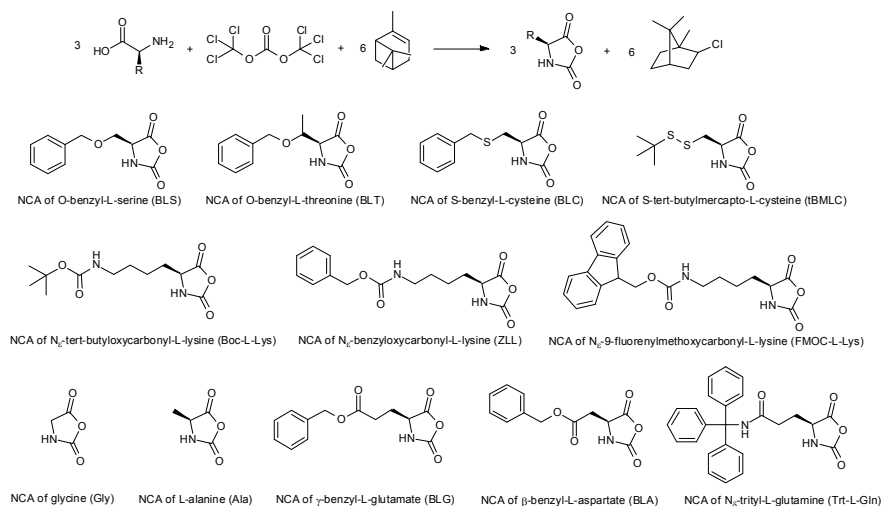
**Synthesis of NCA of N<sub>ε</sub>-*t*-butyloxycarbonyl-L-lysine.** This compound was synthesized following a literature procedure.<sup>37</sup> L-Lysine (15.06 g, 0.103 mmol) was dissolved with NaOH (4.58 g, 0.115 mmol) in 125 ml water and 100 ml *tert*-butanol. Over a period of 1 hour *t*-BOC anhydride (54.8 g, 0.251 mmol) was added. After 48h 250 ml of ethylacetate was added with 150 ml of water ad 23 g of KHSO<sub>4</sub>. The water layer was extracted with ethylacetate and the combined organic layers were washed with water and dried with MgSO<sub>4</sub> and concentrated by vacuum. The yellowish oil was dissolved in 100 ml diethylether and 20 ml of dicyclohexylamine precipitated in 2 L of *n*-heptane and *n*-pentane (1:1). After filtration and drying 41.6 g, 78.9 mmol of Na<sub>ε</sub>,N<sub>ε</sub>-di-(*tert*-butyloxycarbonyl)-L-lysine dicyclohexylamine salt remained. The Na<sub>ε</sub>,N<sub>ε</sub>-di-(*tert*-butyloxycarbonyl)-L-lysine dicyclohexylamine (28.9, 54.8 mmol) was added to 150 ml ethylacetate. To this 1M of H<sub>2</sub>SO<sub>4</sub> was added until all solids were dissolved. The organic phase was extracted with water. The ethylacetate was subsequently dried with MgSO<sub>4</sub> and dried in vacuum. The Na<sub>ε</sub>,N<sub>ε</sub>-di-(*tert*-butyloxycarbonyl)-L-lysine (18.4 g, 53.1 mmol) was dissolved in 400 ml ethylacetate and subsequently triphosgene (8.6 g, 29 mmol) was added. After 10 minutes triethylamine (6.0 g, 59 mmol) was added. After 7 hours the reaction medium was cooled to -18 °C and filtered. The solution was washed with a saturated NaHCO<sub>3</sub> solution repeatedly and subsequently dried with MgSO<sub>4</sub>. 2/3 Of the solvent was removed by vacuum and *n*-heptane was added to recrystallize the NCA. After repeated recrystallization from ethylacetate and *n*-heptane the NCA crystals were filtered and dried by vacuum. Yield: 7.9 g (29,0 mmol); 40.5 %. <sup>1</sup>H-NMR (400 MHz, DMSO,  $\delta$ , ppm ): 1.26 (m, 4H, CH<sub>2</sub>CH<sub>2</sub>), 1.35 (s, 9H, ((CH<sub>3</sub>)<sub>3</sub>C)), 1.67 (m, 2H, CH<sub>2</sub>CH), 2.89 (q, 2H, CH<sub>2</sub>-NH, J=6.3Hz), 4.40 (t, 1H, (CH), J=5.3 Hz), 6.75 (s, 1H, (NH)), 9.04 (s, 1H, (NH)); <sup>13</sup>C-NMR (400 MHz, DMSO,  $\delta$ , ppm ): 22.03 (CH<sub>2</sub>CH<sub>2</sub>CH), 28.57 ((CH<sub>3</sub>)<sub>3</sub>C), 28.69 (CH<sub>2</sub>CH<sub>2</sub>NH), 29.30 (CH<sub>2</sub>CH), 31.08 (CH<sub>2</sub>NH), 57.46 (CH), 77.80 (C(CH<sub>3</sub>)<sub>3</sub>), 152.39 (NHC(O)O), 156.02 (C(O)OC(CH<sub>3</sub>)<sub>3</sub>), 172.07 (C(O)OCH<sub>2</sub>),

**NCA homopolymerization with different temperatures.** The NCA monomer of O-benzyl-L-serine (1.02 g, 4.61 mmol) was dissolved in 9 ml DMF in a Schlenk tube. To this a solution of benzylamine (12 mg,  $11 \times 10^{-1}$  mmol) in 1 ml DMF was added. The reaction was left to stir in a cold water bath of 0 °C or 10 °C, at room temperature or in an oilbath of 60 °C for 4 days under a dry nitrogen atmosphere. The solution was precipitated in diethylether, the polymer was filtered and dried in vacuo. Yield: 0.53 g, 64 wt%.

**NCA ROP Conversion experiments.** NCA of  $\beta$ -benzyl-L-aspartate (1.89 g, 7.60 mmol) was dissolved in 18.1 g DMF in a 40 ml Schlenk tube. A solution of benzylamine (20.49 mg,  $1.91 \times 10^{-1}$  mmol) in 0.80 g of DMF was added to the dissolved NCA. The solution was stirred thoroughly and distributed over 3 other Schlenk tubes as well. Two were left at room temperature under a nitrogen flow or under high vacuum of  $1 \times 10^{-5}$  bar. Both of these Schlenk tubes were connected to a gasline with dry nitrogen gas and an Edwards oil pump with a cold trap between the gasline and the pump. The other two were put in a cooled waterbath under a nitrogen flow or under high vacuum. Samples were taken periodically for IR and SEC. The samples under high vacuum were purged with nitrogen before a sample was taken. After the full conversion was obtained for the polymerizations at 20 °C samples were taken for MALDI-ToF-MS over time. Finally the polymer was precipitated in diethylether.

## 2.3 Results & discussion

### 2.3.1 Monomer synthesis



**Scheme 2.1.** N-Carboxyanhydrides (NCAs) of amino acids applied in the polymerizations at 0 °C.

Most of the NCA monomers were synthesized following a standard literature procedure by reacting the (protected) amino acids with triphosgene in the presence of an HCl scavenger such as  $\alpha$ -pinene

(Scheme 2.1).<sup>17</sup> For all the reactions the solution became clear over time with the conversion of the amino acids to the better soluble NCA monomer. The purification of the NCA monomers was done by repeated recrystallization from *n*-heptane and ethylacetate, yielding white crystals for all reactions. <sup>1</sup>H-NMR did indicate that apart from small traces of solvent the NCA monomers were completely pure. The yields for the  $\alpha$ -pinene route did vary between 70%-90%. The NCAs were stored with P<sub>2</sub>O<sub>5</sub> in the fridge and most could be used months after the preparation. In the case of the NCAs of L-alanine and glycine the quality of the monomer decreased rapidly with increasing storage time.

With the synthesis of the NCA of O-benzyl-L-threonine an adaptation was made with the use of an amino acid HCl salt. Here an additional equivalent of  $\alpha$ -pinene was added to scavenge the HCl. A lower yield of 60.2% was obtained for this reaction. This was most probably due to the purification from a solution with a higher  $\alpha$ -pinene quantity.

The synthesis of the NCA of N $\delta$ -trityl-L-glutamine has not been reported before. When the standard procedure was applied the NCA of 2-amino-4-cyano(S)-butanoic acid was formed.<sup>38</sup> Since the trityl group is removed in the presence of HCl, the free amide can be converted to the nitrile group by phosgene. By altering the concentration of  $\alpha$ -pinene and decreasing the reaction time to under an hour the product could be isolated as a white powder.

N-carboxyanhydrides with a *tert*-butyloxycarbonyl protected amine can be synthesized using triphosgene and triethylamine as HCl scavenger. In the case of the NCA of N $\epsilon$ -*tert*-butyloxycarbonyl-L-lysine this method was applied. First N $\alpha$ ,N $\epsilon$ -di-(*tert*-butyloxycarbonyl)-L-lysine was prepared by reacting L-lysine to *t*-Boc anhydride and after purification the NCA ring was made with triphosgene and triethylamine as HCl scavenger.<sup>37</sup> The yield was lower for this reaction route, especially due to the washing step with water to remove the formed salt after the reaction with phosgene.

**Table 2.1.** SEC results of temperature-dependent NCA polymerization of BLG, BLA and BLS. All reactions were carried out for four days at a monomer to initiator ratio of 40. Values were measured after precipitation by HFIP-SEC and were calibrated by PMMA standards.

| Reaction temperature<br>T(°C) | PBLG                         |      | PBLA                         |      | PBLs <sup>(a)</sup>          |      |
|-------------------------------|------------------------------|------|------------------------------|------|------------------------------|------|
|                               | <i>M<sub>n</sub></i> (g/mol) | PDI  | <i>M<sub>n</sub></i> (g/mol) | PDI  | <i>M<sub>n</sub></i> (g/mol) | PDI  |
| 0                             | 9,300                        | 1.06 | 7,300                        | 1.08 | 7,600                        | 1.18 |
| 10                            | 9,600                        | 1.13 | 10,900                       | 1.09 | 6,700                        | 1.15 |
| 20                            | 11,000                       | 1.09 | 8,600                        | 1.13 | 7,500                        | 1.16 |
| 60                            | 9,100                        | 1.27 | 8,000                        | 1.10 | 6,200                        | 1.18 |

(a) bimodal distributions.

### 2.3.2 Effect of temperature on polypeptide structure

First the effect of temperature on the polypeptide structure by NCA ROP was determined for the polymerization of three NCA monomers, i.e.  $\gamma$ -benzyl-L-glutamate (BLG),  $\beta$ -benzyl-L-aspartate (BLA)



and O-benzyl-L-serine (BLS). All polymerizations were initiated with benzylamine (monomer to initiator ratio ( $M/I$ ) = 40) in DMF and carried out at four different temperatures (0, 10, 20 and 60 °C) for four days under an inert atmosphere. After precipitation, the polypeptides were analyzed by Size Exclusion Chromatography (SEC) and MALDI-ToF-MS. SEC does not reveal a conclusive effect of the reaction temperature on the obtained molecular weights. Within reasonable variations the molecular weights are comparable for a temperature series (Table 2.1). Noteworthy is that the polydispersity index (PDI) of the PBLG sample obtained at 60 °C (1.27) is higher than the PDI obtained at lower temperature (1.06 – 1.13) and that all PBLG samples have a bimodal distribution.

All final polymer samples were further analyzed by MALDI-ToF-MS to determine the chemical composition (for all spectra see the supporting information). For PBLG it is known that pyroglutamate groups can be formed by intramolecular cyclization of the amino end-group with the adjacent benzyl ester.<sup>39</sup> The effect of the reaction temperature on this reaction is clearly visible from the PBLG spectra shown in Figure 2.1. While at 0 °C only PBLG macromolecules with intact amino end-groups are detected (structure A, Figure 2.2) the relative amount of pyroglutamate (structure B, Figure 2.2) successively increases with increasing temperature. At 20 °C already a substantial fraction of the chains are terminated by pyroglutamate and at 60 °C all end-groups are pyroglutamates. The kinetics of this chain end termination cannot be concluded from these measurements, but it is reasonable to assume that it happens throughout the polymerization and leads to an increasing number of dead chain-ends as the polymerization proceeds. This would explain the higher polydispersity observed for the PBLG obtained at 60 °C as compared to the polypeptides obtained at lower temperature.

Also for the PBLA the MALDI-ToF spectrum for the polypeptide obtained at 0 °C confirms the presence of only one polymer species, namely PBLA with amino end-groups (structure C, Figure 2.2). At higher temperatures the spectra become more complex with a series of peaks suggesting the formation of copolypeptides. These side reactions are the result of an intramolecular amidation leading to the formation of succinimide units in the main chain (structure D, Figure 2.2). For the reaction at 60 °C PBLA with at least five succinimide units per chain could be identified. In increasing amount of formamide groups was also found at the chain ends (structure E, Figure 2.2) in addition to the succinimide formation. This chain end termination is the result of the reaction of the amine end-group with the solvent DMF, yielding formamide terminated polypeptide chains and dimethylamine.<sup>24</sup> As an end-capping reaction, the formamide formation will terminate polypeptide growth. However, compared to the chain-end termination of the PBLG, the effect on the molecular weight and polydispersity seems to be minor. The presence of the succinimide groups could be more problematic if the polymer comes into contact with water, which could result in a ring opening reaction producing either a normal  $\alpha$  amide or a  $\beta$  peptide bond.<sup>40</sup>

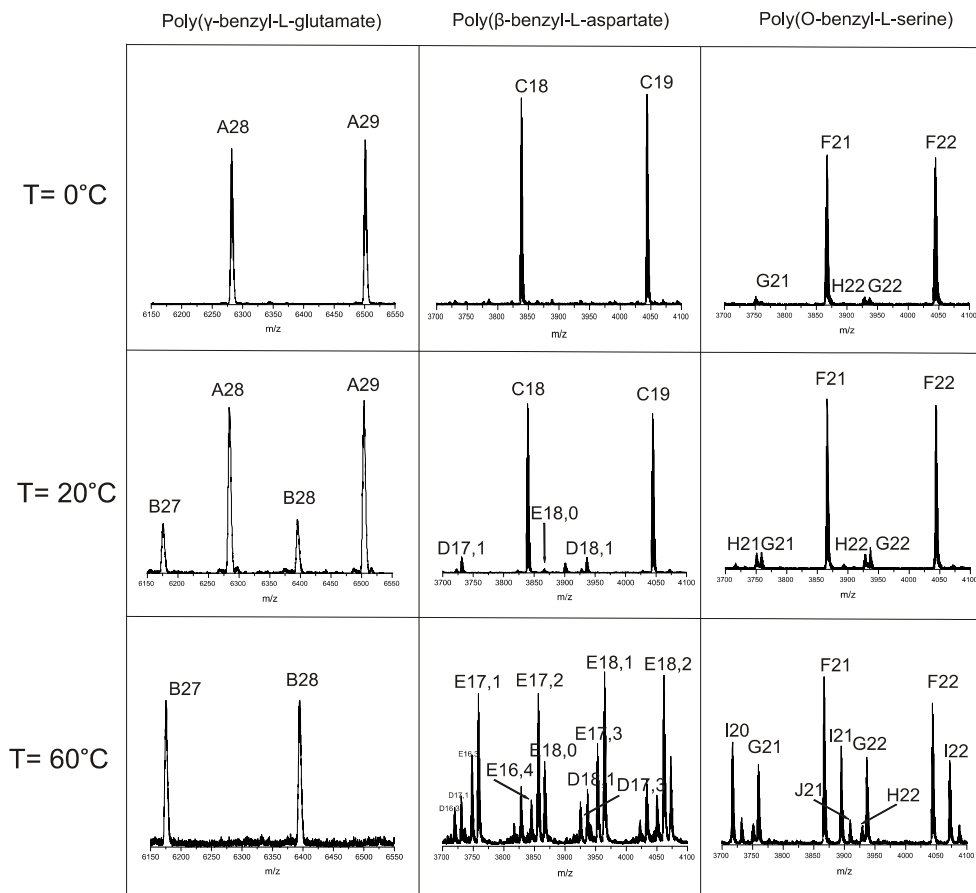


**Figure 2.1.** MALDI-ToF-MS results of PBLG, PBLA and PBLS obtained at different temperatures. Letters in peak assignments refer to structures shown in Figure 2.2; numbers denote the degree of polymerization. For the poly( $\beta$ -benzyl-L-aspartate) the first number refers to the  $\beta$ -benzyl-L-aspartate units and the second number to the succinimide units in the formed copolymers. All samples were measured with potassium trifluoroacetic acid (KTFA).

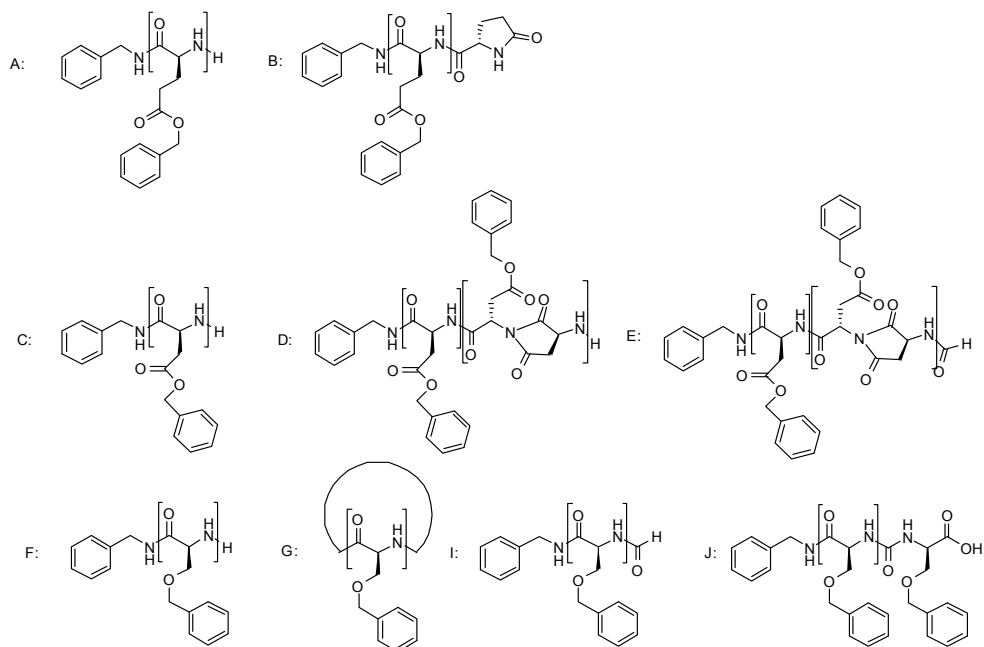


**Figure 2.2.** Structures identified in the NCA polymerization of BLG, BLA and BLS. The letters refer to the MALDI-ToF peak assignment in Figure 2.1.

For the PBLS some side products can be determined even for the polymerization at 0 °C. Besides the benzylamine-initiated and unterminated chains (structure F, Figure 2.2) also cyclic structures (structure G, Figure 2.2) and a so far unidentified species (structure H, Figure 2.2) were found.<sup>25</sup> The full MALDI-ToF-MS spectrum (supportive information) shows that for the lower degrees of polymerization a relatively larger amount of cyclic structures (structure G, Figure 2.2) is present, which implies that there is a molecular weight dependency. At higher temperature in particular an increase of the relative amounts of larger cyclic structures is observed. Moreover, at 60 °C other side reactions occur, for example formamide formation by reaction with DMF (structure I, Figure 2.2). Structure J (Figure 2.2) was identified as a product of a polymer chain, which had reacted with isocyanatocarboxylic acid. The latter is most likely formed at the higher temperature from the deprotonated NCA resulting in the so-called hydantoic acid end group.<sup>26</sup>

In conclusion, for all investigated samples a significant effect of the reaction temperature on the polymer structure was observed. With the exception of PBLG, which shows an increase in PDI at higher reaction temperatures, these effects are not evident from SEC. Striking is the difference between the side reactions of the three investigated polypeptides. For the PBLG only end-group termination occurs, while for PBLA succinimide formation and end-group termination by reaction with DMF was detected. The latter was also observed for PBLS alongside with cyclization reactions. Without exception, the best results were obtained for the polymerizations performed at 0 °C resulting in high structural control with

retention of the active amino end-groups.

The feasibility of the NCA polymerization at 0 °C in DMF was then investigated for a series of other monomers. With a few exceptions these polymerizations resulted in polypeptides with a low PDI and a molecular weight as targeted between 4,000 and 9,000 g/mol (Table 2.2). It has to be noted that due to the calibration of the SEC with PMMA a quantitative comparison with the theoretical molecular weight is difficult. For the L-alanine and the *S*-*tert*-butylmercapto-L-cysteine NCA a high PDI (> 2.0) was obtained, suggesting a limited control over the reaction. This is due to the observed precipitation or aggregation of polymers during the polymerization. For PZLL no side reaction products were found in the MALDI-ToF-MS spectra, except for a small amount of cyclics under both conditions at 20 °C, which are absent at 0 °C. The PAla did not show to have any side reactions over time at all.<sup>26</sup> Both polymerizations seem to remain controlled for a longer period of time. Measurements of poly(*S*-*tert*-butylmercapto-L-cysteine) also confirmed side reactions such as cyclization and chain end termination.

**Table 2.2.** SEC results of polymerization at 0 °C of several NCA monomers. All reactions were carried out for four days. Values measured after precipitation by HFIP-SEC calibrated with PMMA standards.

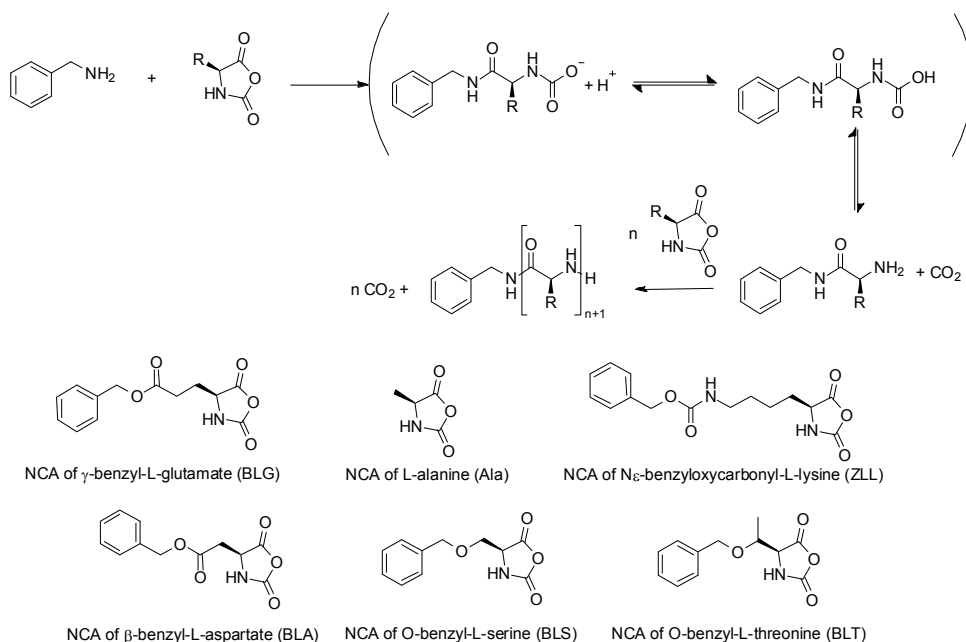
| Entry | Polypeptide  | M/I | $M_{n,theo}$ (g/mol) <sup>b</sup> | $M_n$ (g/mol) | PDI  |
|-------|--|-----|-----------------------------------|---------------|------|
| 1     | Poly( $\gamma$ -benzyl-L-glutamate)                  | 41  | 9,100                             | 9,300         | 1.1  |
| 2     | Poly( $N_\epsilon$ - <i>t</i> -Boc-L-lysine)         | 40  | 9,200                             | 6,500         | 1.2  |
| 3     | Poly( $N_\epsilon$ -Z-L-lysine) with LiBr            | 14  | 3,800                             | 8,100         | 1.1  |
| 4     | Poly( $N_\epsilon$ -Fmoc-L-lysine) <sup>(a)</sup>    | 20  | 7,100                             | 5,100         | 1.25 |
| 5     | Poly(O-benzyl-L-serine)                              | 12  | 2,200                             | 6,200         | 1.1  |
| 6     | Poly(O-benzyl-L-threonine)                           | 40  | 7,800                             | 6,400         | 1.15 |
| 7     | Poly( <i>S</i> -benzyl-L-cysteine)                   | 15  | 3,000                             | 4,700         | 1.1  |
| 8     | Poly( <i>S</i> - <i>t</i> -butylmercapto-L-cysteine) | 18  | 3,500                             | 3,900         | 2.0  |
| 9     | Poly( $N_\delta$ -trityl-L-glutamine)                | 35  | 13,100                            | 6,300         | 1.1  |
| 10    | Poly( $\beta$ -benzyl-L-aspartate)                   | 40  | 8,300                             | 7,300         | 1.08 |
| 11    | Poly(glycine)  | 40  | 2,400                             | (c)           | (c)  |
| 12    | Poly(L-alanine)                                      | 40  | 2,900                             | 4,400         | 2.15 |

(a) Measured with DMF-SEC, calibrated with polystyrene standards. (b) Calculated from the M/I ratio. (c) not measured.

### 2.3.3. Effect of temperature and pressure on NCA ROP: monomer conversion

The effect of temperature on the polypeptide is established, but after a reaction time of 4 days for all reactions. Which makes it hard to distinguish between side reactions that occurred during or after the polymerization. So, the relevant reaction time needs to be determined for every NCA monomer. To determine the optimal polymerization conditions with respect to temperature and pressure a series of the amino acid NCAs shown in Scheme 2.2 was investigated. In order to monitor the NCA conversion under different polymerization conditions, FTIR spectroscopy was used. Upon ring opening the NCA carbonyl peaks of the anhydride at 1786 cm<sup>-1</sup> and 1857cm<sup>-1</sup> are reduced while amide peaks of the polypeptide products increase. A calibration curve was made by plotting the area under the NCA

carbonyl peak at  $1786\text{ cm}^{-1}$  against the NCA solution concentration for all used NCAs. In the reactions under high vacuum there is the possibility that the actual concentration is altered by the evaporation of solvent (DMF), which could lead to an error in the calculation of the NCA conversion. Therefore an additional calibration line was made for the benzyl group containing NCAs using the signal at  $700\text{ cm}^{-1}$  to correct for any change in NCA monomer concentration. Since the quantity of benzyl groups does not change during the polymerization the absorption of this group could be used as an internal standard for the polymerization of the well-soluble polypeptides PZLL, PBLG and PBLT. The resulting calibration plot is shown in Figure 2.3 from which it can be observed that the peak areas measured as a function of concentration are almost identical for all NCAs.



**Scheme 2.2.** NCA ROP according to normal amine mechanism (NAM), initiated by benzylamine and structures of the NCAs investigated in the monomer conversion study.

For the polymerization experiments NCA monomer solutions were prepared and a solution of benzylamine initiator added. This stock solution was then divided over four Schlenk tubes, two of which were polymerized under nitrogen at a temperature of  $0\text{ }^{\circ}\text{C}$  and  $20\text{ }^{\circ}\text{C}$ , respectively. The other two tubes were polymerized at the same two temperatures but were exposed to a pressure of  $1 \times 10^{-5}$  bar. Samples were taken from the reaction solution by a  $\mu\text{L}$  Finn pipet at time intervals and analysed by Size Exclusion Chromatography (SEC) in 1,1,1,3,3,3-hexafluoroisopropanol (HFIP) for molecular weight analysis and by FTIR for monomer conversion analysis. The high vacuum reaction flask was purged with nitrogen gas prior to sampling and subsequently evacuated again. Different degrees of

polymerization (DP) were aimed at by altering the monomer to initiator ratio. As a standard a target degree of polymerization of 40 was used for all polypeptides. In addition, for polymers well soluble in DMF, such as PBLG reactions aiming at higher DPs of 100 and 400 were performed.

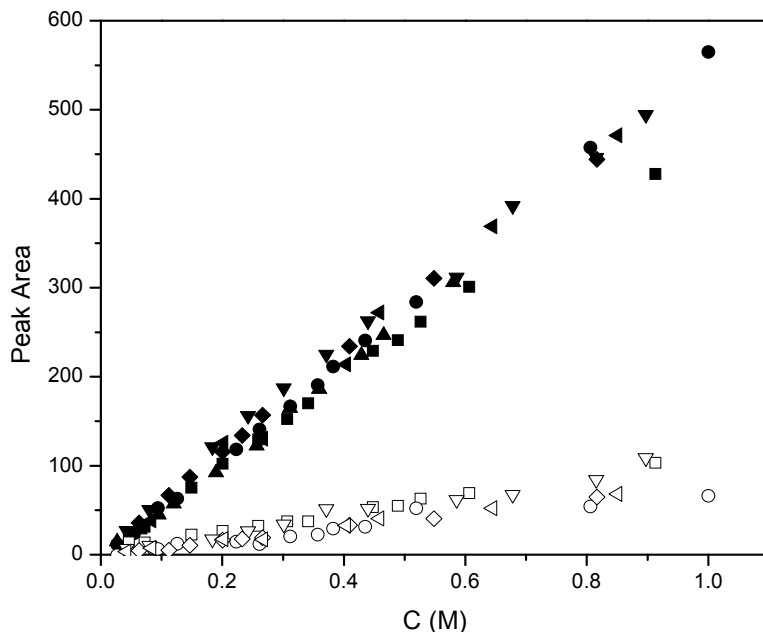


**Figure 2.3.** Calibration plot of the peak areas of the carbonyl peak measured by FTIR at  $1786\text{ cm}^{-1}$  (filled symbols) and benzyl peaks at  $700\text{ cm}^{-1}$  (open symbols) versus the NCA monomer concentration (mol/l) in DMF for the NCAs of BLG (■), Ala (▲), ZLL (●), BLA (▼), BLS (◆) and BLT (◄). For the NCA abbreviations, see Scheme 2.2.

A typical result is shown in Figures 2.4 and 2.5 for the polymerization of PBLG with DP = 100. Inspection of Figure 2.5 shows that at both temperatures the NCA conversion is higher, i.e. the reaction is faster, at the lower pressure (Figure 2.5a and b). This effect is more pronounced at the higher temperature of  $20\text{ }^{\circ}\text{C}$ . At both temperatures and pressures the molecular weight increases linearly with the conversion and low polydispersity indices (PDI) < 1.2 suggests the good control over the polymerization (Figure 2.5c and d). In order to be able to compare the results, the points of full conversion were determined for the different reaction conditions and NCAs and listed in Table 2.3. For the example of BLG (DP = 100) the time to reach full conversion was 70 h at  $0\text{ }^{\circ}\text{C}$  irrespective of the pressure while it was much shorter for the higher temperature with 12 h at 1 bar and 5 hours and 20 minutes at  $1 \times 10^{-5}$  bar, respectively.

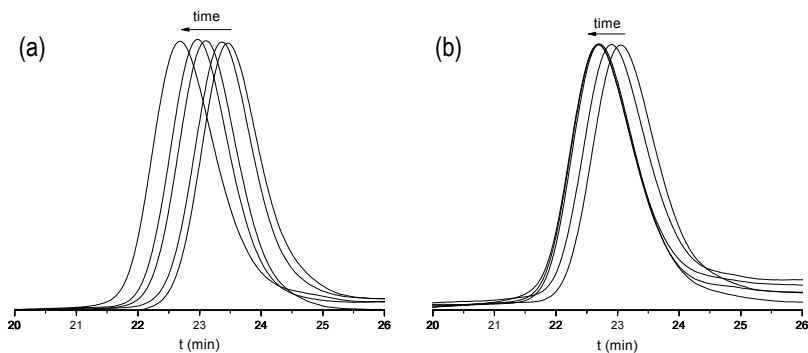


**Figure 2.4.** HFIP SEC measurements of PBLG DP: 100 (a) at 20 °C under N<sub>2</sub> flow and at 20 °C under high vacuum ( $1 \times 10^{-5}$  bar) (b).

Due to the good solubility of PBLG in DMF a polymerization to high molecular weight was attempted. When the initiator to monomer ratio was increased to 400, the time to reach full monomer conversion was considerably longer. In fact, the reaction at 0 °C did not even reach full conversion after 237 hours, while at 20 °C full conversion was obtained after about 31 h under nitrogen and 23 h under high vacuum (Table 2.3). Noticeable was high viscosity of the reaction medium at 0 °C which probably led to a physical retardation of the polymerization. Especially for the high vacuum polymerizations at 20 °C it was found that the polymerization solution was concentrated by 23% due to solvent evaporation, while for the polymerization at 0 °C it was only 2-3%. However, as stated above, due to the use of an internal standard in the FTIR calculations this had no influence on the determination of the monomer conversion. The obtained molecular weights were in the range with the expected molecular weights for this and all other polymerizations.

The results shown for the BLG NCA clearly confirm the positive effect of the high vacuum on the polymerization kinetics of this monomer. All other NCAs investigated can be divided into two groups, i.e. those where a similar effect was observed and those where the applying the high vacuum did not lead to an acceleration of the polymerization. Examples for the latter group are the NCAs of BLA, BLS and BLT. Compared to the polymerization of BLG NCA the monomer conversions of these NCAs were considerably slower under identical conditions and leveled off quickly (Figure 2.6). For BLA and BLS this can be mostly ascribed to the low solubility of the formed polypeptides as evident from precipitation or gelation observed during the polymerization. This is more evident at the lower polymerization temperature, where full conversion could not be reached for either of these NCAs. Furthermore, BLT is known for its slow polymerization kinetics and did require long reaction times to achieve full monomer conversion.<sup>41</sup> However, the polymer has an excellent solubility in many different solvents including DMF and the molecular weight increase was linear. For these three monomers, the difference between the high vacuum and nitrogen conditions was insignificant.

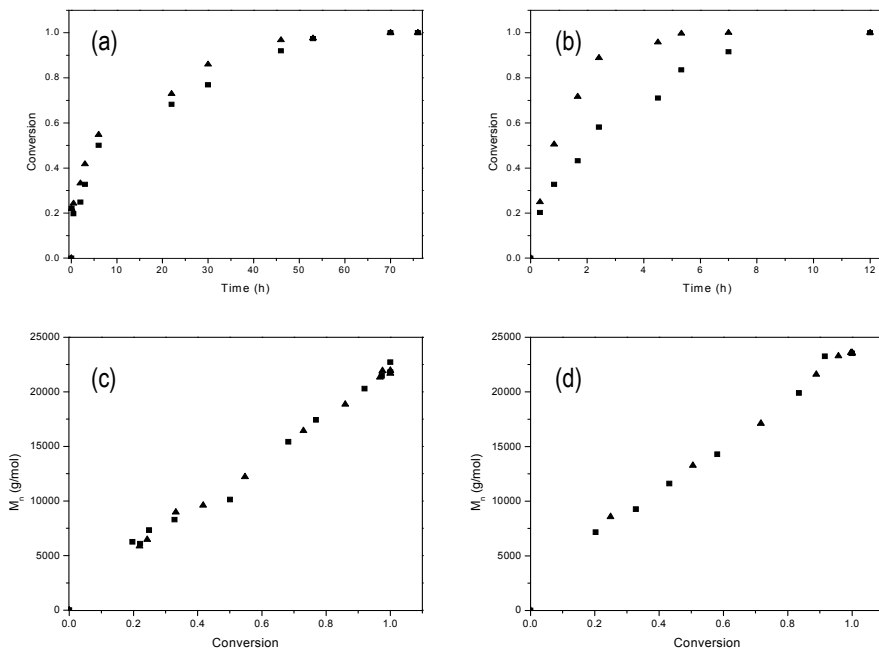


**Figure 2.5.** Polymerization of BLG NCA at a monomer of BLG NCA to initiator ratio of 100: (a) monomer conversion at 0 °C, (b) monomer conversion at 20 °C, (c)  $M_n$  vs conversion at 0 °C, (d)  $M_n$  vs conversion at 20 °C. (▲) reaction under high vacuum of  $1 \times 10^{-5}$  bar and (■) reaction under nitrogen at 1 bar.

In contrast, a clear effect of the vacuum was seen for the BLG NCA, as discussed above and for ZLL and Ala. Interestingly all these monomers have their rapid polymerization in common (Figure 2.6). A fast polymerization was observed for the Ala NCA, but due to precipitation during the polymerization the reaction resulted in a broad PDI of the polymer.

When seeking for an explanation of the different effect of the  $\text{CO}_2$  removal on the two groups of monomers, it is noticeable that the slow polymerizing monomers have a hydrogen bond accepting group next to the  $\beta$ -carbon of the NCA monomer ( $\gamma$ -carbon for  $\beta$ -benzyl-L-aspartate). It was already hypothesized for the slow propagation of L-threonine that the nucleophilicity of the corresponding amine group at the chain end could be lower, thereby lowering the propagation speed.<sup>41</sup> Intrachain hydrogen bonds between the Asp, Thr and Ser side group and the primary amine could decrease the nucleophilicity of the amine chain end.<sup>42</sup>

Another important influence on the polymerization kinetic might arise from the secondary structures of the polypeptides in the studied solvent. DMF is known to be an inefficient hydrogen bond breaking solvent for some of the polypeptide species (PBLG, PZLL).<sup>43</sup> Preliminary FTIR measurements of the polypeptides in DMF (and chloroform for comparison) did indicate that different secondary structures were present in the reaction medium. Although the solvent peaks are partly overlapping the amide



signals for  $\alpha$ -helices in the amide I bond regime,  $\beta$ -sheets as well as the  $\alpha$ -helices in the amide II bond regime could be assigned. For PBLG and PZLL the presence of  $\beta$ -sheets were found, while for PBLG, PBLA and PZLL  $\alpha$ -helices were identified. PBLT did not show to form a secondary structure. For PAla FTIR did not offer any conclusive result on the polypeptide structure in DMF due to precipitation, but it is expected to contain both  $\beta$ -sheets and  $\alpha$ -helices.<sup>44</sup> In general, the  $\alpha$ -helical forming polypeptides appear to have higher polymerization reactivity, but that cannot explain the slow polymerization speed of PBLA. However, at this point we cannot offer a conclusive explanation for these observations. Recently density functional theory (DFT) calculations were used for the determination of the NCA ring opening mechanism.<sup>45</sup> Possibly, DFT calculations could help to solve the reactivity problem found here.

**Table 2.3.** Results of conversion experiments of NCA ROP of different NCA monomers. BLG:  $\gamma$ -benzyl-L-glutamate, ZLL: N<sub>ε</sub>-benzyloxycarbonyl-L-lysine, Ala: L-alanine, BLA:  $\beta$ -benzyl-L-aspartate, BLS: O-benzyl-L-serine, BLT: O-benzyl-L-threonine. Conversion measured by FTIR and molecular weights measured by HFIP-SEC.

| Polymer | DP  | Conc (M) | Temp (°C) | $M_n$ (g/mol) | PDI  | Time (N <sub>2</sub> ) <sup>a</sup> | Time (HV) <sup>a</sup> |
|---------|-----|----------|-----------|---------------|------|-------------------------------------|------------------------|
| PBLG    | 40  | 0.38     | 0         | 8,900         | 1.08 | 30h                                 | 23h                    |
|         | 40  | 0.38     | 20        | 10,900        | 1.17 | 3h                                  | 2h 30m                 |
|         | 100 | 0.76     | 0         | 21,800        | 1.08 | 70h                                 | 70h                    |
|         | 100 | 0.76     | 20        | 23,500        | 1.16 | 12h                                 | 5h 20m                 |
|         | 400 | 0.76     | 0         | 78,800        | 1.14 | 237h (93%)                          | 237h (99%)             |
|         | 400 | 0.76     | 20        | 80,000        | 1.08 | 31h 15m                             | 23h 15m                |
| PZLL    | 40  | 0.38     | 0         | 10,700        | 1.12 | 47h 10m                             | 21h 40m                |
|         | 40  | 0.38     | 20        | 10,300        | 1.17 | 2h 36m                              | 1h 45m                 |
| PAla    | 40  | 0.38     | 0         | 5,700         | 1.69 | 32h                                 | 22h                    |
|         | 40  | 0.38     | 20        | 6,700         | 1.80 | 5h                                  | 3h 30m                 |
| PBLA    | 40  | 0.38     | 0         | 10,500        | 1.20 | 79.5h (97%)                         | 79.5h (93%)            |
|         | 40  | 0.38     | 20        | 11,900        | 1.09 | 30h 30m                             | 30h 30m                |
|         | 100 | 0.76     | 0         | 22,200        | 1.28 | 336h (88.6%)                        | 336h (91.7%)           |
|         | 100 | 0.76     | 20        | 16,600        | 1.17 | 54h                                 | 54h                    |
| PBLT    | 40  | 0.76     | 0         | 10,400        | 1.09 | 480h (80%)                          | 480h (80%)             |
|         | 40  | 0.76     | 20        | 11,000        | 1.11 | 192h (93%)                          | 192h (80%)             |
| PBLG    | 40  | 0.38     | 0         | 8,300         | 1.26 | 412h (93%)                          | 412h (90%)             |
|         | 40  | 0.38     | 20        | 7,500         | 1.23 | 76h (90%)                           | 76h (89%)              |

(a) Time to reach full conversion determined by FTIR. In cases where full conversion was not reached, the maximum conversion is mentioned in brackets.

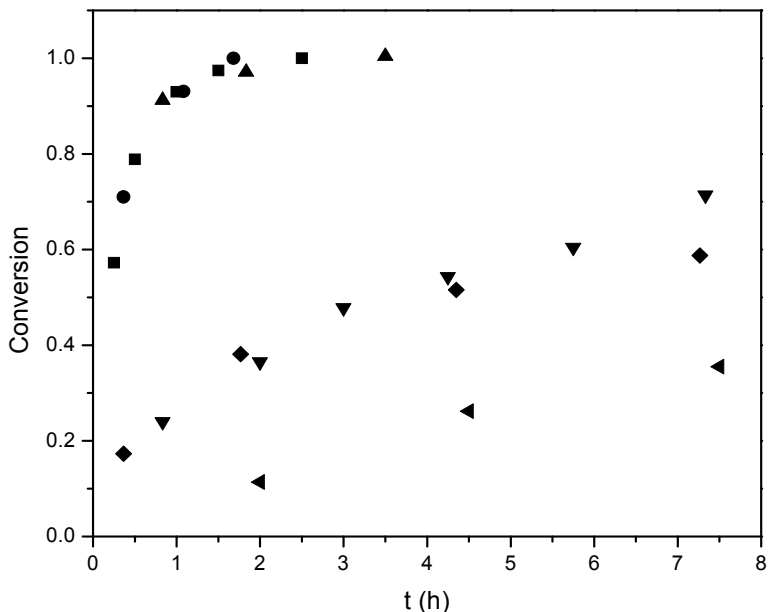


**Figure 2.6.** Conversion plots of BLG (■), Ala (▲), ZLL (●), BLA (▼), BLS (◆), BLT (◄) (0.76 M) for a monomer to initiator ratio of 40 at 20 °C and  $1 \times 10^{-5}$  bar.

### 2.3.4 Polypeptide structure analysis: temperature & pressure

In the study on the effect of temperature the occurrence of side reaction in the polymerization of various NCAs was investigated by MALDI-ToF-MS analysis after a standard reaction time of 4 days. It was found that there is an increase in these side and termination reactions when the polymerization temperature is increased to 20 °C, while at 0 °C almost no side reactions were observed. Here we expand this investigation to a structure analysis of samples taken during polymerization and after full conversion has been reached. This provides important information as to when a reaction has to be stopped at a given reaction temperature to avoid termination reactions or other unwanted structural changes on the polymer. A series of MALDI-ToF-MS spectra were recorded of samples taken at different times after full monomer conversion of the NCA polymerization mixtures listed in Table 2.3 with a targeted DP of 40 at 20 °C. It should be noted that quantification of MALDI-ToF-MS spectra is not possible and the obtained data were thus compared only qualitatively. The samples were taken directly after full monomer conversion was reached and subsequently after several hours and days. Figure 2.7 depicts the example of the BLG NCA polymerization. Besides the expected peaks of the PBLG with amino end-groups (A), the peak series of PBLG with pyroglutamate (B) end-groups can be identified. This reaction is caused by the intramolecular amidation of the amino end-group with the adjacent benzyl ester side chain of the PBLG and terminates the chain growth. While this reaction is totally

absent at 0 °C even after four days, from Figure 2.7 it can be seen that the formation of the pyroglutamate at 20 °C increased over time but only after all monomer was consumed. A first detectable signal for the pyroglutamate end-group was apparent three hours after full monomer conversion was reached (six hours reaction time). No difference was observed between the reactions with the nitrogen flow and the high vacuum technique. This suggests that this termination reaction is absent as long as monomer is present and that the polymerization of BLG NCA is well-controlled at 20 °C. Lowering the reaction temperature only provides an advantage if the polymer is to be stored in the reaction medium for a longer period of time or if monomer conversion is not carefully monitored.

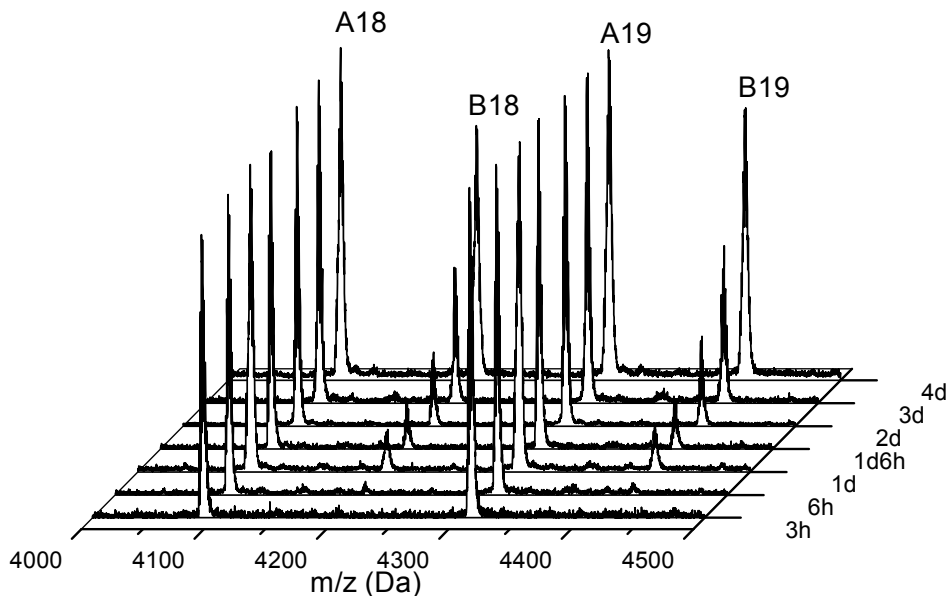


**Figure 2.7.** MALDI-ToF-MS spectra of samples taken from the polymerization reaction of BLG NCA at 20 °C under nitrogen at different storage times after complete monomer conversion. The spectra were normalized using peak A. The corresponding structures can be found in Figure 2.2.

For PZLL no side reaction products were found with the exception of a small amount of cyclic structures under both conditions at 20 °C, while these structures were absent at 0 °C. PAla showed no side reactions at all over time.<sup>26</sup> Both polymerizations appear to remain controlled for a longer period of time. For the other investigated NCA polymerizations such as the BLA, BLS and the BLT more side reactions were found directly after full conversion at 20 °C. As already demonstrated earlier, the formation of succinimides is a side reaction that occurs in the case of PBLA. Figure 2.8 shows that the formation of succinimides (peak D) begins directly after full conversion is obtained irrespective of the pressure applied in the polymerization. However, the formation of formamide terminated amine group due to the reaction with the solvent DMF seems to be slightly lower under high vacuum conditions, while under

both conditions it increased over time. For BLS the formation of the cyclic structures was found. This was not influenced by the reaction conditions suggesting that it occurred during the polymerization. The side reactions identified in the BLT NCA polymerization include cyclics formation, water- and dimethylamine-initiated polymers as well as formamide terminated chains. Compared to the 0 °C degree reaction under a nitrogen atmosphere there were significantly more side products at 20 °C. For PBLA, PBLS and PBLT the results suggest that to overcome the multiple side reactions the polymerizations should preferably be performed at 0 °C.

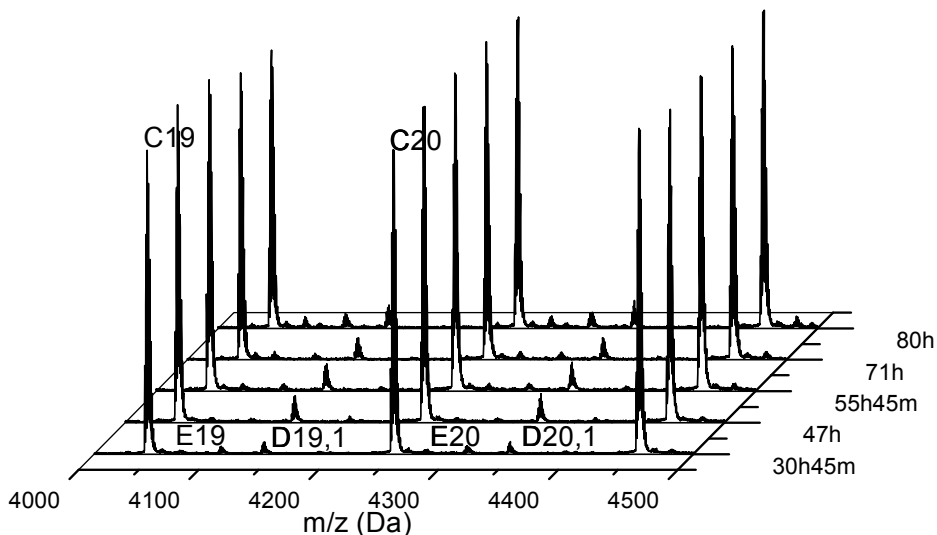


**Figure 2.8.** MALDI-ToF-MS spectra of samples taken from the polymerization reaction of BLA NCA at 20 °C and 0.01 mbar at different reaction times. The spectra were normalized using peak C.

For the different NCAs examined in this investigation the polymerization characteristics of the reaction kinetics and structural control have been determined. When taking both factors into account, recommendations on the preferred polymerization conditions can be given and these are summarized in Table 2.4. For example, BLG NCA can be best polymerized under high vacuum at 20 °C since those conditions allow a fast polymerization and a short reaction time. However, if further extension of the PBLG block is desired and monomer conversion is not monitored, polymerization at 0 °C is advantageous as it prevents end group termination. Also ZLL and Ala NCA polymerization work the best at 20 °C under high vacuum. Generally, the reaction at 0 °C should be used if termination reactions occur more frequently like in BLA, BLS and BLT. For these NCAs the vacuum did not increase the polymerization kinetics and can thus be omitted. It should be noted that reaction control is

also drastically affected by the precipitation or formation of secondary structures during the polymerization.

**Table 2.4.** Recommended NCA polymerization reaction conditions in DMF based on the analysis of monomer conversion and structural control (derived from MALDI-ToF-MS spectra). The reaction conditions are qualitatively valued in terms of reaction speed and structural control. Keys: ++ = high, + = good, - = moderate, -- = low, HV = high vacuum.

| Monomer | 0°C, N <sub>2</sub> |       | 0°C, HV |       | 20°C, N <sub>2</sub> |       | 20°C, HV |       | Remarks:   |
|---------|---------------------|-------|---------|-------|----------------------|-------|----------|-------|--|
|         | Control             | Speed | Control | Speed | Control              | Speed | Control  | Speed |  |
| BLG     | ++                  | --    | ++      | -     | +                    | +     | +        | ++    | Limited time and DP for 20°C.<br>Viscous for higher DPs at both temperatures |
| ZLL     | ++                  | --    | ++      | -     | +                    | +     | +        | ++    | Minor formation of cyclics   |
| Ala     | ++                  | -     | ++      | -     | +                    | +     | +        | ++    | Precipitation for both temperatures  |
| BLA     | ++                  | -     | ++      | -     | --                   | +     | --       | +     | Precipitation for both temperatures  |
| BLS     | ++                  | -     | ++      | -     | --                   | +     | --       | +     | Precipitation for both temperatures  |
| BLT     | ++                  | --    | ++      | --    | --                   | -     | --       | -     | Extremely slow   |

## 2.4 Conclusions

The polymerization by the NAM mechanism of several NCA monomers were studied to determine the best reaction conditions of temperature, pressure in DMF. First, we investigated the polymerization of various amino acid NCAs at 0 °C. Detailed MALDI-ToF-MS analysis clearly confirms the positive effect of the lower reaction temperature on the frequency of end-group termination and side-reactions for all tested NCA monomers. When the effects of the reaction pressure were studied NCAs can be divided into two groups: In the first group monomers of BLG, ZLL and Ala polymerized considerably faster when a lower pressure of  $1 \times 10^{-5}$  bar was applied. MALDI-ToF-MS analysis confirmed that the formation of side products for these monomers continues after full monomer conversion is achieved. This was particularly prominent for the pyroglutamate formation in PBLG. The second group of monomers, i.e. BLA, BLS and BLT polymerized considerably slower than the first group and no effect of the lower pressure was observed. On the other hand, the number of side reactions was significant at 20 °C, so that the polymerizations for the latter monomers should preferably be done at 0 °C. Temperature and pressure can thus be used to balance polymerization kinetics and structural control in NCA polymerizations. However, monomer conversion is an important parameter in the reaction control. The combination of the parameters temperature and pressure proved to be useful for a more efficient controlled ring opening polymerization of NCAs.

## References

- <sup>1</sup> H.R. Kricheldorf, *Angew. Chem. Int. ed.* **2006**, 45, 572-5784
- <sup>2</sup> E.P. Holowka, V.Z. Sun, D.T. Kamei and T.J. Deming, *Nature Mat.* **2007**, 6, 52-57.
- <sup>3</sup> J. Rodriguez-Hernandez and S. Lecommandoux, *J. Am. Chem. Soc.* **2005** 127, 2026-2027.
- <sup>4</sup> H. Iatrou, H. Frielinghaus, S. Hanski, N. Ferderigos, J. Ruokolainen, O. Ikkala, D. Richter, J. Mays and N. Hadjichristidis, *Biomacromolecules* **2007**, 8, 2173-2181.
- <sup>5</sup> E.P. Holowka, D.J. Pochan and T.J. Deming, *J. Am. Chem. Soc.* **2005**, 127, 12423-12428.
- <sup>6</sup> A. Sulistio, A. Widjaya, A. Blencowe, X. Zhang and G. Qiao, *Polym. Prepr. (Am. Chem. Soc., Div. Polym. Chem.)* **2010**, 51, 121-122
- <sup>7</sup> T.J. Deming, *Prog. Polym. Sci.* **2007**, 32, 858-875.
- <sup>8</sup> A.P. Nowak, V. Breedveld, L. Pakstis, B. Ozbas, D.J. Pine, D. Pochan and T.J. Deming, *Nature* **2002**, 417, 424-428
- <sup>9</sup> M.I. Gibson and N. Cameron, *Angew. Chem. Int. Ed.* **2008**, 47, 5160–5162
- <sup>10</sup> H.-A. Klok, *Macromolecules* **2009**, 42, 7990-8000
- <sup>11</sup> H.-A. Klok, S. Lecommandoux, *Adv. Polym. Sci.* **2006**, 202, 75-111
- <sup>12</sup> R.J.I. Knoop, G.J.M. Habraken, N. Gogibus, S. Steig, H. Menzel, C.E. Koning, A. Heise, *J. Polym. Sci. A: Polym. Chem.* **2008**, 46, 3068-3077
- <sup>13</sup> H. Schlaad, *Adv. Polym. Sci.* **2006**, 202, 53-73
- <sup>14</sup> S. Steig, F. Cornelius, P. Witte, C.E. Koning, A. Heise and H. Menzel, *Chem. Commun.* **2005**, 43, 5420-5422
- <sup>15</sup> F. Audouin, R.J.I. Knoop, J. Huang, A. Heise, *J. Polym. Sci. Part A: Polym. Chem.* **2010**, 48, 6402
- <sup>16</sup> N.M.B. Smeets, P.L.J. van der Weide, J. Meuldijk, J.A.J.M. Vekemans, L.A. Hulshof, *Org. Process Res. Dev.* **2005**, 9, 757-763
- <sup>17</sup> F. Corneille, J.-L. Copier, J.-P. Senet and Y. Robin, EP 1201659, **2002**
- <sup>18</sup> W. Vayaboury, O. Giani, H. Collet, A. Commeyras and F. Schu e, *Amino Acids* **2004**, 27, 161-167
- <sup>19</sup> Y. Fujita, K. Koga, H.-K. Kim, X.-S. Wang, A. Sudo, H. Nishida and T. Endo, *J. Polym. Sci. Part A: Polym. Chem.* **2007**, 45, 5365-5370
- <sup>20</sup> T.J. Deming, *Adv. Polym. Sci.* **2006**, 202, 1-18
- <sup>21</sup> H.R. Kricheldorf, *Angew. Chem. Int. ed.* **2006**, 45, 572-5784
- <sup>22</sup> N. Hadjichristidis, H. Iatrou, M. Pitskalis and G. Sakellariou, *Chem. Rev.* **2009**, 109, 5528-5578
- <sup>23</sup> H.R. Kricheldorf,  *$\alpha$ -Aminoacid-N-Carboxyanhydrides and Related Heterocycles*, **1987**, Berlin, Springer-Verlag
- <sup>24</sup> H.R. Kricheldorf, C. von Lossow, G. Schwarz, *Macromolecules* **2005**, 38, 5513-5518
- <sup>25</sup> H.R. Kricheldorf, C. von Lossow and G. Schwarz, *Macromol. Chem. Phys.* **2005**, 206, 282-290
- <sup>26</sup> H.R. Kricheldorf, C. von Lossow and G. Schwarz, *Macromol. Chem. Phys.* **2004**, 205, 918-924
- <sup>27</sup> T.J. Deming, *Nature* **1997**, 390, 386-389
- <sup>28</sup> H. Lu and J. J. Cheng, *J. Am. Chem. Soc.* **2007**, 129, 14114-14115
- <sup>29</sup> I. Dimitrov and H. Schlaad, *Chem. Commun.* **2003**, 2944-2945
- <sup>30</sup> J. Muzart, *Tetrahedron* **2009**, 65, 8313-8323
- <sup>31</sup> T. Aliferis, H. Iatrou and N. Hadjichristidis, *Biomacromolecules* **2004**, 5, 1653-1656
- <sup>32</sup> D.L. Pickel, N. Politakos, A. Avgeropoulos and J.M. Messman, *Macromolecules* **2009**, 42, 7781-7788
- <sup>33</sup> W. Vayaboury, O. Giani, H. Cottet, A. Deratani and F. Schu e, *Macromol. Rapid Commun.* **2004**, 25, 1221–1224
- <sup>34</sup> W. Vayaboury, O. Giani, H. Cottet, S. Bonaric and F. Schu e, *Macromol. Chem. Phys.* **2008**, 209, 1628–1637

- <sup>37</sup> J. Rodríguez-Hernandez and H.-A. Klok, *J. Polym. Sci. Part A: Polym. Chem.* **2003**, 41, 1167-1187
- <sup>38</sup> M. Wilchek, S. Ariely and A. Patchornik, *J. Org. Chem.* **1968**, 33, 1258-1259
- <sup>39</sup> J. Johnes, In *Amino acid and peptide synthesis*. **1992**, Oxford, Oxford University Press.
- <sup>40</sup> V. Saudak, H. Pivcová and J. Drobník, *Biopolymers* **1981**, 20, 1615-1623
- <sup>41</sup> M.I. Gibson and N.R. Cameron, *J. Polym. Sci. Part A: Polym. Chem.* **2009**, 47, 2882-2891
- <sup>42</sup> B. Brulc, E. Žagar, M. Gadzinowski, S. Stomkowski and M. Žigon, *Macromol. Chem. Phys.* **2011**, 212, 550-562
- <sup>43</sup> A. Teramoto and H. Fujita, *Adv. Polym. Sci.* **1975**, 18, 68-147.
- <sup>44</sup> H.R. Kricheldorf, M. Mutter, F. Maser, D. Müller and H. Förster, *Biopolymers* **1983**, 22, 1357-1372
- <sup>45</sup> J. Ling and Y. Huang, *Macromol. Chem. Phys.* **2010**, 211, 1708-1711

# Chapter 3

## Random Copolypeptides, Graft Copolypeptides and Block Copolypeptides by NCA ROP

### Abstract

*In the previous Chapter a study was performed on the livingness of N-carboxyanhydride ring opening polymerization (NCA ROP). The goal of this chapter is to study the synthesis of polymer architectures prepared with the use of living NCA ROP methods, such as copolymers, graft copolymers and (multi) block copolymers using the previously studied methods. Copolypeptides of several NCA monomers were synthesized. MALDI-ToF-MS contour plot analysis confirmed the randomness of the copolypeptides. Graft copolypeptides were obtained by grafting of  $\gamma$ -benzyl-L-glutamate NCA monomers from lysine-containing copolypeptides. The controlled character of the NCA polymerization performed at low temperature and low pressure was further confirmed by the successful block copolypeptides synthesis from polypeptide macroinitiators, which confirms the availability of the amino end-groups for chain extension. The formation of gels from the graft and corresponding block copolypeptides was investigated. While for the block copolypeptides interconnected polypeptide particles were observed by optical microscopy, the graft copolypeptides form an open cell structure.*

This chapter is partially based on G.J.M. Habraken, M. Peeters, C.H.J.T. Dietz C.E. Koning and A. Heise, *Polym. Chem.* **2010**, 1, 514-524 and G.J.M. Habraken, C.H.R.M. Wilsens, C.E. Koning and A. Heise, *Polym. Chem.* Accepted



### 3.1 Introduction

The versatility of controlled and living polymerizations allows the synthesis of challenging polymer architectures, such as copolymers, (multi) block copolymers, star, grafted and branched polymers. Examples can be found in the field of controlled radical polymerization and anionic polymerizations.<sup>1,2</sup> The introduction of the living N-carboxyanhydride ring opening polymerization (NCA ROP) techniques enabled the access to more advanced polymer structures. Specifically the synthesis of well-defined block copolypeptides was improved.<sup>3,4</sup> As a continuation of the investigation of the controlled living NCA ROP techniques based on the normal amine mechanism (NAM), as mentioned in Chapter 2, these methods will be tested for the generation of other polymer architectures: random, grafted and block copolypeptides.

Copolypeptides prepared by NCA ROP have been prepared mostly without the use of specific beneficial living ring opening techniques, such as the lower temperature and high vacuum approaches.<sup>5,6</sup> The synthesis of the copolypeptides is straightforward by using two species of NCA monomers in the reaction. Similar to other copolymers the reaction products have combined properties of the two homopolymers, such as hydrophilicity and hydrophobicity. Copolypeptides can also possess other particular features, such as the secondary peptide structure. An example is the combination of hydrophobic and hydrophilic amino acid monomers both with a preference to form a  $\alpha$ -helical structure, such as L-glutamic acid and L-leucine or lysine and L-alanine, resulting in altered pH dependency of the helix to coil transition.<sup>7,8</sup> Combinations of specific amino acids have been selected for biological applications, such as drug therapy, antibacterial coatings and biomineralization.<sup>9-11</sup> A functional copolypeptide was prepared with the structure poly(N-2-hydroxyethyl-L-glutamate-co-3,4-dihydroxyphenyl-L-alanine) (P(HEGlu-co-DOPA)).<sup>12</sup> The rare amino acid residue DOPA can cross-link upon oxidation and is associated to the advanced adhesion properties of mussel peptides.<sup>13</sup> Other combinations have recently been found in the hydrophobic blocks of PLys-*b*-PLeu where the leucine was copolymerized with DOPA. In the vesicle structure of PLys-*b*-P(Leu-co-DOPA) this results in a cross-linked vesicle.<sup>14</sup>

Star, graft and branched copolypeptides have been prepared by different methods involving NCA ROP. For methods using the NAM mechanism a precursor (initiator or polypeptide) with multiple amine groups is required. Multi-amine initiators were used for the preparation of star polypeptides with 3, 4, 6, 8 or 64 arms.<sup>15-18</sup> Examples of a dendritic-graft and a branched copolypeptide prepared by living NCA ROP were performed with the use of lysine NCA monomers with different protecting groups and selective deprotection strategies.<sup>19,20</sup> Grafted copolypeptides have been prepared by the addition of amino acids on the side groups of poly(L-lysine) or from poly((2-aminoethyl)-L-glutamate).<sup>21,22</sup>

For block copolypeptide synthesis the livingness of the polymerization is of great importance. All used

methods are targeted to avoid chain end termination.<sup>6,23-26</sup> Most of the living NCA ROP polymerization techniques have been used for the synthesis of block copolypeptides. This is of specific relevance since polypeptide block copolymers show interesting self-assembly behavior and were applied in responsive and biomedical materials.<sup>27-34</sup> Both of the NAM-based techniques have been used for the synthesis of block copolypeptides, although with a limited variety of NCA monomers.<sup>6,26</sup> The maximum number of block additions published for both techniques was one, resulting in a diblock, triblock or even a hybrid pentablock copolymer if a diamine (macro)initiator was used.<sup>35,36</sup> For the silazane method not many examples are reported, except for PBLG-*b*-PZLL in the initial publication.<sup>24</sup> However, it was shown to be successful for the synthesis of the novel core cross-linked PZLL-*b*-P(L-cystine) structure.<sup>37</sup> The most frequently applied NCA ROP technique for the synthesis of block copolypeptides is the nickel-mediated ROP (Table 1.1). Many different combinations of NCA monomers have been reported. Also the highest number of five individual polypeptide blocks was reported for the pentablock copolypeptide PZLL-*b*-PLeu-*b*-PZLL-*b*-PLeu-*b*-PZLL.<sup>38</sup> Most combinations that are mentioned start with PZLL or PBLG and are followed by a less soluble polypeptide species, such as leucine, alanine or phenylalanine (Table 1.1). When considering all the potential applications of (multi)block copolypeptides, the optimization of the metal-free controlled/living NAM methods are highly promising as it represents a less elaborate synthetic approach to obtain block copolypeptides.

In this chapter the synthesis of different polymer architectures by NCA ROP is performed by living NCA ROP using NAM. First the random copolymerization of different NCA monomers is described. The copolypeptide composition is determined by known methods as well as with MALDI-ToF-MS. Subsequently, graft copolypeptides are prepared from a copolypeptide of L-lysine and  $\gamma$ -benzyl-L-glutamate followed by NCA ROP from the pendant primary amines of the L-lysine residues. Finally, the living NCA ring opening polymerization techniques as discussed in Chapter 2 were used for the synthesis of block copolypeptides.

## 3.2 Experimental

### Materials

Benzylamine 99.5% purified by redistillation, DMAc, *S-tert*-butylmercapto-L-cysteine, *S*-benzyl-L-cysteine, L-alanine, piperidine,  $\alpha$ -pinene 98% and bis(trichloromethyl) carbonate (triphosgene) 99% were purchased from Aldrich. L-Glutamic acid,  $\gamma$ -benzyl ester, L-aspartic acid,  $\beta$ -benzyl ester, *O*-benzyl-L-serine,  $N_{\epsilon}$ -benzyloxycarbonyl-L-lysine,  $N_{\epsilon}$ -9-fluorenylmethoxycarbonyl-L-lysine and  $N_{\delta}$ -trityl-L-glutamine were supplied by Bachem. DMF (extra dry), chloroform, ethylacetate, *n*-heptane, and diethylether were purchased from Biosolve. All chemicals were used without any purification unless mentioned. DMF and ethylacetate were used directly from the bottle or stored under an inert, dry atmosphere. NCA monomers were prepared according to procedures described in Chapter 2.

## Characterization

1,1,1,3,3,3-Hexafluoroisopropanol size exclusion chromatography (HFIP SEC) was performed on a system equipped with a Waters 1515 Isocratic HPLC pump, a Waters 2414 refractive index detector (40 °C), a Waters 2707 autosampler, a PSS PFG guard column followed by 2 PFG-linear-XL (7 µm, 8\*300 mm) columns in series at 40°C. HFIP (Apollo Scientific Limited) with potassium trifluoro acetate (3 g/L) was used as eluent at a flow rate of 0.8 mL min<sup>-1</sup>. The molecular weights were calculated against polymethyl methacrylate standards (Polymer Laboratories,  $M_p = 580$  Da up to  $M_p = 7.1 \times 10^6$  Da).

N,N-dimethylformamide size exclusion chromatography (DMF SEC) was measured on a Waters Alliance system equipped with a Waters 2695 separation module, a Waters 2414 refractive index detector (40 °C), a Waters 2996 photo diode array detector, a PSS GRAM guard column followed by 2 PSS GRAM columns in series of 100 Å (10 µm particles) and 3000 Å (10 µm particles) respectively at 60 °C. DMF was used as an eluent at a flow rate of 1 mL min<sup>-1</sup>. The molecular weights were calculated against polystyrene standards (Polymer Laboratories,  $M_p = 580$  Da up to  $M_p = 7.1 \times 10^6$  Da). Before SEC analysis was performed, the samples were filtered through a 0.2 µm PTFE filter (13mm, PP housing, Alltech).

N,N-dimethylacetamide size exclusion chromatography (DMAc SEC) was measured on a Waters Alliance system equipped with a Waters 2695 separation module, a Waters 2414 refractive index detector (40 °C), a Waters 2996 photo diode array detector, a PSS GRAM guard column followed by 2 PSS GRAM columns in series of 100 Å (10 µm particles) and 3000 Å (10 µm particles) respectively at 60 °C. DMAc was used as an eluent at a flow rate of 1 mL min<sup>-1</sup>. The molecular weights were calculated against polystyrene standards (Polymer Laboratories,  $M_p = 580$  Da up to  $M_p = 7.1 \times 10^6$  Da). Before SEC analysis was performed, the samples were filtered through a 0.2 µm PTFE filter (13mm, PP housing, Alltech).

FTIR measurements were performed on a PerkinElmer SpectrumOne FTIR Spectrometer, using a universal ATR sampling accessory (resolution 1 cm<sup>-1</sup>). Samples for the monomer conversion were taken from the reaction mixtures and analyzed without any further modification.

<sup>1</sup>H-NMR analyses were performed on a 400 MHz Mercury 400. For most of the polypeptides deuterated TFA were used. DMSO-d<sub>6</sub> was used for Fmoc-L-Lys containing copolymers.

Matrix Assisted Laser Desorption / Ionization - Time of Flight - Mass Spectroscopy analysis was carried out on a Voyager DE-STR from Applied Biosystems (laser frequency 20 Hz, 337 nm and a voltage of 25 kV). The matrix material used was DCTB (40 mg/ml). Potassium trifluoroacetic acid (KTFA) was added as cationic ionization agent (5 mg/ml). The sample was dissolved in HFIP (1 mg/ml), to which the matrix material and the ionization agent were added (5:1:5), and the mixture was placed on the target plate. Samples were precipitated from the reaction medium in diethylether, filtered and placed in a freezer before measuring.

Samples for microscopy were prepared by dissolving the polypeptides (1.0 mg) in 0.1 g TFA and subsequently in 10 ml CHCl<sub>3</sub>. The solution was brought on a glass plate or grid and dried under an

argon flow. The solvent was finally removed by vacuum and the sample was sputtered for 3 minutes. Dark field optical microscopy was done with a Zeiss axioplan 2 using an LD epiplan 50x objective.

### Synthesis

**Random NCA copolymerizations.** The NCA monomers of  $\gamma$ -benzyl-L-glutamate (1.437 g, 5.46 mmol) and O-benzyl-L-serine (1.21 g, 5.46 mmol) were dissolved in 20 ml DMF in a Schlenk tube. The solution was stirred at 0 °C until all NCA monomer was completely dissolved. To this a solution of benzylamine (29.5 mg, 0.272 mmol) in 5 ml DMF was added. The reaction was left to stir in a cold water bath of 0 °C for 4 days under a dry nitrogen atmosphere. The solution was precipitated in diethylether, the polypeptide was filtered and dried in vacuo. Yield: 1.70 g, 77.4 wt%.

**Selective deprotection of P(BLG-co-FmocLLys).** The copolypeptide P(BLG-co-FmocLLys) (1.69 g, 0.197 mmol) was dissolved in 15 ml DMF. To this 4 ml of piperidine was added. The solution was stirred for 2 hours at room temperature. After precipitating twice and filtration the polypeptide was dried in a vacuum oven at room temperature. Yield: 1.03 g, 60.9 wt%.

**NCA ROP for grafted copolymerizations.** The selectively deprotected copolypeptide P(BLG-co-Lys) (0.201 g, 27.9  $\mu$ mol) was dissolved in 10 ml DMF. Once the polypeptide was completely dissolved the NCA of  $\gamma$ -benzyl-L-glutamate (0.96 g, 3.65 mmol) was added. The reaction was left to stir in a cold water bath of 0 °C for 4 days under a dry nitrogen atmosphere. After precipitation the sample was dried in a vacuum oven. Yield: 0.54 g, 54 wt%.

**NCA ROP for block copolymerizations one-pot reaction.** The NCA monomer of  $\gamma$ -benzyl-L-glutamate (0.994 g, 3.78 mmol) was dissolved in 9 ml DMF in a Schlenk tube. To this a solution of benzylamine (20.9 mg, 0.193 mmol) in 1 ml DMF was added. The reaction was left to stir in a cold water bath of 0 °C for 4 days under a dry nitrogen atmosphere. After 4 days the second NCA monomer, O-benzyl-L-serine (0.830 g, 3.75 mmol), and 10 ml DMF were added. The solution was precipitated after another 4 days in diethylether, the polypeptide was filtered and dried in vacuo. Yield: 1.24 g, 81.9 wt%.

**NCA ROP tetrablock copolymerization of PBLG<sub>80</sub>-b-PAIa<sub>25</sub>-b-PZLL<sub>80</sub>-b-PBLA<sub>40</sub>.** NCA of  $\gamma$ -benzyl-L-glutamate (1.00 g, 3.80 mmol) was dissolved in 4.0 g DMF in a 40 ml Schlenk tube. Benzylamine (5.06 mg, 4.72  $\times 10^{-2}$  mmol) in 1.00 g DMF was added quickly with a syringe. The polymerization was performed at 20 °C under high vacuum of 1  $\times 10^{-5}$  bar for 3 hours. Of the solution 16.7 wt% was removed and precipitated in water. The NCA of L-alanine (113 mg, 9.81  $\times 10^{-1}$  mmol) was dissolved in 2.92 g DMF and added to the solution with the PBLG macroinitiator. The reaction was maintained for 1 hour at 20 °C and under 1  $\times 10^{-5}$  bar. Of the solution 7.6 wt% was removed for precipitation. The NCA of

N<sub>ε</sub>-benzyloxycarbonyl-L-lysine (0.89 g, 2.91 mmol) in 2.10 g DMF was added. The reaction was maintained for 3 hours at 20 °C and under 1x 10<sup>-5</sup> bar. Of the solution 9.1 wt% was removed. The NCA of β-benzyl-L-aspartate (0.333 g, 1.36 mmol) in 1.7 g DMF was added. The Schlenk tube was placed in a cooled waterbath at 0 °C under a nitrogen flow for 7 days. Finally, the polypeptide was precipitated in water. After each polymerization step a sample was taken and measured by IR to determine the conversion and subsequently precipitated and analyzed by SEC.

### 3.3 Results and discussion

#### 3.3.1 Copolymerization

In order to investigate the applicability of the low temperature synthesis for copolymerizations, γ-benzyl-L-glutamate (BLG) was copolymerized with several NCAs. Both comonomers were dissolved in DMF at 0 °C, followed by the addition of a solution of DMF containing benzylamine. After a reaction time of four days the polymer solutions were precipitated in diethylether and the obtained polypeptide investigated by SEC and MALDI-ToF-MS. Initially the effect of the monomer feed composition on the molecular weights and final composition of the copolypeptide was examined for O-benzyl-L-serine (BLS) and BLG. Three experiments were carried out with comonomer ratios of 1:3, 1:1 and 3:1 (Table 3.1, entries 1-3). A precipitation was observed for the polymerization with higher BLS quantities (entries 2 and 3). The obtained molecular weights were comparable for all three reactions (8,300 – 11,000 g/mol), but a bimodal distribution was obtained for the partially precipitated samples. This also resulted in a higher PDI of >1.2 as compared to the 1.08 of the homogeneous reaction (entry 1). All other reactions were homogeneous and produced polypeptides with PDIs of around 1.2. For the N<sub>ε</sub>-trityl-L-glutamine and γ-benzyl-L-glutamate copolypeptide a lower than expected molecular weight was found, which was also observed for the N<sub>ε</sub>-trityl-L-glutamine homopolypeptide (Table 2.2). This might possibly be due to the bulkiness of the trityl-side group.

The MALDI-ToF-MS analysis of the copolypeptides was in agreement with the results obtained for the homopolypeptides (Chapter 2). For copolymerizations performed at 0 °C no side reaction products were found by MALDI-ToF-MS with the exception of the BLS copolymerization. As in the homopolymerization an increasing relative amount of cycles was seen with increasing amount of BLS in the monomer feed.

A first indication of the monomer composition in the copolypeptides was obtained from <sup>1</sup>H-NMR (Table 3.1). Generally, good agreement was found between the monomer feed ratios and the compositions determined by <sup>1</sup>H-NMR. However, this method provides only information on the overall composition of the copolypeptide, but not on the monomer distribution along the polypeptide chain. While NCA copolymerizations have been reported before, copolymerization parameters of these reactions are not wide spread and mostly determined under different reaction conditions.<sup>7,39-41</sup> We were able to apply a software based MALDI-ToF-MS deconvolution method developed in our group, which allows converting

the spectra into composition contour plots.<sup>42-44</sup> The shape of the contour plot allows to draw conclusions concerning the molecular distribution of the comonomers in the chain, i.e. whether it is a random or a block structure. For example, for the contour plot of copolypeptide 1 (Table 3.1) a single distribution was found to exhibit a maximum for 25 BLG and 7 BLS units (Figure 3.1a). This is characteristic for a random copolymer and in agreement with the monomer feed ratio. From the directional coefficient of the contour plot of copolypeptide 2 (Figure 3.1b) a random copolymerization with a monomer composition of 1:1 can be concluded, again in agreement with the feed ratio. Similarly, the contour plot of copolypeptide 3 confirms the random structure with the expected comonomer composition (Figure 3.1c). It has to be noted, that due to the mass discrimination in the MALDI-ToF-MS spectra the bimodal character of the distribution is increased and the composition of the maxima cannot directly be determined from the contour plots.<sup>44</sup>

**Table 3.1.** NCA copolymerization of with various monomers (M1: monomer 1; M2: monomer 2) 0 °C in DMF (4 days). All samples measured by HFIP-SEC, calibrated with PMMA standards.

| Entry | M1                        | M2  | Feed ratio | $M_n$<br>(g/mol) | PDI  | Composition ( <sup>1</sup> H-NMR) |
|-------|---------------------------|-----|------------|------------------|------|-----------------------------------|
| 1     | BLS                       | BLG | 10:30      | 10,300           | 1.08 | 1.0 : 3.6                         |
| 2     | BLS                       | BLG | 20:20      | 11,000           | 1.24 | 1.0 : 1.0                         |
| 3     | BLS                       | BLG | 30:10      | 8,300            | 1.27 | 2.0 : 1.0                         |
| 4     | Ala                       | BLG | 20:20      | 8,600            | 1.10 | 1.0: 1.0                          |
| 5     | Fmoc-L-Lys <sup>(a)</sup> | BLG | 10:41      | 8,600            | 1.18 | 1.0 : 3.5                         |
| 6     | Fmoc-L-Lys <sup>(a)</sup> | BLG | 9:37       | 7,800            | 1.11 | 1.0 : 2.6                         |
| 7     | Fmoc-L-Lys                | BLG | 20:59      | 12,700           | 1.23 | 1.0 : 2.3                         |
| 8     | Gln(Trt)                  | BLG | 19:18      | 3,500            | 1.20 | 1.0 : 1.2                         |

(a) Measured by DMF-SEC with PS standards.

A similar contour plot was constructed from a MALDI-ToF spectrum of P(BLG-co-Ala) (entry 4, Table 3.1) with a targeted composition of 20:20. The SEC of this copolypeptide showed a Gaussian distribution with a low polydispersity and no side-reactions were detected in the MALDI-ToF-MS. As for the P(BLG-co-BLS) (entry 2, Table 3.1) the contour plot confirms that the composition is in the range of the weighed-in 50:50 ratio with a random monomer distribution. The results provide evidence that the copolymerization at 0 °C results in random copolypeptide with comonomer ratios close to the monomer feed ratios.

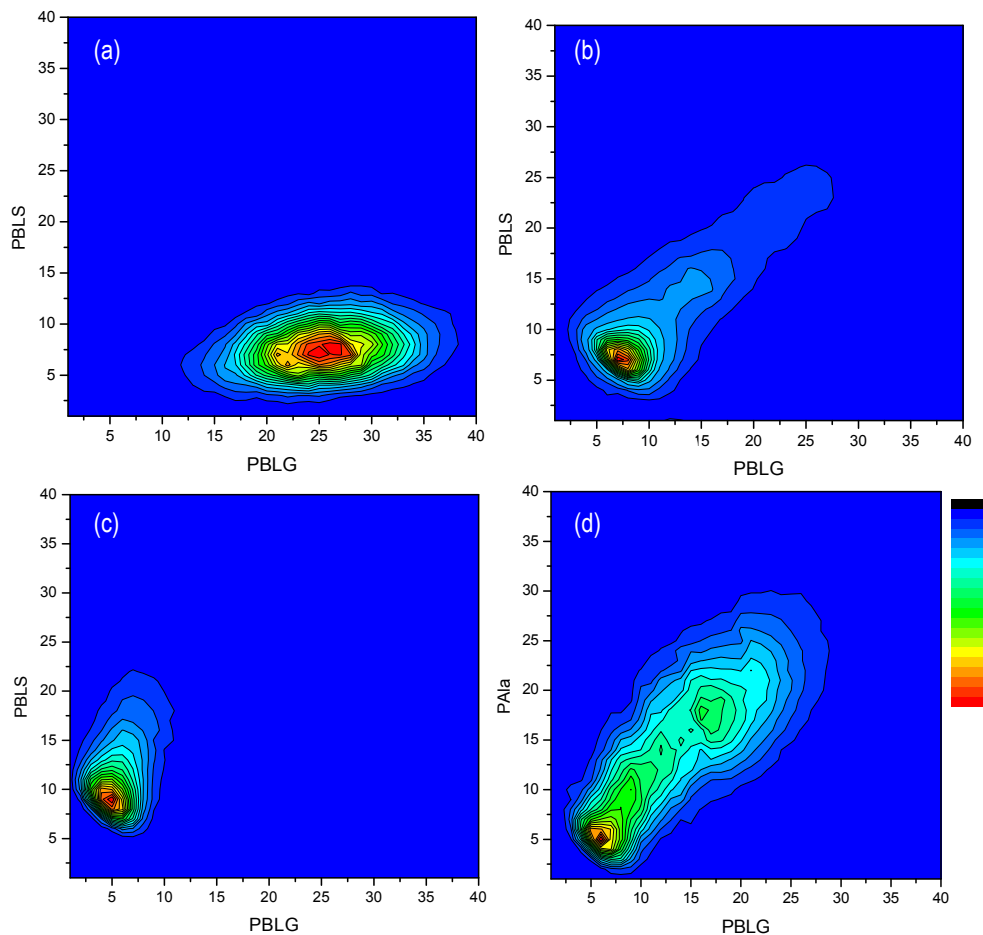
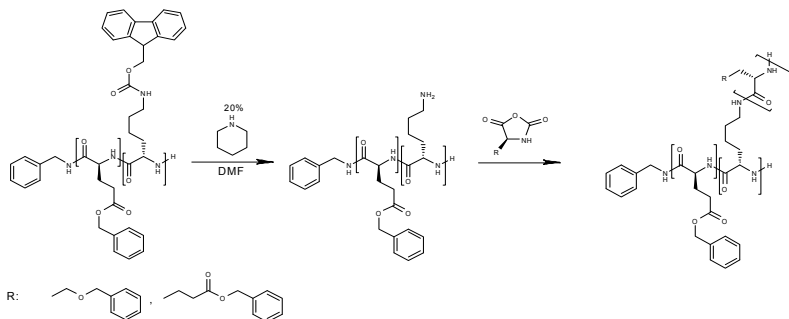


**Figure 3.1.** MALDI-ToF-MS contour plots of P(BLS-co-BLG) for monomer feed ratios 10:30 (a), 20:20 (b) and 30:10 (c) (Table 3.1, entries 1-3) and P(BLG-co-Ala) (d) (Table 3.1, entry 4).

### 3.3.2 Graft copolymerization

For the manufacturing of graft copolypeptides the copolypeptides of  $\gamma$ -benzyl-L-glutamate and  $N_\epsilon$ -Fmoc-L-lysine (Table 3.1, entry 5) were selectively deprotected, resulting in a backbone of PBLG and L-lysine with functional amines present as pendant groups for further polymerization (Scheme 3.1).<sup>45,46</sup> Approximately 200 mg of deprotected copolypeptide was dissolved in DMF and different amounts of BLG and BLS NCA were added. Figure 3.2 shows the clear increase in molecular weight, corresponding to the ratio of NCA to the PBLG : L-Lys (Table 3.2). The PDI of the graft copolypeptides increases to 1.6-1.9, which suggests a somewhat higher PDI of the grafted blocks. This increase in the PDI can be caused by the different number of initiating amine groups in the chain due to the random character of the polypeptide. Moreover, SEC traces reveal a peak at lower molecular weight which is

believed to be caused by a secondary initiation mechanism. Indeed MALDI-ToF-MS confirms that homopolypeptide PBLG is present in these samples. Whether this is caused by impurities in the reaction mixture or by initiation of the activated monomer mechanism from the sterically hindered amines present along the grafted main chain cannot be concluded from the obtained data.



**Scheme 3.1.** Polymerization and deprotection reactions for grafted NCA-prepared polypeptide.

**Table 3.2.** Molecular weights of graft copolypeptides obtained from P(BLG-co-Lys). All samples entry 1-3 measured by DMF-SEC calibrated with PS, entry 4 measured by HFIP-SEC calibrated with PMMA.

| Entry | Grafted NCA | Target DP of graft | $M_n$ (g/mol) | PDI  |
|-------|-------------|--------------------|---------------|------|
| 1(a)  | BLG         | 10                 | 14,000        | 1.64 |
| 2(a)  | BLG         | 20                 | 20,200        | 1.66 |
| 3(a)  | BLG         | 40                 | 30,300        | 1.92 |
| 4(b)  | BLS         | 15                 | 21,400        | 1.51 |

(a) obtained from deprotected P(BLG-co-FmocLLys) entry 5 Table 3.1. (b) obtained from deprotected P(BLG-co-FmocLLys) entry 6, Table 3.1.

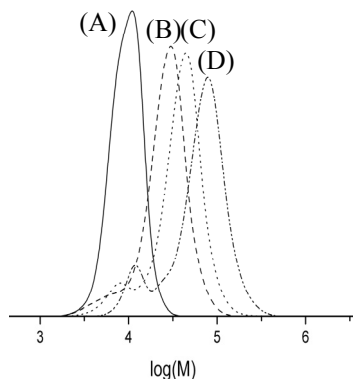


**Figure 3.2.** SEC traces of (A) P(BLG-co-FmocLLys), (B) P(BLG<sub>40</sub>-co-(Lys<sub>10</sub>-g-PBLG<sub>10</sub>)), (C) P(BLG<sub>40</sub>-co-(Lys<sub>10</sub>-g-PBLG<sub>20</sub>)) and (D) P(BLG<sub>40</sub>-co-(Lys<sub>10</sub>-g-PBLG<sub>40</sub>)) measured by DMF-SEC calibrated with polystyrene standards. Subscript numbers denote the targeted degree of polymerization.



### 3.3.3 Block copolymerization

Block copolymer synthesis by sequential monomer addition (macroinitiation) is ideally suited to investigate the degree of control of a polymerization. A successful macroinitiation is dependent on the presence of active chain ends on the polymer after the first polymerization and on an efficient initiation step. Any deactivation of chain ends or inefficient macroinitiation will inevitably result in unreacted macroinitiator and thus in homopolymer residues. Our results so far confirmed that the NCA polymerization at 0 °C fulfils the first requirement, i.e. polypeptides with active amino end-groups are obtained (Chapter 2).

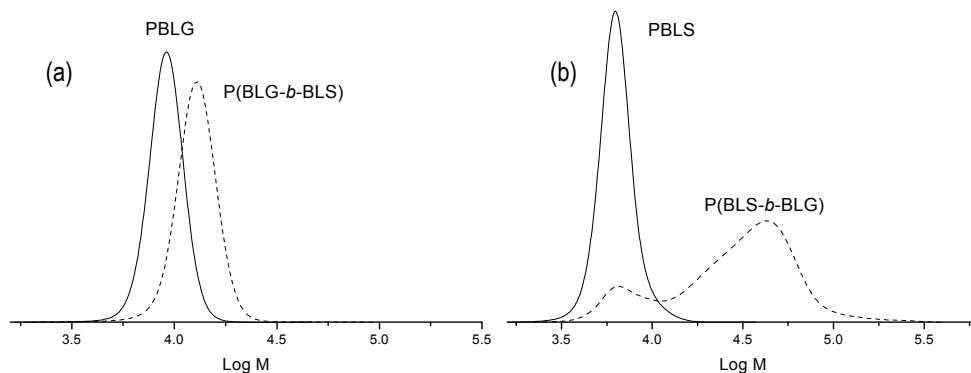


**Figure 3.3.** SEC (HFIP) results of P(BLS-*b*-BLG) synthesis by sequential monomer addition. (a) Addition of BLG NCA to a PBLG macroinitiator (entry 1, Table 3.3) and (b) addition of BLS NCA to a PBLG macroinitiator (entry 2, Table 3.3).

A first attempt was made for the synthesis of P(BLS-*b*-BLG) from a well-defined isolated PBLG macroinitiator of 6,100 g/mol (Table 3.3, entry 1). The synthesis of the blocks was performed by adding the NCA of  $\gamma$ -benzyl-L-glutamate to the solution of the first block for 4 days.<sup>26</sup> As can be seen from the SEC plot in Figure 3.3a, a block copolypeptide with a broad distribution (PDI = 1.89) and a significant amount of unreacted macroinitiator was obtained. PBLG is a strong  $\beta$ -sheet forming polypeptide and the reaction solvent DMF does not disrupt the hydrogen bonds to make all PBLG chain ends equally available for macroinitiation. Since PBLG is much better soluble in DMF, inverting the order of monomer addition was expected to improve the results. Indeed when BLG was polymerized first, followed by the addition of the NCA of BLS without isolation and purification of the first block, a complete shift from the macroinitiator to the block copolypeptide was observed in SEC (Figure 3.3b). The molecular weight increased from 6,400 g/mol for the PBLG macroinitiator to 9,700 g/mol for the block copolypeptide with a PDI of 1.06 (Table 3.3, entry 4). Moreover, by changing the monomer ratios PBLG-*b*-PBLG block copolypeptides with various block length ratios and low polydispersities were successfully synthesized (Table 3.3, entries 2-6) even when a gelation effect was seen upon the polymerization for approximately 10 wt% monomer in DMF for most entries. This seems to be

contradictive with the low PDI, but the gelation occurs only after 2 to 3 days when a considerable amount of the second block is already formed. With a uniform gelation all polymerizations are quenched, due to a lack of mobility.

The MALDI-ToF-MS contour plot of the block copolypeptides clearly differ from the corresponding contour plots of the random copolypeptides in that there is no directional coefficient (Figure 3.4a). The circular distribution with a clear maximum, as seen for the example of P(BLG-*b*-Ala) in Figure 3.4a, is typical for block copolymers. The block structure was only evident from  $^{13}\text{C}$ -NMR for P(BLG-*b*-Ala).<sup>47,48</sup> The contour plot of P(BLG-*b*-BLS) shows two different maxima at the monomer composition of 15/15 and 17/17, respectively. This might indicate that there was still a small amount the first monomer present at the time of the addition of the second monomer, which might give rise to some copolymerization in the second block. This could be due to the gelation in the reaction mixture, which was seen at the end of the first polymerization.

The block copolypeptide synthesis by addition of different cysteine NCAs to the PBLG macroinitiator was successful when a low degree of polymerization was targeted for the cysteine block. For higher degrees of polymerization the polydispersities increased for the *S*-*tert*-butylmercapto-L-cysteine a bimodal distribution was visible.

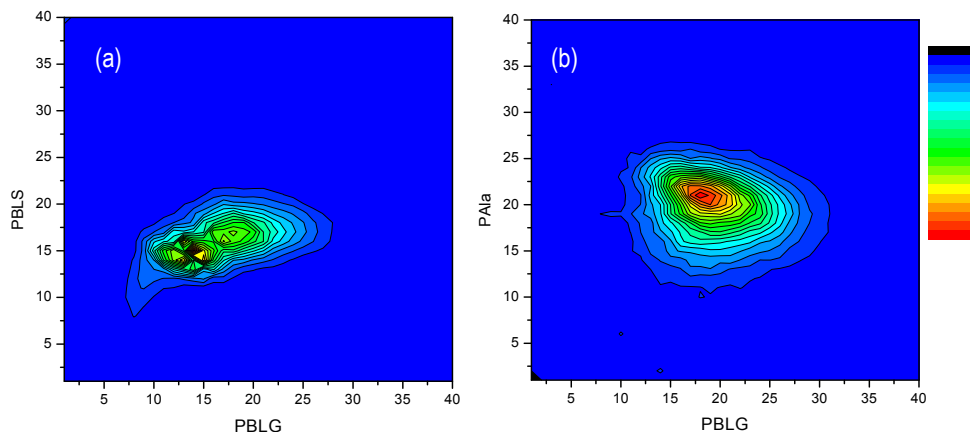


**Figure 3.4.** (a) Contour plot of MALDI-ToF-MS spectrum of P(BLG-*b*-BLS) (entry 4, Table 3.3) (b) Contour plot of MALDI-ToF-MS spectrum of P(BLG-*b*-Ala) (entry 9, Table 3.3).

**Table 3.3.** Synthesized block copolypeptides by NCA ROP at 0 °C. All samples measured by HFIP-SEC calibrated by PMMA standards. Subscript numbers indicate the degrees of polymerization.

| Entry | Block 1                           | Block 2              | Block 1          |      | Block 2          |      |
|-------|-----------------------------------|----------------------|------------------|------|------------------|------|
|       |                                   |                      | $M_n$<br>(g/mol) | PDI  | $M_n$<br>(g/mol) | PDI  |
| 1     | PBLS <sub>12</sub> <sup>(a)</sup> | PBLG <sub>24</sub>   | 6,100            | 1.06 | 19,800           | 1.89 |
| 2     | PBLG <sub>39</sub>                | PBLS <sub>15</sub>   | 8,900            | 1.04 | 12,400           | 1.06 |
| 3     | PBLG <sub>42</sub>                | PBLS <sub>33</sub>   | 9,000            | 1.04 | 13,900           | 1.07 |
| 4     | PBLG <sub>20</sub>                | PBLS <sub>20</sub>   | 6,400            | 1.06 | 9,700            | 1.06 |
| 5     | PBLG <sub>20</sub>                | PBLS <sub>40</sub>   | 5,500            | 1.07 | 11,000           | 1.09 |
| 6     | PBLG <sub>40</sub>                | PBLS <sub>20</sub>   | 9,200            | 1.07 | 14,700           | 1.10 |
| 7     | PBLG <sub>44</sub>                | PBLC <sub>16</sub>   | 8,800            | 1.08 | 12,800           | 1.08 |
| 8     | PBLG <sub>40</sub>                | PfBMLC <sub>15</sub> | 8,100            | 1.10 | 11,700           | 1.15 |
| 9     | PBLG <sub>41</sub>                | PfBMLC <sub>41</sub> | 16,000           | 1.09 | 21,300           | 1.44 |
| 10    | PBLG <sub>20</sub>                | PAla <sub>20</sub>   | 6,300            | 1.05 | 7,500            | 1.05 |

(a) prepared from precipitated macroinitiator

The information obtained from the homopolymerizations in Chapter 2 was used for the improved synthesis of block copolypeptides. The 0 °C method did increase the livingness, by decreasing the number of side reactions, but also increased the reaction time to obtain full conversion. In Chapter 2 it was shown that the livingness for the polymerization of certain NCA monomers (BLG, ZLL and Ala) was maintained over the time needed for a NCA ROP at 20 °C under high vacuum ( $1 \times 10^{-5}$  bar). A novelty for the block copolypeptide synthesis is the combination of the investigated techniques according to Table 2.4.

The optimized polymerization conditions obtained from the homo polymerizations were validated by performing the synthesis of a tetrablock copolypeptide PBLG<sub>80</sub>-*b*-PAla<sub>25</sub>-*b*-PZLL<sub>80</sub>-*b*-PBLa<sub>40</sub> (Table 3.4). The monomer conversion was followed by FTIR spectroscopy and individual NCA monomers were added to the polymerization solution consecutively when full conversion was reached of the previous NCA monomer without intermediate work-up. The polymerization was started with the synthesis of the well soluble PBLG block at 20 °C under high vacuum. After three hours, full monomer conversion was reached and for a sample withdrawn from the reaction solution the  $M_n$  of the PBLG block was determined to be 15,700 g/mol with a PDI of 1.06 (Entry 1A, Table 3.4). Ala NCA was then directly added to the polymerization solution and the reaction continued for 90 min at 20 °C under high vacuum. For the Ala block the number of repeating units was kept low (25) to maintain the solubility of the block copolypeptide for the subsequent monomer addition of the ZLL NCA. Consequently, only a small increase of the molecular weight to 18,400 g/mol (PDI: 1.07) was obtained (entry 1B, Table 3.4). From Figure 3.5 it can be seen that a full shift of the SEC trace to higher molecular weight was achieved of

the PBLG macroinitiator to the diblock copolypeptide. Without further work-up ZLL NCA was added to the reaction and polymerized at 20 °C under high vacuum for 3.5 hours. A larger block of 80 monomer units was aimed at in order to obtain a significant increase in the molecular weight. Indeed, the SEC trace of the triblock copolypeptide shows a corresponding significant shift to higher molecular weight as compared to the diblock copolypeptide macroinitiator. The trace remains narrow (PDI 1.14) and a total molecular weight of 34,700 g/mol was determined (Entry 1C, Table 3.4). However, the trace also reveals the presence of a small amount of remaining macroinitiator, suggesting a non-quantitative initiation. This might be attributed to steric hindrance in the macroinitiation process. Finally, a PBLA block was polymerized at 0 °C over a much longer time scale of 168 h due to increasingly lowered concentration of the initiating amine end group with every monomer addition and lower reaction temperature. The reaction for the last block did not reach full conversion. The entire procedure yielded the final tetrablock copolypeptide with a total  $M_n$  of 36,400 g/mol and a PDI of 1.33 (Entry 1D, Table 3.4). Other samples showed that tri- and tetrablock copolypeptides with similar combinations were attempted using the same conditions for the blocks of 1A to 1D. With less L-alanine a better peak shift was seen for the polymerizations. Still the polydispersity index of the final material was relatively high due to some lower molecular weight left of terminated material. Although this approach pushes the limits of block copolypeptide synthesis by NCA polymerization and the applied reaction conditions resulted in a fast and very controlled synthesis.

**Table 3.4.** Block copolymerizations of NCA applying the conditions outlined in Table 2.4

| Entry | Polymer   | Conditions                          | RT<br>(h) | $M_n^{(a)}$<br>(g/mol) | $M_w^{(a)}$<br>(g/mol) | PDI <sup>(a)</sup> |
|-------|---|-------------------------------------|-----------|------------------------|------------------------|--------------------|
| 1A    | PBLG <sub>80</sub>  | 20 °C, HV                           | 3         | 15,700                 | 16,600                 | 1.06               |
| 1B    | PBLG <sub>80</sub> - <i>b</i> -PAla <sub>25</sub>   | 20 °C, HV                           | 1.5       | 18,400                 | 19,700                 | 1.07               |
| 1C    | PBLG <sub>80</sub> - <i>b</i> -PAla <sub>25</sub> - <i>b</i> -PZLL <sub>80</sub>                                      | 20 °C, HV                           | 3.5       | 34,700                 | 41,900                 | 1.14               |
| 1D    | PBLG <sub>80</sub> - <i>b</i> -PAla <sub>25</sub> - <i>b</i> -PZLL <sub>80</sub> - <i>b</i> -<br>PBLA <sub>40</sub>   | 0 °C, N <sub>2</sub>                | 168       | 36,400                 | 47,300                 | 1.30               |
| 2     | PBLG <sub>100</sub> - <i>b</i> -PZLL <sub>100</sub> - <i>b</i> -PAla <sub>20</sub>                                    | 20 °C, HV                           | 72        | 47,100                 | 54,400                 | 1.15               |
| 3     | PBLG <sub>50</sub> - <i>b</i> -PAla <sub>15</sub> - <i>b</i> -PZLL <sub>50</sub> - <i>b</i> -<br>PBLA <sub>40</sub>   | 20 °C, HV / 0 °C,<br>N <sub>2</sub> | 96        | 30,700                 | 36,400                 | 1.19               |
| 4     | PBLG <sub>100</sub> - <i>b</i> -PAla <sub>15</sub> - <i>b</i> -PZLL <sub>100</sub> - <i>b</i> -<br>PBLA <sub>40</sub> | 20 °C, HV / 0 °C,<br>N <sub>2</sub> | 168       | 47,500                 | 51,100                 | 1.31               |

(a) DMAc SEC calibrated with polystyrene standards. (b) Reactions conditions for entries 2 to 4 were similar as described for the blocks 1A to 1D. RT: Reaction time.

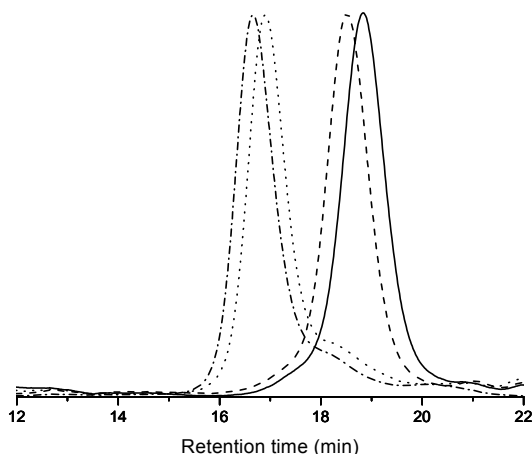


**Figure 3.5.** DMAC-SEC results of PBLG<sub>80</sub>-*b*-PAla<sub>25</sub>-*b*-PZLL<sub>80</sub>-*b*-PBLA<sub>40</sub> tetrablock copolymerization. Traces represent the sequentially extended block copolymers from from right to left (entries 1A to 1D in Table 3.4).

### 3.3.4 Polypeptide organogels

Block and graft copolypeptides of PBLG and PBLS form gels at concentrations of around 10 wt% in DMF. As reported earlier for similar block copolypeptides this is due to an  $\alpha$ -helix and  $\beta$ -sheet formation in the solvent. FTIR results confirmed the presence of the orientation of the peptide bonds in organogel in chloroform with 4 wt% of PBLG-*b*-PBLS solids (Figure 3.6). The spectra show the peak around 1652  $\text{cm}^{-1}$  for the  $\alpha$ -helix of a PBLG homopolypeptide. The PBLS homopolypeptide shows the peaks characteristic for antiparallel  $\beta$ -sheets at 1670-1675 and 1630  $\text{cm}^{-1}$ . The measured block and graft copolypeptides all display a mixture of these supramolecular structures. Depending on the block length and overall composition of the block copolypeptide the  $\alpha$ -helix or  $\beta$ -sheets is more prominent. This is illustrated by the difference between PBLG<sub>40</sub>-*b*-PBLS<sub>20</sub> (Entry 6, Table 3.3) and PBLG<sub>20</sub>-*b*-PBLS<sub>40</sub> (Entry 5, Table 3.3). To compare the self-assembly structures of the block and grafted copolypeptides, a solution of < 0.1 mg/ml of the polypeptides in chloroform containing 1 vol% TFA was placed on a glass slide. TFA was added to disrupt the hydrogen bonds between the polypeptide chains of the otherwise insoluble material. Dark field optical microscopy did show a difference between the obtained structures (Figure 3.7). For the block copolypeptides (Table 3.3, entry 4 and 6) two types of structures were found, namely a flat layer and a dense three-dimensional structure. During the evaporation of the solvent a gel formed in the concentrated regime, caused by the hydrogen bonding between the O-benzyl-L-serine blocks. For the corresponding graft copolypeptide of  $\gamma$ -benzyl-L-glutamate and L-lysine, P(BLG-*co*-(Lys-*g*-PBLS)) (Table 3.2, entry 4), on the other hand, completely different structures were obtained. The polypeptides resemble a three-dimensional open structure of interconnected fibers on the glass slide (Figure 3.7).

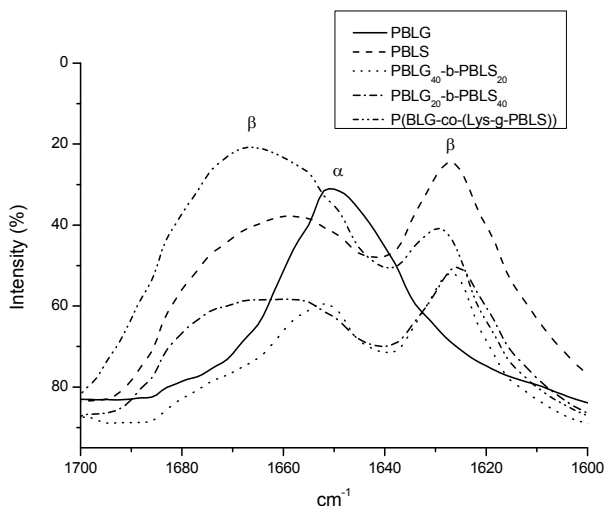


**Figure 3.6.** FTIR of PBLG-*b*-PBLS organogels in chloroform for PBLG<sub>40</sub>-*b*-PBLS<sub>20</sub> 9 wt% (entry 6, Table 3.3), PBLG<sub>20</sub>-*b*-PBLS<sub>40</sub> 4 wt% (entry 5, Table 3.3) and P(BLG-*co*-(Lys-*g*-PBLS)) 6 wt% in DMF (entry 4, Table 3.2)

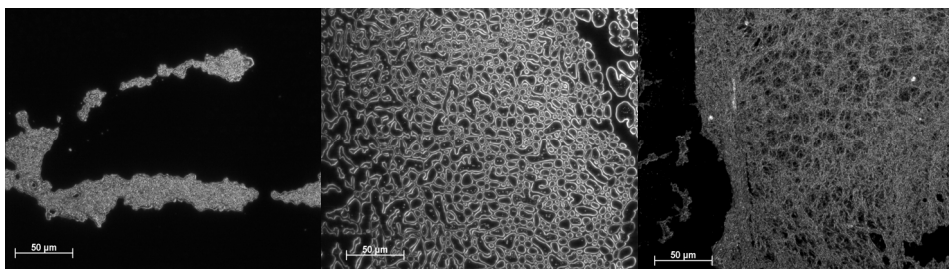


**Figure 3.7.** Optical microscopy pictures of dried organogels, from left to right: P(BLG-*b*-BLS) (entry 4, Table 3.3), P(BLG-*b*-BLS) (entry 6, Table 3.3), P(BLG-*co*-(Lys-*g*-PBLS)) (entry 4, Table 3.2).

### 3.4 Conclusions

We have investigated the successful use of NCA ROP at 0 °C for the synthesis of random copolypeptides. MALDI-ToF-MS was used to confirm the copolypeptide compositions. Moreover, graft copolypeptides were obtained by NCA grafting from well-defined lysine containing copolypeptides. The information obtained in Chapter 2 was applied for the synthesis of block copolypeptides. Block copolypeptides with low polydispersities were prepared with the low temperature method. The additional use of the high vacuum technique was shown for the synthesis of tetrablock copolypeptides comprising PBLG, PAla, PZLL and PBLA blocks. For this tetrablock different reaction conditions were combined to result in low polydispersities and high structural control. The combination of the parameters temperature and pressure proved to be useful for a more efficient controlled ring opening polymerization of NCAs. Finally the organogelation of PBLG PBLS block and graft copolypeptides was

investigated. It was shown that the organogelation was a result of the secondary structures of the separate blocks.

The presented results confirm that NCA ROP at 0 °C is a simple and feasible method to obtain a variety of well-defined copolypeptides as well as more complex polypeptide architectures. The use of the NCA ROP at 20 °C at  $1 \times 10^{-5}$  bar showed the advantage of enabling a quick block copolypeptide synthesis for a selection of NCA monomers.

## References

- <sup>1</sup> W.A. Braunecker and K. Matyjaszewski, *Prog. Polym. Sci.* **2007**, 32, 93–146
- <sup>2</sup> N. Hadjichristidis, H. Iatroua, M. Pitsikalisa and J. Mays, *Prog. Polym. Sci.* **2006**, 31, 1068–1132
- <sup>3</sup> H.R. Kricheldorf, *Angew. Chem. Int. ed.* **2006**, 45, 572-5784
- <sup>4</sup> N. Hadjichristidis, H. Iatrou, M. Pitskalis and G. Sakellariou, *Chem. Rev.* **2009**, 109, 5528-5578
- <sup>5</sup> W. Vayaboury, O. Giani, H. Cottet, A. Deratani and F. Schué, *Macromol. Rapid Commun.*, **2004**, 25, 1221–1224
- <sup>6</sup> T. Aliferis,; H. Iatrou and N. Hadjichristidis, *Biomacromolecules* **2004**, 5, 1653-1656
- <sup>7</sup> R.E. Nylund and W.G. Miller, *J. Am. Chem. Soc.* **1965**, 87, 3537-3542
- <sup>8</sup> H. Sugiyajia and H. Soda, *Biopolymers* **1970**, 9, 459-469
- <sup>9</sup> S. Hayashi, K. Ohkawa and H. Yamamoto, *Macromol. Biosci.* **2006**, 6, 228–240
- <sup>10</sup> M.B. Bornstein, A.I. Miller, D. Teitelbaum, R. Arnon and M. Sela, *Ann. Neurol.* **1982**, 11, 317–319
- <sup>11</sup> C. Zhou, X. Qi, Peng Li, W.N. Chen, L. Mouad, M.W. Chang, S. Su Jan Leong and M.B. Chan-Park, *Biomacromolecules* **2010**, 11, 60–67
- <sup>12</sup> T.H. Anderson, J. Yu, A. Estrada, M.U. Hammer, J.H. Waite and J.N. Israelachvili, *Adv. Funct. Mater.* **2010**, 20, 4196-4205
- <sup>13</sup> M. Yu and T.J. Deming, *Macromolecules* **1998**, 31, 4739-4745
- <sup>14</sup> E.P. Holowka and T.J. Deming, *Macromol. Biosci.* **2010**, 10, 496–502
- <sup>15</sup> T. Aliferis, H. Iatrou, N.Hadjichristidis, J. Messman and J. Mays, *Macromol. Symp.* **2006**, 240, 12-17
- <sup>16</sup> H.-A. Klok, J.R. Hernandez, S. Becker and K. Müllen, *J. Polym. Sci. Part A: Polym. Chem.* **2001**, 39, 1572-1583
- <sup>17</sup> K. Inoue, S. Horibe, M. Fukae, T. Muraki, E. Ihara and H. Kayama, *Macromol. Biosci.* **2003**, 3, 26-33
- <sup>18</sup> D. Appelhans, H. Komber, R. Kirchner, J. Seidel, C.-F. Huang, D. Voigt, D. Kuckling, F.-C. Chang and B. Voit, *Macromol. Rapid Commun.* **2005**, 26, 586-591
- <sup>19</sup> H.-A. Klok and J. Rodriguez-Hernández, *Macromolecules* **2002**, 35, 8718-8723
- <sup>20</sup> J. Rodriguez-Hernandez, M. Gatti and H.-A. Klok, *Biomacromolecules* **2003**, 4, 249-258
- <sup>21</sup> G. Mezö, J. Reményi, J. Kajtár, K. Barna, D. Gaál and F. Hudecz, *J. Controlled Release* **2000**, 63, 81-95.
- <sup>22</sup> C. Cai, W. Zhu, T. Chen, J. Lin and X. Tian, *J. Polym. Sci. Part. A: Polym. Chem.* **2009**, 47, 5967–5978
- <sup>23</sup> T.J. Deming, *Nature* **1997**, 390, 386-389
- <sup>24</sup> H. Lu and J.J. Cheng, *J. Am. Chem. Soc.* **2007**, 129, 14114-14115
- <sup>25</sup> I. Dimitrov and H. Schlaad, *Chem. Commun.* **2003**, 2944-2945
- <sup>26</sup> W. Vayaboury, O. Giani, H. Cottet, S. Bonaric and F. Schué, *Macromol. Chem. Phys.* **2008**, 209, 1628–1637
- <sup>27</sup> V. Breedveld, A.P. Povak, J. Sato, T.J. Deming, and D.J. Pine, *Macromolecules* **2004**, 37, 3943-3953
- <sup>28</sup> E.P. Holowka, D.J. Pochan and T.J. Deming, *J. Am. Chem. Soc.* **2005**, 127, 12423-12428
- <sup>29</sup> M.I. Gibson and N. Cameron, *Angew. Chem. Int. Ed.* **2008**, 47, 5160-5162
- <sup>30</sup> J.Rodriguez-Hernandez and S.Lecommandoux, *J. Am. Chem. Soc.* **2005**, 127, 2026-2027
- <sup>31</sup> J. Sun, X. Chen, C. Deng, H. Yu, Z. Xie and X. Jing, *Langmuir* **2007**, 23, 8308-8315
- <sup>32</sup> E.P. Holowka, V.Z. Sun, D.T. Kamei and T.J. Deming, *Nature Mat.* **2007**, 6, 52-57
- <sup>33</sup> V.Z. Sun, Z. Li, T.J. Deming and D.T. Kamei, *Biomacromolecules*, **2011**, 12, 10-13
- <sup>34</sup> C.-Y. Yang, B. Song, Y. Ao, A.P. Nowak, R.B. Abelowitz, R.A. Korsak, L.A. Havton, T.J. Deming and M.V. Sofroniew, *Biomaterials* **2009**, 30, 2881–2898
- <sup>35</sup> A. Karatzas, H. Iatrou, N. Hadjichristidis, K. Inoue, K. Sugiyama, and A. Hirao, *Biomacromolecules* **2008**, 9, 2072-2080



- <sup>36</sup> H. Iatrou, H. Frielinghaus, S. Hanski, N. Ferderigos, J. Ruokolainen, O. Ikkala, D. Richter, J. Mays, and N. Hadjichristidis, *Biomacromolecules* **2007**, 8, 2173-2181
- <sup>37</sup> A. Sulistio, A. Widjaya, A. Blencowe, X. Zhang and G. Qiao, *Polym. Prepr. (Am. Chem. Soc., Div. Polym. Chem.)* **2010**, 51, 121-122
- <sup>38</sup> Z. Li and T.J. Deming, *Soft Matter* **2010**, 6, 2546–2551
- <sup>39</sup> M. Atreyi, M.V.R. Rao and S. Kumar, *Biopolymers* **1983**, 22, 747-753
- <sup>40</sup> K. Ishiwari, T. Hayashi and A. Nakajima; *Bull. Inst. Chem. Res., Kyoto Univ.* **1977**, 55, 366-375
- <sup>41</sup> A. Wamsley, J. Bhaskara, P. Phiasivongsa and X. Li, *J. Polym. Sci. Part A: Polym. Chem.* **2004**, 42, 317-325
- <sup>42</sup> R.X.E. Willemsse, B.B.P. Staal, E.H.D. Donkers and A.M. Herk, *Macromolecules* **2004**, 37, 5717-5723
- <sup>43</sup> R.X.E. Willemsse and A.M. Herk, *J. Am. Chem. Soc.* **2006**, 128, 4471-4480
- <sup>44</sup> S. Huijser, In *Synthesis and characterization of biodegradable polyesters: polymerization mechanisms and polymer microstructures revealed by MALDI-ToF-MS.* **2009**, thesis Technische Universiteit Eindhoven
- <sup>45</sup> J. Rodriguez-Hernandez, M. Gatti and H.-A. Klok, *Biomacromolecules* **2003**, 4, 249-258
- <sup>46</sup> G. Mezö, J. Reményi, J. Kajtár, K. Barna, D. Gaál and F. Hudecz, *J. Controlled Release* **2000**, 63, 81-95
- <sup>47</sup> H.R. Kricheldorf and G. Schillig, *Makromol. Chem.* **1978**, 179, 1175-1191
- <sup>48</sup> H.R. Kricheldorf, *Makromol. Chem.* **1979**, 180, 147-159

# Chapter 4

## Thiol Chemistry on Well-Defined Synthetic Polypeptides

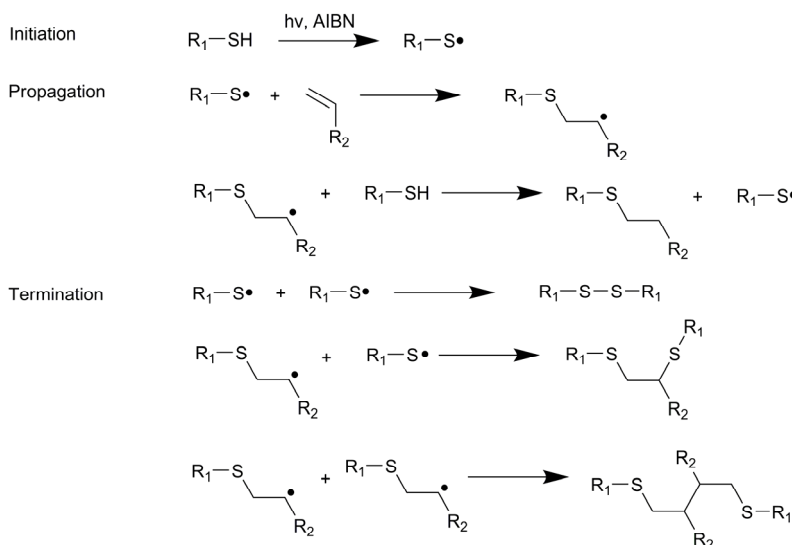
### Abstract

*Well-defined cysteine-containing synthetic polypeptides were synthesized using N-carboxyanhydride ring opening polymerization (NCA ROP) of the NCAs of S-tert-butylmercapto-L-cysteine in combination with  $\gamma$ -benzyl-L-glutamate and N $\epsilon$ -benzyloxycarbonyl-L-lysine. The thiol groups of the copolypeptide were selectively deprotected with the removal of the disulfides by reduction with dithiothreitol. The versatility of various chemical reactions on the deprotected thiol groups was investigated subsequently. Cross-linking was studied for polypeptides in solution. Thiol-ene reactions by Michael addition and the free radical catalyzed mechanism were studied for the addition of PEG acrylates and fluorescein-O-acrylate. The chain transfer properties of the free thiols in free radical polymerizations were used to make hybrid graft copolymers.*

Part of this chapter was published in G.J.M. Habraken, C.E. Koning, J.P.A. Heuts and A. Heise, *Chem. Commun.* **2009**, 3612-3614

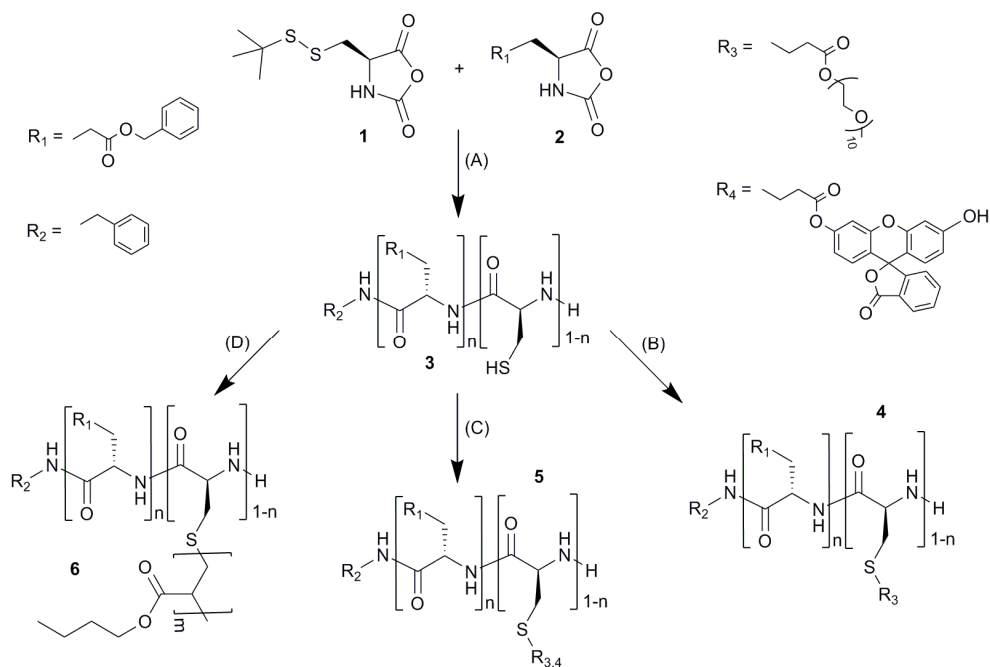
## 4.1 Introduction

The high potential of protein-(polymer) conjugates in biomedical applications has triggered increased research activity towards their synthesis.<sup>1-5</sup> While in principle any functional group in natural peptides can be utilized for conjugation, thiols present in the form of the amino acid L-cysteine (Cys) have specifically been targeted due to their versatility in a wide variety of reactions. For the same reason, thiol reactions are also increasingly investigated in synthetic (bio)materials. For example, Michael additions have been successfully performed on the Cys of natural proteins as well as on synthetic polymers. Furthermore, the cross-linking of polymers comprising thiol-containing monomers has been reported targeting degradable drug delivery materials.<sup>6</sup> Already known for a long time and used in many commercial polymerizations is the role of thiols as chain transfer agents in free radical polymerizations.<sup>6</sup> In the presence of a radical a thiol can transfer a hydrogen to a growing radical (Scheme 4.1). The thiyl radical reacts with another monomer. Termination can occur through radical-radical coupling. In this process the thiols can thus be used to decrease and reasonably control the molecular weight of the polymers. Obeying the same mechanism, in the case of equimolar amounts of the alkene and the thiols, this process is referred to as thiol-ene chemistry.<sup>7</sup> The renewed interest in thiol-ene chemistry is due to the fact that these reactions are extremely fast and open new possibilities for rapid photopolymerization of a large variety of monomers to yield polymers for special applications, including biomedical materials. Furthermore, thiol-ene chemistry can be used as a metal free 'click' polymer functionalization reaction.<sup>8-10</sup>



**Scheme 4.1.** Thiol-ene reaction scheme.

Our research is focused on bridging natural and synthetic polymers with the long term goal to develop a new material platform for biomedical applications. While modern controlled polymerization techniques offer the possibility to access and design a wide range of (bio)functional polyacrylates, these materials are not based on natural building blocks and are intrinsically non-degradable. On the other hand, natural functional biopolymers like proteins are too complex to be synthetically accessible in large quantities (except by fermentation). Functional synthetic polypeptides have the potential to close the gap between synthetic and biopolymers provided they can be produced with good control over molecular weight and decorated with functional groups, which allow further modification of the material.



**Scheme 4.2.** Synthesis and chemical modification of (co)polypeptides based on NCAs. (A) Polymerization/deprotection: 1. Benzylamine, DMF, 0 °C, 4 days. 2. Dithiothreitol. (B) Michael addition: PEG acrylate, pyridine, DMF, room temperature, 5 days. (C) Thiol-ene addition: PEG acrylate (or fluorescein), AIBN, DMF, 70 °C, 1 hour. (D) Chain transfer grafting: PEG acrylate, AIBN, DMF, 60 °C, 16 hours.

The synthesis of polypeptides from N-carboxyanhydrides (NCAs) has been known for quite some time.<sup>11</sup> However, only recent developments made it possible to control the polymerization and obtain polypeptides with defined molecular weight and polydispersity. The most prominent method was initially reported by Deming and makes use of a metal (e.g. nickel) complex regulating monomer addition without any chain end termination.<sup>12</sup> Very good control over the NCA ring

opening polymerization (NCA ROP) was also achieved by the addition of salts to form a dormant chain-end for poly(*N*<sub>ε</sub>-benzyloxycarbonyl-L-lysine) and poly( $\gamma$ -benzyl-L-glutamate) (PBLG).<sup>13,14</sup> Good results were obtained under high vacuum conditions as well.<sup>15</sup> Recently Vayaboury showed that NCA polymerization at 0 °C resulted in a well controlled polymerization of poly(*N*<sub>ε</sub>-trifluoroacetyl-L-lysine) owing to the fact that side reactions are considerably slower at this temperature.<sup>16</sup>

Here we investigate the synthesis of well-defined Cys containing polypeptides and the versatility of the thiol groups for secondary modification. With the use of NCA ROP high cysteine-containing peptides were synthesized. The polypeptides were selective deprotected by reduction of dithiothreitol to remove the disulfide bonds on the cysteines. The deprotected peptides were then cross-linked by oxidation. Furthermore, the polypeptides were functionalized by grafting (meth)acrylate monomers and polymers by Michael addition and radical chain transfer on the thiols (Scheme 4.2).

## 4.2 Experimental

### Materials

All materials and solvents were used without any purification, unless otherwise mentioned. Benzylamine 99,5% purified by redistillation, *S*-*tert*-butylmercapto-L-cysteine, *N*-(*tert*-butyloxycarbonyl)-L-cysteine methyl ester 97%, DL-dithiothreitol  $\geq 99\%$ ,  $\alpha$ -pinene 98%, bis(trichloromethyl) carbonate (triphosgene) 99%, *n*-butylacrylate, methylmethacrylate, fluorescein O-acrylate and polyethyleneglycol methyl ether acrylate ( $M_n = 450$  g/mol), were purchased from Aldrich.  $\gamma$ -benzyl-L-glutamate was supplied from Bachem. Potassium hydroxide was purchased from VWR. 2,2'-Azobis(2-methylpropionitrile) was purchased from Merck. Cobalt phtalocyanine 90% was purchased from Acros. HFIP, DMF (extra dry), ethylacetate, *n*-heptane and diethylether were purchased from Biosolve. DMF and ethylacetate were used directly from the bottle or stored under an inert, dry atmosphere. *n*-Butylacrylate and methylmethacrylate were purified by passing through a silica column twice before polymerization. NCA monomers were prepared according to procedures mentioned in Chapter 2.

### Characterization

For the SEC analysis using HFIP (Biosolve, AR-S from supplier or redistilled) as eluent measurements were done using a Shimadzu LC-10AD pump (flow rate 0.8 ml/min) and a WATERS 2414, differential refractive index detector (at 35 °C). Injections were done by a Spark Holland, MIDAS injector, a 50  $\mu$ L injection volume was used. The column is a PSS, 2\* PFG-lin-XL (7  $\mu$ m, 8\*300 mm) column at 40°C. Calibration has been done using poly(methyl methacrylate) standards.

For the SEC analysis using DMF as eluent measurements were done on a Waters Alliance system equipped with a Waters 2695 separation module, a Waters 2414 refractive index detector (40 °C), a Waters 486 UV detector, a PSS GRAM guard column followed by 2 PSS GRAM columns in series of

100 Å (10 µm particles) and 3,000 Å (10 µm particles) respectively at 60°C. The flow rate was 1 mL min<sup>-1</sup>. The molecular weights were calculated using polystyrene standards. Before SEC analysis was performed, the samples were filtered through a 0.2 µm PTFE filter (13 mm, PP housing, Alltech) <sup>1</sup>H-NMR analyses were performed on a Mercury 400. For the monomers deuterated chloroform was used. For the polymers DMSO-d<sub>6</sub> and deuterated TFA were used.

Gradient polymer elution chromatography was done using a Zorbax Eclipse XDB-C8 column, 4.6 x 150 mm, 5 µm on an Agilent 1100 series setup. The eluents were toluene and DMF of which the gradient was initially toluene for 2 minutes and then increased to 50 : 50 in 25 minutes. The flow rate was 1 ml/min. The temperature of the column was 50 °C. Detection was done by a Polymer Labs ELSD detector.

### Synthesis

**Synthesis of P(BLG-co-tBMLC):** The γ-benzyl-L-glutamate NCA (6.00 g, 22.8 mmol) and the *S*-tert-butylmercapto-L-cysteine NCA (1.33 g, 5.7 mmol) were dissolved in 45 ml DMF. A solution of benzylamine (123 mg, 1.14 mmol) in 5 ml DMF was added once all NCA monomer had been completely dissolved. The reaction was maintained for 4 days at 0°C and the polypeptide was precipitated in diethylether, washed with diethylether and dried under vacuum at 20°C. Yield: 4.70 g, 0.770 mmol (*M<sub>n</sub>*: 6100), 76 wt%

**Synthesis of P(BLG-co-tBMLC) with sampling:** The γ-benzyl-L-glutamate NCA (5.05 g, 19.2 mmol) and the *S*-tert-butylmercapto-L-cysteine NCA (1.12 g, 4.8 mmol) were dissolved in 35 ml DMF. A solution of benzylamine (64 mg, 0.60 mmol) in 5 ml DMF was added once all NCA monomer had been completely dissolved. The reaction was maintained for 4 days at 0°C. Samples were taken and precipitated in diethylether, washed and dried under vacuum.

**Synthesis of P(BLG-co-Cys) 3:<sup>2</sup>** The P(BLG-co-tBMLC) (*M<sub>n</sub>*: 4,200 g/mol) (2.25 g, 0.54 mmol) and dithiothreitol (2.15 g, 13.9 mmol) were dissolved in 20 ml DMF. The reaction was maintained for 5 days at 60 °C under a nitrogen atmosphere. After 5 days the polymer was precipitated in diethylether, washed with diethylether and dried under vacuum at 20°C. Yield: 1.16 g, 57.7 wt%

**Cross-linking of 3:** **3** (54 mg, 13µmol) and cobalt phtalocyanine (6.0 mg, 10 µmol) were dissolved in 0.2 ml of DMF in a 1.5 ml vial with an opening to the ambient atmosphere. The reaction was left at room temperature for 24 hours and a sample was taken and dissolved in DMF. After filtration of the sample it was immediately measured by the DMF-SEC.

**Cross-linking of 3 in basic environment:** **3** (53 mg, 13 µmol), cobalt phtalocyanine (6.0 mg, 10 µmol) and potassium hydroxide (5.3 mg, 94 µmol) were dissolved in 0.2 ml of DMF in a 1.5 ml vial with an

opening to the ambient atmosphere. The reaction was left at room temperature for 24 hours and a sample was taken and dissolved in DMF. After filtration of the sample it was immediately measured by the DMF-SEC.

**Michael Addition of polyethylene glycol methyl ester acrylate to 3:** **3** (50 mg, 11  $\mu\text{mol}$ ) was dissolved with the poly(ethylene glycol) methyl ether acrylate ( $M_n$ : 454 g/mol) (28 mg, 62  $\mu\text{mol}$ ) in 0.7 ml DMF in a 1.5 ml vial. The reaction mixture was shaken for 5 days at room temperature. After 5 days the solvent was evaporated under vacuum.

**Michael Addition of polyethylene glycol methyl ester acrylate to 3 in the presence of pyridine:** **3** (50 mg, 11  $\mu\text{mol}$ ) was dissolved with the poly(ethylene glycol) methyl ether acrylate ( $M_n$ : 454 g/mol) (28 mg, 62  $\mu\text{mol}$ ) and pyridine (85 mg, 1.1 mmol) in 0.7 ml DMF in a 1.5ml vial. The reaction mixture was shaken for 5 days at room temperature. After 5 days the solvent was evaporated under vacuum. A sample was taken from the dried material for SEC measurements.

**Thiol-ene addition of polyethylene glycol methyl ester acrylate to 3.** **3** (209 mg, 31  $\mu\text{mol}$ ), poly(ethylene glycol) methyl ether acrylate ( $M_n$ : 454 g/mol) ( 50 mg, 0.11 mmol) and  $\alpha,\alpha'$ -azoisobutyronitrile (1.2 mg, 7.3  $\mu\text{mol}$ ) were dissolved in 0.6 ml DMF. The mixture was heated to 70°C for 1 hour under ambient atmosphere. After the reaction the solvent was removed under vacuum. A sample was taken from the dried material for SEC measurements.

**Thiol-ene addition of fluorescein O-acrylate to 3.** **3** (48 mg, 11  $\mu\text{mol}$ ), fluorescein O-acrylate (22 mg, 57  $\mu\text{mol}$ ) and  $\alpha,\alpha'$ -azoisobutyronitrile (0.2 mg, 1  $\mu\text{mol}$ ) were dissolved in 0.3 ml DMF. The mixture was heated to 60°C for 1 hour under ambient atmosphere. The polymer was purified by two precipitations in diethylether. After the reaction the material was dried under vacuum. Yield: 11 mg, 16 wt%

**Free Radical Chain Transfer of *n*-butylacrylate with 3.** **3** (100 mg, 2.22 x 10<sup>-2</sup> mmol) and *n*-butylacrylate (720 mg, 5.62 mmol) were dissolved in DMF.  $\alpha,\alpha'$ -Azoisobutyronitrile (1.2 mg, 7.3  $\mu\text{mol}$ ) was added from a DMF solution. The total amount of DMF was 2 ml. Oxygen was removed by three freeze / thaw cycles. The reaction was maintained at 60°C for 16 hours under a nitrogen atmosphere. After the reaction the material was precipitated in methanol and dried under vacuum. Yield: 450 mg, 55 wt%

**Free Radical Chain Transfer of *n*-butylacrylate.** *n*-Butylacrylate (720 mg, 5.62 mmol) was dissolved in DMF.  $\alpha,\alpha'$ -Azoisobutyronitrile (1.2 mg, 7.3  $\mu\text{mol}$ ) was added from a solution. Total amount of DMF was 2 ml. Oxygen was removed by three freeze / thaw cycles. The reaction was maintained at 60°C for 16 hours under a nitrogen atmosphere. After the reaction the material was

precipitated in methanol and dried under vacuum. Yield: 325 mg, 45 wt%.

**Free radical chain transfer of L-cysteine.**  $N_\epsilon$ -*t*-butyloxycarbonyl-L-cysteine, methyl ester (35 mg, 0.15 mmol) and *n*-butylacrylate (982 mg, 7.66 mmol) were dissolved in DMF.  $\alpha,\alpha'$ -Azobisisobutyronitrile (2.8 mg, 17.4  $\mu$ mol) was added from a DMF solution. The total amount of DMF was 2.7 ml. Oxygen was removed by three freeze / thaw cycles. The reaction was maintained at 60°C for 17 hours under a nitrogen atmosphere. After the reaction the polymer did not precipitate in methanol, so solvent and monomer were removed under vacuum. Yield: 562 mg, 55 wt%.

### 4.3 Results and discussion

The polypeptides were prepared by ring opening copolymerization of protected amino acid *N*-carboxyanhydrides (NCAs) such as  $\gamma$ -benzyl-L-glutamate NCA (BLG) **1** or  $N_\epsilon$ -benzyloxycarbonyl-L-lysine NCA (ZLL) with a protected Cys-NCA. Cys-NCAs are often prepared using a thiol-protecting group like *S*-benzyl-L-cysteine and *S*-benzyloxycarbonyl-L-cysteine.<sup>17-19</sup> We decided to use *S*-*tert*-butylmercapto-L-cysteine (*t*BMLC) because this protecting group can selectively be removed in the presence of other amino acid protecting groups such as benzyl esters, leaving the latter unaffected.<sup>20</sup>

**Table 4.1.** Results of the copolymerization of  $\gamma$ -benzyl-L-glutamate NCA (BLG) or  $N_\epsilon$ -benzyloxycarbonyl-L-lysine NCA (ZLL) and *S*-*tert*-butylmercapto-L-cysteine NCA (*t*BMLC).

| Entry | Monomers           | Feed ratio <sup>a</sup> | $M_{n, \text{theo}}$ (g/mol) | Monomer ratio <sup>b</sup> | $M_n$ (g/mol) <sup>c</sup> | PDI <sup>c</sup> |
|-------|--------------------|-------------------------|------------------------------|----------------------------|----------------------------|------------------|
| 1     | BLG, <i>t</i> BMLC | 4.0 : 1.0               | 5,400                        | 4.0 : 1.0                  | 6,100                      | 1.16             |
| 2     | BLG, <i>t</i> BMLC | 7.4 : 1.0               | 8,100                        | 4.5 : 1.0                  | 7,800                      | 1.11             |
| 3     | BLG, <i>t</i> BMLC | 4.1 : 1.0               | 13,000                       | 4.1 : 1.0                  | 12,700                     | 1.20             |
| 4     | BLG, <i>t</i> BMLC | 4.0 : 1.0               | 8,700                        | 4.0 : 1.0                  | 10,800                     | 1.12             |
| 5     | BLG, <i>t</i> BMLC | 4.0 : 1.0               | 8,700                        | 3.8 : 1.0                  | 9,200                      | 1.21             |
| 6     | ZLL, <i>t</i> BMLC | 4.0 : 1.0               | 6,400                        | 4.3 : 1.0                  | 5,400                      | 1.35             |
| 7     | ZLL, <i>t</i> BMLC | 4.0 : 1.0               | 12,600                       | 3.5 : 1.0                  | 6,900                      | 1.61             |

<sup>a</sup> Ratio based on molar amounts of used monomers. <sup>b</sup> Determined by <sup>1</sup>H-NMR analysis by comparison of the signals at 7.0 ppm (BLG, ZLL) with 1.4 ppm (*t*BMLC). <sup>c</sup> Determined by SEC in HFIP with PMMA standards.

Following this approach, all copolymerizations were carried out in DMF at 0 °C with benzylamine as initiator (Table 4.1) at a 1:4 monomer ratio for *t*BMLC-NCA to ZLL-NCA or BLG-NCA, respectively. The evolution of the molecular weight and the composition was monitored during the polymerization. After three days no further increase of the molecular weight was measured by size exclusion chromatography (SEC). Over time the solutions became opaque, indicating that not all the polypeptides were dissolved well. All PBLG copolypeptides were found to have a low polydispersity ( $\leq 1.2$ ) with good agreement between the monomer feed ratio and the copolymer composition (with one exception, entry 2, Table 4.1). On the other hand, the polydispersities of the



copolypeptides obtained from ZLL-NCA were slightly higher and a low molecular weight shoulder was observed in the SEC trace, indicating the formation of aggregates during the NCA ROP as seen for the homopolymerizations in Chapter 2.

The selective deprotection of the copolypeptides was performed in DMF with dithiothreitol (DTT) at 60 °C under a nitrogen atmosphere for several days. After precipitation and drying, analysis of the polypeptides by <sup>1</sup>H-NMR confirmed that the *S*-*t*-butylmercapto groups were removed with 90% to 100% yield (Figure 4.1). The signal at 1.4 ppm, corresponding to the *tert*-butyl group decreases after the reaction compared to the signal for the benzyl groups at 7.4 ppm and the protons of the peptide main chain at 4.8 ppm. The spectroscopic difference coincided with a small molecular weight decrease in the SEC as compared to the protected copolypeptide.

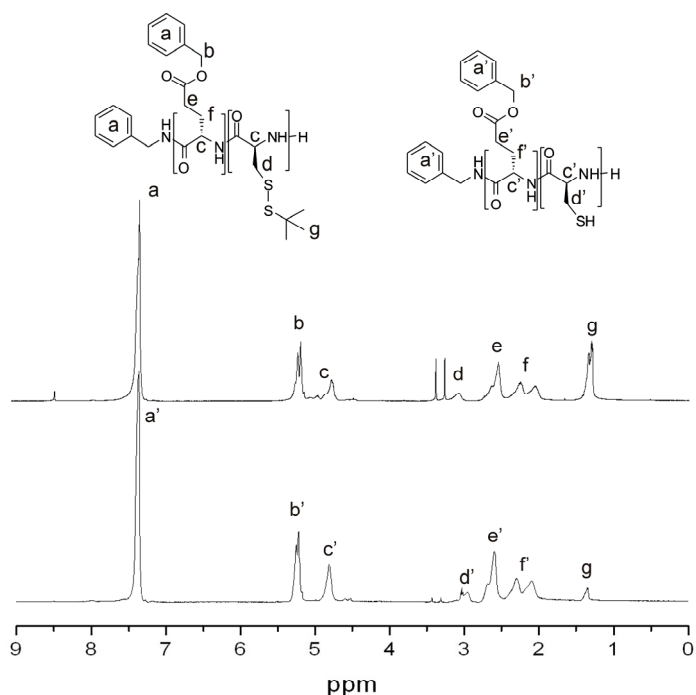


**Figure 4.1.** <sup>1</sup>H-NMR spectra: deprotection of P(BLG-*co*-*t*BMLC) with dithiothreitol.

A slow oxidative cross-linking of the polypeptides was observed under ambient atmosphere. The oxidative cross-linking of the Cys-thiol groups could be accelerated by the addition of cobalt phthalocyanines. The weight average molecular weight increased from 5,800 to 12,200 g/mol (PDI: 2.1) within 1 day (Figure 4.2). This reaction is known to be pH dependent as with the addition of KOH the weight average molecular weight increased significantly to 22,100 g/mol (PDI: 2.8). The disadvantage

of this reaction is that either a higher concentration or a higher initial molecular weight is needed for significant molecular weight increase resulting in a fully cross-linked system. The product obtained here should be considered as a branched polymer.

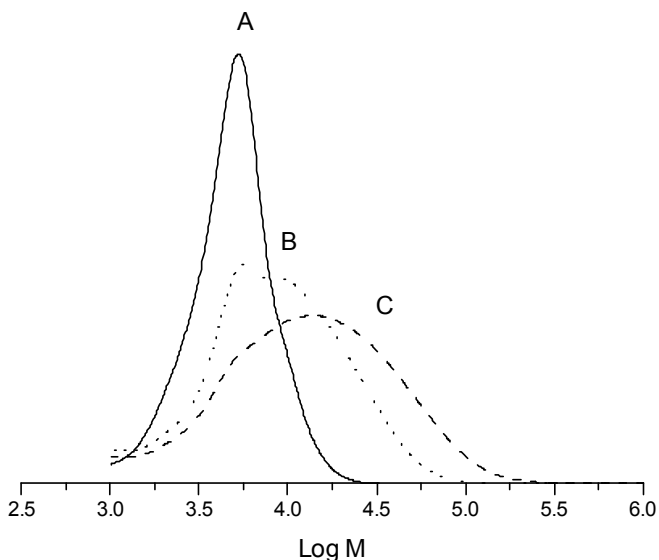


**Figure 4.2.** HFIP SEC traces of cross-linking of P(BLG-co-Cys). A), P(BLG-co-Cys), B) cross-linking by phthalocyanine, C) cross-linking by phthalocyanine in presence of potassium hydroxide.

The Michael addition to the Cys-copolypeptide was tested with poly(ethylene glycol) methyl ether acrylate ( $M_n$ : 454 g/mol) in DMF with and without the presence of the basic pyridine at room temperature. SEC showed a clear increase of the molecular weight of the reaction product **4** (9,300 g/mol) compared to the starting material **3** (7,100 g/mol) for both reactions. However, the product trace was bimodal, which suggests a low efficiency of this reaction. The presence of the pyridine did not show any effect.

Better results were obtained when the reaction was carried out under conditions promoting thiol-ene addition (ratio SH to acrylate 1:1). The basic reaction conditions were similar to the Michael addition, but  $\alpha,\alpha'$ -azoisobutyronitrile (AIBN) was added as a radical source. After heating the reaction mixture to 70 °C for 1 hour, SEC analysis showed that the molecular weight of the formed P(BLG-co-(Cys-g-PEGA)) **5** had shifted completely compared to the starting material (Figure 4.3). Only a small additional low molecular weight peak can be observed in the chromatogram, which we believe to be the product of the free radical polymerization of the PEGA. The observed complete shift of the molecular weight distribution confirms that the thiol-ene addition is the dominant process in this reaction. As a further control, a similar mixture without the copolypeptide was treated under the same conditions, causing free radical polymerization of the PEGA. When

the SEC trace of this reaction product was compared to the trace of the material that was obtained in the presence of **3** it can be seen that the free radical polymerization resulted in a much higher molecular weight (32,900 g/mol).

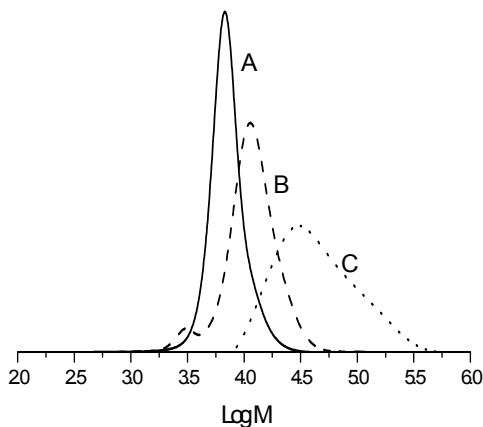


**Figure 4.3.** HFIP-SEC traces of products from thiol-ene addition of PEG-acrylate (PEGA) to P(BLG-co-Cys) **3**. (A) P(BLG-co-Cys) **5**; (B) P(BLG-co-(Cys-g-PEGA)); (C) Control: P(PEGA) obtained under conditions of thiol-ene addition without P(BLG-co-Cys).

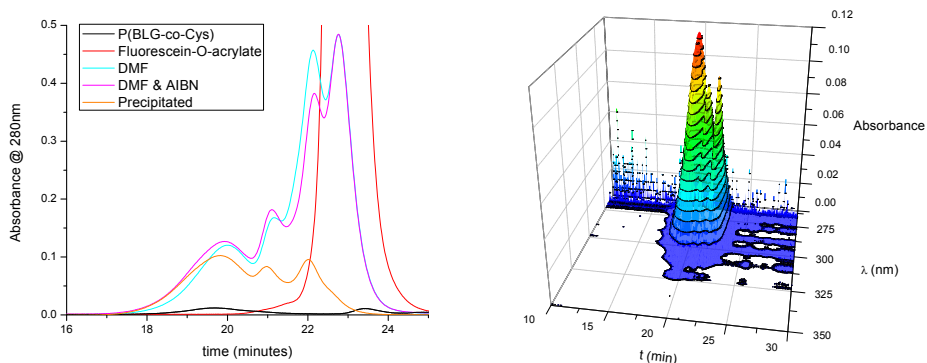


**Figure 4.4.** Product of fluorescein attachment to P(BLG-co-Cys) by thiol-ene coupling.

The thiol-ene reactions on the Cys-copolypeptide were then successfully extended to other acrylates such as isobornyl acrylate and fluorescein O-acrylate. While expectably in this case only a small molecular weight increase of 500 g/mol was measured, the absence of any acrylate double bond was confirmed by  $^1\text{H-NMR}$ . Moreover, the UV absorbance at 280 nm from the SEC of the reaction product with fluorescein O-acrylate further confirmed the successful thiol-ene reaction (Figure 4.4). At 280 nm the starting material only gives a small absorption at 20 minutes, while after the reaction a much higher absorption was found. Most of the unreacted fluorescein-O-

acrylate was removed by precipitation.

By increasing the ratio of the acrylate to SH higher values than 1:1, free radical polymerization can occur with the thiols acting as a chain transfer (CT) agent. Commonly, mono-functional thiols are added to free radical polymerizations to reasonably control and reduce the average degree of polymerization. According to its function as a chain transfer agent, the thiol will form the initiating end-group of the polymer. In our case the copolypeptide contains several thiol functionalities and a successful reaction would open a simple way to obtain grafted copolymers with a well-defined polypeptide backbone and polyacrylate grafts. We choose a low AIBN concentration in order to increase the amount of grafted PBA chains. At a lower radical concentration the importance of CT as the main chain stopping event will become even larger, thus enhancing the efficiency of the grafting process.

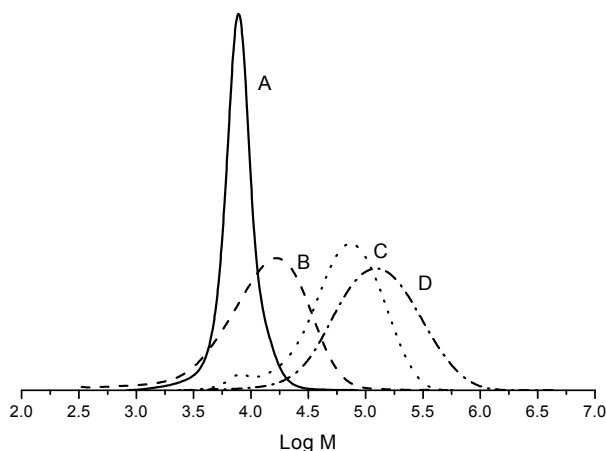


**Figure 4.5.** HFIP-SEC traces of graft copolymer obtained by free radical polymerization of butyl acrylate in the presence of P(BLG-co-Cys). (A) P(BLG-co-Cys) **3**, (B) PBA with *N*<sub>ε</sub>-*tert*-butyloxycarbonyl-L-cysteine methyl ester as CT agent, (C) P(BLG-co-(Cys-*g*-PBA)), (D) PBA

The reaction was carried out with *n*-butyl acrylate (BA) in DMF under nitrogen at 60 °C for 16 hours after which the product was precipitated. Two additional control experiments were conducted under the same reaction conditions and concentrations. In the first one the polypeptide copolymer was replaced by a C- and N-protected Cys, namely *N*<sub>ε</sub>-*tert*-butyloxycarbonyl-L-cysteine methyl ester. The thiol concentration was kept constant for this experiment. In the second one no thiol group was present at all, making this a free radical polymerization without a chain transfer agent.

The SEC results (Figure 4.5) confirm an increase of molecular weight from 7,100 g/mol (PDI: 1.2) of the polypeptide copolymer to 43,000 g/mol for the product obtained after the polymerization.

Evidence for the graft copolymer structure was obtained from  $^1\text{H-NMR}$ , showing prominent signals of both the polypeptide and PBA. Moreover, the elution time of this material in Gradient Polymer Elution Chromatography (GPEC) was between those of PBA and **3** (see Figure 4.6), which is typically the case for copolymers comprising two individual block units. Figure 4.6 also reveals a small peak at the elution time of the peptide copolymer. While the GPEC results suggest that no P(BLG-co-Cys) remains after the radical polymerization, it confirms the presence of PBA.

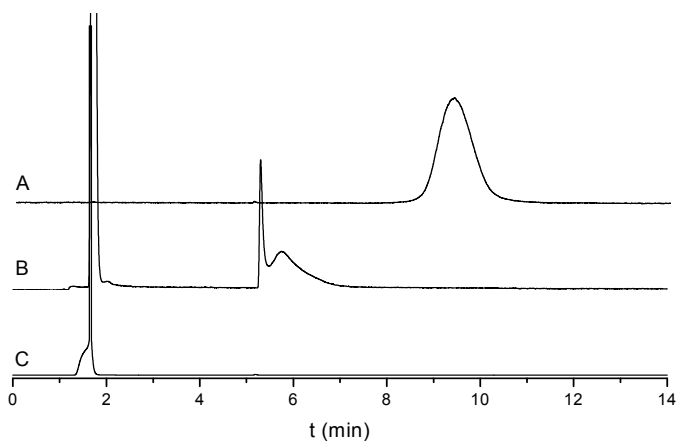


**Figure 4.6.** GPEC traces of (A) P(BLG-co-Cys), (B) P(BLG-co-(Cys-g-PBA)), (C) PBA

The control experiment without **3** yielded a PBA with a molecular weight of 84,000 g/mol. This shows qualitatively the efficiency of the chain transfer process in the presence of the Cys copolymer. The control experiment with  $N_\epsilon$ -*tert*-butyloxycarbonyl-L-cysteine methyl ester resulted in a PBA of 7,300 g/mol (PDI: 2.5), which gives an indication of the molecular weight of the grafted chains. It has to be noted that direct comparison of the SEC results of both polymers has to be performed with caution since the graft copolymer contains not only a flexible coil PBA but also a polypeptide block. The contribution to the hydrodynamic volume and its relation to the linear standards of the latter is unknown. Moreover, the accuracy of this comparison will also depend on the difference in chain transfer constant ( $C_T$ ) between the poly- and the mono-thiol. Similar results on the chain transfer were obtained from experiments with PMMA (Figure 4.7).

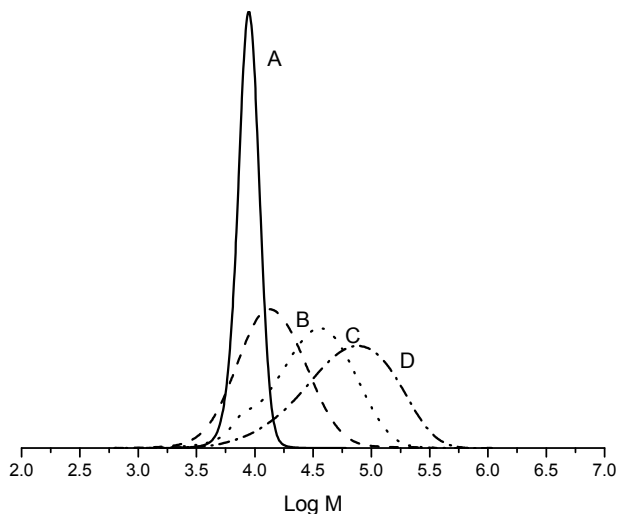


**Figure 4.7.** HFIP-SEC traces of graft copolymer obtained by free radical polymerization of methylmethacrylate in the presence of P(BLG-co-Cys). (A) P(BLG-co-Cys) **3**, (B) PMMA with *N*<sub>ε</sub>-*tert*-butyloxycarbonyl-L-cysteine methyl ester as CT agent, (C) P(BLG-co-(Cys-g-PMMA)), D) PMMA

#### 4.4 Conclusions

In summary we have shown that well-defined Cys-containing polypeptides can be obtained by NCA polymerization at 0°C. These can form a useful platform for further reactions making use of the thiol functionality. While cross-linking reactions and Micheal additions to the thiol group are possible, the most promising reactions are thiol-ene additions and radical grafting by chain transfer. Further experiments are currently under way to provide insights into the chain transfer process and to extend the range of monomers so as to obtain functional materials.

## References

- <sup>1</sup> K. Velonia, A. E. Rowan and R. J. M. Nolte, *J. Am. Chem. Soc.* **2002**, 124, 4224-4225
- <sup>2</sup> A. Chilkoti, G. H. Chen, P. S. Stayton and A. S. Hoffman, *Bioconjugate Chem.* **1994**, 5, 504-507
- <sup>3</sup> R.J. Pounder, M.J. Standford, P. Brooks, S.P. Richards and A.P. Dove, *Chem. Commun.* **2008**, 5158-5160
- <sup>4</sup> J. Rieger, K. van Butsele, P. Lecomte, C. Detrembleur, R. Jérôme and C. Jérôme, *Chem. Commun.* **2005**, 274-276
- <sup>5</sup> I.V. Dimitrov, I.V. Barlinova, P.V. Ilieva and N.G. Vladimirov, *Macromolecules* **2008**, 41, 1045-1049
- <sup>6</sup> G. Moad and D.H. Solomon, *The Chemistry of Radical Polymerization*, 2nd edition, **2006**
- <sup>7</sup> C.E. Hoyle, T.Y. Lee and T. Roper, *J. Polym. Sci. Part A: Polym. Chem.* **2004**, 42, 5301-5338
- <sup>8</sup> L.M. Campos, I. Meinel, R. G. Guino, M. Schierhorn, N. Gupta, G. D. Stucky and C. J. Hawker, *Adv. Mater.* **2008**, 20, 3728-3733
- <sup>9</sup> P. Jonkheijm, D. Weinrich, M. Koehn, H. Engelkamp, P. C. M. Christianen, J. Kuhlmann, J. C. Maan, D. Nuesse, H. Schroeder, R. Waker, R. Breinbauer, C. M. Niemeyer and H. Waldmann, *Angew. Chem. Int. Ed.* **2008**, 47, 4421-4424
- <sup>10</sup> N.B. Cramer, S.K. Reddy, H. Lu, T. Gross, R. Raj and C.N. Bowman, *J. Polym. Sci. Part A: Polym. Chem.* **2004**, 42, 1752-1757
- <sup>11</sup> H.R. Kricheldorf, *Angew. Chem. Int. Ed.* **2006**, 45, 5752-5784
- <sup>12</sup> T.J. Deming, *Nature* **1997**, 390, 386-389
- <sup>13</sup> I. Dimitrov and H. Schlaad, *Chem. Commun.* **2003**, 2944-2945
- <sup>14</sup> W. Agut, A. Briet, D. Taton and S. Lecommandoux, *Langmuir* **2007**, 23, 11526-11533
- <sup>15</sup> T. Aliferis, H. Iatrou and N. Hadjichristidis, *Biomacromolecules* **2004**, 5, 1653-1656
- <sup>16</sup> W. Vayaboury, O. Giani, H. Cottet, A. Deratani and F. Schué, *Macromol. Rapid Commun.* **2004**, 25, 1221-1224
- <sup>17</sup> S. Abraham, I. Kim and C.A. Batt, *Angew. Chem. Int. Ed.* **2007**, 46, 5720-5723
- <sup>18</sup> S. Jing, C. Xuesi, L. Tiancheng, L. Shi, T. Huayu, G. Zhaopei and J. Xiabin, *Langmuir* **2008**, 24, 10099-10106
- <sup>19</sup> A. Berger, J. Noguchi and E. Katchalski, *J. Am. Chem. Soc.* **1956**, 78, 4483-4488
- <sup>20</sup> H.R. Kricheldorf,  *$\alpha$ -Aminoacid-N-carboxyanhydrides and Related heterocycles*, **1987**, Berlin, Springer Verlag

## Chapter 5

# Biomimetic CaCO<sub>3</sub> Crystallization with Fluorescent Polypeptides Prepared by N- Carboxyanhydride Ring Opening Polymerization.

### Abstract

*In nature organisms are known to alter the growth of minerals to their advantage with highly developed and complicated shapes. In the case of calcium carbonate nacre and coral are nice examples. One of nature's tools for biomineralization is the use of peptide material to direct the growth of calcium carbonate. The specific knowledge about the peptide composition (amino acids) and crystal structure and growth characteristics is not yet available. With the use of N-carboxyanhydride ring opening polymerization (NCA ROP) random fluorescent copolypeptides of L-glutamic acid, L-aspartic acid and L-alanine were prepared and these were used to control the crystallization of calcium carbonate. SEM showed clear differences in the crystal structures depending on the used copolypeptide. Where P(Glu-co-Ala) gave round calcite crystals the P(Asp-co-Ala) did show the altered growth, resulting in elongated crystals. With the use of the fluorescent label the occlusion of the polypeptide during the crystallization could be proven. This work shows the use of NCA ROP-prepared copolypeptides in the biomimetic crystallization to study the role of the polypeptide additive on the crystal structure.*

This work was done in collaboration with Z. Deng and N.A.J.M. Sommerdijk



## 5.1 Introduction

In nature biomineralization is known to result in highly advanced structures such as mother of pearl, coccolith scales, the exoskeleton of sea urchins and coral. To mimic the fabulous materials nature produces, all of nature's tools to accomplish this need to be studied and understood. One of these is the crucial part biological polymers like peptides play in biomineralization. For example, in the crystallization of calcium carbonate peptides can affect polymorphs, morphology, nucleation or growth of the crystals (Figure 5.1). The general aim of research conducted in this field is to use the knowledge obtained from studying and elucidating biological systems and to apply this for other inorganic systems to obtain materials with advanced properties.

### 5.1.1 Calcium carbonate crystallization

Calcium carbonate has many polymorphs, such as calcite, vaterite and aragonite. The difference between the crystal structure is determined by the thermodynamics of the controlled growth of the polymorphs. The Ostwald step rule explains this to some extent, suggesting that in a cascade of crystal phases a final low energy phase is obtained. An instable crystal form of calcium carbonate is vaterite. Low in energy and most stable is calcite. Aragonite is high in energy and can be made under certain conditions using an increased reaction temperature and a higher magnesium (additive) concentration in the reaction medium. Apart from salt hydrates also amorphous calcium carbonate exists. This is also an unstable species and can be transformed into a crystal form lower in energy.<sup>1</sup>

Crystal nucleation can occur with or without an alien (precritical) nucleus. Homogeneous nucleation is the clustering of ions forming small clusters. Depending on the solvent conditions, such as the pH either nucleation is observed or the formation of amorphous calcium carbonate (ACC) nanoparticles.<sup>2,3</sup> Growth is then achieved by addition of ions or further aggregation of clusters. Heterogeneous nucleation occurs from surfaces, where the interaction of the ACC nanoparticle with the surface decreases the surface energy, making it easier to reach the critical size of the amorphous particle. Nucleation on the finished flat crystal surface or from crystal imperfections, such as screw dislocations, enable the growth of another layer. The steps or kinks are then the place where the growth of the layer takes place due to the lower energy cost. Growth planes depend on the surface energies of all the present planes.<sup>1</sup> High surface energy surfaces will grow quickly compared to low energy surfaces, meaning that high surface energies surfaces are the growing planes, while the low energy surfaces will dominate the crystal morphology.

### 5.1.2 Polymer additives

Organic additives, among which polymers, are known to have a significant effect on the nucleation and growth of calcium carbonate crystals, resulting in different polymorphs, orientation and shapes of crystals.

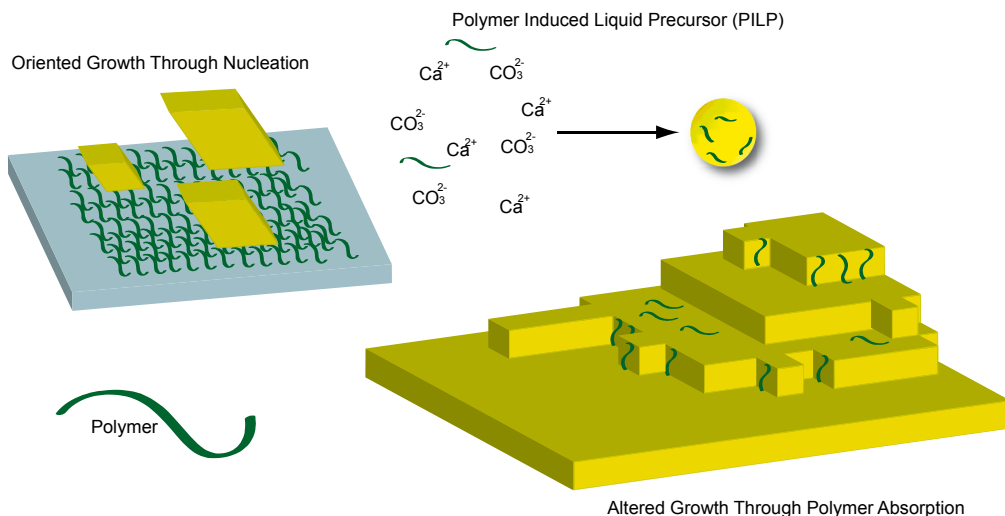


**Figure 5.1.**  $\text{CaCO}_3$  crystallization with peptide / polymer additives: polymer induced liquid precursor (PILP), nucleation from a polymer / peptide covered surface and influenced crystal growth on the steps by interaction with peptide / polymer additives.

Additives can, for example, influence the crystallization by controlling the crystallization speed by inhibition. Moreover, stabilized by a polymer additive an amorphous phase consisting of calcium carbonate, water and additive can be formed, known as a polymer induced liquid precursor (PILP).<sup>4</sup> By a heterogeneous nucleation these moldable ACC precursors can be crystallized. The formed ACC particles can be transported and deposited on a growing crystal surface. It is thought that these stabilized precursors play an important role in the formation of exoskeletons of bivalves, searhchins and coccolithophores. The natural peptides found to be involved in the formation of these amorphous particles seem to be rich in aspartic acid, glutamic acid and hydroxyamino acids.<sup>4,5</sup> Phosphorylated peptides and glycopeptides are also known to enhance the PILP process. All of the above mentioned peptides are known to bind to calcium ions and stabilize the amorphous particles. Crystallization is promoted with the addition of polymer that interacts with the carbonate ions. For example poly(L-lysine) is known to increase the crystallization speed.<sup>6</sup>

In order to mimic biomineralization a number of polymers have been investigated ranging from natural peptides to synthetic polymers. Synthetic polymers like poly(L-aspartic acid) and poly(acrylic acid) are known to be very effective additives to produce ACC for the PILP process. However, it is found that they also stabilize the polymorph vaterite crystals.<sup>1,7</sup> Usually, vaterite crystals are transformed into calcite crystals by Ostwald riping, the dissolution and recrystallization of the calcium carbonate. The molecular weight of the polymer did seem to have an effect as well. For poly(acrylic acid) with lower molecular weight the ACC was better stabilized and the higher molecular weight poly(acrylic acid)

stabilized the formed vaterite crystals better.<sup>8</sup> Thus, with the addition of the highly acidic polymer the crystal polymorph was controlled.

Another form of polymorph control was shown by Freeman et al. for the crystallization of calcite.<sup>9</sup> Here a chicken eggshell protein adsorbs by several cationic arginine groups to an ACC particle thereby forcing the particle to form a calcite structure. These nuclei promote the growth of calcite crystals. The protein is subsequently released and can nucleate new ACC particles.

Another important aspect of the crystal growth is the surface from which the crystal is grown, since the nature of the surface can alter the crystal orientation.<sup>2,10</sup> In studies where the surface is covered by an organic layer different crystal orientations are induced. In the case of a P(Glu-*alt*-Leu) Langmuir layer some crystals showed to yield a (01.2) oriented pyramidal crystal.<sup>11</sup> Crystallization from non-peptide functionalized surfaces containing either phosphate, sulfate, alcohol, ammonium, alkyl or acidic acid groups showed similar results.<sup>12,13</sup> On the different surfaces (gold, silver and silicon wafers) the crystals were oriented differently depending on the substrate and the functional group. This is thought to be the result of the nucleation of the crystals by the surface, favoring other crystal planes compared to the 'normal' (104) orientation.

By addition of the organic molecules to the growing crystal the surface energy is lowered. Hereby the growth of the crystal can be directed towards another surface (Figure 5.1). When a selective adsorption occurs the blocked surfaces will not grow, leaving the highest energy surface to continue the growth.

For amino acids it was shown that the chirality has an effect on the growth of calcium carbonate crystals.<sup>14</sup> In peptides the number of the repeating units of the amino acids does play a role in the formation of steps in the growth of the crystal, as was shown for L-aspartic acid.<sup>15</sup> The side chains of the acidic amino acids can bind to the calcium ions. Other amino acids play a role as well. For example, the hydrophilic character of the amino acids does have an effect on the crystallization. It was shown by Elhadj et al. that the overall hydrophilicity of (short) peptide could be the main driving force for the displacement of water molecules during the crystallization.<sup>16,17</sup>

Natural peptides extracted from the shells of organisms or expressed in microorganisms have also been studied for biomineralization.<sup>17,18</sup> An example is the aragonite peptide AP8 obtained from abalone shell nacre.<sup>17,19</sup> The peptides consist approximately out 35 mol% aspartic acid derivative (not further specified in the original article), 38 mol% Gly and the rest were nine other amino acids. It was shown by AFM that for the calcite crystals the acute surfaces were selectively targeted by the AP8 peptides, resulting in rounded shapes. Crystal growth was increased for both acute and obtuse steps, but was substantially higher for the obtuse steps. By binding to the surface the growth into one direction was preferred, resulting in a stretched crystal.

During the crystallization the additives can also be incorporated into the crystals. For the natural Asperich peptides this was shown with X-ray absorption spectroscopy.<sup>20</sup> This family of peptides found in

the *Atringa rigida* shell has a repeating Asp-Glu-Ala-Asp-Ala-Asp sequence.<sup>21</sup> According to simulations the acidic groups bind to the calcium ions, forming nanoclusters and finally ordering these into an aggregate from which water is excluded to finally form the crystal structure. With the use of fully fluorescent polymers or fluorescent labels the position of the polymers in the crystal can be easily tracked.<sup>22,23</sup> This was done, for example, for an incorporated peptide in the calcite binding  $\alpha$ -helical peptide CBP-1 (77% Ala and 17% Asp).<sup>24</sup> Here the labeled peptide keeps the functionalities that alter the crystallization, without any effect of the fluorescent label, which also keeps its fluorescent property. From calcite seed crystals the addition of the new layers showed incorporated fluorescent peptides.

To find a correlation between the amino acid species and crystal growth is difficult for the natural peptides. The specific order, the high number of amino acids and the protein structure make it complex to compare the different peptides with one another.<sup>18,25</sup> Moreover, they are difficult to obtain or synthesize. For these crystallization experiments polypeptides prepared by N-carboxyanhydride ring-opening polymerization (NCA ROP) could be excellent models.<sup>26-29</sup> Polypeptides with different amino acid compositions can be made as shown in Chapter 3. Easily higher numbers of amino acids (resulting in higher degrees of polymerization) can be incorporated in the polypeptide, but also low molecular weights can be acquired if needed.<sup>30</sup> It has to be noted, though, that the sequence distribution of the amino acid residues in these NCA ROP products will be random and that the NCA ROP products are not monodisperse, contrary to the well-defined natural peptides, making it less likely that secondary and almost impossible that tertiary protein structures are formed solely from one molecule. The random character of the polymerization will not yield a uniform folded structure for all polypeptide molecules. Thus using NCA-based polypeptides eliminates a steric effect from the polypeptide, where otherwise the amino acids on the outer side had the highest probability to affect the biomineralization.<sup>9</sup> However, the importance of the sequential control of the amino acid residues and consequently their folding on the biomineralization is unknown.

In this work we describe the synthesis of fluorescently labeled copolypeptides of L-glutamic acid, L-aspartic acid and L-alanine prepared by NCA ROP. This combination is based on earlier findings with natural peptides containing these amino acids, such as CBP-1, AP-8 and Asprich peptides.<sup>17,21,24</sup> It is known that pure PAsp and PGlu stabilize ACC particles and vaterite, while it was shown that with the addition of hydrophobic amino acids altered calcite crystals are formed. We show the effect of the different compositions of the amino acids in the NCA-based polypeptide on the formation of CaCO<sub>3</sub> crystals. Of interest is the effect of the different used amino acid residues with on the formation of crystal morphology.<sup>6,16</sup> With the use of the fluorescent label we are able to localize the polypeptide during the crystallization in solution as well in the final crystal.

## 5.2 Experimental

### Materials

L-Alanine, L-glutamic acid benzyl ester and L-aspartic acid benzyl ester were ordered from Bachem. Triphosgene,  $\alpha$ -pinene, benzylamine, 5(6)-carboxyfluorescein, TFA, HBr / acetic acid, N-dicyclohexylcarbodiimide, N-hydroxysuccinimide and deuterated TFA were purchased from Sigma-Aldrich. DMF, THF, ethylacetate, n-heptane and diethylether were purchased from Biosolve. NCAs were prepared following procedures as described in Chapter 2.

### Methods

1,1,1,3,3,3-Hexafluoroisopropanol size exclusion chromatography (HFIP SEC) was performed at 40 °C on a system equipped with a Waters 1515 Isocratic HPLC pump, a Waters 2414 refractive index detector (40 °C), a Waters 2707 autosampler, a PSS PFG guard column followed by 2 PFG-linear-XL (7  $\mu$ m, 8\*300 mm) columns in series. HFIP (Apollo Scientific Limited) with potassium trifluoro acetate (3 g/L) was used as eluent at a flow rate of 0.8 mL min<sup>-1</sup>. The molecular weights were calculated against polymethyl methacrylate standards (Polymer Laboratories, M<sub>p</sub> = 580 Da up to M<sub>p</sub> = 7.1\*10<sup>6</sup> Da).

N,N-dimethylformamide size exclusion chromatography (DMF SEC) was performed at 60 °C on a system equipped with a Waters 2695 separation module, a Waters 2414 refractive index detector (40 °C), a Waters 486 UV detector, a PSS GRAM guard column followed by 2 PSS GRAM columns in series of 100 Å (10  $\mu$ m particles) and 3000 Å (10  $\mu$ m particles) respectively. DMF was used as eluent at a flow rate of 1 mL min<sup>-1</sup>. The molecular weights were calculated using polystyrene standards. Before SEC analysis was performed, the samples were filtered through a 0.2  $\mu$ m PTFE filter (13mm, PP housing, Alltech).

<sup>1</sup>H-NMR analyses were performed on a Mercury 400. For the polymers deuterated TFA was used. The composition of the copolymers (Table 5.1) was determined by comparing the integral values of  $\gamma$ -benzyl-L-glutamate at 2.2 ppm (2H),  $\beta$ -benzyl-L-aspartate at 3.2 ppm (2H) and L-Alanine at 1.5 ppm (3H).

Matrix Assisted Laser Desorption / Ionization - Time of Flight - Mass Spectroscopy analysis was carried out on a Voyager DE-STR from Applied Biosystems (laser frequency 20 Hz, 337nm and a voltage of 25kV). The matrix material used was T-2-(3-(4-*t*-Butyl-phenyl)-2-methyl-2-propenylidene)malononitrile (DCTB) (40 mg/ml). Potassium trifluoroacetic acid (KTFA) was added as cationic ionization agent (5 mg/ml). The polymer sample was dissolved in HFIP (1 mg/ml), to which the matrix material and the ionization agent were added (5:1:5), and the mixture was placed on the target plate. Samples were precipitated from the reaction medium in diethylether, filtered and placed in a freezer before measuring. CD-spectroscopy was performed on a Jasco J-815 spectrometer with 0.0045 mM solutions of the polypeptides. With the addition of the salts, 2.9 mM CaCl<sub>2</sub> and 4.8 mM NaHCO<sub>3</sub> concentrations were obtained, while the polypeptide concentration was maintained at 0.0045 mM.

UV-vis absorption spectra were recorded with a Hewlett Packard 8453 between 200 nm and 1000 nm. Samples of the crystallization medium were taken over time from the same experiment. The sample was taken from the middle part of the solution.

Confocal Laser Scanning Microscopy was carried out on a Zeiss LSM 510 META. An argon laser was used for the excitation at 488 nm. 63x C-Apochromat and 20x Plan-Apochromat objectives were used. Fluorescent Laser Microscopy was performed on a Zeiss Axioplan 200M. Plan neofluor 10 x objectives were used.

Scanning electron microscopy studies on the CaCO<sub>3</sub> crystals grown on glass plates were performed on a FEI Quanta 3D FEG at an accelerating voltage of 20 kV, after sputter-coating the samples with gold to increase the conductivity.

Powder X-ray diffraction was performed with a Rigaku Geigerflex instrument equipped with a Cu LF X-ray tube operating at 40 kV and 30 mA. The XRD patterns were recorded for 2 $\theta$  values ranging from 10° to 80° using a scanning rate of 0.02 degrees per second.

## Synthesis

**Synthesis of succinimide ester of 5(6)-carboxyfluorescein.**<sup>31</sup> 5(6)-carboxyfluorescein (2.79 g, 7.41 mmol) was dissolved in 25 ml THF. A second THF solution (25 ml) with N-hydroxy succinimide (1.01 g, 8.78 mmol) and dicyclohexylcarbodiimide (1.71 g, 8.78 mmol) was prepared to which the 5(6)-carboxyfluorescein solution was added slowly. The reaction mixture was left to stir for 2 hours. The solution was filtered and concentrated and precipitated in pentane. After filtration it was dried in a vacuum oven at 40 °C. Yield: 3.30 g, 6.99 mmol, 94%. LC-MS: 474.1 Da (M+H<sup>+</sup>)

**Synthesis of P(BLG-co-Ala).** The NCA monomers of  $\gamma$ -benzyl-L-glutamate (1.99 g, 7.56 mmol) and L-alanine (0.890 g, 7.73 mmol) were dissolved in 25 ml DMF in a Schlenk tube. The solution was stirred at 0 °C until all monomer was completely dissolved. To this a solution of benzylamine (41.1 mg, 0.38 mmol) in 5 ml DMF was added. The reaction mixture was left to stir in a cold water bath of 0 °C for 4 days under a dry nitrogen atmosphere. 4 ml of the solution was precipitated in diethylether, the polypeptide was filtered and dried in vacuo. Yield: 0.261 g, 62.3 wt%.

**Synthesis of fluorescein-labeled P(BLG-co-Ala).** After 4 days of polymerization of P(BLG-co-Ala) the succinimide ester of 5(6)-carboxyfluorescein (0.890 g, 1.89 mmol) was added to the solution. The reaction was stirred for another 24 hours and precipitated twice in diethylether after redissolving in NMP. After this the polymer was dissolved in NMP and dialyzed (membrane cut-off of 3500 Da) for 16 hours. After filtration the solution was precipitated in diethylether. The polypeptide was dried in vacuo at ambient temperature. Yield: 1.71 g, 84.0 wt%

**Synthesis of P(BLA-co-Ala).** The NCA monomers of  $\beta$ -benzyl-L-aspartate (3.00 g, 12.0 mmol) and L-alanine (1.38 g, 12.0 mmol) were dissolved in 40 ml DMF in a Schlenk tube. The solution was stirred at 0 °C until all monomer was completely dissolved. To this a solution of benzylamine (64.9 mg, 0.600 mmol) in 4 ml DMF was added. The reaction mixture was left to stir in a cold water bath of 0 °C for 4 days under a dry nitrogen atmosphere. 20 ml of the solution was precipitated in diethylether, the polypeptide was filtered and dried in vacuo at ambient temperature. Yield: 0.96 g, 62 wt%.

**Synthesis of fluorescein-labeled P(BLA-co-Ala).** After 4 days of polymerization of P(BLA-co-Ala) the succinimide ester of 5(6)-carboxyfluorescein (0.772 g, 1.63 mmol) was added to the solution. The reaction mixture was stirred for another 24 hours and precipitated twice in diethylether after redissolving in NMP. After this the polymer was dissolved in NMP and dialyzed (membrane cut-off of 3500 Da) for 16 hours. After filtration the solution was precipitated in diethylether. The polypeptide was dried in vacuo at ambient temperature. Yield: 0.83 g, 42 wt%

**Synthesis of P(BLA-co-BLG-co-Ala).** The NCA monomers of  $\beta$ -benzyl-L-aspartate (1.89 g, 7.58 mmol),  $\gamma$ -benzyl-L-glutamate (1.98 g, 7.52 mmol) and L-alanine (0.878 g, 7.62 mmol) were dissolved in 44 ml DMF in a Schlenk tube. The solution was stirred at 0 °C until all monomer was completely dissolved. To this a solution of benzylamine (61.8 mg, 0.572 mmol) in 4 ml DMF was added. The reaction mixture was left to stir in a cold water bath of 0 °C for 6 days under a dry nitrogen atmosphere. 18 ml of the solution was precipitated in diethylether, the polypeptide was filtered and dried in vacuo at ambient temperature. Yield: 0.67 g, 48 wt%.

**Synthesis of fluorescein-labeled P(BLA-co-BLG-co-Ala).** After the 6 days of polymerization time of P(BLA-co-BLG-co-Ala) the succinimide ester of 5(6)-carboxyfluorescein (0.840 g, 1.78 mmol) was added to the solution. The reaction mixture was stirred for another 24 hours and precipitated twice in diethylether after redissolving in NMP. After this the polymer was dissolved in NMP and dialyzed (membrane cut-off of 3500 Da) for 16 hours. After filtration the solution was precipitated in diethylether. The polypeptide was dried in vacuo at ambient temperature. Yield: 0.670 g, 27.1 wt%

**Deprotection of fluorescein-labeled P(BLG-co-Ala).** The polypeptide (0.980 g) was dissolved in 12 ml TFA. To this 4 ml of HBr in acetic acid solution was added. The reaction mixture was stirred for 16 hours. Then the solution was precipitated in diethylether. The polypeptide was allowed to settle on the bottom and the solution was decanted. Diethylether was added and the mixture was stirred for 10 minutes after which the solvent was removed again by decantation. This procedure was performed 5 times to get a clear diethylether solution. After filtration residual solvent was removed in vacuo at ambient temperature. Yield: 0.306 g, 45.3 wt%

**Calcium carbonate crystallization (biomimetic crystallization).** The CaCO<sub>3</sub> crystallization experiment was performed following the Kitano procedure.<sup>32</sup> Briefly, all glassware used in the crystallization experiment was thoroughly cleaned with soap, nitric acid solution (10%, overnight), and methanol. The glassware was rinsed three times with ultrapure water (18MΩ/cm) after each cleaning step. A 9 mM supersaturated Ca(HCO<sub>3</sub>)<sub>2</sub> solution was prepared by bubbling CO<sub>2</sub> gas through a suspension of CaCO<sub>3</sub> (3.5-4 g) in ultrapure water (1.5 L) for 90 min to shift the CaCO<sub>3</sub>/ Ca(HCO<sub>3</sub>)<sub>2</sub> equilibrium towards the more water-soluble Ca(HCO<sub>3</sub>)<sub>2</sub>, followed by filtration and bubbling CO<sub>2</sub> gas for another 30 min to dissolve all remaining CaCO<sub>3</sub> particles. For all crystallization reactions the 4.5×10<sup>-3</sup> mM fluorescent-labeled polypeptides solution in pure water was prepared, which was injected into 25 mL of the supersaturated calcium bicarbonate solutions. The solutions were left in unsealed vessels. The crystallization of CaCO<sub>3</sub> was accompanied by the slow loss of CO<sub>2</sub> gas from the supersaturated solution. All crystallization experiments were carried out at room temperature for 72 h.

**Calcium carbonate crystal etching.** The glass slides with the crystals were placed in a 1.0M acetic acid solution for 30 seconds. After this the slides were immediately placed in a beaker with demineralized water. The glass plates were left to dry in a covered container.

## 5.3 Results & discussion

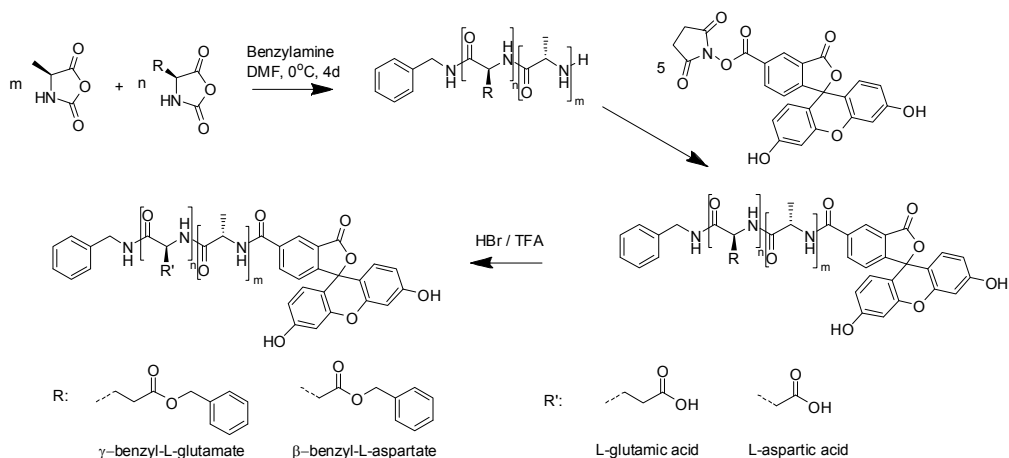
### 5.3.1 Polypeptide preparation

The goal was to prepare copolypeptides of Glu, Asp and Ala, where the both acidic amino acids were combined with the hydrophobic alanine. To study the effect of the different acidic amino acids on the CaCO<sub>3</sub> crystal growth P(Glu-co-Ala) and P(Asp-co-Ala) were prepared with similar quantities of acidic amino acids. P(Asp-co-Glu-co-Ala) was prepared to determine the effect of the simultaneous presence of both acidic monomers in one and the same molecule. The synthesis of the copolypeptides was achieved by living NCA ROP at 0°C for four or six days (Scheme 5.1) with benzyl ester-protected acidic amino acids. The targeted degree of polymerization was kept constant at 40 amino acid units, using equimolar ratios of monomers. The synthesis resulted in polypeptides with expected molecular weights and polydispersity indices in the range of 1.1 - 1.2. As shown previously in Chapter 2 the lower temperature method suppresses the side reactions at the chain ends and prevents the formation of ring structures and chain end termination, as well as main chain side reactions.<sup>33,34</sup> With the amine end group still intact after full monomer conversion this allows further polymer functionalization. From the reaction mixtures approximately one third to a half of the solution was removed for analysis or deprotected with HBr (Table 5.1). The remainder of the prepared polypeptide solution was functionalized with fluorescein. The succinimide ester of 5(6)-carboxylfluorescein was added in an equivalence of 5:1 to the end groups directly into the reaction solution after 4 days. After an additional reaction time of 1 day at 0 °C, the polypeptide solution was precipitated in diethylether, redissolved in NMP and dialyzed to remove the excess of fluorescein and finally was precipitated in diethylether. In



Table 5.1 it can be seen that the polydispersity and the molecular weight increased compared to the unfunctionalized polypeptide. This could be due to a residual amount of NCA monomer that enables continuous chain growth in combination with the extra molecular weight of the fluorescein, which results in a higher hydrodynamic volume. The attachment of one fluorescent group per polypeptide molecule was shown by MALDI-ToF-MS by an increase in the molecular mass of 358 g/mol (Figure 5.2a) for P(Glu-co-Ala) and P(Asp-co-Ala). For the terpolymer P(Asp-co-Glu-co-Ala) the MALDI-ToF-MS spectrum was too complex due to the large number of peaks to indisputably identify a clear shift in the spectrum. SEC combined with UV detection showed the presence of the fluorescent group at 494 nm in the higher molecular weight part of the polypeptide and a small contamination of unreacted fluorescein in the lower molecular weight area of the chromatogram for all functionalized peptides (Figure 5.2b). The <sup>1</sup>H-NMR signals of the side chains of the glutamic acid (2.2 ppm), the aspartic acid (3.2 ppm) and the methyl group of the alanine (1.3 ppm) were used to confirm the agreement of the present amino acid residues in the copolypeptide with the monomer feed ratio.

The polypeptides were deprotected by removal of the benzyl esters with HBr in TFA. The conversion of the benzyl esters was monitored by <sup>1</sup>H-NMR, which showed the decrease of the signal of the benzyl groups at 7.0 ppm and at 5.0 ppm for the two methylene protons.



**Scheme 5.1.** NCA copolymerization, functionalization with fluorescein and deprotection.

The deprotected polypeptides were dispersed in demineralized water using ultrasound to yield a 0.0045 mM polypeptide solution. Due to the lack of counter ions in the solution for the acid side groups of Asp and Glu and due to the hydrophobic character of the polypeptides these were not well dissolved. From the DLS measurements of the 'solutions' particle sizes between 100 nm to 200 nm were determined.

**Table 5.1.** Copolypeptides of Glu, Asp and Ala synthesized for the calcium carbonate mineralization.

| Copolypeptides       | After polymerization <sup>(a)</sup> |                              |      | After deprotection                          |   |
|----------------------|-------------------------------------|------------------------------|------|---|---|
|                      | #                                   | <i>M<sub>n</sub></i> (g/mol) | PDI  | <i>M<sub>n</sub></i> (g/mol) <sup>(b)</sup> | monomer ratio<br>( <sup>1</sup> H-NMR) <sup>(c)</sup> |
| P(BLG-co-Ala)        | 1                                   | 7,300                        | 1.15 | 5,100                                       | 1.0 : 1.0   |
| + fluorescein        | 2                                   | 8,900                        | 1.18 | 6,300                                       | 1.0 : 1.0   |
| P(BLA-co-Ala)        | 3                                   | 6,800                        | 1.13 | 4,600                                       | 1.0 : 1.0   |
| + fluorescein        | 4                                   | 8,100                        | 1.23 | 5,100                                       | 1.0 : 1.1   |
| P(BLA-co-BLG-co-Ala) | 5                                   | 9,000                        | 1.12 | 5,800                                       | 1.0 : 1.0 : 1.0                                       |
| + fluorescein        | 6                                   | 10,000                       | 1.18 | 6,500                                       | 1.0 : 1.0 : 1.0                                       |

a) Measured by HFIP-SEC, calibrated by PMMA standards. b) Approximated by subtracting the weight of the removed benzyl esters. c) The composition is listed in the order of the monomers.

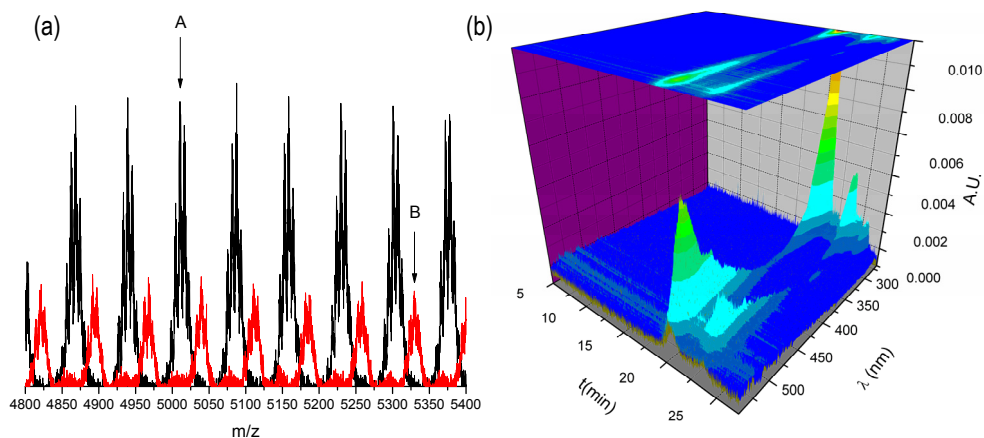


**Figure 5.2.** MALDI-ToF-MS of P(BLG-co-Ala) (black) and fluorescein functionalized (red), P(BLG<sub>17</sub>-co-Ala<sub>16</sub>) (+K<sup>+</sup>) unfunctionalized (A) and functionalized (+H<sup>+</sup>) (B) are pointed out. Difference between A and B is 358 g/mol minus the mass of potassium (39 g/mol) (a). DMF-SEC with UV detection of P(BLG-co-Ala)fluorescein (Entry 2, Table 5.1) (b)

To determine the secondary structure of the copolypeptides CD spectroscopy was performed (Figure 5.3). The calcium carbonate crystallization would be done in a saturated calcium bicarbonate solution. To simulate the effect of the ions on the polypeptide conformation, without the formation of calcium carbonate, polypeptide solutions with 2.9 mM CaCl<sub>2</sub> and 4.8 mM NaHCO<sub>3</sub> were prepared. For P(Asp-co-Ala) and P(Asp-co-Glu-co-Ala) the CD spectra did resemble the typical spectrum of an unordered polypeptide. Calculations with CDPro confirmed that mostly unordered peptide bonds were found. The only one that did show a secondary structure was P(Glu-co-Ala) (Entry 2, Table 5.1), with a dominant  $\alpha$ -helix structure. From the literature it is known that copolypeptides of glutamic acid with a maximum of

30% leucine do resemble an  $\alpha$ -helix structure.<sup>35,36</sup> The preference of L-alanine copolypeptides to form an  $\alpha$ -helix was found for other systems as well. For example, the random copolymers of P(Lys-co-Ala) did show to have an  $\alpha$ -helix conformation for pHs above 9.0.<sup>37</sup> In block copolypeptides of P(BLG-b-Ala) the preference of the separate Ala block to form the helix formation was found as well.<sup>38</sup> The obtained result for P(Glu-co-Ala) was therefore not unexpected. Nevertheless, the differences between the copolypeptides based on the different acidic monomers and the combination of Glu, Asp and Ala are interesting. It seems that the presence of the aspartic acid residue in the copolypeptide does inhibit the formation of a secondary structure. In a 2.9 mM CaCl<sub>2</sub> solution P(Glu-co-Ala) did change partially to a random coil and a distorted  $\alpha$ -helix. A similar effect was seen for the same polypeptide in a 4.8 mM NaHCO<sub>3</sub> solution. For the P(Asp-co-Ala) and P(Asp-co-Glu-co-Ala) the addition of the ions in the solution did not have any effect whatsoever (Figure 5.3c). The fluorescein-labeled polypeptides had the same conformations as the unfunctionalized ones.

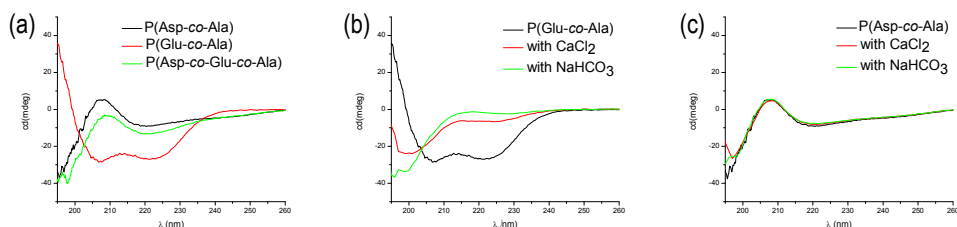


**Figure 5.3.** CD spectra of  $4.5 \times 10^{-3}$  M P(Asp-co-Ala)fluorescein, P(Glu-co-Ala)fluorescein and P(Asp-co-Glu-co-Ala)fluorescein in water (a) and P(Glu-co-Ala)fluorescein (b) and P(Asp-co-Ala)fluorescein (c) in a 2.9 mM CaCl<sub>2</sub> solution or a 4.8 mM NaHCO<sub>3</sub> solution.

### 5.3.2 Crystallization experiments

For the crystallization experiments 1 to 3 ml of the aqueous polypeptide solution was added to 25 ml of the saturated Ca(HCO<sub>3</sub>)<sub>2</sub> solution in a beaker with glass slides at the bottom. The polypeptide concentration was respectively 0.17  $\mu$ M, 0.33  $\mu$ M and 0.48  $\mu$ M in the saturated Ca(HCO<sub>3</sub>)<sub>2</sub> solutions. A saturated calcium bicarbonate solution releases CO<sub>2</sub> resulting in insoluble calcium carbonate and gaseous CO<sub>2</sub>. The crystallization medium was left for three days in a fumehood covered with alumina foil. During this time crystals formed on the glass slides, which in all cases were confirmed by XRD to be calcite crystals. However, clear differences between the crystal morphology could be seen by SEM, both depending on the used copolypeptide and in comparison to the blank experiments (no polypeptide present), which formed orthorhombic crystals.

The P(Glu-co-Ala)-mediated crystals differed from the crystal obtained from the blank in that it shows many planes with round features. Depending on the amount of the polypeptide solution added to the 25

ml of the calcium bicarbonate solution the shape of the crystal is altered (Figure 5.4). At a low polypeptide concentration already some fractured edges were found on the surface of the crystal. The crystal structure with straight edges at low polypeptide concentration progresses towards a crystal with complete round features. For these crystals a flat plateau on top of the crystal is visible.

For P(Asp-co-Ala)-manipulated crystals a similar structure as for P(Glu-co-Ala) with rounded features was found for a low concentration of polypeptide in the solution. As the quantity of the polypeptide was increased, the crystals got elongated features along the crystallographic c-axis with their {104} faces expressed at the end of the crystals (Figure 5.5).<sup>17,18</sup> The steps on the crystal did have more straight features, all sharing the same direction. The number of steps also seems to increase with the increasing concentration of the polypeptide.

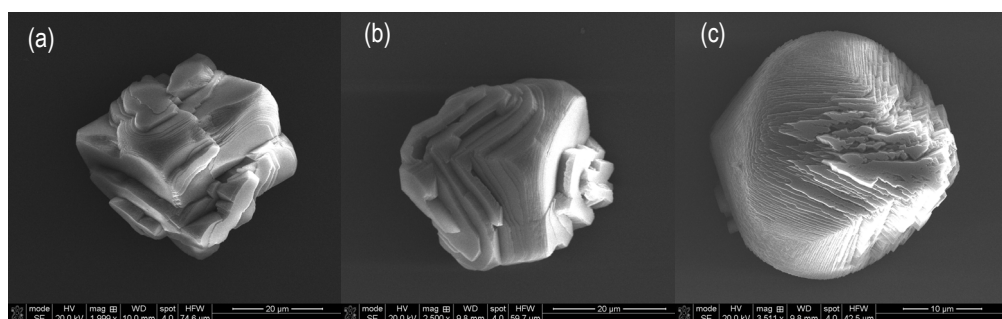


**Figure 5.4.** SEM pictures of calcium carbonate crystals grown in P(Glu-co-Ala)fluorescein (entry 2, Table 5.1) solutions for (a) 0.17  $\mu\text{M}$ , (b) 0.33  $\mu\text{M}$  and (c) for 0.48  $\mu\text{M}$  of P(Glu-co-Ala)fluorescein solution. The scale bars of (a) and (b) are 20  $\mu\text{m}$ . For (c) the scale bar is 10  $\mu\text{m}$ .

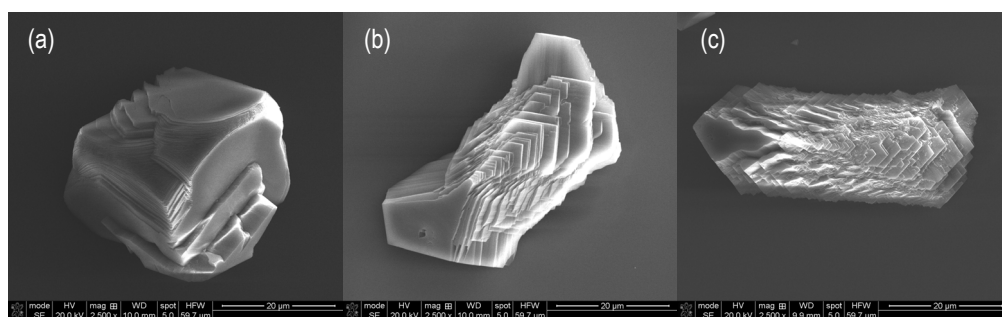


**Figure 5.5.** SEM pictures of calcium carbonate crystals grown in P(Asp-co-Ala)fluorescein (entry 4, Table 5.1) solutions for (a) 0.17  $\mu\text{M}$ , (b) 0.33  $\mu\text{M}$  and (c) for 0.48  $\mu\text{M}$  of P(Asp-co-Ala)fluorescein. The scale bars of (a), (b) and (c) are 20  $\mu\text{m}$ .

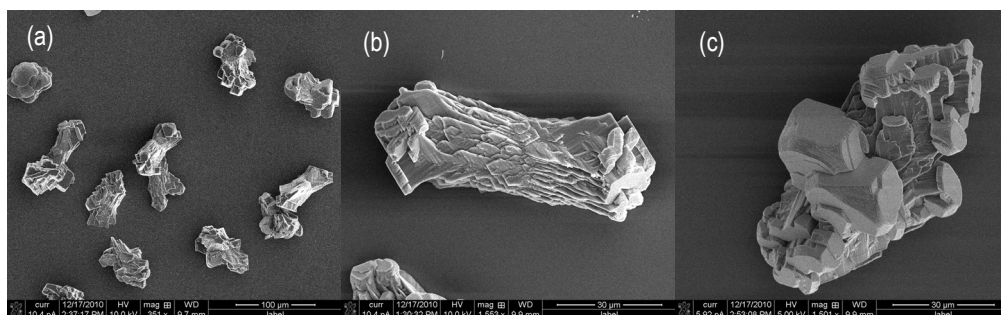


**Figure 5.6.** SEM pictures of calcium carbonate crystals grown with 0.33  $\mu\text{M}$  P(Asp-co-Glu-co-Ala)fluorescein (entry 6, Table 5.1). The scale bar for (a) is 100  $\mu\text{m}$ . The scale bars of (b) and (c) are 30  $\mu\text{m}$ .

Crystals grown in the presence of P(Asp-co-Glu-co-Ala)fluorescein (Figure 5.6a, b) had more resemblance to the features of the crystals grown in the presence of P(Asp-co-Ala). The elongated crystal shape could be obtained with an increase in the concentration from 0.17  $\mu\text{M}$  to 0.33  $\mu\text{M}$ . For 0.48  $\mu\text{M}$  the elongated crystal shape could be observed, however, also impurities of spherical particles were found again. Due to the impurities observed with the crystals grown from the 0.48  $\mu\text{M}$  polypeptide solution, further analysis was done with the crystals prepared in the 0.33  $\mu\text{M}$  solution. Here the crystals could be reproducibly prepared and the shape was uniform. The crystal shapes were not completely identical to the crystals formed in the presence of P(Asp-co-Ala), since some of the crystals were overgrown with rounded calcite rhombs which are crystallographically aligned with the elongated core (Figure 5.6c). The most interesting (and obvious) differences between the crystallization results were found for the P(Asp-co-Ala) and the P(Glu-co-Ala). The role of these polypeptides on the crystallization was thus investigated further.

For the blank crystals, the P(Glu-co-Ala) and for the P(Asp-co-Ala)-mediated crystals the bottom sides of the crystals were inspected by SEM. Instead of a flat surface, in many cases a step-wise structure was found. This could imply that the crystals grow from the bottom of the crystal, pushing the rest of the crystal up while because of the steric limitation of the crystal the calcium carbonate ions cannot be added to the growing crystal in the middle part (Figure 5.7).

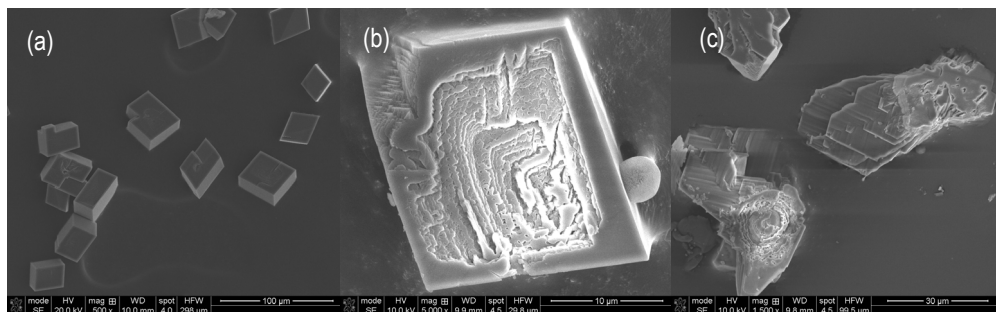


**Figure 5.7.** Bottom side of the crystals blank (a) grown in the presence of P(Glu-co-Ala) (b) and grown in the presence of P(Asp-co-Ala) (c).

To determine the effect of the peptides on the growth process of the surface planes crystals were overgrown to yield a crystal shape that is easier to recognize. The small steps that make the recognition of the calcite crystal harder are then overgrown to yield the more recognizable orthorhombic calcite structure (Figure 5.8). The crystals grown from 0.48  $\mu\text{M}$  polypeptide solution were put in a saturated  $\text{Ca}(\text{HCO}_3)_2$  solution to continue the crystal growth on the surfaces.<sup>39</sup> After 3 days the crystals were taken from the solution and analyzed with SEM. In the case of the crystals grown in the presence of P(Asp-co-Ala) the elongated structure remained. The original crystal was simply overgrown with calcite rhombohedral crystals. The surfaces of the overgrown crystals were mostly aligned in the same direction, showing that the crystals are single crystals and not a cluster of different crystals. When the crystals at the surface were compared not one specific orientation could be found. This indicates that the crystals grown from the glass plates did not have a specific preference for the initiation of a certain crystal orientation.

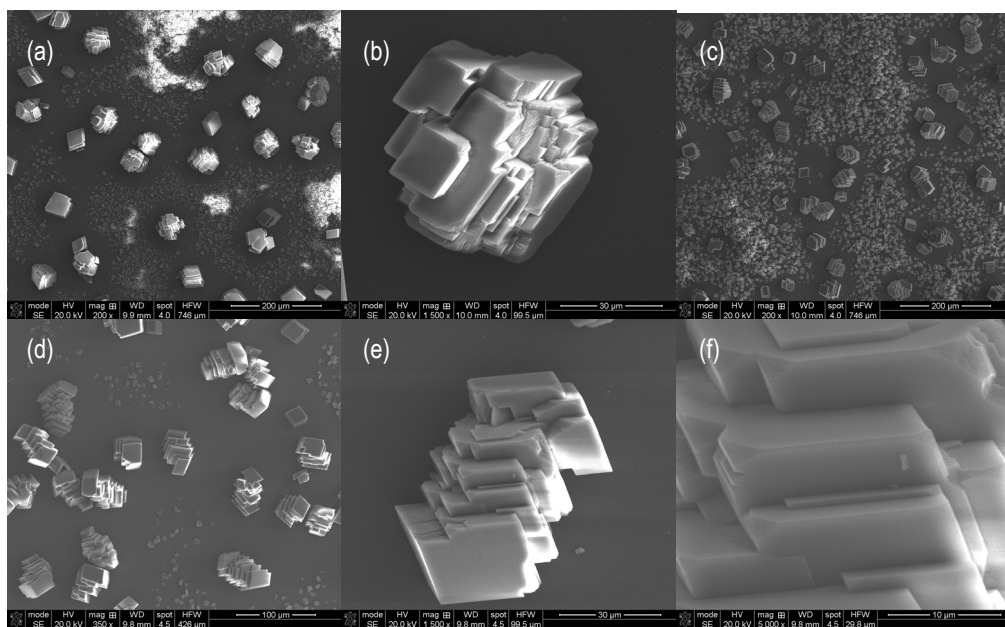


**Figure 5.8.** Overgrown crystals grown in the presence of P(Glu-co-Ala) 0.33  $\mu\text{M}$  (a) and (b), 0.48  $\mu\text{M}$  (c) and those grown in the presence of P(Asp-co-Ala) 0.48  $\mu\text{M}$  (d), (e), (f).

### 5.3.3 Determination of the location of fluorescent polypeptide

To monitor the polypeptide concentration during the crystallization, UV-spectrometry was used. In Figure 5.9a the values of the absorption peaks at 494 nm, characteristic of the fluorescein chain end, are shown during the crystallization at time intervals after 16, 24, 48 and 72 hours. The increase of the absorption signal from the first measurement at the beginning of the crystallization compared to that after 16 hours is due to the sensitivity of the fluorescein to the pH change that occurs during the reaction. The slightly acidic bicarbonate is partially converted into CO<sub>2</sub> and the insoluble calcium carbonate, results in a pH raise from 6.0 to 6.7. The absorption spectrum of the fluorescein responded to this pH range with a shift and increasing peak intensity at 494 nm. The change in the absorption spectrum with pH was confirmed by recording the UV spectrum of the polypeptide of P(Asp-co-Ala) in different buffer solutions in between pH 5.24 and 7.15 (Figures 5.9b, c). The experiments show that the signal at 494 nm is increasing with increasing pH. However, during the crystallization reaction the absorption at 494 nm decreases, which provides qualitative evidence for the incorporation of the polypeptides into the growing crystal. Due to the two opposite effects of the pH and the incorporation into the crystal, the latter cannot be quantified.

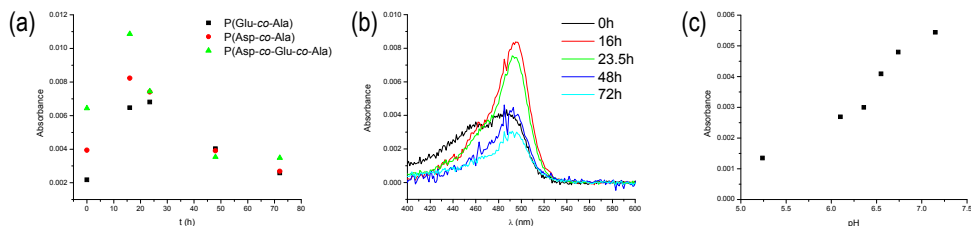


**Figure 5.9.** (a) UV-vis absorbance at  $\lambda=494$  nm of polypeptide solutions P(Glu-co-Ala), P(Asp-co-Ala) and P(Asp-co-Glu-co-Ala) measured over time during the crystallization from the supersaturated Ca(HCO<sub>3</sub>)<sub>2</sub>. (b) UV measurements over time for P(Asp-co-Ala). (c) Absorbance at 494 nm of P(Asp-co-Ala) at a different pH.

Growth of the altered crystal shapes shown by SEM (Figures 5.4 / 5.5 / 5.6) confirmed the effect of the peptide on the crystal growth. Results of UV measurements suggest that during the growth of the crystal the polypeptide was removed from the solution. If the polypeptides are indeed incorporated into the growing crystal, they should be detectable by fluorescence microscopy. First the glass surface surrounding the crystals was investigated but this area did not contain any fluorescent material, which indicates that no physisorption of the polypeptide onto the surface occurs. Images of cross-sections of the crystals, which were 1 to 2  $\mu\text{m}$  apart, were made with the use of confocal scanning laser microscopy (CSLM). For all the crystals the polypeptides could be found inside the crystal, which was evident from their fluorescence. Some regions of the crystals did show more fluorescence than others, suggesting a higher concentration of polypeptide in these areas. For the P(Glu-co-Ala) (Figures 5.10a, b, c) and P(Asp-co-Glu-co-Ala) (Figures 5.10i, j, k) clear fluorescent lines could be found throughout the crystal from top to bottom. For the P(Asp-co-Glu-co-Ala) crystals this line appeared in general in the middle of the crystal. For the P(Asp-co-Ala) (Figures 5.10e, f, g) the crystal showed regimes where less fluorescence was found. This was mostly the case at the straight end of the crystal in the opposite direction of the steps. With the use of a 3D construction of the CSLM pictures the empty parts in the crystals were better identified.



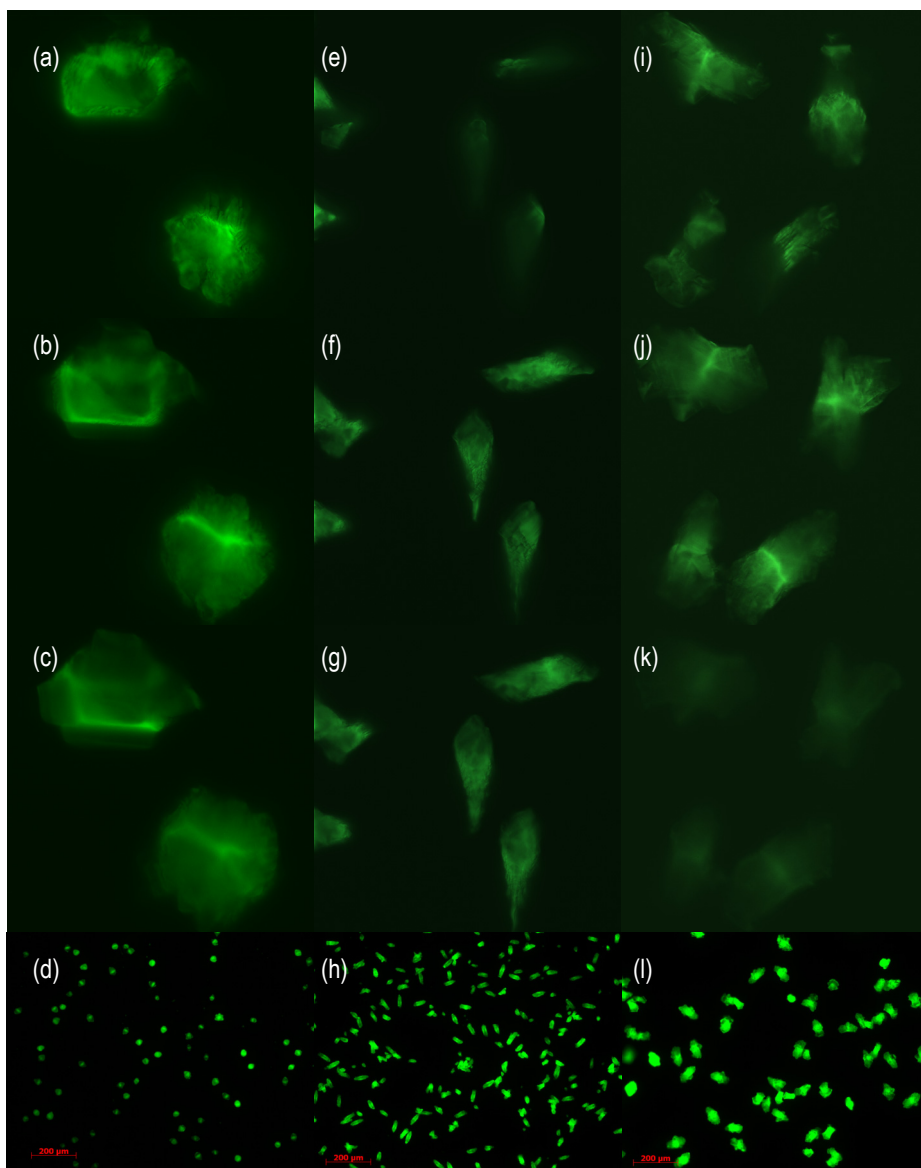


**Figure 5.10.** Confocal scanning laser microscopy (a,b,c) and fluorescence microscopy (d) of crystals grown in the presence of 0.48  $\mu\text{M}$  P(Glu-co-Ala)fluorescein (Entry 2, Table 5.1). The distance between the slices of the CSLM images is 3  $\mu\text{m}$ . Dimensions of the CSLM pictures are 114.4  $\mu\text{m}$  x 114.4  $\mu\text{m}$ . Confocal laser scanning microscopy (e,f,g) and fluorescence microscopy (h) of crystals grown in the presence of 0.48  $\mu\text{M}$  P(Asp-co-Ala)fluorescein (Entry 4, Table 5.1). The distance between the slices of the CSLM images is 6  $\mu\text{m}$ . Dimensions of the CSLM pictures are 142.9  $\mu\text{m}$  x 142.9  $\mu\text{m}$ . Confocal laser scanning microscopy (i,j,k) and fluorescence microscopy (l) of crystals grown in the presence of 0.33  $\mu\text{M}$  P(Asp-co-Glu-co-Ala)fluorescein (Entry 6, Table 5.1). The distance between the slices of the CSLM images is 8  $\mu\text{m}$ . Dimensions of the CSLM pictures are 178.2  $\mu\text{m}$  x 178.2  $\mu\text{m}$ .

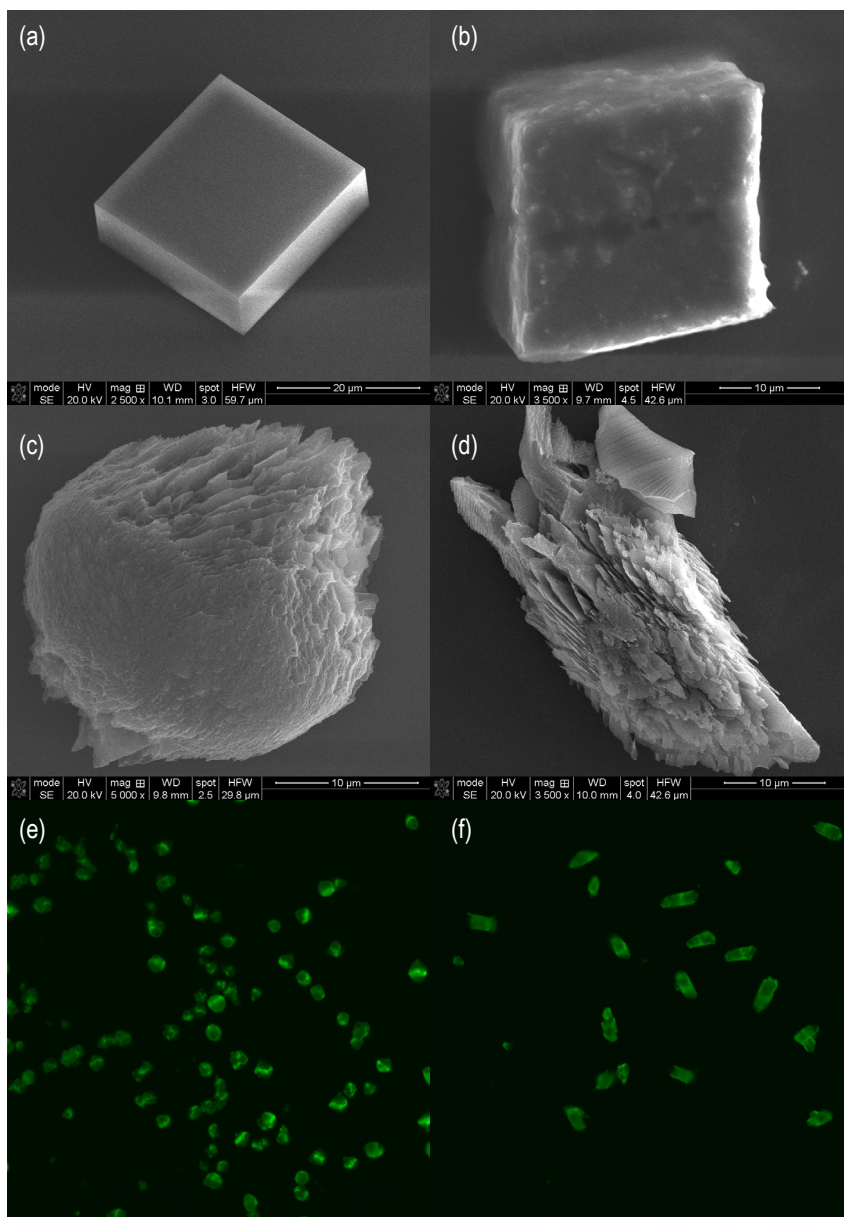


**Figure 5.11.** SEM images of blank (a) and etched blank (b) CaCO<sub>3</sub> crystals. SEM pictures of the etched CaCO<sub>3</sub> crystal grown in the presence of P(Glu-co-Ala)fluorescein (c) and CaCO<sub>3</sub> crystal grown in the presence of P(Asp-co-Ala)fluorescein (d). CSLM of etched CaCO<sub>3</sub> crystal grown in the presence of P(Glu-co-Ala)fluorescein (e) and CaCO<sub>3</sub> crystal grown in the presence of P(Asp-co-Ala)fluorescein (f). The size of the CSLM pictures is 636.4 μm x 636.4 μm. The CSLM image was taken in the centre of the crystals.

To further confirm the presence of the fluorescent marker inside the crystals further experiments were done. The crystals grown on a glass slide were etched in a solution of 1.0 M acetic acid for 30 seconds and then were washed in water. The polypeptide manipulated crystals did lose their original structure (Figure 5.11). For the crystal grown in the presence of 0.48  $\mu\text{M}$  P(Asp-co-Ala)fluorescein the stretched features from the crystal were still visible although the surface had changed drastically. A highly open structure consisting out of elongated plates were found. The direction of these plates was easily determined for the P(Asp-co-Ala)fluorescein modified crystals, due to their elongated character. For the crystals grown in the presence of 0.48  $\mu\text{M}$  P(Glu-co-Ala)fluorescein the alteration from the original crystal towards the etched crystal is harder to recognize. If the parts of the crystal with more steps is etched quicker, then the rounded part should be in the area where originally the flat plateau could have been located.

The fluorescence was measured before and after the etching. Fluorescence did remain in the crystals, confirming that the polypeptide must have been incorporated in the crystals. It has been shown that incorporated additives might alter the dissolution properties of CaCO<sub>3</sub>.<sup>40,41</sup> In this case the same might be proposed, although the polypeptide inside the crystal could have preserved some inner parts of the crystal better than the parts on the outer side during the etching. From this the direction of the crystal surfaces on which the peptides are attached can be found.

## 5.4 Conclusions

In summary, the fluorescein-labeled random copolypeptides consisting of L-aspartic acid, L-glutamic acid and L-alanine have successfully been applied to investigate the effect on CaCO<sub>3</sub> mineralization. Living NCA ROP at 0 °C was used for the synthesis of the random copolypeptides followed by the functionalization with fluorescein. All copolypeptides showed an unordered chain structure, apart from the P(Glu-co-Ala), which showed an  $\alpha$ -helix configuration. This was altered in the presence of ions resulting in a more unordered conformation. P(Asp-co-Ala) and P(Asp-co-Glu-co-Ala) did seem to have a random structure and were not altered by the presence of ions during the crystallization. The formed crystal structures proved to greatly depend on the added polypeptide solution. The crystals P(Asp-co-Ala) were elongated along the crystallographic axis with straight steps, while the crystals grown in a P(Glu-co-Ala) solution were round with rounded steps. For the P(Asp-co-Glu-co-Ala) again elongated crystals were found, however also crystal structures attached to the centre of the crystal were found. The overgrown crystal structures formed in the presence of P(Asp-co-Ala) and P(Glu-co-Ala) did show that the crystal orientation of the surface was not specific. With the use of the fluorescent label it was shown that the polypeptide was removed from the solution during the crystallization and was incorporated into the crystals. Upon etching of the formed crystals the used fluorescence techniques were validated and the altered solubility properties of the polypeptide in the crystals were shown.

## References

- <sup>1</sup> F. Meldrum and H. Cölfen, *Chem. rev.* **2008**, 108, 4332-4432
- <sup>2</sup> D. Gebauer, A. Völkel and H. Cölfen, *Science* **2008**, 322, 1819-1822
- <sup>3</sup> E. Pouget, P.H. H. Bomans, J. A. C. M. Goos, P.M. Frederik, G. de With and N.A.J.M. Sommerdijk, *Science* **2009**, 323, 1455-1458
- <sup>4</sup> L.B. Gower, *Chem. Rev.* **2008**, 108, 4551-4627
- <sup>5</sup> J. Aizenberg, G. Lambert, S. Weiner and L. Addadi, *J. Am. Chem. Soc.* **2002**, 124, 32-39
- <sup>6</sup> B. Njagic-Dzakula, L. Brecevic, G. Falini and D. Kralj, *Cryst. Growth Des.* **2009**, 9, 2425-2434
- <sup>7</sup> N. Loges, K. Graf, L. Nasdala and W. Tremel, *Langmuir* **2006**, 22, 3073-3080
- <sup>8</sup> S.-C. Huang, K. Naka and Y. Chujo, *Polym. J.* **2008**, 40, 154-162
- <sup>9</sup> C.L. Freeman, J.H. Harding, D. Quigley and P.M. Rodger, *Angew. Chem. Int. Ed.* **2010**, 49, 5135 - 5137
- <sup>10</sup> N.A.J.M. Sommerdijk and G. de With, *Chem. Rev.* **2008**, 108, 4499-4550
- <sup>11</sup> S. Cavalli, D.C. Popescu, E.E. Tellers, M.R.J. Vos, B.P. Pichon, M. Overhand, H. Rapaport, N.A.J.M. Sommerdijk and A. Kros, *Angew. Chem. Int. Ed.* **2006**, 45, 739-744
- <sup>12</sup> D.D. Archibald, S.H. Qadri and B.P. Gaber, *Langmuir* **1996**, 12, 538-546
- <sup>13</sup> J. Aizenberg, A.J. Black and G.M. Whitesides, *J. Am. Chem. Soc.* **1999**, 121, 4500-4509
- <sup>14</sup> C.A. Orme, A. Noy, A. Wierzbicki, M. T. McBride, M. Grantham, H.H. Teng, P.M. Dove and J.J. DeYoreo, *Nature* **2001**, 411, 775-779
- <sup>15</sup> S. Elhadj, E.A. Salter, A. Wierzbicki, J.J. De Yoreo, N. Han and P.M. Dove, *Cryst. Growth Des.* **2006**, 6, 197-201
- <sup>16</sup> S. Elhadj, J.J. De Yoreo, J.R. Hoyer and P.M. Dove, *Proc. Natl. Acad. Sci. U. S. A.*, **2006**, 103, 19237-19242
- <sup>17</sup> G. Fu, S.R. Qui, C.A. Orme, D.E. Morse and J.J. De Yoreo, *Adv. Mater.* **2005**, 17, 2678-2683
- <sup>18</sup> Y. Yamamoto, T. Nishimura, A. Sugawara, H. Inoue, H. Nagasawa and T. Kato, *Cryst. Growth Des.* **2008**, 8, 4062-4065
- <sup>19</sup> G. Fu, S. Valiyaveetil, B. Wopenka and D.E. Morse, *Biomacromolecules* **2005**, 6, 1289-1298
- <sup>20</sup> R.A. Metzler, G.A. Tribello, M. Parrinello and P.U.P.A. Gilbert, *J. Am. Chem. Soc.* **2010**, 132, 11585-11591
- <sup>21</sup> B.-A. Gottiv, N. Kessler, J.L. Sumerel, D.E. Morse, N. Tuross, L. Addadi and S. Weiner, *ChemBioChem* **2005**, 6, 304-314
- <sup>22</sup> L. Dai, X. Cheng and L.B. Gower, *Chem. Mater.* **2008**, 20, 6917-6928
- <sup>23</sup> S. Sindhu, S. Jegadesan, L. Hairong, P.K. Ajikumar, M. Vetrichelvan and S. Valiyaveetil, *Adv. Funct. Mat.* **2007**, 17, 1698-1704
- <sup>24</sup> D.B. Deoliveira and R.A. Laursen, *J. Am. Chem. Soc.* **1997**, 119, 10627-10631
- <sup>25</sup> D.L. Masica, S.B. Schrier, E.A. Specht and J.J. Gray, *J. Am. Chem. Soc.* **2010**, 132, 11252-12262
- <sup>26</sup> Y. Yao, W. Dong, S. Zhu, X. Yu and D. Yan, *Langmuir* **2009**, 25, 13238-13243
- <sup>27</sup> S. Hayashi, K. Ohkawa and H. Yamamoto, *Macromol. Biosci.* **2006**, 6, 228-240
- <sup>28</sup> P. Kašparová, M. Antonietti and H. Cölfen, *Colloids Surf. A* **2004**, 250, 153-162
- <sup>29</sup> J.N. Cha, G.D. Stucky, D.E. Morse and T.J. Deming, *Nature*, **2000**, 403, 289-292
- <sup>30</sup> H.R. Kricheldorf, *Angew. Chem. Int. Ed.* **2006**, 45, 572-5784
- <sup>31</sup> G. Ye, N.-H. Nam, A. Kumar, A. Saleh, D.B. Shenoy, M.M. Amiji, X. Lin, G. Sun and K. Parang, *J. Med. Chem.* **2007**, 50, 3604-3617
- <sup>32</sup> Y. Kitano, K. Park and D.W. Hood, *J. Geophys. Res.* **1963**, 67, 4873-4874
- <sup>33</sup> G.J.M. Habraken, M. Peeters, C.H.J.T. Dietz, C.E. Koning, A. Heise, *Polym. Chem.* **2010**, 1, 514-524

- <sup>34</sup> W. Vayaboury, O. Giani, H. Cottet, A. Deratani and F. Schué, *Macromol. Rap. Commun.* **2004**, 25, 1221-1224
- <sup>35</sup> R.E Nylund and W.G. Miller, *J. Am. Chem. Soc.* **1965**, 87, 3537-3542
- <sup>36</sup> R.E Nylund and W.G. Miller; *J. Am. Chem. Soc.* **1965**, 87, 3542-3547
- <sup>37</sup> H. Sugiyama and H. Noda, *Biopolymers* **1970**, 9, 459-469
- <sup>38</sup> A. Gitsas, G. Floudas, M. Mondeshki, H.W. Spiess, T. Aliferis, H. Iatrou and N. Hadjichristidis, *Macromolecules* **2008**, 41, 8072 - 8080
- <sup>39</sup> J. Aizenberg, G. Lambert, S. Weiner and L. Addadi, *J. Am. Chem. Soc.* **2002**, 124, 32-39
- <sup>40</sup> L.A. Estroff, L. Addadi, S. Weiner and A.D. Hamilton, *Org. Biomol. Chem.* **2004**, 2, 137-141
- <sup>41</sup> H. Li and L.A. Estroff, *Adv. Mat.* **2009**, 21, 470-473

# Chapter 6

## Peptide Block Copolymers by N-Carboxyanhydride Ring Opening Polymerization and Atom Transfer Radical Polymerization

### Abstract

*The synthesis of polypeptide-containing block copolymers combining N-carboxyanhydride (NCA) ring opening polymerization (ROP) and atom transfer radical polymerization (ATRP) was investigated. An amide initiator comprising an amine function for the NCA polymerization and an activated bromide for ATRP was used. Well-defined polypeptide macroinitiators were obtained from  $\gamma$ -benzyl-L-glutamate NCA, O-benzyl-serine NCA, and N $\epsilon$ -benzyloxycarbonyl-L-lysine. Subsequent ATRP macroinitiation from the polypeptides resulted in higher than expected molecular weights. Analysis of the reaction products and model reactions confirmed that this is due to the high frequency of termination reactions by disproportionation in the initial phase of the ATRP, which is inherent in the amide initiator structure. In some cases selective precipitation could be applied to remove unreacted macroinitiator to yield well-defined block copolymers.*

Chapter based on G.J.M. Habraken, C.E. Koning and A. Heise, *J. Polym. Sci. A: Polym. Chem.* **2009**, 47, 6883-6892

## 6.1 Introduction

The conjugation of natural polymers like proteins with synthetic polymers can result in novel materials for biomedical applications and has therefore created increased interest recently.<sup>1</sup> The availability of controlled radical polymerization techniques accelerated the development of a wide range of peptide-polymer conjugates as it conveniently allows control over the polymer end-groups, the molecular weight and the polydispersity index (PDI) of the synthetic polymer block. In particular, atom transfer radical polymerization (ATRP) has been applied in the synthesis of bioconjugates because of the straightforward functionalization of biomolecules with the ATRP initiator via amine functionalities, leading to amide ATRP initiator units. The wide range of monomers polymerizable by this method further explains the popularity of ATRP in the synthesis of bioconjugates.

In some reported examples, polypeptides were synthesized by step-wise condensation of amino acids, either on solid supports or in solution, and, after functionalization with an ATRP initiator, used as oligo-initiators.<sup>2-5</sup> While this method allows for the defined synthesis of (sequenced) peptide blocks, the synthesis is tedious and the molecular weight of the peptide limited by the step-wise addition chemistry under protection-deprotection conditions. Another approach to polypeptide blocks is the ring opening polymerization (ROP) of amino acid N-carboxyanhydrides (NCAs).<sup>6</sup> Traditionally NCA polymerization conveniently allows for the preparation of high molecular weight polypeptides, however without much control over PDI and polymer architecture. This changed in recent years with the development of several synthetic approaches towards controlled NCA polymerization.<sup>7-11</sup> The combination of both controlled NCA and radical polymerization techniques can thus lead to a variety of well-defined functional bioconjugates with interesting self-assembly properties.<sup>12</sup> Consequently, a number of block and graft copolymers have been reported in the literature applying both techniques. Zhang et al. reported the combination of reversible addition-fragmentation transfer (RAFT) with  $\gamma$ -benzyl-L-glutamate (BLG) NCA polymerization<sup>13</sup>, whilst the combination of ATRP with NCA polymerization was initially described by Deming.<sup>14</sup> Both approaches have in common that the controlled radical polymerization was conducted first, producing an amino-terminated macroinitiator for the NCA polymerization. The inversed strategy, i.e. NCA polymerization followed by controlled radical polymerization was also applied; for example, Menzel investigated ATRP from polypeptides obtained by metal-mediated NCA polymerization.<sup>15</sup> Previously, our group reported the synthesis of polypeptide-based block copolymers by the combination of NCA ring opening polymerization and nitroxide mediated radical polymerization (NMRP).<sup>16</sup> In our approach we first synthesized a PBLG macroinitiator end-functionalized with an NMP initiator group by well-controlled NCA polymerization at 0 °C followed by the polymerization of styrene. The NCA polymerization at 0 °C was initially described by Vayaboury et al. and has the advantage that it is synthetically less demanding than other controlled NCA polymerization techniques, whilst offering very good control over the molecular weight and polydispersity.<sup>9</sup> However, its versatility for the polymerization of a larger range of amino acid NCAs has not yet been shown. Moreover, we are aiming

to combine this technique with ATRP, as the latter is capable of polymerizing a much larger variety of vinyl monomers than NMRP.

In this paper we investigate the feasibility of combining both approaches with the goal to develop a synthetic strategy that allows the combination of a variety of amino acids for the peptide block with a variety of vinyl monomers for the synthetic block. Special attention was given to the elucidation of a side-reaction promoted by the amide ATRP initiator.

## 6.2 Experimental

### Materials

CuBr, CuCl, 1,1,4,7,10,10-hexamethyltriethylenetetramine (HMTETA), anisole, TFA, NaOH, MgSO<sub>4</sub>, Al<sub>2</sub>O<sub>3</sub>, L-lysine, S-benzyl-L-cysteine, N<sub>ε</sub>-benzyloxycarbonyl-L-lysine, *tert*-butyloxycarbonyl anhydride,  $\alpha$ -pinene, bis(trichloromethyl) carbonate and P<sub>2</sub>O<sub>5</sub> were purchased from Sigma-Aldrich. O-Benzyl-L-serine,  $\gamma$ -benzyl-L-glutamate were purchased from Bachem. Dichloromethane, ethylacetate, diethylether, methanol, DMSO and DMF were purchased from Biosolve and kept under nitrogen. HFIP was purchased from Biosolve, AR-S from supplier or redistilled. Methylmethacrylate, methylacrylate and *tert*-butylmethacrylate were purified over an Al<sub>2</sub>O<sub>3</sub> column. All NCAs were prepared according to methods described in Chapter 2. Tris(2-dimethylaminoethyl)amine (Me<sub>6</sub>TREN) was synthesized according to literature procedures.<sup>17</sup>

### Methods

SEC analysis using HFIP (Biosolve, AR-S from supplier or redistilled) as eluent was carried out using a Shimadzu LC-10AD pump (flow rate 0.8ml/min) and a WATERS 2414 with a differential refractive index detector (at 35 °C) calibrated with poly(methyl methacrylate). Two PSS PFG-lin-XL (7  $\mu$ m, 8\*300 mm) columns at 40 °C were used. Injections were done by a Spark Holland MIDAS injector using a 50  $\mu$ L injection volume.

High Performance Liquid Chromatography - Mass Spectroscopy was carried out on an Agilent 1100 series setup with an Agilent MSD type SL (G1946D). The column used was a Zorbax RX-C8; 2.1 x 150 mm; 5 $\mu$ m. The eluent was methanol at 25 °C with a flow of 0.25 ml/min. Detection was done by UV and MS with Atmospheric Pressure Electrospray Interface. The conditions for the AP-ESI: pressure: 30 psi; capillary voltage: 4000V; and dry gas: 13 L/min; 350 °C.

Matrix Assisted Laser Desorption/Ionization - Time of Flight - Mass Spectroscopy (MALDI-ToF-MS) analysis was carried out on a Voyager DE-STR from Applied Biosystems (laser frequency 20 Hz, 337nm and a voltage of 25kV). The matrix material that was used was DCTB (40mg/ml). Potassium trifluoroacetic acid was added as cationic ionization agent (5mg/ml). The polymer sample was dissolved in HFIP (1mg/ml). A mixture of the matrix material, the ionization agent and the polymer sample was made (5:1:5) and placed on the target plate.



$^1\text{H-NMR}$  was performed on a Mercury 400 or Mercury 200 in deuterated chloroform and deuterated DMSO. For the polymers deuterated TFA was used.

Gas Chromatography analysis was performed on a Hewlet Packard 5890 Series II GC with an Agilent 6890 series injector. Samples of the ATRP reaction were taken with the use of a three-way valve by which nitrogen was pumped through the needle to prevent the introduction of oxygen to the system. The samples were precipitated in 40 ml methanol per 1 ml of DMF solution. From this the GC samples were taken with the use of a syringe and a filter. Calculations were made with the use of an internal standard (anisole).

## Synthesis

**Synthesis of Initiator 2.** *tert*-Butyl-2-(2-bromo-2-methylpropanamido)ethylcarbamate, initiator **1**, was prepared following a literature procedure.<sup>18</sup> For the deprotection it was dissolved in a 25 % TFA/dichloromethane solution (1.5 g, 4.9 mmol). After 3 hours the dichloromethane was removed by evaporation. To this first water and then a NaOH solution was added until the pH was above 11. The aqueous solution was extracted by dichloromethane. After drying with  $\text{MgSO}_4$  the sample was concentrated and a yellowish oil remained. Yield: 0.98 g (4.7 mmol), 96 %.  $^1\text{H-NMR}$  (400 MHz,  $\text{CDCl}_3$ ,  $\delta$ , ppm): 1,95 ppm (s, 6H,  $\text{CH}_3$ ), 2,51 ppm (s, 2H,  $\text{NH}_2$ ) 2,85 ppm (t, 2H,  $J = 5.9$ ,  $\text{CH}_2\text{NH}_2$ ), 3,30 ppm (q, 2H,  $J = 5.9$ ,  $\text{CH}_2\text{NH}$ ), 7,24 ppm (s, 1H, NH),  $^{13}\text{C-NMR}$  (400 MHz,  $\text{CDCl}_3$ ,  $\delta$ , ppm): 32.36 ( $\text{CH}_3$ ), 40.77 ( $\text{CH}_2\text{NH}_2$ ), 42.35 ( $\text{CH}_2\text{NH}$ ), 63.34 (CBr), 172.40 (C(O)NH), LC-MS: 209.1 Da  $[\text{M}+\text{H}]^+$ , 211.1 Da  $[\text{M}+\text{H}]^+$ .

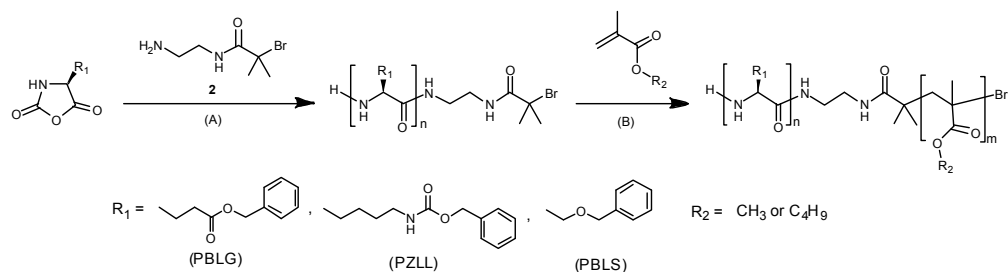
**Typical NCA polymerization.** NCA of  $\gamma$ -benzyl-L-glutamate (11.2 g, 42.6 mmol) was dissolved in dry DMF (50 ml). The bifunctional initiator **2** (588 mg, 2.84 mmol) was also dissolved in dry DMF (5 ml) and added to the NCA solution. The reaction mixture was stirred at 0 °C for 4 days. After precipitation in diethylether the polymer was dried in a vacuum oven overnight at room temperature. Yield: 7.7 g, 78 wt%.

**Model ATRP reactions.** CuBr (115 mg, 0.80 mmol) and HMTETA (185 mg, 0.80 mmol) were dissolved in DMF (10 ml) after deoxygenation by  $\text{N}_2$  and heated to 60 °C. *tert*-Butyl-2-(2-bromo-2-methylpropanamido)ethylcarbamate, initiator **1**, was added (255 mg, 0.82 mmol) and after 0.5 hour the copper was removed with a  $\text{Al}_2\text{O}_3$  column. The reaction mixture was evaporated to dryness.

**ATRP from polypeptide macroinitiator.** The macroinitiator of poly( $\gamma$ -benzyl-L-glutamate) (PBLG) (310 mg, 0.11 mmol), CuCl (12 mg, 0.12 mmol) and MMA (2.58 g, 26 mmol) were dissolved in 6 ml DMF in a Schlenk tube. In a second Schlenk tube a solution of HMTETA (44 mg, 0.19 mmol) in 3 ml DMF was prepared. After three freeze-thaw cycles of both Schlenk tubes the HMTETA solution was added to the reaction mixture. The temperature was first kept at 25°C for one hour, then raised to 60 °C. Conversion

was measured by GC with anisole as an internal standard. After polymerization the polymer was precipitated in methanol, filtered and dried in a vacuum oven.

### 6.3 Results and discussion



**Scheme 6.1.** Synthesis of polypeptide conjugates; (A) 0 °C, DMF, 4 days; (B) RT-60 °C, 5h, HMTETA, CuCl, DMF, anisole.

The synthetic strategy towards the polypeptide bioconjugates is shown in Scheme 6.1. In the first step we employ a bifunctional initiator **2**, which contains a primary amine as the initiator for the NCA ROP and an activated bromide for the ATRP. The amide structure of the initiator was specifically chosen so as to avoid the presence of any ester group in the polymer. Due to the higher susceptibility to hydrolysis as compared to polypeptide amide bonds, an ester bond in the polymer main chain would represent a potentially weak link between the two blocks. For example, in the polymer analogous deprotection of the  $\gamma$ -benzyl-L-glutamate, this could lead to scission of the two blocks.

The feasibility of this double-headed initiator in the NCA polymerization of various NCAs was first investigated with the aim of obtaining well-defined polypeptides with the ATRP initiator attached to the polypeptide-chain end. The initiation of ATRP was then carried out from the polypeptide macroinitiator in a second step.

#### 6.3.1 NCA polymerizations

All monomers were first polymerized in DMF at 0 °C using benzylamine as an initiator in order to determine their polymerization behavior and then using initiator **2** to obtain ATRP macroinitiators (Table 6.1). After precipitation in diethylether, white powders were obtained in all cases and characterized by SEC in hexafluoroisopropanol (HFIP SEC) and MALDI-ToF-MS. Under the applied conditions all polymerizations produced polypeptides with low polydispersities between 1.1 and 1.2. The SEC traces were monomodal, except for poly( $N_\epsilon$ -benzyloxycarbonyl-L-lysine) (PZLL) and poly( $N_\epsilon$ -*t*-butyloxycarbonyl-L-lysine), where a bimodal distribution was observed. During the NCA polymerizations,  $\beta$ -sheet conformation of the latter two polypeptides can compete with the  $\alpha$ -helix conformation.<sup>19</sup> The extent of both conformations is dependent on the molecular weight and the solvent

conditions, but it also depends on the nature of the amino acid itself. A bimodal distribution suggests that  $\beta$ -sheet-organized polypeptides exist alongside the  $\alpha$ -helix conformation.

**Table 6.1.** Polymerization results of NCAs of various amino acids initiated by the bifunctional initiator **2**. All SEC data were obtained in HFIP calibrated with PMMA standards.

| Entry | Polymer   | $M_{n,theor}$<br>(g/mol) <sup>(a)</sup> | $M_n$<br>(g/mol) | $M_w$<br>(g/mol) | PDI | $M_n$ ( <sup>1</sup> H-NMR) <sup>(b)</sup> |
|-------|---|---|------------------|------------------|-----|--|
| 1     | poly( $\gamma$ -benzyl-L-glutamate)                       | 2,800                                   | 3,700            | 4,100            | 1.1 | 2,600                                      |
| 2     | poly( $\gamma$ -benzyl-L-glutamate)                       | 2,800                                   | 5,600            | 6,100            | 1.1 | 3,100                                      |
| 3     | poly( $\gamma$ -benzyl-L-glutamate)                       | 3,500                                   | 5,100            | 5,500            | 1.1 | 4,200                                      |
| 4     | poly( $N_\epsilon$ -benzyloxycarbonyl-L-lysine)           | 5,300                                   | 7,600            | 8,400            | 1.1 | 5,200                                      |
| 5     | poly( $N_\epsilon$ - <i>t</i> -butyloxycarbonyl-L-lysine) | 2,700                                   | 6,300            | 7,700            | 1.2 | -  |
| 6     | poly(O-benzyl-L-serine)                                   | 3,800                                   | 5,700            | 6,100            | 1.1 | 3,800                                      |

(a) Theoretical molecular weight calculated from the monomer to initiator ratio.

(b) Calculated from integral ratio of the benzyl protons (7.3 ppm) to that of the *tert*-butyl protons (2.0 ppm).

While all polymers have a low PDI (1.1 – 1.2), the molecular weights obtained from SEC analysis are higher than the corresponding theoretical molecular weights. This is presumably an effect of the helical structure and the different chemical nature of the polypeptide as compared to the PMMA standards. When the  $M_n$  values were calculated from <sup>1</sup>H-NMR better agreement with the theoretical values was found. MALDI-ToF-MS analysis shows that all polymers were indeed initiated from the bifunctional initiator. Figure 6.1 shows the example of PBLG with the respective peak assigned to the polymer with the initiator end-group at  $m/z$  3,536 (DP = 15). In addition, polymer chains terminated with the pyroglutamate chain end were found at  $m/z$  3,428. The latter is caused by intramolecular ring closure and is typically observed for PBLG upon storage at room temperature (Chapter 2). Moreover, all samples show several other small peaks due to end-group fragmentation presumably occurring during the ionization process.

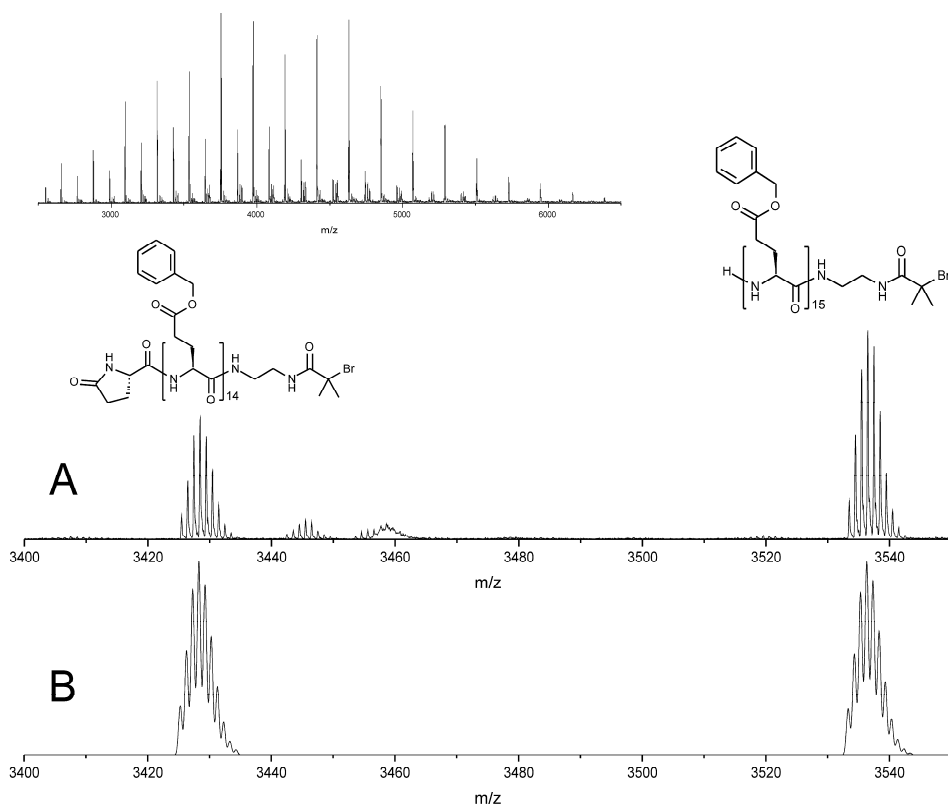


**Figure 6.1.** Measured (A) and calculated (B) MALDI-ToF-MS spectrum of poly( $\gamma$ -benzyl-L-glutamate) initiated from the bifunctional ATRP initiator 1.

### 6.3.2 ATRP macroinitiation

$\alpha$ -Halogen amide initiators have been used only rarely in ATRP (as opposed to ester-based initiators) because of their problematic reaction control.<sup>20</sup> It is generally observed that when amide-based initiators are used the obtained molecular weights are significantly higher than the theoretical ones. In a systematic study on amide-based initiators Haddleton concluded that a high termination rate during the initiation step leads to a decrease of the actual initiator concentration, resulting in higher than calculated molecular weights. This can be overcome by reducing the initiation rate by altering the reaction conditions and the catalyst, for example by using CuCl as the catalyst.<sup>21</sup> Several papers have also appeared, describing the ATRP from either amino acid or oligo-peptide amides.<sup>5,22</sup> Previously, Adams and coworker systematically investigated ATRP from oligo(phenyl alanine) (up to trimers) and again found higher than expected molecular weights and higher polydispersities than for ester-based initiators.<sup>3</sup> Although the discrepancy between theoretical and obtained molecular weight due to a high termination rate in the initiation step has been acknowledged by several authors, there is no study

describing the nature of this termination. Moreover, all studies were done on amino acid or oligomeric peptides. Since our goal is the synthesis of higher molecular weight peptide conjugates of various amino acids employing ATRP, we attempted the ATRP macroinitiation from the polypeptides listed in Table 6.1. Initially, the PBLG end-capped with the ATRP amide initiator was used as a model system. The PBLG macroinitiator was dissolved in DMF or DMSO, respectively, together with the copper catalyst (CuBr/Me<sub>6</sub>TREN or CuBr/HMTETA) and MMA monomer. Notably, the monomodal molecular weight distribution of the PBLG macroinitiator does not merely gradually shift to higher molecular weight with the reaction time of the ATRP (Figure 6.2). Instead, the macroinitiator trace decreases during the course of the polymerization while the molecular weight of the block copolymer increases, as evident from the peak shift in Figure 6.2. A significant amount of macroinitiator remains unreacted, even after prolonged reaction time. The conversion of the monomer shows a very fast increase at the start of the reaction, followed by a slower consumption of monomer at a later stage (Figure 6.3). The molecular weight increases quickly with monomer conversion in the beginning of the reaction, after which a linear increase can be seen (data not shown). This indicates that there is a period of uncontrolled initiation in this macroinitiation, similar to what was observed for low molar mass amide initiators. The efficiency of the macroinitiation was only 17 % under these conditions.

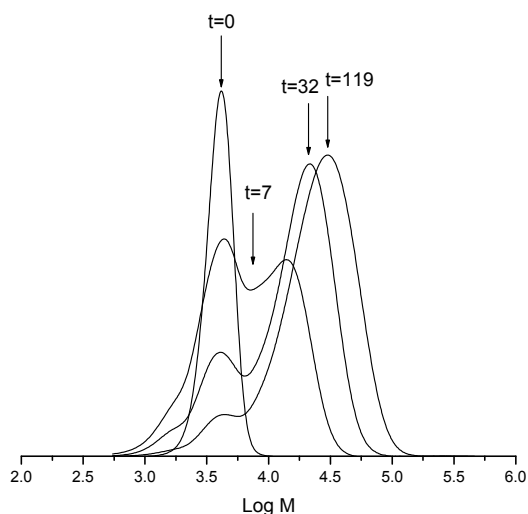


**Figure 6.2.** Evolution of molecular weight of MMA ATRP from the PBLG macroinitiator (Table 6.1, entry 1) in DMF (CuBr/Me<sub>6</sub>TREN at 60 °C), where *t* is the reaction time in minutes.

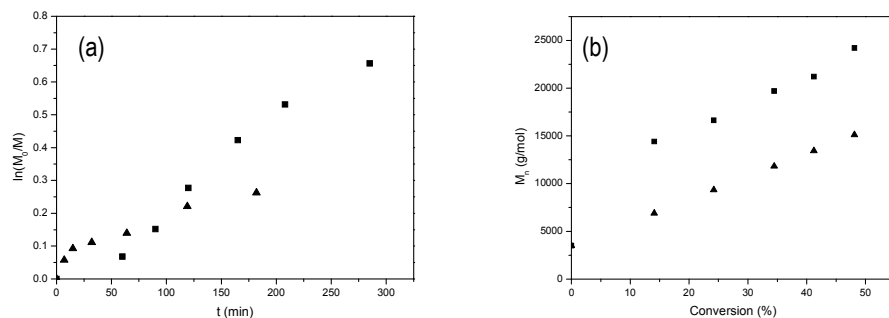
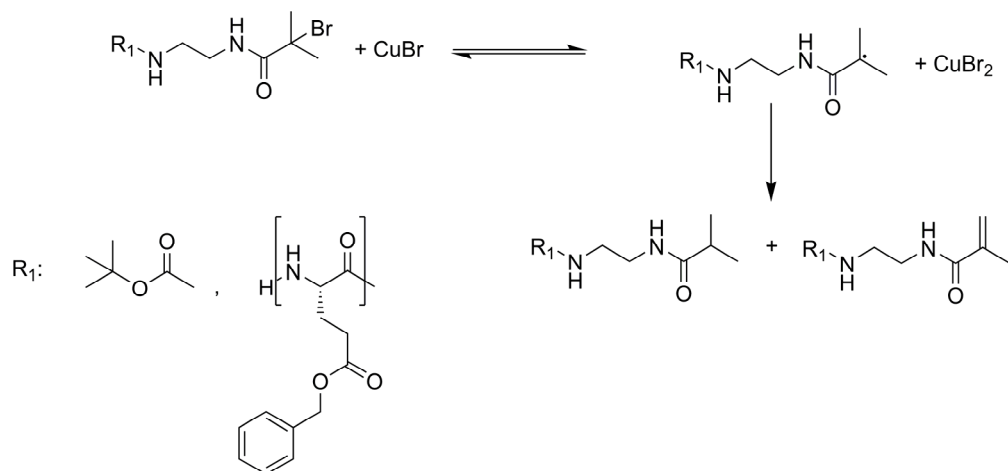


**Figure 6.3.** Kinetic plot of ATRP of MMA initiated by the PBLG macroinitiator in DMF for CuCl/HMTETA(■) and CuBr/HMTETA (▲) at 60 °C (a). Evolution of number average molecular weight of the block copolymer (■) for ATRP of MMA initiated by the PBLG macroinitiator (Table 6.1, entry 1) in DMF for CuCl/HMTETA at 60 °C compared to theoretical values (▲). Values acquired by HFIP-SEC with PMMA calibration (b).

It was proposed by Haddleton for bromo-2-methylpropionamide initiators that the bond strength of the carbon bromide is too weak.<sup>21</sup> This results in an uncontrolled initiation period with a high possibility of termination reactions. By reducing the initiation rate using CuCl and decreasing the reaction temperature, control in the reaction was improved. When this was applied in the PBLG macroinitiation, a slow conversion of monomer after the first hour was observed followed by near-linear reaction kinetics at a later stage (Figure 6.3a). Compared to the ATRP with CuBr there is a more constant conversion and the kinetic plot largely resembles a controlled polymerization. However, an induction period with slow initiation is still visible during the first hour of the reaction. Even though the molecular weight increased linearly with conversion under these reaction conditions, it was still higher than the theoretical molecular weight (Figure 6.3b). It has to be noted that, although the contribution of the PBLG block (random coil in HFIP) to the hydrodynamic volume of the block copolymer is unknown and an absolute comparison with theoretical values is difficult, the difference is significant and not due to SEC effects. Although the macroinitiation is significantly better controlled under these conditions, the initiator efficiency remains low (55%), due to the obvious loss of macroinitiator in the initial phase of the reaction.

To investigate the nature of the termination reactions in the initial phase of the ATRP macroinitiation, model reactions with amine (*t*-Boc) protected bifunctional initiator **1** were performed without monomer. In the literature the termination during radical polymerization of polymethacrylamide macroradicals is mentioned to be predominately by disproportionation.<sup>23</sup> Analysis of the products obtained from the model reaction by <sup>1</sup>H-NMR and LC-MS indeed showed disproportionation products of the initiator radical obtained after Br transfer to CuBr, namely 2-methylpropionamide and a methacrylamide (Scheme 6.2), which are very similar to the corresponding products obtained upon disproportionation of polymethacrylamide macroradicals. The <sup>1</sup>H-NMR spectrum shows a clear decrease of 34% of the

methyl protons positioned adjacent to the bromide at 1.9 ppm and the formation of the peaks at 1.14 ppm due to the removal of the halogen. Carbon double bond signals of the reaction product 2-methylpropionamide were also identified in the spectrum at 5.76 ppm and 5.28 ppm (Figure 6.4). Under ATRP conditions the latter could act as a monomer and indeed SEC confirmed the formation of oligomers in this experiment (Figure 6.5).<sup>24,25</sup>



**Scheme 6.2.** Proposed termination reaction of amide-based model- and macroinitiator.

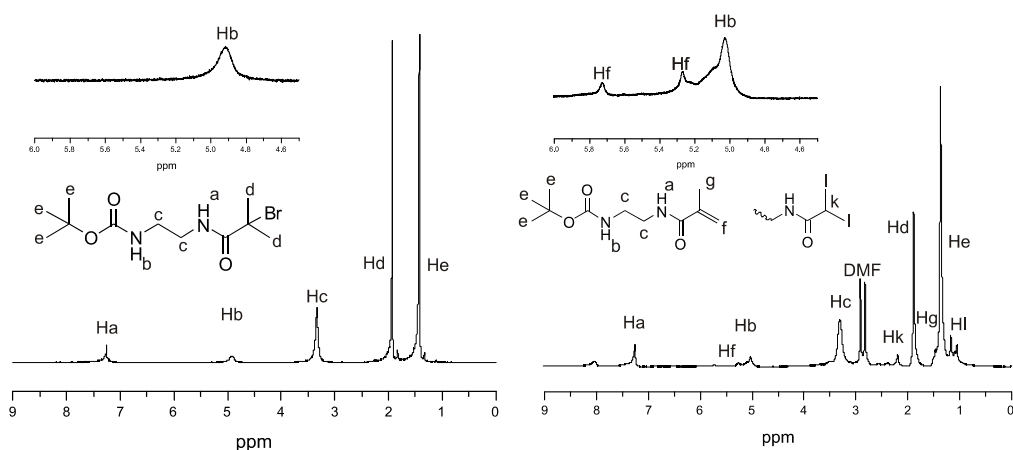


**Figure 6.4.** <sup>1</sup>H-NMR of *t*-Boc-protected initiator **1** before and after applying ATRP conditions.

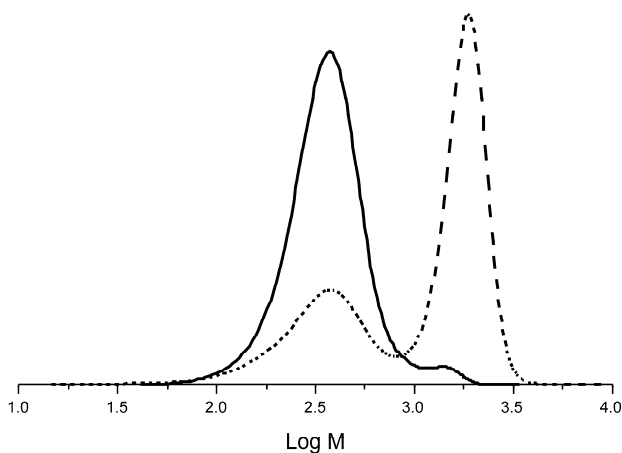


**Figure 6.5:** SEC traces of *t*-Boc-protected amide containing initiator **1** before (solid line) and after ATRP conditions (dashed line). Measured in HFIP-SEC with PMMA standards.

The same reaction was then repeated in the presence of a small quantity of monomer (MMA:initiator 5:1) under otherwise identical reaction conditions. Again, the molecular weight was higher than theoretically expected ( $M_{n,theo}$ : 700 g/mol,  $M_{n,obs}$ : 20,800 g/mol, PDI 1.4). MALDI-ToF-MS confirmed that the lower molecular weight fraction consists of pure PMMA initiated by the initiator and terminated by disproportionation. However, no incorporation of methacrylamide could be concluded from MALDI-ToF-MS or  $^1\text{H-NMR}$ , which indicates that no copolymer was formed.

The ATRP reaction was then carried out with the PBLG macroinitiator and MMA. MALDI-ToF-MS revealed the presence of the two disproportionation products predominantly in the lower molecular weight fractions. Figure 6.6 shows the example at 1,373 m/z and 1,592 m/z. These chains must have terminated at an early stage of the polymerization in agreement with the suggestion in the literature and our model reaction. Although this disproportionation reaction produces a PBLG macromonomer (methacrylamide end-capped PBLG), we did not find any evidence of its incorporation into the PMMA block. Therefore, the main consequence of this side reaction is the reduction of the initiator concentration, which results in the observed higher molecular weight and can explain the discrepancy between the theoretical and experimental molecular weight.



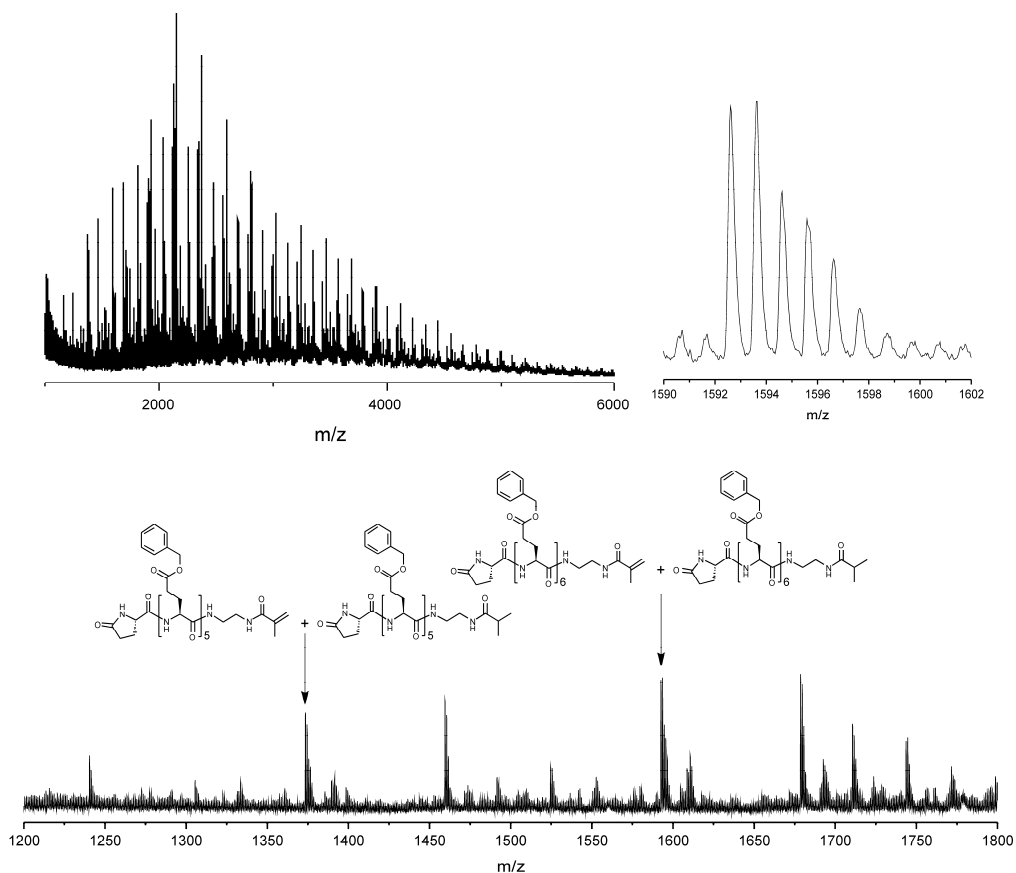


**Figure 6.6.** MALDI-ToF-MS spectrum of PBLG macroinitiator (Table 1, entry 2) after the ATRP reaction with MMA.

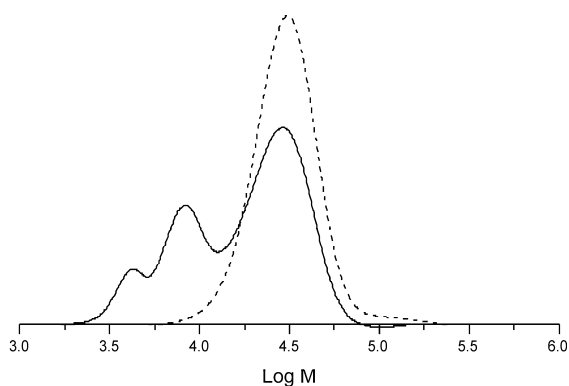


**Figure 6.7.** SEC of PBLG-*b*-PMMA before (solid line) and after precipitation in methanol (dashed line).

Although the side-reaction implies that the block copolymer molecular weight cannot be exactly predicted from the macroinitiator to monomer ratio for amide ATRP macroinitiators, the system can be

used to obtain well-defined block copolymers. Table 6.2 summarizes the results for the block copolymer syntheses from different polypeptide macroinitiators. PBLG (3,300 g/mol) was first used in the macroinitiation of MMA. Under the optimized conditions with CuCl as a catalyst, the ATRP in DMF is reasonably well controlled, leading to block copolymers of 24,200 g/mol with a PDI of 1.3. In DMSO, however, the molecular weight distribution is broader (1.5) at a higher monomer conversion of 64% after 3 hours compared to DMF (48% after 5 hours). ATRP from the PBLG macroinitiator is thus faster in DMSO compared to DMF and also proves to have more termination of the active chain ends. Due to the termination reaction described above, the reaction product always contains PBLG macroinitiator, as is evident from the multimodal SEC distribution of a crude sample shown in Figure 6.7. However, the unreacted macroinitiator and catalyst could be removed by selective precipitation in MeOH to yield the pure block copolymer as the insoluble part.

**Table 6.2.** Results of the synthesis of block copolymers by ATRP macroinitiation from various polypeptides.

| Biohybrid block copolymer | polypeptide macroinitiator <sup>(a)</sup> | $M_n$ (g/mol) | $M_w$ (g/mol) | PDI                | Solvent |
|---------------------------|---|---------------|---------------|--------------------|---------|
| PBLG- <i>b</i> -PMMA      | Entry 3                                   | 24,200        | 30,900        | 1.3                | DMF     |
| PBLG- <i>b</i> -PMMA      | Entry 3                                   | 42,100        | 64,400        | 1.5                | DMSO    |
| PBLG- <i>b</i> -PBMA      | Entry 3                                   | 17,500        | 22,900        | 1.3 <sup>(b)</sup> | DMF     |
| PBLG- <i>b</i> -PBMA      | Entry 3                                   | 29,400        | 45,100        | 1.5 <sup>(b)</sup> | DMSO    |
| PZLL- <i>b</i> -PMMA      | Entry 4                                   | 26,800        | 36,100        | 1.3                | DMF     |
| PZLL- <i>b</i> -PBMA      | Entry 4                                   | 36,000        | 64,400        | 1.9 <sup>(b)</sup> | DMSO    |
| PBLS- <i>b</i> -PMMA      | Entry 6                                   | 27,900        | 56,200        | 2.0 <sup>(b)</sup> | DMSO    |

(a) Entries of Table 1, (b) bimodal distribution.

The use of other monomers than MMA for the ATRP reactions was successful for *tert*-butylmethacrylate (PBMA). However, PBMA is better soluble in methanol than PMMA, making the selective precipitation of P(BLG-*b*-MMA) impossible.

Other polypeptides were also tested in the ATRP with MMA. The use of PZLL was successful in both DMF and DMSO with similar results as for the PBLG. As seen before, the molecular weight as well as the PDI is much higher for the reactions in DMSO for the same reaction time. The separation of the unreacted PZLL from the P(ZLL-*b*-BMA) was less successful than for the other block copolymers, resulting in a bimodal distribution. ATRP with the PBLS was only possible using DMSO as a solvent and did not result in a good separation in methanol.

## 6.4 Conclusions

We have expanded the NCA polymerization at low temperatures in DMF to several amino acids. Well-defined polypeptides were obtained except for polypeptides with a low solubility in the reaction medium.

When an amide initiator comprising an amine function for initiating the NCA polymerization and an activated bromide for ATRP was employed polypeptide macroinitiators were obtained from  $\gamma$ -benzyl-L-glutamate NCA, O-benzyl-serine NCA and N $\epsilon$ -benzyloxycarbonyl-L-lysine. Subsequent ATRP macroinitiation from the polypeptides resulted in higher than expected molecular weights. Analysis of the reaction products and model reactions confirmed that this is due to the high frequency of termination reactions by disproportionation in the initial phase of the ATRP, which is inherent in the amide initiator structure. Nevertheless, well-defined block copolymers could be obtained in some cases by selective precipitation.

## References

- <sup>1</sup> K.L. Heredia and H.D. Maynard, *Org. Biomol. Chem.* **2007**, 1, 45-53
- <sup>2</sup> L.Ayres, P. Hans, J. Adams, D.W.P.M. Lowik and J.C.M. van Hest, *J. Polym. Sci. A: Polym. Chem.* **2005**, 24, 6355-6366
- <sup>3</sup> D.J. Adams and I. Young, *J. Polym. Sci. A: Polym. Chem.* **2008**, 18, 6082-6090
- <sup>4</sup> M.L. Becker, J.Q. Liu and K.L. Wooley, *Biomacromolecules* **2005**, 1, 220-228
- <sup>5</sup> H. Rettig, E. Krause, H.G. Börner, *Macromol. Rapid Commun.* **2004**, 13, 1251-1256
- <sup>6</sup> H.R. Kricheldorf, *Angew. Chem. Int. Ed.* **2006**, 35, 5752-5784
- <sup>7</sup> I. Dimitrov and H. Schlaad, *Chem. Commun.* **2003**, 23, 2944-2945
- <sup>8</sup> T. Aliferis, H. Iatrou and N. Hadjichristidis, *Biomacromolecules* **2004**, 5, 1653-1656
- <sup>9</sup> W. Vayaboury, O. Giani, H. Cottet, A. Deratani and F.Schue, *Macromol. Rapid Commun.* **2004**, 13, 1221-1224
- <sup>10</sup> H. Lu and J. Cheng, *J. Am. Chem. Soc.* **2007**, 46, 14114-14115
- <sup>11</sup> T. J. Deming, *Nature*, **1997**, 390, 386-389
- <sup>12</sup> H.G. Boerner and H. Schlaad, *Soft Matter* **2007**, 4, 394-408
- <sup>13</sup> X. Zhang, J. Li, W. Li, A. Zhang, *Biomacromolecules* **2007**, 11, 3557-3567
- <sup>14</sup> K.R. Brzezinska and T.J. Deming, *Macromol. Biosci.* **2004**, 6, 566-569
- <sup>15</sup> S. Steig, F. Cornelius, P. Witte, B.B.P. Staal, C.E. Koning, A. Heise and H. Menzel, *Chem. Commun.* **2005**, 43, 5420-5422
- <sup>16</sup> R.J.I. Knoop, G.J.M. Habraken, N. Gogibus, S. Steig, H. Menzel, C.E. Koning and A. Heise, *J. Polym. Sci. A: Polym. Chem.* **2008**, 9, 3068-3077
- <sup>17</sup> M. Ciampoli and N. Nardi, *Inorg. Chem.* **1966**, 5, 41-44
- <sup>18</sup> V.B. Sadhu, J. Pionteck, D.Voigt, H. Komber and B.Voit, *Macromol. Symp.* **2004**, 147-155
- <sup>19</sup> H.R. Kricheldorf, C. von Lossow and G. Schwarz, *Macromol. Chem. Phys.* **2004**, 7, 918-924
- <sup>20</sup> Y.T. Li, Y.Q. Tang, R. Narain, A.L. Lewis and S.P. Armes, *Langmuir* **2005**, 22, 9946-9954
- <sup>21</sup> A. Limer and D.M. Haddleton, *Macromolecules* **2006**, 4, 1353-1358
- <sup>22</sup> S. Venkataraman and K.L. Wooley, *Macromolecules* **2006**, 26, 9661-9664
- <sup>23</sup> K. Ulbrich and J. Kopecek, *Eur. Polym. J.* **1976**, 3, 183-187
- <sup>24</sup> B. Zhang, K. Fischer and M. Schmidt, *Macromol. Chem. Phys.* **2005**, 206, 157-162
- <sup>25</sup> F. Audouin, R.J.I. Knoop, J. Huang and A. Heise, *J. Polym. Sci. A: Polym. Chem.* **2010**, 48, 4602-4610



# Chapter 7

## Selective Enzymatic Degradation of Biohybrid Block Copolymers Particles

### Abstract

*Biohybrid block copolymers are proposed for many different applications, such as biomedical applications and anti-bacterial particles. By combining controlled radical polymerization techniques and controlled polypeptide synthesis, such as N-carboxyanhydride ring opening polymerization (NCA ROP), these block copolymers are easily accessible. Here we apply NCA polymerization and nitroxide mediated radical polymerization (NMRP) of poly(*n*-butylacrylate) and polystyrene using 2,2,5-trimethyl-4-phenyl-3-azahexane-3-nitroxide (TIPNO) and N-tert-butyl-N-(1-diethylphosphono-2,2-dimethylpropyl) nitroxide (SG1) based bifunctional initiators. The polypeptide block itself consists of (block) copolymers of poly(L-glutamic acid) with various quantities of L-alanine. The formed superstructures (vesicles and micelles) of the block copolymers were exposed to elastase and thermolysin in a phosphate buffer solution to investigate their enzymatic degradation. The PBA-containing block copolymers with 50% L-alanine in the polypeptide block showed a high degradation response compared to polymer containing lower L-alanine quantities. The particles stabilized by copolypeptides with L-alanine near the hydrophobic block showed full degradation within four days. A clear difference was observed for the particles containing polystyrene blocks, for which no degradation was observed under the same conditions. However, when the degradation temperature was increased to 70 °C, degradation could be achieved due to the higher block copolymer exchange between the particle and the solution.*

## 7.1 Introduction

Biohybrid polymers combine natural polymers with synthetic polymers and are frequently proposed as natural mimics for biomedical applications. Superstructures, like micelles and vesicles are often the target structures for biohybrid polymers being considered, for example for drug delivery applications.<sup>1-4</sup> When a peptide block is used as the hydrophilic component the core of the micelle or the membrane of the vesicle is formed by the hydrophobic synthetic polymer block. In many cases hydrophobic interactions are sufficient to stabilize the polymer assembly while some authors choose chemical cross-linking to further stabilize the structures. For example, our group prepared pH-responsive core cross-linked core-shell particles from block copolymers of polystyrene and poly(L-glutamate).<sup>5,6</sup> Another example are micelles prepared with the peptide tripticin attached to poly(acrylic acid)-*b*-polystyrene.<sup>7</sup> The micelles of these biohybrid block copolymers showed anti-bacterial properties. Micelles and vesicles of poly(butadiene)-*b*-poly(L-glutamic acid) were prepared with iron oxide nanoparticles. These magnetic particles could have an application in external magnetic therapy or for MRI labeling.<sup>8</sup> Micelles of graft and block copolymers of poly(L-lysine) and poly(caprolactone) have been prepared and considered to be fully degradable and useful for drug-delivery systems.<sup>9,10</sup>

Degradation of biohybrid block copolymers is a critical factor for the lifetime of the superstructures in a biological environment. It is known that polypeptides are susceptible to enzymatic hydrolysis and that some enzymes selectively hydrolyze bonds between a certain pair of amino acids. Selectivity of the enzymes for the hydrolysis of certain amide bonds involves the placement of the bond that should be cleaved (endo- and exopeptidases) and the combination with the adjacent amino acid residues.<sup>11,12</sup> Examples are copolypeptides of poly(L-glutamic acid) or poly(L-lysine) in combination with small hydrophobic monomers, such as L-alanine, L-leucine and L-valine, which are degradable by endopeptidases such as trypsin and papain.<sup>13,14</sup>

For biohybrid micelles or vesicles enzymatic degradation of parts of the polypeptide block should result in particle destabilization. Conceptually this was shown for the enzymatic ester degradation of the hydrophobic block of poly(trimethylene carbonate)-*b*-L-glutamic acid vesicles.<sup>15</sup> With the use of DLS measurements the enzymatic degradation was confirmed by the decreasing light scattering intensity of the reaction medium. The light scattering is dependent on the concentration and size of the particles in the solution. Lipases have also been used to degrade the core of polyethylene glycol and oligo(caprolactone) micelles.<sup>16,17</sup> This method allowed for a full degradation of the hydrophobic core, resulting in fully dispersed polymer chains. The degradation of this block copolymer was suggested to occur in the bulk solution by unimer exchange from the micelles above the critical micelle concentration (CMC).

Selective enzymatic degradation has been shown in other hybrid systems, such as hydrogels, where enzymatic hydrolysis was used as a release trigger. In oligopeptide (Asp-Ala-Ala-Arg)-functionalized cross-linked PEG hydrogels, the Ala-Ala bonds were selectively cleaved resulting in swelling of the nanoparticles due to the increased positive ionic repulsion of the remaining L-arginine-containing

dipeptide.<sup>18,19</sup> Swollen PEG networks, where a peptide sequence was used as a cross-linker, have been degraded by the enzyme trypsin resulting in a fully degraded network.<sup>20</sup> Recently, the same enzymatic trigger mechanism was used in a two-phase system with Asp-Ala-Ala-Arg oligopeptides-coated porous silica particles to show the release of a fluorescent dextran.<sup>21</sup> Another enzymatic response was found for a peptide monolayer on gold nanoparticles as the cleavage and release of the fluorescent label at the end of the peptide.<sup>22</sup> In addition, polystyrene particles with poly(acrylic acid) brushes were functionalized with well-defined fluorescent-labeled peptides immobilized in the PAA corona.<sup>23</sup> These examples illustrate the accessibility of the enzyme to the corona or peptide layer close to a hydrophobic surface, which is the case in micelles and vesicles.

However, to our knowledge the effect of enzymatic polypeptide degradation in amphiphilic hybrid block copolymers on micelle or vesicle destabilization had not previously been investigated. Clearly, the effect of enzymatic degradation on amphiphilic block copolymers might be complex. For example, the nature of the hydrophobic, enzymatic-neutral part of the block copolymers might have an effect on the degradation. The unimer exchange process determines whether the majority of the degradation occurs in the particle corona or in the solution in the unimer state, influencing the speed of degradation and particle stability. Hydrophobic blocks with different properties need to be tested to determine these effects. By using non-crystalline, hydrophobic polymer blocks with high and low glass transition temperatures the difference between both processes can be studied.

In this chapter the synthesis of block copolymers of polystyrene and poly(*n*-butylacrylate) with homopolypeptides and copolypeptides of L-glutamic acid and L-alanine via a (macro)initiation from bifunctional primary amine-containing initiators for nitroxide mediated radical polymerization (NMRP) (Scheme 7.1) is described. The deprotected polypeptide-based block and the hydrophobic *n*-butylacrylate or polystyrene block give the block copolymers amphiphilic properties. Micelles and vesicles were prepared from the deprotected hybrid block copolymers and the effect of peptidases tested was on these particles. By altering the amino acid composition of the polypeptide block, the enzymatic degradation was tuned and a correlation could be made for low and high  $T_g$  hydrophobic block copolymer material.

## 7.2 Experimental

### Materials

THF, pentane, diethylether, DMF, NMP, DMSO, HFIP and dichloromethane were purchased from Biosolve. DMAc was purchased from Aldrich. N-hydroxysuccinimide dicyclohexylcarbodiimide, diaminoethane, MgSO<sub>4</sub>, TFA, HBr 33% / acetic acid solution, styrene, *n*-butylacrylate, 5(6)-carboxyfluorescein, thermolysin and lipase from *Thermomyces lanuginosus* were purchased from Sigma. Elastase was purchased from Worthington Biochemical Corporation. Palladium (10%) / carbon was purchased from Merck. All materials were used as received. Bifunctional initiator **2** was prepared according to procedures mentioned in literature.<sup>24</sup> NCAs of  $\gamma$ -benzyl-L-glutamate and L-alanine were



prepared following literature procedures reported in Chapter 2.<sup>25</sup> The succinimide ester of 5(6)-carboxyfluorescein was prepared following literature procedures.<sup>26</sup>

## Methods

NMR was performed on a 400 MHz Varian Mercury 400 and 200 MHz Varian Mercury 200. Deuterated chloroform was used for the characterization of the NCA monomers and NMRP initiators. Deuterated TFA was used for analyzing the polypeptide macroinitiators and the poly(*n*-butylacrylate) block copolymers. The polystyrene block copolymers were analyzed in deuterated DMF.

N,N-dimethylacetamide size exclusion chromatography (DMAc SEC) was performed at 60 °C on a system equipped with a Waters 2695 separation module, a Waters 2414 refractive index detector (50 °C), a Waters 486 UV detector, a PSS GRAM guard column followed by 2 PSS GRAM columns in series of 100 Å (10 µm particles) and 3000 Å (10 µm particles), respectively. DMAc was used as eluent at a flow rate of 1 ml/min. The molecular weights were calculated using polystyrene standards. Before SEC analysis was performed, the samples were filtered through a 0.2 µm PTFE filter (13mm, PP housing, Alltech).

Matrix Assisted Laser Desorption / Ionization - Time of Flight - Mass Spectroscopy analysis was carried out on a Voyager DE-STR from Applied Biosystems (laser frequency 20 Hz, 337nm and a voltage of 25kV). The matrix material used was T-2-(3-(4-*tert*-Butyl-phenyl)-2-methyl-2-propenylidene)malononitrile (DCTB) (40 mg/ml). Potassium trifluoroacetic acid (KTFA) was added as cationic ionization agent (5 mg/ml). The polymer sample was dissolved in HFIP (1 mg/ml), to which the matrix material and the ionization agent were added (5:1:5), and the mixture was placed on the target plate.

Fourier Transform - Infra Red spectroscopy analyses were performed on a PerkinElmer SpectrumOne FTIR Spectrometer, using a universal ATR sampling accessory. Samples for IR spectroscopy were taken from the reaction mixtures and analyzed without any further modification.

High performance liquid chromatography mass spectroscopy was carried out on an Agilent 1100 series setup with an Agilent MSD type SL (G1946D). The column used was a Zorbax RX-C18; 2.1 x 50 mm<sup>2</sup>; 5 µm. The eluent was 90% water and 10% methanol at 25 °C with a flow of 0.2 ml/min. Detection was done using UV and MS with an atmospheric pressure electrospray interface. The conditions for the APESI were: pressure 30 psi; capillary voltage 4000 V; dry gas 13 l/min, 350 °C.

Gradient polymer elution chromatography was performed on an Agilent 1100 with a Alltech ELSD 2000 detector. The column used was a Zorbax SB-C18. The eluent was 100% toluene for the first 2 minutes which was then changed to toluene with 20 vol% - 15 vol% DMF over a period of 28 or 30 minutes. In a period of 2 minutes the eluent was then changed to 100% toluene and this was maintained for 3 minutes. The flow rate was kept constant at 1 ml/min at 25 °C. The injection volume was 2-10 µl of a 10 mg/ml solution.

Dynamic light scattering was performed on a Coulter N4 plus in a 1cm quartz cuvet at 90°.

Static light scattering was performed with a Wyatt Dawn Heleos-II at 90°.

Cryogenic transmission electron microscopy (cryo-TEM) measurements were performed on a FEI Tecnai 20, type Sphera TEM instrument (with a LaB6 filament, operating voltage=200 kV). The sample vitrification procedure was performed using an automated vitrification robot (FEI Vitrobot Mark III). A 3  $\mu\text{L}$  sample was applied to a Quantifoil grid (R 2/2, Quantifoil Micro Tools GmbH; freshly glow discharged for 40 s just prior to use) within the environmental chamber of the Vitrobot and the excess liquid was blotted away. The thin film thus formed was shot into melting ethane. The grid containing the vitrified film was immediately transferred to a cryoholder (Gatan 626) and observed under low dose conditions at -170 °C.

## Synthesis

**Synthesis of 2-methyl-2-[N-*tert*-butyl-N-(1-diethoxyphosphoryl-2,2-dimethylpropyl)aminoxy]-N-propionyloxysuccinimide.**<sup>27</sup> The (MAMA-SG1) (11.36 g, 29.80 mmol) and the N-hydroxysuccinimide (4.10 g, 35.6 mmol) were dissolved in 25 ml THF. To this 25 ml of THF with dicyclohexylcarbodiimide (6.72 g, 32.6 mmol) was added. The reaction was left for 3 hours, then filtered, concentrated and precipitated in pentane. The solid was subsequently dried under vacuum at ambient temperature.

Yield: 8.14 g, 17.0 mmol. <sup>1</sup>H-NMR (400 MHz, CDCl<sub>3</sub>,  $\delta$ , ppm): 1.13 (18H, s), 1.17 (18H, s), 1.26 (12H, q, J= 7.1 Hz, 9.0 Hz), 1.78 (6H, s), 1.85 (6H, s), 2.80 (8H, s), 3.24 (1H, s), 3.31 (1H, s), 3.9-4.3 (8H, m) (both stereoisomers) <sup>13</sup>C-NMR (400 MHz, CDCl<sub>3</sub>,  $\delta$ , ppm): 16.17 (d, POCH<sub>2</sub>C $\underline{\text{H}}$ <sub>3</sub>, J(C,P)= 6.6 Hz), 16.57 (d, POCH<sub>2</sub>C $\underline{\text{H}}$ <sub>3</sub>, J(C,P)= 6.6 Hz), 21.91 (CHC(CH<sub>3</sub>)<sub>3</sub>), 25.63 ((C $\underline{\text{H}}$ <sub>3</sub>)<sub>2</sub>CON), 28.18 (s, (C $\underline{\text{H}}$ <sub>3</sub>)CN), 29.33 (s, C $\underline{\text{H}}$ <sub>2</sub>(CO)), 30.06 (d, (C $\underline{\text{H}}$ <sub>3</sub>)<sub>3</sub>CH, J= 5.6 Hz), 58.81 (d, POCH<sub>2</sub>C $\underline{\text{H}}$ <sub>3</sub>, J= 7.2 Hz), 61.90 (d, POCH<sub>2</sub>C $\underline{\text{H}}$ <sub>3</sub>, J= 6.2 Hz), 62.63 (s, NC(CH<sub>3</sub>)<sub>3</sub>), 69.21 (d, NCHP, J= 137.51 Hz), 83.67 (s, C(CH<sub>3</sub>)<sub>2</sub>O), 168.91 (s, CH<sub>2</sub>(CO)N), 170.25 (s, OC(O)C(CH<sub>3</sub>)) <sup>31</sup>P-NMR (200 MHz, CDCl<sub>3</sub>,  $\delta$ , ppm): 25.8 (s)

**Synthesis of 2-methyl-2-[N-*tert*-butyl-N-(1-diethoxyphosphoryl-2,2-dimethylpropyl)aminoxy]-N-aminoethyl propionamide (Initiator 1).** 2-methyl-2-[N-*tert*-butyl-N-(1-diethoxyphosphoryl-2,2-dimethylpropyl)aminoxy]-N-propionyloxysuccinimide (5.00 g, 10.5 mmol) was dissolved in 50 ml dichloromethane. This was added slowly to a solution of diaminoethane (32.0 g, 532 mmol) in 100 ml of dichloromethane. After 5 hours the solution was extracted with 3 x 30 ml water. The water fraction was extracted with dichloromethane. The organic fractions were collected and dried with MgSO<sub>4</sub>. The solution was subsequently concentrated at 20 °C and under vacuum, by which the remaining solvent and diaminoethane were removed. The oil was stored in a freezer at -18 °C. Yield: 3.25 g, 7.67 mmol, 73.3%, LC-MS: 424 Da (M+H)<sup>+</sup>, 446 Da (M+Na)<sup>+</sup>, <sup>1</sup>H-NMR (400 MHz, CDCl<sub>3</sub>,  $\delta$ , ppm): 1.03 (18H, s), 1.15 (18H, s), 1.28 (12H, m), 1.50 (6H, s), 1.63 (6H, s), 2.74 (4H, t, J=6.1), 3.24 (1H, s), 3.30 (1H, s), 3.36 (4H, q, J=6.1 Hz) 3.9-4.2 (4H, m), 5.22 (2H, s), 8.32 (2H, s) (both stereoisomers) <sup>13</sup>C-NMR (400 MHz, CDCl<sub>3</sub>,  $\delta$ , ppm): 16.10 (d, POCH<sub>2</sub>C $\underline{\text{H}}$ <sub>3</sub>, J(C,P)= 6.8 Hz), 16.57 (d, POCH<sub>2</sub>C $\underline{\text{H}}$ <sub>3</sub>, J(C,P)= 5.7 Hz), 24.34 (s, CHC(CH<sub>3</sub>)<sub>3</sub>), 27.34 (s, (C $\underline{\text{H}}$ <sub>3</sub>)<sub>2</sub>CON), 29.35 (s, (C $\underline{\text{H}}$ <sub>3</sub>)CN), 29.54 (d, (C $\underline{\text{H}}$ <sub>3</sub>)<sub>3</sub>CH, J= 5.4 Hz),

41.82 (s, CH<sub>2</sub>CH<sub>2</sub>NHC(O)), 42.89 (s, CH<sub>2</sub>NH<sub>2</sub>), 59.81 (d, POCH<sub>2</sub>CH<sub>3</sub>, J= 8.1 Hz), 61.56 (d, POCH<sub>2</sub>CH<sub>3</sub>, J= 3.7 Hz), 62.57 (s, NC(CH<sub>3</sub>)<sub>3</sub>), 69.55 (d, NCHP, J= 133.66 Hz), 85.82 (s, C(CH<sub>3</sub>)<sub>2</sub>O), 176.87 (s, OC(O)C(CH<sub>3</sub>)) <sup>31</sup>P-NMR (200 MHz, CDCl<sub>3</sub>, δ, ppm): 28.0 (s)

**Polymerization of NCAs initiated by initiator 1.** The following general procedure was applied for all combinations of BLG and Ala NCA. The bifunctional initiator **1** (134 mg, 0.316 mmol) was dissolved in 5 ml of DMF. The NCA of  $\gamma$ -benzyl-L-glutamate (5.02 g, 19.1 mmol) was dissolved in 20 ml DMF in a Schlenk tube. The initiator solution was added quickly. The reaction was maintained under 0 °C for 4 days. The reaction mixture was precipitated in diethylether and filtered. The sample was stored in the freezer. Yield: 3.10 g, 71.8 wt%

**Block copolymerization of poly( $\gamma$ -benzyl-L-glutamate<sub>15</sub>-co-L-alanine<sub>15</sub>)-b-poly( $\gamma$ -benzyl-L-glutamate<sub>25</sub>-co-L-alanine<sub>5</sub>) initiated by 1.** The bifunctional initiator **1** (95.8 mg, 0.226 mmol) was dissolved in 1 ml DMF and added to a solution of the NCAs of  $\gamma$ -benzyl-L-glutamate (1.50 g, 5.70 mmol) and L-alanine (0.133 g, 1.16 mmol) in 16 ml DMF. The polymerization was performed at 0 °C under a nitrogen flow. After 3 days FTIR analysis pointed to full conversion and a solution of the NCAs of  $\gamma$ -benzyl-L-glutamate (0.900 g, 3.42 mmol) and L-alanine (0.393 g, 3.41 mmol) in 10 ml DMF was added. The reaction mixture was precipitated in diethylether after reaching full conversion after 2 days. The polymer was dried under vacuum at room temperature. Yield: 2.29 g, 95.0 wt%

**NCA random copolymerization for MALDI-ToF-MS analysis.** The NCA monomers of  $\gamma$ -benzyl-L-glutamate (0.500 g, 1.90 mmol) and L-alanine (0.219 g, 1.90 mmol) were dissolved in 4 ml DMF in a Schlenk tube. The solution was stirred at 0 °C until all monomer was completely dissolved. To this a solution of benzylamine (0.510 mg, 0.272 mmol) in 1 ml DMF was added. Samples were taken over time for IR and MALDI-ToF-MS analyses. For the MALDI-ToF-MS 100  $\mu$ l was dissolved in 1 ml HFIP with 1.5 M benzylamine and the mixture was placed in the freezer at -18 °C.

**NMRP of *n*-butylacrylate with a poly( $\gamma$ -benzyl-L-glutamate)-SG1 macroinitiator.** The macroinitiator (310 mg, 2.38 x 10<sup>-2</sup> mmol), *n*-butylacrylate (0.85 g, 6.6 mmol), free SG1 nitroxide (0.65 mg, 2.2 x 10<sup>-3</sup> mmol) were dissolved in 2.0 ml NMP. The solution was deoxygenized by three freeze thaw cycles. The solution was subsequently placed in an oil bath of 60 °C. The temperature was increased to 90 °C for 1 hour and then increased to 100 °C for 2.5 hours. Monomer and solvent were removed by precipitation in methanol and filtration. Yield: 0.450 g

**Deprotection of poly( $\gamma$ -benzyl-L-glutamate)-b-poly(*n*-butylacrylate).** The hybrid block copolymer PBLG<sub>60</sub>-b-PBA (0.95 g) and 100 mg of palladium on carbon catalyst were dissolved in 20 ml DMF and deoxygenized by a nitrogen flow. In a Parr setup the hydrogenation was performed under a 6 bar

hydrogen gas atmosphere. After several hours of reaction the catalyst was removed by filtration. Most of the solvent was removed by high vacuum and the polymer was precipitated in pentane. Yield: 110 mg, 17.2 wt%

**Deprotection of poly( $\gamma$ -benzyl-L-glutamate)-*b*-polystyrene.** The hybrid block copolymer PBLG<sub>60</sub>-*b*-PS (1.07 g) was dissolved in 20 ml dichloromethane. To this solution 6 ml of HBr 33% / acetic acid solution was added. The reaction was precipitated in diethylether after 24h. The precipitated polymer was dried in a vacuum oven. Yield: 0.600 g, 95.9 wt%

**Particle formation of deprotected hybrid block copolymers.** The block copolymer of PGIu<sub>60</sub>-*b*-PBA (44 mg) was dissolved in 10 ml DMSO. To this 10 ml of phosphate buffer solution was added slowly over 3 hours. The solution was dialyzed with a PBS buffer for 48 hours.

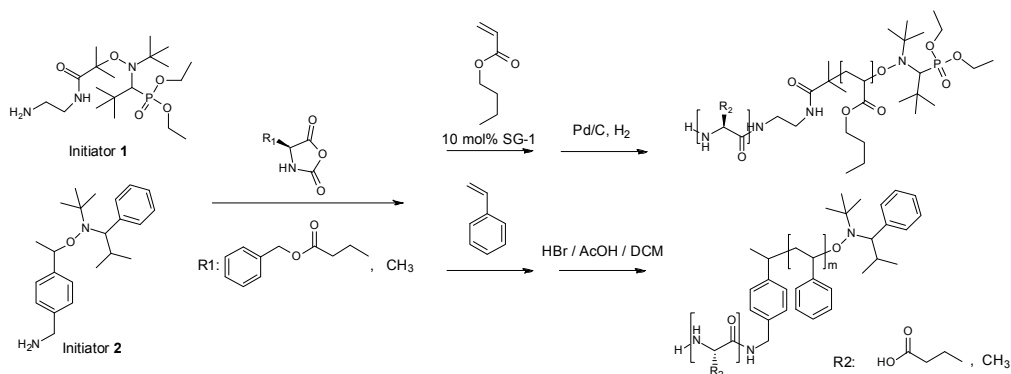
**Synthesis of fluorescein-labeled poly( $\gamma$ -benzyl-L-glutamate).** The NCA monomers of  $\gamma$ -benzyl-L-glutamate (1.50 g, 5.70 mmol) was dissolved in 14 ml DMF in a Schlenk tube. To this a solution of benzylamine (15.3 mg, 0.141 mmol) in 1 ml DMF was added. The reaction was left to stir in a cold water bath of 0 °C for 4 days under a dry nitrogen atmosphere. The succinimide ester of 5(6)-carboxyfluorescein (0.200 g, 0.424 mmol) was added to the solution. The reaction was stirred for another 24 hours and precipitated in diethylether twice, the second time after redissolving in NMP. After this the polymer was dissolved in NMP and dialyzed (membrane cut-off of 3500 Da) for 16 hours. After filtration the solution was precipitated in diethylether. Polymer was dried in vacuo at ambient temperature. Yield: 0.39 g, 29.3 wt%

**Deprotection of fluorescein-labeled poly( $\gamma$ -benzyl-L-glutamate).** The fluorescein-labeled PBLG (0.300 g,  $6.35 \times 10^{-2}$  mmol) was dissolved in 7 ml TFA. To this 3 ml of HBr / acetic acid solution was added. The reaction was maintained overnight. After precipitation in diethylether the product was filtered and washed in diethylether three times. Finally the polymer was dried in a vacuum oven overnight at room temperature and stored in a freezer. Yield: 0.105 g, 51.3 wt%

**Enzymatic degradation of fluorescent-functionalized (co)polypeptides.** The deprotected fluorescent-labeled poly(L-glutamic acid) (6.1 mg) and elastase (2.2 mg) or thermolysin (2.2 mg) were dissolved in 1.5 ml PBS buffer with 50  $\mu$ l of concentrated NaHCO<sub>3</sub> solution. The reaction was shaken at room temperature and after 24 hours the solution was analyzed by LC-MS.

**Enzymatic degradation of the selectively deprotected biohybrid block copolymers.** 4.5 ml of the particle solution (1.25 mg/ml) of the biohybrid block copolymers were filtered through a 0.2  $\mu$ m filter and added to a solution of 6.6 mg elastase (4 units/mg) or 1 mg of thermolysin (42 units/mg) in 1.5 ml of

PBS buffer. The solution was divided over three reaction tubes. The solutions were shaken in a water bath at 37 °C and taken out for DLS analysis.



**Scheme 7.1.** NCA ROP of PBLG from bifunctional initiators **1** and **2**. NMRP macroinitiation of PBA and PS followed by deprotection of the benzyl esters.

## 7.3 Results & discussion

### 7.3.1 Synthesis of polypeptide-based NMRP macroinitiators

The most commonly used synthetic strategies for peptide-containing block copolymers are solid phase peptide synthesis (SPPS) and N-carboxyanhydride ring opening polymerization (NCA ROP). In both methods convergent synthetic methods, such as Huisgens cycloaddition, and divergent methods, such as macroinitiation for controlled polymerizations, have been used to synthesize block copolymers.<sup>28-35</sup> Alternatively, we have previously reported the use of bifunctional initiators, combining the initiator function for NCA ROP with that for controlled radical polymerizations in one and the same molecule.<sup>36-39</sup> In particular the synthesis of polystyrene-*b*-poly( $\gamma$ -benzyl-L-glutamate) was successfully performed with an amine-functionalized initiator for nitroxide-mediated radical polymerization (NMRP).<sup>36</sup> This 2,2,5-trimethyl-4-phenyl-3-azahexane-3-nitroxide (TIPNO) based initiator was also applied in this study (initiator **2**). Due to the tedious synthetic procedure of the amine-functionalized TIPNO initiator, we decided to explore another bifunctional initiator based on the commercial N-(2-methylpropyl)-N-(1-diethylphosphono-2,2-dimethylpropyl)-O-(2-carboxyprop-2yl)hydroxylamine (MAMA-SG1) (initiator **1**). This initiator was synthesized with an overall yield of 42 % in two steps based on a modified procedure reported by Vinas et al.,<sup>27</sup> reacting the N-succinimide-activated MAMA-SG1 with an excess of 1,2-diaminoethane. This resulted in a lightly yellow oil that solidified into a wax upon storage in the freezer. For both initiators the synthesis of biohybrid block copolymers begins with the initiation of a living NCA ROP at 0 °C from the primary amine group of the initiator, followed by a controlled radical polymerization. The polypeptide block was then deprotected by removal of the benzyl esters to obtain an amphiphilic biohybrid block copolymer.

For the NCA polymerization the bifunctional initiator **1** (Scheme 7.1) was dissolved in DMF and added to a solution of NCA monomers in DMF. The conversion of the reactions was monitored by FTIR following the characteristic peak of the NCA monomers at 1786 cm<sup>-1</sup>. At full conversion the polypeptides were precipitated in diethylether and filtered. Homopolymers of poly( $\gamma$ -benzyl-L-glutamate) and (block) copolymers with different chain compositions and L-alanine content were prepared (Table 7.1). Although the copolymers with 50% alanine did form a gel during the polymerization, this did not influence the polymerization of the second PBLG block for entry 6, Table 7.1 (Figure 7.2). All polypeptides were obtained with low polydispersities of around 1.1 and molecular weights close to the expected value. Moreover, the determined chemical compositions of the polypeptides were in good agreement with the NCA feed ratio.

The same polymerization procedure was applied for the bifunctional TIPNO initiator **2**, according to our procedure published elsewhere.<sup>36</sup> As addition to the previously mentioned procedure, the NCA monomer composition was altered to obtain a P(Glu<sub>30</sub>-co-Ala<sub>30</sub>) copolypeptide as the TIPNO-functionalized macroinitiator.

**Table 7.1.** Entries of polypeptide blocks prepared by NCA ROP using bifunctional initiators **1** (SG1) and **2** (TIPNO).

| Entry | Polymer <sup>a</sup>  | $M_n^b$<br>(g/mol) | $M_w$<br>(g/mol) | PDI  | Glu : Ala <sup>c</sup> |
|-------|---|--------------------|------------------|------|------------------------|
| 1     | PBLG <sub>60</sub> -SG1   | 13,000             | 13,700           | 1.05 | -                      |
| 2     | P(BLG <sub>50</sub> -co-Ala <sub>10</sub> )-SG1   | 14,500             | 15,500           | 1.07 | 5.0 : 1.0              |
| 3     | P(BLG <sub>30</sub> -co-Ala <sub>30</sub> )-SG1   | 11,200             | 12,200           | 1.09 | 1.0 : 1.0              |
| 4     | P(BLG <sub>15</sub> -co-Ala <sub>15</sub> )- <i>b</i> -PBLG <sub>30</sub> -SG1                        | 13,300             | 14,200           | 1.06 | 2.5 : 1                |
| 5     | P(BLG <sub>15</sub> -co-Ala <sub>15</sub> )-SG1   | 7,600              | 8,800            | 1.16 | 1.1 : 1                |
| 6     | PBLG <sub>30</sub> - <i>b</i> -P(BLG <sub>15</sub> -co-Ala <sub>15</sub> )-SG1                        | 13,600             | 15,300           | 1.12 | 2.6 : 1                |
| 7     | P(BLG <sub>25</sub> -co-Ala <sub>5</sub> )-SG1  | 7,100              | 8,000            | 1.12 | 5.0 : 1.0              |
| 8     | P(BLG <sub>15</sub> -co-Ala <sub>15</sub> )- <i>b</i> -P(BLG <sub>25</sub> -co-Ala <sub>5</sub> )-SG1 | 11,600             | 12,400           | 1.08 | 2.0 : 1.0              |
| 9     | PBLG <sub>20</sub> -TIPNO   | 5,900              | 6,100            | 1.04 | -                      |
| 10    | PBLG <sub>60</sub> -TIPNO   | 13,500             | 15,200           | 1.13 | -                      |
| 11    | P(BLG <sub>30</sub> -co-Ala <sub>30</sub> )-TIPNO   | 12,100             | 13,900           | 1.14 | 1.0 : 1.0              |

a) Superscript numbers refer to target degree of polymerization based on monomer to initiator ratio. b) Measured in DMAc-SEC. c) Compositions determined by <sup>1</sup>H-NMR: 1.5 ppm (methyl of L-alanine) and 3.0 - 2.0 ppm ( $\gamma$ -benzyl-L-glutamate) measured in d-TFA.

We previously studied the composition of copolymers obtained by NCA polymerizations, performed under the same conditions, by <sup>13</sup>C-NMR and MALDI-ToF-MS contour plot analysis in Chapter 3.<sup>25</sup> When applied to the P(BLG-co-Ala) copolypeptide the contour plot confirms that the obtained copolymer composition is close to the diagonal (Figure 7.1). This indicates that the calculated composition is not

far from the 1:1 experimental feed composition. It also confirms that the composition of the copolymer is highly random throughout the polypeptide chains. This is of great importance for the properties of the copolypeptide. Firstly, when using a selective enzyme for the degradation of Ala-Ala bonds only a random distribution allows to relate the degradation results to the copolymer composition. Secondly, if the L-glutamic acid monomers are well distributed over the chain, this will improve the water solubility of the polypeptide block as opposed to a blocky copolypeptide structure.<sup>40,41</sup>

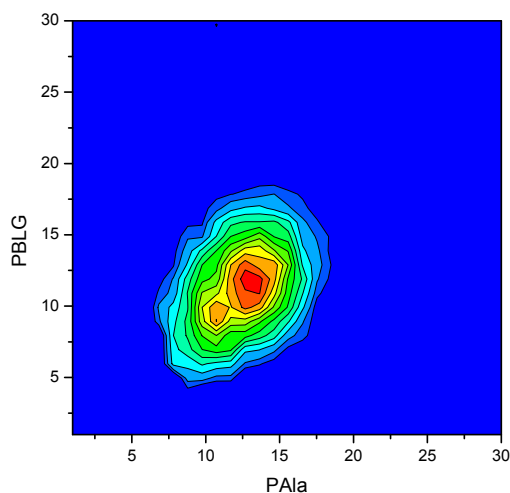


**Figure 7.1.** Contour plot of the copolymer P(BLG-co-Ala) analyzed by MALDI-ToF-MS at 5% monomer conversion.

### 7.3.2 NMRP reactions and deprotection

The polypeptide macroinitiators containing the SG1- and TIPNO-based NMRP groups were used for the initiation of the polymerizations of styrene (S) and *n*-butylacrylate (BA) (Table 7.2). For the BA polymerizations the macroinitiators were dissolved in N-methylpyrrolidone (NMP) together with BA and 10 mol% of the corresponding free nitroxide in a Schlenk tube. According to literature reports better control over the polymerization reaction is achieved in the presence of additional free SG1 and if the polymerization is performed at a lower reaction temperature.<sup>42,43</sup> Specifically, for a SG-1 functionalized peptide the temperature was increased slowly.<sup>33</sup> These reports were combined for the used procedure. The polymerization temperature was increased to 60 °C for several minutes and subsequently to 90 °C and kept at this temperature for 1 hour. Although initially at 90 °C a clear increase in molecular weight was observed with respect to the low temperature product, the reaction seemed to stop. However, by increasing the temperature to above 100 °C the molecular weight was found to increase again, although at this temperature high quantities of low molecular weight poly(*n*-butylacrylate) (PBA) were found. In conventional free radical polymerization of polyacrylates it was found that radical backbiting

occurs during the polymerization.<sup>44</sup> The radical transferred onto the polymer chain, facilitating fragmentation and branching, resulting in free PBA. The termination of the polyacrylates occurs predominantly by combination, but this can be confused with the fragmentation process. During nitroxide-mediated radical polymerization (NMRP) the same side reactions do occur. The solution was finally cooled to room temperature and the block copolymer was selectively precipitated in methanol to remove most of the free PBA. Both types of nitroxide radicals, *viz.* TIPNO and SG1, worked sufficiently well for the polymerization initiation and resulted in block copolymers with relatively low polydispersities (Figure 7.2). For the styrene polymerization both nitroxide macroinitiators were efficient initiators, although lower polydispersities were obtained using the TIPNO initiator. Gradient polymer elution chromatography (GPEC) was performed to determine the chain composition of the reaction product of the radical polymerization. For PBLG<sub>30</sub>-*co*-P(BLG<sub>15</sub>-*co*-Ala<sub>15</sub>)-*b*-PBA a clear shift of the peak was found compared to the macroinitiator (Figure 7.3). The shift was towards the homopolymer of PBA, indicating that the block copolymer was formed. GPEC also showed the formation of traces of PBA and PS homopolymers in some reactions (Entries 2, 3, 4, 6 and 8, Table 7.2).

Since no kinetic study was carried out for initiator **1** no claim can be made about the livingness of the polymerization. However, from the increasing molecular weight, the copolymer composition (Table 7.2) and from the GPEC results it can be concluded that a block copolymer had indeed been formed.

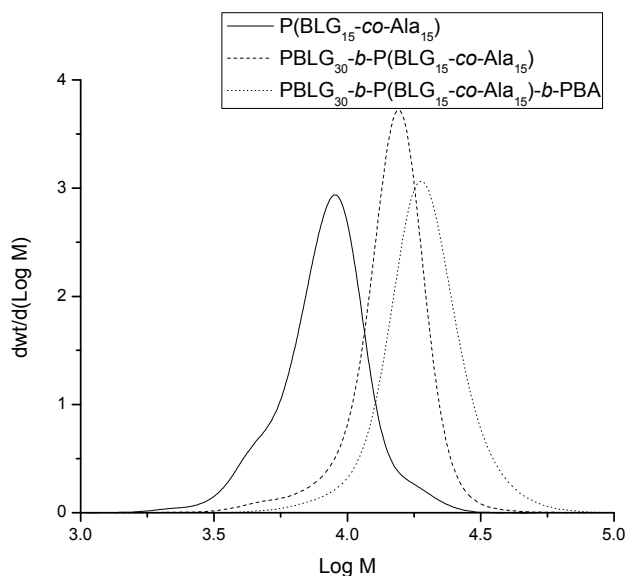


**Figure 7.2.** DMAc-SEC plots of P(BLG<sub>15</sub>-*co*-Ala<sub>15</sub>) (Entry 5, Table 7.1), PBLG<sub>30</sub>-*b*-P(BLG<sub>15</sub>-*co*-Ala<sub>15</sub>)-SG1 macroinitiator (entry 6, Table 7.1) and PBLG<sub>30</sub>-*b*-P(BLG<sub>15</sub>-*co*-Ala<sub>15</sub>)-*b*-PBA block copolymer (entry 6, Table 7.2).



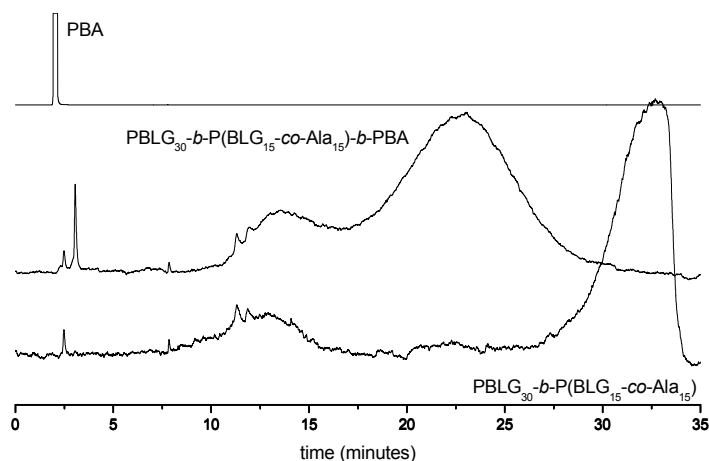


**Figure 7.3.** Gradient polymer elution chromatography of PBA, PBLG<sub>30</sub>-*b*-P(BLG<sub>15</sub>-*co*-Ala<sub>15</sub>)-*b*-PBA (entry 6, Table 7.2) and PBLG<sub>30</sub>-*b*-P(BLG<sub>15</sub>-*co*-Ala<sub>15</sub>)-SG1 (entry 6, Table 7.1). The eluent was 100% toluene for the first 2 minutes and gradually changed to 80% toluene/20% DMF over 30 minutes. After that, in 2 minutes the eluent was changed to 100% toluene and maintained for another 3 minutes.

**Table 7.2.** Bioconjugate block copolymers from the NMRP of polypeptide macroinitiators.

| Entry | Polymer  | Nitroxide | $M_n^a$ (g/mol) | PDI  | ratio BA/St:<br>amino acid <sup>b</sup> |
|-------|--|-----------|-----------------|------|---|
| 1     | PBLG <sub>20</sub> - <i>b</i> -PBA   | TIPNO     | 7,500           | 1.21 | 1.08 : 1                                |
| 2     | PBLG <sub>60</sub> - <i>b</i> -PBA   | SG1       | 19,000          | 1.47 | 2.86 : 1                                |
| 3     | P(BLG <sub>50</sub> - <i>co</i> -Ala <sub>10</sub> )- <i>b</i> -PBA  | SG1       | 20,400          | 1.17 | 2.64 : 1                                |
| 4     | P(BLG <sub>30</sub> - <i>co</i> -Ala <sub>30</sub> )- <i>b</i> -PBA  | SG1       | 19,500          | 1.38 | 3.70 : 1                                |
| 5     | P(BLG <sub>15</sub> - <i>co</i> -Ala <sub>15</sub> )- <i>b</i> -PBLG <sub>30</sub> - <i>b</i> -PBA                                 | SG1       | 20,300          | 1.33 | 2.97 : 1                                |
| 6     | PBLG <sub>30</sub> - <i>b</i> -P(BLG <sub>15</sub> - <i>co</i> -Ala <sub>15</sub> )- <i>b</i> -PBA                                 | SG1       | 18,000          | 1.14 | 0.55 : 1                                |
| 7     | P(BLG <sub>15</sub> - <i>co</i> -Ala <sub>15</sub> )- <i>b</i> -P(BLG <sub>25</sub> - <i>co</i> -Ala <sub>5</sub> )- <i>b</i> -PBA | SG1       | 14,400          | 1.08 | 0.41 : 1                                |
| 8     | PBLG <sub>60</sub> - <i>b</i> -PS  | TIPNO     | 19,900          | 1.33 | 1.74 : 1                                |
| 9     | P(BLG <sub>50</sub> - <i>co</i> -Ala <sub>10</sub> )- <i>b</i> -PS   | SG1       | 25,200          | 1.60 | 4.13 : 1                                |
| 10    | P(BLG <sub>30</sub> - <i>co</i> -Ala <sub>30</sub> )- <i>b</i> -PS   | TIPNO     | 18,200          | 1.31 | 1.86 : 1                                |

a) All block copolymers measured by DMAc-SEC; b) Compositions determined by <sup>1</sup>H-NMR. For PBA-based copolymers these were determined in *d*-TFA using signals at 4.9 ppm (protons of the amino acid residues in the main chain of the polypeptide) and 1.1 ppm (*n*-butyl). Compositions of PS-based polymers were determined in *d*<sub>7</sub>-DMF using signals at 5.3 ppm (methylene of benzylesters) and 6.6-7.8 ppm for PS.

The benzylesters on the PBA block copolymers were selectively deprotected by catalytic hydrogenation with the use of palladium catalyst to preserve the esters of the *n*-butylacrylate. The polymers were dissolved in DMF or NMP with a few milligrams of the catalyst. The conversion of the hydrogenation was monitored by <sup>1</sup>H-NMR by recording the disappearance of the peak of the aromatic protons at 7.4 ppm (see Table 7.3). While full conversion was not achieved for the catalytic deprotections, conversion exceeded 90% for all reactions. A selective catalytic deprotection was not necessary for polystyrene-*b*-poly( $\gamma$ -benzyl-L-glutamate), due to the absence of labile ester bonds in the PS blocks. The block copolymers with polystyrene were therefore deprotected quantitatively by dissolving them in DCM followed by the addition of HBr in acetic acid. After precipitation in diethylether the polymer was dried in a vacuum oven.

### 7.3.3 Particle formation in phosphate buffer solution

The synthesized amphiphilic block copolymers were dissolved in DMSO or NMP (the latter for the polystyrene block copolymers). A 0.10 M phosphate buffer solution with a pH of 7.4 was added slowly over 3 hours and the solution was dialyzed against the phosphate buffer solution buffer for 2 days. The critical micelle concentrations (CMCs) of the deprotected block copolymer solutions were determined using SLS and proved to be in the range from  $2 \times 10^{-3}$  to  $1.5 \times 10^{-1}$  mg/ml (Table 7.3), depending on the block copolymer composition. DLS was used to identify the particle size of the formed particles. The deprotected copolymers gave particles in the nanometer range. For some of the polymers with a polypeptide block with a higher L-alanine content larger overall particle sizes with bimodal distributions were found, such as for P(Glu<sub>30</sub>-co-Ala<sub>30</sub>)-*b*-PS (entry 7, Table 7.3). Cryo-TEM was used to determine the particle shape of selected samples. For the analyzed Glu<sub>60</sub>-*b*-PBA and P(Glu<sub>30</sub>-co-Ala<sub>30</sub>)-*b*-PBA block copolymers, large spherical particles were found ranging from 20 to 80 nm (Figures 7.4 a, b and c). The large particles are unlikely to be pure micelles, but might also contain some PBA homopolymer (as was detected by GPEC).<sup>45</sup> For the P(Glu<sub>30</sub>-co-Ala<sub>30</sub>)-*b*-PS solution cryo-TEM showed the presence of vesicles as well as micelles (Figures 7.4 d, e and f). The combination of these different sized particles in the solution explains the broader particle size distribution (higher PI values, see Table 7.3). Vesicles were only found for P(Glu<sub>30</sub>-co-Ala<sub>30</sub>)-*b*-PS, while for P(Glu<sub>60</sub>-*b*-PS only micelles could be identified.

**Table 7.3.** Deprotection efficiency, particle size, CMC and enzymatic stability of particles of deprotected bioconjugate block copolymers.

| Entry | Polymer  | Deprotection (%) <sup>a</sup> | Z <sub>Av</sub> (nm) <sup>b</sup> | PI <sup>b</sup> | CMC (mg/ml) <sup>c</sup> | Precipitation (# days) <sup>b</sup> |
|-------|--|-------------------------------|-----------------------------------|-----------------|--------------------------|-------------------------------------|
| 1     | PGlu <sub>60</sub> - <i>b</i> -PBA   | 91                            | 129.6                             | 0.139           | 8.0 x 10 <sup>-3</sup>   | none                                |
| 2     | P(Glu <sub>50</sub> - <i>co</i> -Ala <sub>10</sub> )- <i>b</i> -PBA  | 90                            | 168.8                             | 0.101           | 9.0 x 10 <sup>-3</sup>   | none                                |
| 3     | P(Glu <sub>30</sub> - <i>co</i> -Ala <sub>30</sub> )- <i>b</i> -PBA  | 93                            | 149.7                             | 0.084           | 7.0 x 10 <sup>-3</sup>   | 4                                   |
| 4     | PGlu <sub>30</sub> - <i>b</i> -P(Glu <sub>15</sub> - <i>co</i> -Ala <sub>15</sub> )- <i>b</i> -PBA   | 94                            | 63.2                              | 0.186           | 1.5 x 10 <sup>-1</sup>   | 4                                   |
| 5     | P(Glu <sub>15</sub> - <i>co</i> -Ala <sub>15</sub> )- <i>b</i> -P(Glu <sub>25</sub> - <i>co</i> -Ala <sub>5</sub> )- <i>b</i> -PBA                             | 90                            | 37.7                              | 0.165           | 1.5 x 10 <sup>-1</sup>   | None                                |
| 6     | PGlu <sub>60</sub> - <i>b</i> -PS  | 100                           | 48.5                              | 0.117           | 2.5 x 10 <sup>-1</sup>   | None                                |
| 7     | P(Glu <sub>30</sub> - <i>co</i> -Ala <sub>30</sub> )- <i>b</i> -PS   | 100                           | 129.5                             | 0.298           | 2.0 x 10 <sup>-3</sup>   | None                                |
| 8     | P(Glu <sub>30</sub> - <i>co</i> -Ala <sub>30</sub> )- <i>b</i> -PS / P(Glu <sub>30</sub> - <i>co</i> -Ala <sub>30</sub> )- <i>b</i> -PBA (1:1) mixed solutions | -                             | 151.3                             | 0.258           | -                        | 4                                   |

a) Conversion for the removal of benzyl esters from PBA-based block copolymers was determined with in d-TFA by monitoring the absorptions at 7.4 ppm (aromatics of benzylester) and at 4.9 ppm (protons of the amino acid residues in the main chain of the polypeptide). For <sup>1</sup>H-NMR in DMF-d<sub>7</sub> on PS-based block copolymers the absorptions at 6.8-7.8 ppm (all aromatics) and 5.3 ppm (methylene of benzylesters) were used. b) Particle size and polydispersity index was determined by DLS. c) Determined by static light scattering. d) Precipitation determined visually during the enzymatic degradation of elastase.

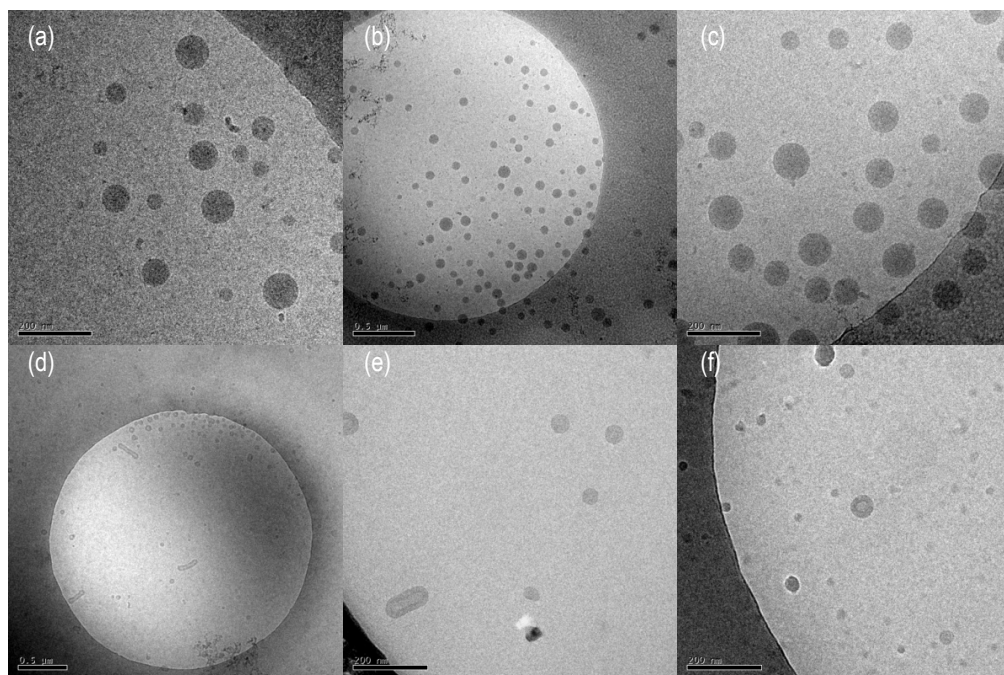


**Figure 7.4.** Cryo-TEM pictures of (a) PGLU<sub>60</sub>-*b*-PBA (2 mg/ml), (b) and (c) P(GLU<sub>30</sub>-*co*-Ala<sub>30</sub>)-*b*-PBA (10 mg/ml) and (d), (e) and (f) P(GLU<sub>30</sub>-*co*-Ala<sub>30</sub>)-*b*-PS (2 mg/ml). Scale bars are 200 nm in pictures (a), (c), (e) and (f). Scale bars are 500 nm in pictures (b) and (d).

### 7.3.4 Enzymatic degradation

To investigate the activity of different enzymes, polypeptides with a degree of polymerization of 40 were fluorescently labeled by reacting PBLG and P(BLG-*co*-Ala) polypeptides with the succinimide ester of 5(6)-carboxyfluorescein after the NCA monomers had been fully converted (See Chapter 5). The fluorescein-functionalized polypeptide was deprotected with HBr in acetic acid and TFA and after purification dissolved in a phosphate buffer solution. To identify the specificity of enzymes two peptidases were added, *viz.* thermolysin and elastase. Elastase is known to selectively cleave Ala-Ala bonds and thermolysin prefers a hydrophobic monomer and is less specific for the Ala-Ala bond. To identify if the observed effect was truly due to the specificity of the peptidases a lipase from *Thermomyces Lanuginosus* was added as a negative control. To the fluorescent polypeptide solutions the enzymes were added and after one day the reaction solutions were analyzed by LC-MS. With the use of the fluorescent label the original polypeptide chain end could be easily detected at 494 nm.

For the copolypeptide of P(Glu-*co*-Ala) mass spectroscopy confirmed that the new LC-MS peaks at 15-16 minutes did represent the fragments of fluorescent-labeled L-alanine and L-glutamic acid after the reaction with both peptidases (Figure 7.5). The same peaks as well as others were found at 9-10 minutes for 280 nm. The mass spectrum of these compounds showed to be newly formed fragments,

formed due to enzymatic degradation. These fragments do not contain any fluorescent endgroups. As a negative control, the homopolymer of poly(L-glutamic acid) gave no response to the peptidases and for the reaction with the lipase from *Thermomyces Lanuginosus* no degradation was found for any of the polypeptides.

**Table 7.4.** Response of (co)polypeptides to enzymes.

| Polypeptide              | Blank | Elastase    | Thermolysin | Lipase |
|--------------------------|-------|-------------|-------------|--------|
| P(Glu)fluorescein        | None  | None        | None        | None   |
| P(Glu-co-Ala)fluorescein | None  | Degradation | Degradation | None   |

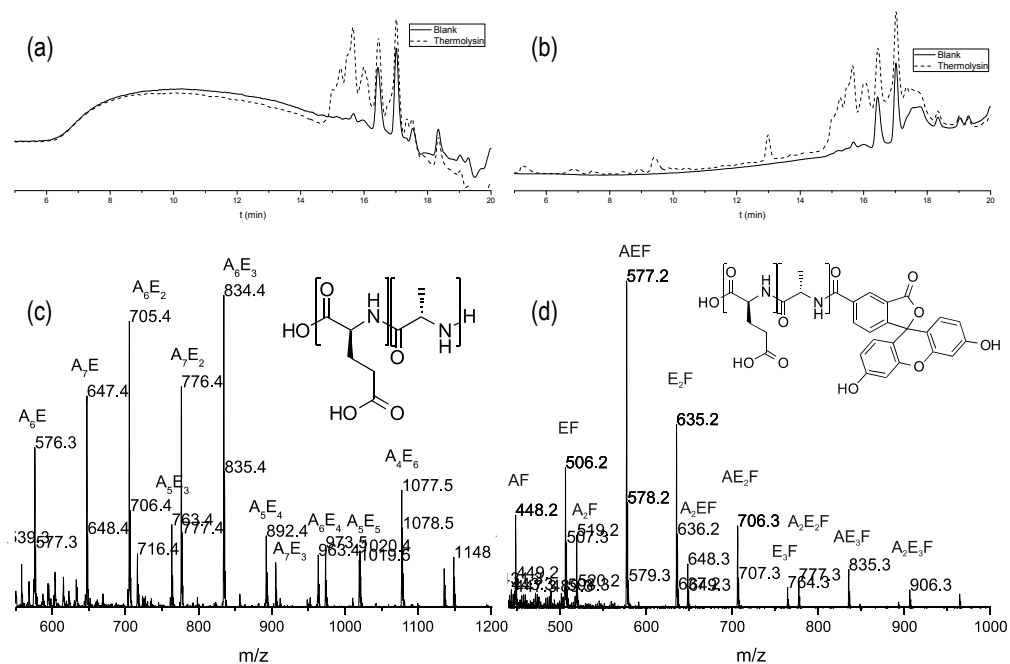


**Figure 7.5.** LC-MS of degradation of fluorescein-labeled P(Glu-co-Ala) with thermolysin. LC UV:  $\lambda=494$  nm (a) and  $\lambda=280$  nm (b) and MS for fluorescein-labeled P(Glu-co-Ala) corresponding to the retention time of 9 to 10 minutes (c) and the retention time of 15 to 16 minutes (d). In the MS spectra A represents the number of L-alanine residues, whereas E represents the number of L-glutamic acid residues.

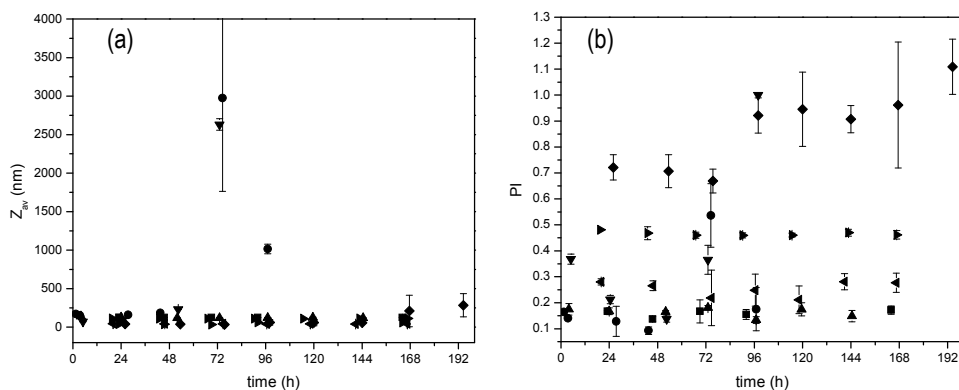


**Figure 7.6.** DLS measurements of enzymatic degradation with elastase: particle size (a) and polydispersity (b) for (■) P(Glu<sub>60</sub>-b-PBA, (●) P(Glu<sub>30</sub>-co-Ala<sub>30</sub>)-b-PBA, (▲) P(Glu<sub>50</sub>-co-Ala<sub>10</sub>)-b-PBA, (▼) P(Glu<sub>30</sub>-b-P(Glu<sub>15</sub>-co-Ala<sub>15</sub>)-b-PBA, (◆) P(Glu<sub>15</sub>-co-Ala<sub>15</sub>)-b-P(Glu<sub>25</sub>-co-Ala<sub>5</sub>)-b-PBA, (◄) PBLG<sub>60</sub>-b-PS and (►) P(Glu<sub>30</sub>-co-Ala<sub>30</sub>)-b-PS.

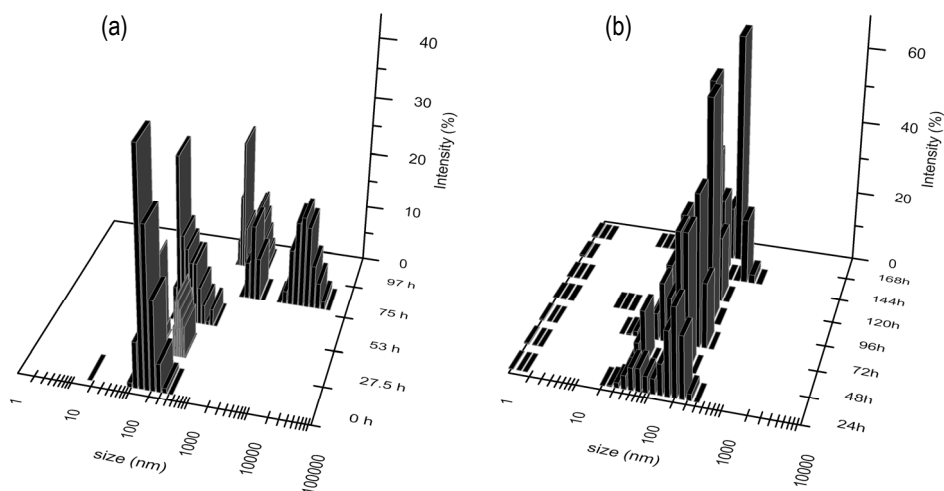


**Figure 7.7.** DLS measurement of enzymatic degradation of P(Glu<sub>30</sub>-co-Ala<sub>30</sub>)-b-PBA (entry 3, Table 7.3) with elastase (a). DLS measurement of enzymatic degradation of P(Glu<sub>30</sub>-co-Ala<sub>30</sub>)-b-PS (entry 7, Table 7.3) with elastase (b).

The enzyme solution was then added to the solution of the biohybrid polymer particles. The particle sizes and polydispersities were monitored over time (Figure 7.6). For the enzymatic degradation using elastase large differences between the different polypeptide compositions were found. For the poly(*n*-butylacrylate)-containing block copolymers with a high content of Ala a quick increase in the particle size and polydispersity was observed after three days and the polymer (partially) precipitated on the fourth day (entry 3, Table 7.3 and Figure 7.7a). For the block copolymer P(Glu<sub>30</sub>-b-P(Glu<sub>15</sub>-co-Ala<sub>15</sub>)-b-

PBA (entry 4, Table 7.3) the same behaviour was observed (Figure 7.8). This again resulted in large clusters of particles with a size of a few micrometers. This indicates that the destabilization of the particles is predominantly dependent on the enzymatic cleavage of the Ala-Ala amide bonds near the hydrophobic core. For the polymers with a lower Ala content in the main chain less degradation was observed. The results so far are as expected, since the bioconjugate polymers with a high Ala content degrade due to the high number of Ala-Ala bonds in the polypeptide block.

For the polystyrene-containing block copolymer particles the particle size remained stable when exposed to the enzyme. More surprisingly, no precipitation was observed for the micelles containing the Ala copolypeptide, while that was clearly the case for the P(Glu<sub>30</sub>-co-Ala<sub>30</sub>)-*b*-PBA. The difference in this degradation behaviour must be due to the hydrophobic blocks of polystyrene and poly(*n*-butylacrylate). One difference is the mobility of the chains due to the low  $T_g$  of poly(*n*-butylacrylate).<sup>46</sup> Firstly, this gives the polymer the opportunity to deform more easily, resulting in the coalescence of particles during the degradation. Secondly it influences the dynamic behaviour of the block copolymers in the micelles, which are known to be in an equilibrium state with free chains in the solution.<sup>47</sup> For polystyrene-containing block copolymers this process is observed only at elevated temperatures due to the high  $T_g$  of the material. This also indicates that because of the low mobility of the chains the polystyrene-containing chains do not easily transfer into the water phase, while the PBA-containing block copolymers are more likely to migrate.<sup>48-50</sup> This could have a significant consequence for the enzymatic degradation, since most of the enzyme is dispersed in the bulk solution. Assuming that the majority of the degradation occurs in the solution, in view of the lower accessibility of the enzyme by the other rigid chains in the micelle shell, a more dynamic system would degrade faster.<sup>16,51</sup> It was found that for gold nanoparticles with a nanolayer of peptides and grafted PEG chains the enzymatic degradation of polypeptide chains on the particle shell decreased. The PEG chains were found to reduce the access of the enzyme to the peptide chains.<sup>22</sup>

In order to provide further evidence for this hypothesis the degradation of the P(Glu<sub>30</sub>-co-Ala<sub>30</sub>)-*b*-PS systems was studied at higher temperatures using thermolysin. Thermolysin is a thermostable enzyme with an optimum activity at 70 °C. Since the mobility of the polystyrene chains is increased above 60 °C, similar conditions as for the poly(*n*-butylacrylate)-containing copolymers with unimer exchange could be achieved.<sup>49</sup> The sample with thermolysin showed a significant increase in particle size compared to the blank sample maintained under the same conditions, indicating that the enzymatic degradation occurred. A comparison was made with the previous degradation conditions by keeping the enzyme activity and temperature in mind. At 37 °C thermolysin showed no reactivity towards either P(Glu<sub>30</sub>-co-Ala<sub>30</sub>)-*b*-PBA or P(Glu<sub>30</sub>-co-Ala<sub>30</sub>)-*b*-PS particles.

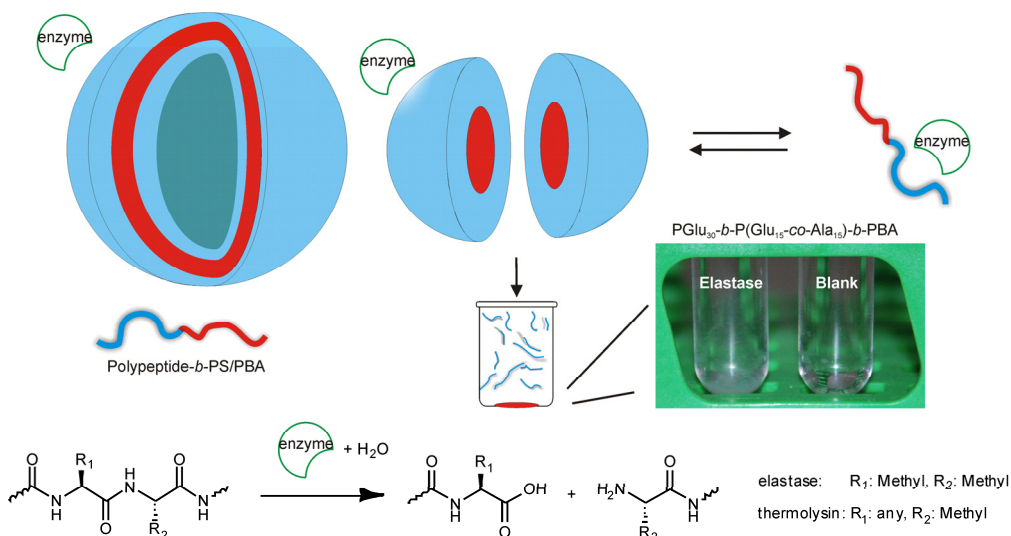


**Figure 7.8.** Schematic degradation of micelles, with a picture of degraded precipitated material.

To show the selectivity of the enzymatic degradation by elastase both P(Glu<sub>30</sub>-co-Ala<sub>30</sub>)-*b*-PS and P(Glu<sub>30</sub>-co-Ala<sub>30</sub>)-*b*-PBA solutions were mixed and elastase was added to the new solution containing both PS- and PBA-containing block copolymers. Precipitation was observed after 3 days, while DLS still showed the presence of particles in the solution. The particle sizes did resemble that of the PS block copolymers. The precipitate was analyzed by <sup>1</sup>H-NMR and proved to be PBA, indicating that the degradation was very selective towards the P(Glu<sub>30</sub>-co-Ala<sub>30</sub>)-*b*-PBA micelles.

## 7.4 Conclusions

Biohybrid block copolymers of poly(*n*-butylacrylate) and (block co)polypeptides of PGlu and P(Glu-co-Ala) have been made using two different amine-functionalized bifunctional NMRP initiators based on the nitroxides TIPNO and SG1. Both bifunctional initiators successfully initiated the ROP of NCA. The polypeptide-based macroinitiators for controlled NMRP were used for the chain extension with polystyrene and poly(*n*-butylacrylate). The benzylesters of poly(*n*-butylacrylate)-containing block copolymers were subsequently selectively deprotected.

A mixture of vesicles and micelles was obtained from the amphiphilic block copolymers and their enzymatic stability was investigated. It was found that for the degradation by elastase the amount of L-alanine in the polypeptide block is of great importance for the hydrolysis and stability of the particles. At a 50% L-alanine composition the particles showed an increase in particle size after three days, due to degradation under the applied conditions. By altering the peptide block copolymer composition it was found that the composition of the polypeptide block near the hydrophobic block had the most profound



effect on the stability of the particles. No effect of the enzymatic degradation was seen at 37 °C for the particles containing a polystyrene block copolymer. This was probably due to the limited unimer exchange between the polymer micelle and the solution and the better particle stability due to the high  $T_g$ . This hypothesis was confirmed by the successful degrading the polystyrene-polypeptide particles at 70 °C with thermolysin. The results suggest that polypeptide hybrid particles (micelles and vesicles) can be degraded selectively depending on the composition of the hydrophilic polypeptide block and the composition of the hydrophobic non-degradable block.

These results give guidelines towards the design of particles with targeted composition for biological processes with respect to their interaction with enzymes.

## References

- <sup>1</sup> H.G. Börner and H. Schlaad, *Soft Matter* **2007**, 3, 394–408
- <sup>2</sup> H.-A. Klok, *Macromolecules* **2009**, 42, 7990–8000
- <sup>3</sup> H.-A. Klok, *J. Polym. Sci. Part. A: Polym. Chem.* **2005**, 43, 1–17
- <sup>4</sup> H.M. Robson and A. Kros, *Macromol. Biosci.* **2009**, 9, 935–1036
- <sup>5</sup> R.J.I. Knoop, M. de Geus, G.J.M. Habraken, C.E. Koning, H. Menzel and A. Heise, *Macromolecules* **2010**, 43, 4126–4132
- <sup>6</sup> F. Audouin, R.J.I. Knoop, J. Huang and A. Heise, *J. Polym. Sci. Part A: Polym. Chem.* **2010**, 48, 4602–4610
- <sup>7</sup> M.L. Becker, J. Liu and K.L. Wooley, *Biomacromolecules* **2005**, 6, 220–228
- <sup>8</sup> S. Lecommandoux, O. Sandre, F. Chécot, J. Rodriguez-Hernandez and R. Perzynski, *Adv. Mater.* **2005**, 17, 712–718
- <sup>9</sup> S. Motala-Timol, D. Jhurry, J. Zhou, A. Bhaw-Luximon, G. Mohun and H. Ritter, *Macromolecules* **2008**, 41, 5571–5576
- <sup>10</sup> B. Nottelet, A. El Ghzaoui, J. Coudane and M. Vert, *Biomacromolecules* **2007**, 8, 2594–2601
- <sup>11</sup> R.H.P. Doezé, B.A. Maltman, C.L. Egan, R.V. Ulijn, and S.L. Flitsch *Angew. Chem. Int. Ed.* **2004**, 43, 3138–3141
- <sup>12</sup> J. Polaina and A.P. MacCabe, *Industrial Enzymes* **2007**, Springer Utrecht
- <sup>13</sup> T. Hayashi, Y. Tabata, A. Nakajima, *Polymer J.* **1985**, 17, 463–471
- <sup>14</sup> H. Sugiyama and H. Noda, *Biopolymers* **1970**, 9, 459
- <sup>15</sup> C. Sanson, C. Schatz, J.-F. Le Meins, A. Brûlet, A. Soum and S. Lecommandoux, *Langmuir* **2010**, 26, 2751–2760
- <sup>16</sup> M.G. Carstens, C.F. van Nostrum, R. Verrijck, L.G.J. De Leede, D.J.A. Crommelin and W.E. Hennink, *J. Pharm. Sci.* **2008**, 97, 506–518
- <sup>17</sup> J.-W. Hofman, M. G. Carstens, F. van Zeeland, C. Helwig, F. M. Flesch, W.E. Hennink and C.F. van Nostrum, *J. Pharm. Sci.* **2008**, 25, 2065–2073
- <sup>18</sup> R.V. Ulijn, *J. Mater. Chem.* **2006**, 16, 2217–2225
- <sup>19</sup> P.D. Thornton, R.J. Mart and R.V. Ulijn, *Adv. Mater.* **2007**, 19, 1252–1256
- <sup>20</sup> M. van Dijk, C.F. van Nostrum, W.E. Hennink, D.T.S. Rijkers and R.M.J. Liskamp, *Biomacromolecules* **2010**, 11, 1608–1614
- <sup>21</sup> P. D. Thornton and A. Heise, *J. Am. Chem. Soc.* **2010**, 132, 2024–2028
- <sup>22</sup> P. Free, C. P. Shaw and R. Lévy, *Chem. Commun.* **2009**, 5009–5011
- <sup>23</sup> B.-C. Yin, M. Zhang, W. Tan and B.-C. Ye, *ChemBioChem* **2010**, 11, 494–497
- <sup>24</sup> A.W. Bosman, R. Vestberg, A. Heumann, J.M.J. Frechet and C. J. Hawker, *J. Am. Chem. Soc.* **2003**, 125, 715–728
- <sup>25</sup> G.J.M. Habraken, M. Peeters, C.H.J.T. Dietz, C.E. Koning and A. Heise, *Polym. Chem.* **2010**, 1, 514–524
- <sup>26</sup> G. Ye, N.-H. Nam, A. Kumar, A. Saleh, D.B. Shenoy, M.M. Amiji, X. Lin, G. Sun and K. Parang, *J. Med. Chem.* **2007**, 50, 3604–3617
- <sup>27</sup> J. Vinas, N. Chagneux, D. Gimes, T. Trimaille, A. Favier and D. Bertin, *Polymer* **2008**, 49, 3639–3647
- <sup>28</sup> W. Agut, D. Taton and S.Lecommandoux, *Macromolecules* **2007**, 40, 5653–5661
- <sup>29</sup> C. Schatz, S. Louguet, J.-F. Le Meins and S. Lecommandoux, *Angew. Chem. Int. Ed.* **2009**, 48, 2572–2575
- <sup>30</sup> H. Rettig, E. Krause and H.G. Börner, *Macromol. Rapid Commun.* **2004**, 25, 1251–1256

- <sup>31</sup> M.L. Becker, J. Liu and K.L. Wooley, *Chem. Commun.* **2003**, 180-181
- <sup>32</sup> M. G. J. ten Cate, H. Rettig, K. Bernhardt and H.G. Börner, *Macromolecules* **2005**, 38, 10643-10649
- <sup>33</sup> T. Trimaille, K. Mabrouk, V. Monnier, L. Charles, D. Bertin and D. Gigmes, *Macromolecules* **2010**, 43, 4864-4870
- <sup>34</sup> K.R. Brzezinska and T. J. Deming, *Macromol. Biosci.* **2004**, 4, 566-569
- <sup>35</sup> I. Dimitrov and H. Schlaad, *Chem. Commun.* **2003**, 2944-2945
- <sup>36</sup> J.R.I. Knoop, G.J.M. Habraken, N. Gogibus, S. Steig, H. Menzel, C.E. Koning and A. Heise, *J. Polym. Sci. Part A: Polym. Chem.* **2008**, 46, 3068-3077
- <sup>37</sup> G.J.M. Habraken, C.E. Koning and A. Heise, *J. Polym. Sci. Part A: Polym. Chem.* **2009**, 47, 6883-6893
- <sup>38</sup> S. Steig, F. Cornelius, A. Heise, J.R.I. Knoop, G.J.M. Habraken, C.E. Koning and H. Menzel, *Macromol. Symp.* **2007**, 248, 199-206
- <sup>39</sup> C.-J. Huang and F.-C. Chang, *Macromolecules* **2008**, 41, 7041-7052
- <sup>40</sup> E.P. Holowka, D.J. Pochan and T.J. Deming, *J. Am. Chem. Soc.* **2005**, 127, 12423-12428
- <sup>41</sup> J. Sun, X. Chen, C. Deng, H. Yu, Z. Xie and X. Jing, *Langmuir* **2007**, 23, 8308-8315
- <sup>42</sup> C.R. Becer, R.M. Paulus, R. Hoogenboom and U.S. Schubert, *J. Polym. Sci. Part A: Polym. Chem.* **2006**, 44, 6202-6213
- <sup>43</sup> D. Benoit, V. Chaplinski, R. Braslau and C.J. Hawker, *J. Am. Chem. Soc.* **1999**, 121, 3904-3920
- <sup>44</sup> G. Moad and D.H. Solomon, *'The chemistry of radical polymerization'* **2006**, second edition, Elsevier
- <sup>45</sup> O. Colombani, M. Ruppel, M. Burkhardt, M. Drechsler, M. Schumacher, M. Gradzielski, R. Schweins and A.H.E. Müller, *Macromolecules* **2007**, 40, 4351-4362
- <sup>46</sup> J. Brandrup, E.H. Immergut and E.A. Grulke, *'Polymer Handbook'* **1999**, fourth edition, John Wiley & Sons, Inc.
- <sup>47</sup> I.W. Hamley, *'Block Copolymers in Solution'* **2005**, John Wiley & Sons, Ltd
- <sup>48</sup> M. Tian, A. Qin, C. Ramireddy, S. E. Webber, P. Munk, Z. Tuzar and K. Prochazka, *Langmuir* **1993**, 9, 1741-1748
- <sup>49</sup> J. van Stam, S. Creutz, F.C. De Schryver, and R. Jérôme, *Macromolecules* **2000**, 33, 6388-6395
- <sup>50</sup> O. Colombani, M. Ruppel, F. Schubert, H. Zettl, D. Pergushov and A.H.E. Müller, *Macromolecules* **2007**, 40, 4338-4350
- <sup>51</sup> K. Letchford, J. Zastre, R. Liggins and H. Burt, *Colloids Surf. B* **2004**, 35, 81-91

## Chapter 8

# Enzymatically Degradable Polypeptide Vesicles with the Potential for Selective Delivery Applications

### Abstract

*Polypeptide vesicles based on different amino acid combinations have been reported with applications such as drug and gene delivery. These polypeptide structures have not yet been tested for enzymatic degradation, though this enzymatic process could be a selective release trigger for payload release. In this study vesicles of L-glutamic acid and L-alanine comprising block copolymers are synthesized and their selective enzymatic degradation by hydrolysis of the hydrophobic L-alanine block is followed by DLS and optical microscopy. The enzymatic degradation was shown to be dependent on the chain length and composition of the block copolymers. For recognition, the vesicles were further functionalized with  $\beta$ -galactose that can interact with RCA 120 lectin. In this work an initial step is made towards fully degradable vesicles for selective delivery.*

## 8.1 Introduction

The formation of vesicles or polymersomes (Scheme 8.1) has been reported for many block copolymers with different combinations of hydrophobic and hydrophilic blocks. Using the solvent solubility as a driving force, membranes are formed from the hydrophobic blocks, which are stabilized on both sides by the hydrophilic block. Applications for such vesicles have been discussed for the use in gene or drug delivery, for example. If properly designed, the membrane can be disrupted and the structure can deliver a payload using external triggers such as pH or the intracellular reduction of disulfide bonds.<sup>1,2</sup> The formation of vesicles for NCA ROP-prepared block copolypeptides has been studied as well.<sup>3,4</sup> Several combinations of peptide blocks have been reported to form vesicles. For example, the synthesis of PLys<sub>(20-80)</sub>-*b*-PLeu<sub>(10-30)</sub> block copolypeptides followed by a phase inversion from THF to demineralized water resulted in micrometer-sized vesicles. Similar results were obtained with PGlu-*b*-PLeu block copolypeptides.<sup>5</sup> The possibility of encapsulation of a fluorescent material was confirmed with the use of confocal scanning laser microscopy. Further studies showed that the hydrophobic block enabling the formation of the membrane can be substituted for phenylalanine, DOPA or PBLG-d<sub>7</sub>.<sup>6-8</sup> The PLys-*b*-PDOPA system was further used as it cross-links upon oxidation and thus a better particle stability is obtained. By substituting lysine with arginine PArg-*b*-PLeu was synthesized, which showed transport through the cell membrane.<sup>9,10</sup> All of these materials are assumed to be enzymatically degradable due to the amino acid residue composition. An interesting NCA ROP hybrid vesicle was reported by Schatz et al. for the combination of PBLG as the hydrophobic block and dextran (branched polysaccharide) as the hydrophilic block.<sup>11</sup> This can be considered a first step towards a synthetic viral capsid, since viruses are known to have carbohydrates for lectin cell-membrane recognition. It is known that specific carbohydrates bind with specific cell-membrane lectins.<sup>12</sup>

Although the preparation of peptide vesicles is well-known, the reported block copolypeptide vesicles lack functionalities for selective cell-recognition. Moreover, tests with peptidases to confirm the degradability have not yet been performed on these materials.

Enzymes occur in higher concentrations in certain places of the human body. For example elastase is found in a layer of cells in the skin.<sup>13</sup> Therefore these localized enzymes might be used for a selective degradation of Ala, Leu or any other hydrophobic peptide block of the vesicle and consequently trigger the release of the vesicles' cargo. The goal set out for this chapter was to synthesize carbohydrate-functionalizable vesicles based on peptide block copolymers, investigate their enzymatic degradation and provide a first proof of principle for lectin recognition.

First the synthesis of vesicles based on PGlu-*b*-PALa will be described (Scheme 8.1). The use of these vesicles will be demonstrated by functionalization with a carbohydrate for cell-membrane recognition. Furthermore, the formed vesicles will be used for a study into the selective enzymatic degradation of the hydrophobic poly(L-alanine) block.

## 8.2 Experimental

### Materials

Diethylether, DMF and NMP were purchased from Biosolve. DMAc was purchased from Aldrich. Propargylamine, PMDETA, CuBr, Lectin RCA 120, Lectin Con A, TFA and HBr 33% / acetic acid solution were purchased from Sigma. Elastase was purchased from Worthington Biochemical Corporation. NCAs of  $\gamma$ -benzyl-L-glutamate and L-alanine were prepared according to the synthetic procedure described in Chapter 2. 1-Azide- $\beta$ -galactose was synthesized according to literature procedures.<sup>14</sup>

### Methods

FTIR measurements were performed on a PerkinElmer SpectrumOne FTIR Spectrometer, using a universal ATR sampling accessory (resolution 1 cm<sup>-1</sup>). Samples for the IR spectroscopy were taken from the reaction mixtures and analyzed without further modification.

N,N,-dimethylacetamide size exclusion chromatography (DMAc SEC) was performed at 60 °C on a system equipped with a Waters 2695 separation module, a Waters 2414 refractive index detector (60 °C), a Waters 486 UV detector and a PSS GRAM guard column followed by 2 PSS GRAM columns in series of 100 Å (10  $\mu$ m particles) and 3000 Å (10  $\mu$ m particles) respectively. DMAc was used as eluent at a flow rate of (1 ml/min). The molecular weights were calculated using polystyrene standards. Before SEC analysis was performed, the samples were filtered through a 0.2  $\mu$ m PTFE filter (13mm, PP housing, Alltech).

<sup>1</sup>H-NMR spectra were measured on a 400 MHz Mercury 400 with deuterated TFA as solvent.

Dynamic light scattering was measured by a Coulter N4 plus in a 1 cm quartz cuvet at 90°.

Differential interference contrast optical microscopy was carried out using a Zeiss axioplan 2.

Transmission electron microscopy measurements were performed on a FEI Tecnai 20, type Sphera TEM instrument (with a LaB6 filament, operating voltage=200 kV). A 3  $\mu$ L sample was applied to a 200 mesh copper carbon only grid and the excess liquid was blotted away. The grid was analyzed under low dose conditions.

### Synthesis

**Synthesis of PBLG<sub>50</sub>-*b*-PAIa<sub>20</sub> with sampling.** The NCA of  $\gamma$ -benzyl-L-glutamate (1.94 g, 7.37 mmol) was dissolved in 10 ml DMF in a 40 ml Schlenk tube. Propargylamine (8.25 mg, 1.50 x 10<sup>-1</sup> mmol) in 1.2 ml DMF was added quickly with a syringe. The polymerization was performed at 20 °C under 0.01 mbar for 4 hours. Part of the solution was removed (6.6 wt%) and precipitated in water. The NCA of L-alanine (322 mg, 2.80 mmol) was dissolved in 4 ml DMF and added to the solution with the PBLG macroinitiator. The reaction was allowed to proceed for 1.5 hour at 20 °C and 0.01 mbar. The solution was finally precipitated in water. Yield: 1.67 g, 91.3 wt%

**Synthesis of PBLG<sub>100</sub>-*b*-PALa<sub>40</sub>.** The NCA of  $\gamma$ -benzyl-L-glutamate (1.060 g, 4.03 mmol) was dissolved in 5 ml DMF in a 40 ml Schlenk tube. Propargylamine (2.36 mg,  $4.23 \times 10^{-2}$  mmol) in 1.1 ml DMF was added quickly with a syringe. The polymerization was performed at 20 °C under 0.01 mbar for 5 hours until full conversion was achieved. The NCA of L-alanine (215 mg, 1.87 mmol) was dissolved in 3 ml DMF and added to the solution with the PBLG macroinitiator. The reaction was allowed to proceed for 1.5 hour at 20 °C and 0.01 mbar. The solution was finally precipitated in water. Yield: 0.922 g, 90.0 wt%

**Synthesis of PGLu<sub>50</sub>-*b*-PALa<sub>20</sub>.** The polypeptide (1.45 g) was dissolved in 12 ml TFA. To this solution 4 ml of HBr in acetic acid solution was added and the reaction was stirred for 16 hours. Then the solution was precipitated in diethylether. The polypeptide was allowed to settle on the bottom of the beaker and the solution was decanted. Diethylether was added and the mixture was stirred for 10 minutes after which the solvent was removed again by decantation. This procedure was repeated until a clear diethylether supernatant was obtained. After filtration, residual solvent was removed in vacuo at ambient temperature. Yield: 0.678 g, 73.9 wt%

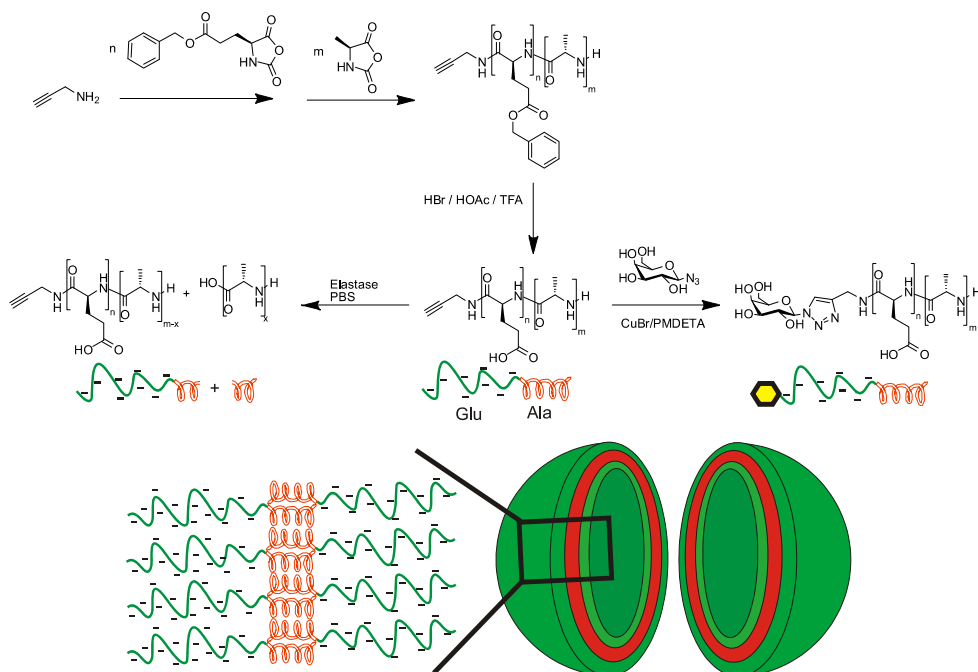
**Preparation of polypeptide block copolymers vesicles.** 50 mg of PGLu<sub>50</sub>-*b*-PALa<sub>20</sub> was dissolved in 5 ml NMP. PBS buffer (5 ml, pH = 7.6) was slowly added drop-wise during one hour. The reaction mixture was transferred into a 3500 Da cut-off membrane and left to dialyze against PBS buffer for two days.

**Example of the enzymatic degradation of PGLu<sub>50</sub>-*b*-PALa<sub>20</sub> in 0.10 M PBS.** 6 ml of the solution of the block copolypeptide (5 mg/ml) was added to a solution of 6.6 mg elastase (4 units/mg) in 1.5 ml of PBS buffer. The solution was divided over three reaction tubes, which were shaken in a waterbath at 37 °C, and periodically removed for measurements by DLS.

**Functionalization of PGLu-*b*-PALa with  $\beta$ -galactose by Huisgen Click reaction.** The propargyl-initiated deprotected polymer PGLu<sub>60</sub>-*b*-PALa<sub>30</sub> (263 mg,  $2.66 \times 10^{-5}$  mmol) was dissolved in 4 ml DMF with 1-azide- $\beta$ -galactose (29 mg,  $4.5 \times 10^{-5}$  mmol). To this solution CuBr (6.0 mg,  $4.2 \times 10^{-5}$  mol) and PMDETA (21 mg,  $1.2 \times 10^{-4}$  mol) were added after degassing. After 2 hours the reaction mixture was dialyzed for several days with NMP using an 8000 Da cut-off membrane to remove the copper catalyst. From the NMP solution 1.6 ml was added to a mixture of 3.4 ml of NMP and 5 ml of PBS buffer. After dialysis against the buffer solution a solution was obtained for lectin testing. After dialysis against demineralized water and freeze drying a white powder was obtained.

**Turbidity lectin test with  $\beta$ -galactose-PGLu<sub>60</sub>-*b*-PALa<sub>30</sub> in 0.10M PBS.** The PBS buffer of the  $\beta$ -galactose-PGLu<sub>60</sub>-*b*-PALa<sub>30</sub> (1 mg/ml) (300  $\mu$ l) was mixed with 30  $\mu$ l of a 2 mg/ml lectin solution in PBS. The turbidity was observed visually.

### 8.3 Results and discussion



**Scheme 8.1.** Reaction sequence of NCA ROP for the synthesis of PBLG-*b*-PAla and subsequent deprotection, their assembly into vesicles and either enzymatic degradation using elastase (left part) or functionalization with β-galactose by azide-alkyne Huisgen cycloaddition (right part).

#### 8.3.1 Synthesis and vesicle formation

A series of block copolymers containing PBLG and PAla were prepared by NCA ROP under vacuum at 20 °C with propargylamine or benzylamine as initiator applying the optimized reaction conditions discussed in Chapters 2 and 3. The synthesis of the PBLG macroinitiator was monitored by FTIR and once full conversion was obtained the NCA of Ala was added. For entry 1, Table 8.1 the macroinitiator and block copolypeptide were characterized with SEC. An increase of the molecular weight was seen from  $M_n$ : 10,900 to  $M_n$ : 13,100 g/mol. Most polymerizations of PBLG-*b*-PAla resulted in the expected molecular weights with low PDIs and a composition close to the expected amino acid quantities as determined by <sup>1</sup>H-NMR (Table 8.1). The block copolymers were subsequently deprotected using HBr in TFA and acetic acid to remove the benzyl ester groups. This reaction was nearly quantitative for all block copolypeptides.



**Table 8.1.** Molecular characteristics of block copolypeptides prepared by NCA ROP initiated by propargylamine and average particle size ( $Z_{Av}$ ) of deprotected block copolypeptides in solution.

| Entry | Polymer  | $M_n$<br>(g/mol) <sup>(b)</sup> | PDI  | Composition <sup>(c)</sup> (Glu :<br>Ala) | $Z_{Av}$ (nm)<br>demi.<br>water | $Z_{Av}$ (nm)<br>0.10 M PBS |
|-------|--|---------------------------------|------|---|---------------------------------|-----------------------------|
| 1     | PBLG <sub>50</sub> - <i>b</i> -PAla <sub>20</sub>                                    | 13,100                          | 1.08 | 2.8 : 1.0                                 | 977 ± 456<br>PI: 1.69           | 309 ± 141<br>PI: 1.29       |
| 2     | PBLG <sub>40</sub> - <i>b</i> -PAla <sub>30</sub> <sup>(a)</sup>                     | 12,400                          | 1.08 | 1.4 : 1.0                                 | 168 ± 77<br>PI: 1.35            | 122 ± 51<br>PI: 0.61        |
| 3     | PBLG <sub>60</sub> - <i>b</i> -PAla <sub>30</sub>                                    | 17,200                          | 1.16 | 2.0 : 1.0                                 | -                               | 59 ± 26<br>PI: 0.73         |
| 4     | PBLG <sub>100</sub> - <i>b</i> -PAla <sub>40</sub>                                   | 22,700                          | 1.11 | 2.5 : 1.0                                 | 348 ± 162<br>PI: 1.51           | 330 ± 149<br>PI: 1.11       |
| 5     | PBLG <sub>60</sub> - <i>b</i> -PAla <sub>30</sub> - <i>b</i> -<br>PBLG <sub>60</sub> | 15,900                          | 1.39 | 3.8 : 1.0                                 | -                               | 286 ± 126<br>PI: 0.85       |
| 6     | PBLG <sub>50</sub> - <i>b</i> -P(Ala <sub>16</sub> -CO-<br>BLG <sub>4</sub> )        | 11,800                          | 1.27 | 3.6 : 1.0                                 | -                               | 896 ± 414<br>PI: 1.46       |
| 7     | PBLG <sub>100</sub> - <i>b</i> -P(Ala <sub>32</sub> -CO-<br>BLG <sub>8</sub> )       | 18,400                          | 1.15 | 3.8 : 1.0                                 | -                               | 779 ± 361<br>PI: 1.54       |

a) Initiated by benzylamine. b) Determined by DMAc-SEC. c) Determined by <sup>1</sup>H-NMR using the signal at 1.5 ppm for L-alanine and at 7.5 ppm for  $\gamma$ -benzyl-L-glutamate.

The deprotected polypeptides were dissolved in NMP and to this solution the phosphate buffer solution (PBS) was added slowly over time. The solution was dialyzed against the phosphate buffer solution for several days. To dissolve the polypeptides in demineralized water the NMP solution was diluted with demineralized water and a sodium bicarbonate solution. The solution was then dialyzed against demineralized water. In most cases this resulted in stable solutions without precipitation. Only for the PGLu<sub>100</sub>-*b*-PAla<sub>40</sub> some precipitation was observed.

The prepared samples displayed large size distribution in the DLS ranging from 10 nm to several micrometers. The measured nanometer-sized particles suggest the presence of micelles, while the particles of several micrometers of aggregates, tapes or vesicles. In general, the size of the particles in demineralized water was larger compared to the particle size in the PBS buffer (Table 8.1). For example, PGLu<sub>50</sub>-*b*-PAla<sub>20</sub> resulted in a size of 977 nm in demineralized water, while the size in 0.10 M phosphate buffer solution was 309 nm (entry 1, Table 8.1). The presence of the large vesicles was confirmed with differential interference contrast optical microscopy. Figure 8.1a shows an example of PGLu<sub>40</sub>-*b*-PAla<sub>30</sub> in demineralized water. An aggregate of vesicles is visible in which the separate vesicles have an average diameter of several micrometers. After the water was evaporated from the glass slide, the intact PGLu<sub>50</sub>-*b*-PAla<sub>20</sub> vesicles could be visualized by DIC microscopy as shown in Figure 8.1b. The shape and size of the micrometer size-range particles are in agreement with literature

reports on block copolypeptide vesicles.<sup>6,9</sup> To further investigate the shape of the particles, transmission electron microscopy (TEM) was used. For PGLu<sub>60</sub>-*b*-PALa<sub>30</sub> in 0.10 M PBS, TEM showed the presence of rounded sub-micrometer particles that were present in the solution, suggesting the presence of vesicles (Figure 8.2). Since there is salt in the solution it is possible that the particles shown are not solely the suprastructure, but also contain some residual buffer salt. The overall shape on the surface is circular with a lighter corona. The black patterns in the particles indicate that a vesicle membrane has dropped to the TEM grid surface, creating areas with a higher density of polypeptide. Vesicle collapse occurred due to the removal of the vesicle content by blotting and the vacuum applied during the sample preparation.

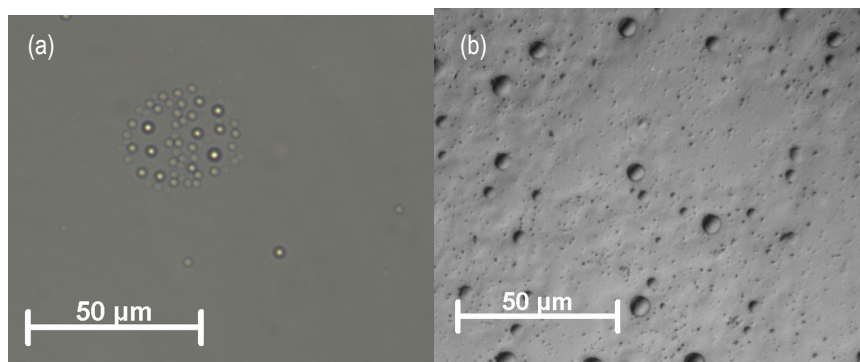


**Figure 8.1.** DIC optical microscopy of giant vesicles of PGLu<sub>40</sub>-*b*-PALa<sub>30</sub> (5 mg/ml) in demineralized water (a) and vesicles of PGLu<sub>50</sub>-*b*-PALa<sub>20</sub> (5 mg/ml) in demineralized water after drying on a glass slide (b).

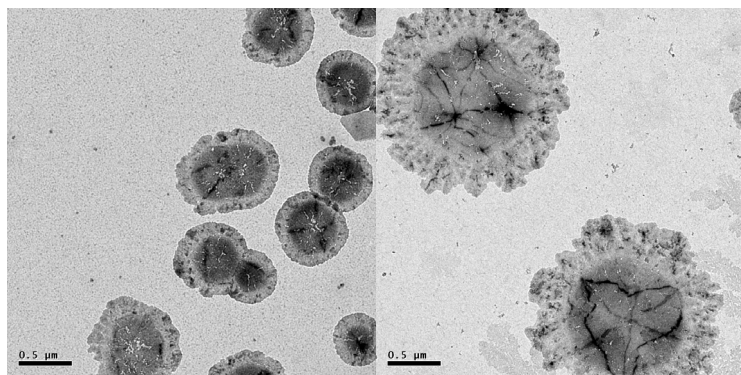


**Figure 8.2.** TEM of collapsed PGLu<sub>60</sub>-*b*-PALa<sub>30</sub> vesicles from a 0.10 M phosphate buffer solution. The bar represents 0.5  $\mu$ m.

### 8.3.2 Enzymatic degradation of polypeptide vesicles

As described in Chapter 7 the enzyme elastase can hydrolyze L-alanine-L-alanine bonds of NCA ROP-prepared polypeptides. As the vesicle membranes consist of pure PAla blocks, it should be possible to selectively hydrolyze them. To our knowledge these block copolypeptide suprastructures have not yet been studied for selective degradation. In order to investigate the degradation, a solution of the copolypeptide (5 mg/ml) in phosphate buffer solution was mixed with a solution of the enzyme and shaken at 37 °C in a water bath. The degradation was monitored by DLS and optical microscopy on samples periodically withdrawn to determine the effect of the enzyme. These results were compared to a blank sample without the enzyme.

As time progressed DLS showed that for the blank samples a clear decrease in particle size occurred (Figures 8.3 and 8.4). In the spectrum, larger particles with a size of several micrometers disappeared after one day, resulting in particles of several hundreds of nanometers. The increased temperature and the effect of mixing by shaking alter the size of the particles, which would mean that at 37 °C a different particle size is more favorable for this system. Cryo-TEM showed that after four days mostly worm-like micelles could be found for PGLu<sub>100</sub>-*b*-PAla<sub>40</sub>, implying that the particle shape is also altered by the increase in temperature. For solutions containing the enzyme the particle size did not decrease (as seen for the blank sample), but in most cases the particle size increased over time (Table 8.2). For PGLu<sub>60</sub>-*b*-PAla<sub>30</sub> (entry 3, Table 8.2) the particle size decreased after one day, but showed an increase in size afterwards. Optical microscopy showed that after two days aggregated vesicles were present in the solution, which were not seen before (Figure 8.5). After four days almost no distinctive vesicles could be found in the solution. Mostly unsymmetrical particles were found consisting of branched worm-like structures. In this specific case this also resulted in an increase of the scattering intensity with time, while most others showed a decrease in light scattering. The decrease in intensity of the scattered light was used previously to monitor the enzymatic degradation of polyester particles and vesicles.<sup>15-17</sup> However, in the case of alteration of the composition or particle size of the newly formed particles an increase in scattering can be found.

For most vesicles the use of diblocks has been reported, however in the case of PLys-*b*-PBLG-*b*-PLys the triblocks were seen to form vesicles of approximately 130 nm.<sup>7</sup> For PGLu<sub>60</sub>-*b*-PA<sub>30</sub>-*b*-PGLu<sub>60</sub> (Entry 5 in Tables 8.1 and 8.2) the presence of larger particle sizes was not observed in the DLS (Figure 8.6). The blank sample was not affected by the temperature or mixing by shaking of the water bath. However, in the presence of protease a huge increase in particle size was again seen. A single cleavage of the central L-alanine block in the triblock with the protease creates two diblocks, resulting in a direct increase of particle size.

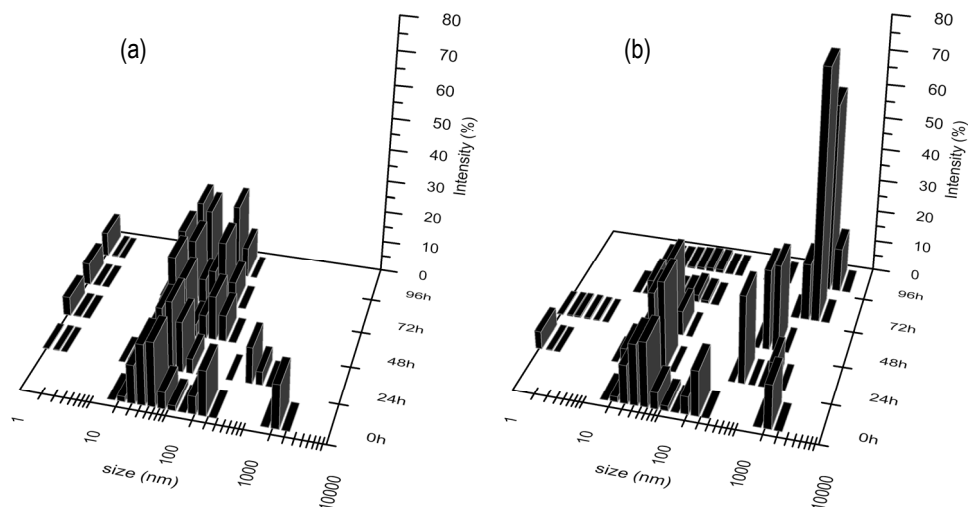


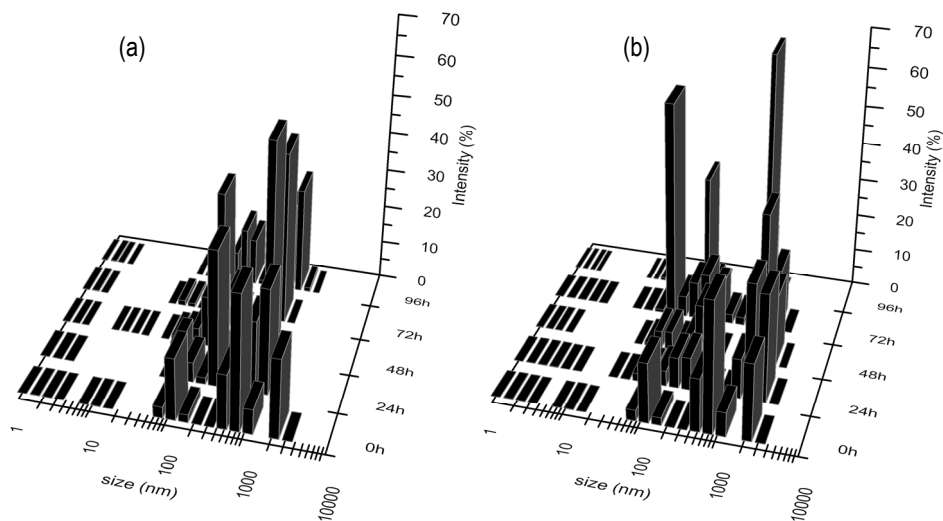
**Figure 8.3.** DLS measurements of PGLu<sub>60</sub>-*b*-PAla<sub>30</sub>, blank (a) and in the presence of the enzyme elastase (b).

Most degradation samples (except entries 6 and 7, Table 8.2) showed the formation of tubular or fibrillar structures in the presence of the enzymes. Similar structures have been reported before for PLYS<sub>40</sub>-*b*-PLEU<sub>20</sub> in demineralized water.<sup>5</sup> The solutions also showed signs of precipitation after two to three days. The degradation products of the enzymatic degradation by the endopeptidase elastase should be L-alanine oligomers and residual PGLu-*b*-PAla block copolypeptides. The length of the L-alanine oligomers should affect the solubility of this formed waste-product. The precipitate was analyzed with <sup>1</sup>H-NMR and showed to contain 3.5 times more L-alanine compared to the amount in the original block copolypeptide. The insolubility of this degradation byproduct is believed to result in a precipitation or an alteration of the vesicle structures, due to the hydrophobic interactions of oligo(L-alanine) with the poly(L-alanine) membrane. For PGLu<sub>100</sub>-*b*-PAla<sub>40</sub> (entry 4, Table 8.2), the particle size did decrease to finally result in the same particle size as found for the blank sample, while the scattering intensity decreased by 44.6 %.

To overcome the problem of precipitation during the enzymatic degradation, entries 6 and 7 (Table 8.2) were prepared with a small quantity of L-glutamic acid in the hydrophobic L-alanine block. During the enzymatic degradation this should result in more soluble waste-products. DLS showed a decrease in particle size for PGLu<sub>100</sub>-*b*-P(Ala<sub>32</sub>-*co*-Glu<sub>8</sub>) from 779 nm to 484 nm upon enzymatic degradation, while for PGLu<sub>50</sub>-*b*-P(Ala<sub>16</sub>-*co*-Glu<sub>4</sub>) an increase was observed from 895 nm to 1.6 μm. For both samples no precipitation was observed for at least six days, while other samples containing no Glu residues showed precipitation after two days. The scattering intensity decreased over time suggesting a decrease in the number of particles

**Table 8.2.** Enzymatic degradation of poly(L-glutamic acid)-*block*-poly(L-alanine) superstructures.

| Entry | Polypeptide  | Blank                |               | Enzyme               |               | Remarks              |
|-------|--|----------------------|---------------|----------------------|---------------|----------------------|
|       |  | Z <sub>Av</sub> (nm) | Intensity (%) | Z <sub>Av</sub> (nm) | Intensity (%) |                      |
| 1     | PGlu <sub>50</sub> - <i>b</i> -PAla <sub>20</sub>                                    | 165 ± 75             | -6.2          | 370 ± 170            | -59.4         | Slight precipitation |
| 2     | PGlu <sub>40</sub> - <i>b</i> -PAla <sub>30</sub>                                    | 89 ± 36              | -21.2         | 71 ± 31              | -59.6         | Precipitation        |
| 3     | PGlu <sub>60</sub> - <i>b</i> -PAla <sub>30</sub>                                    | 62 ± 28              | -10.9         | 2,380 ± 1060         | +1,070        | Precipitation        |
| 4     | PGlu <sub>100</sub> - <i>b</i> -PAla <sub>40</sub>                                   | 200 ± 88             | -6.3          | 206 ± 92             | -44.6         | No Precipitation     |
| 5     | PGlu <sub>60</sub> - <i>b</i> -PAla <sub>30</sub> - <i>b</i> -<br>PGlu <sub>60</sub> | 159 ± 71             | -22.0         | 860 ± 400            | -39.1         | Huge size increase   |
| 6     | PGlu <sub>50</sub> - <i>b</i> -P(Ala <sub>16</sub> -CO-<br>Glu <sub>4</sub> )        | 894 ±<br>417         | -9.6          | 1,660 ± 741          | -43.2         | No precipitation     |
| 7     | PGlu <sub>100</sub> - <i>b</i> -P(Ala <sub>32</sub> -CO-<br>Glu <sub>8</sub> )       | 362 ±<br>157         | +6.0          | 484 ± 215            | -12.4         | No precipitation     |

**Figure 8.4.** DLS measurements of PGlu<sub>100</sub>-*b*-PAla<sub>40</sub>, blank (a) and in the presence of the enzyme elastase (b).

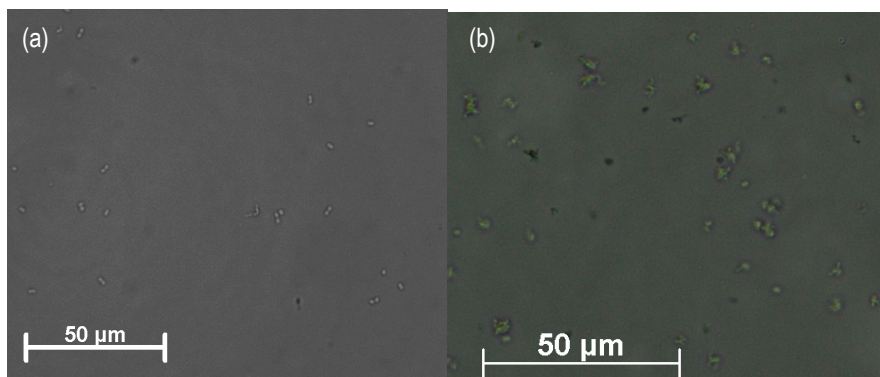


**Figure 8.5.** DIC optical microscopy pictures of enzymatic degradation of PGLu<sub>60</sub>-*b*-PALa<sub>30</sub> after two days (a) and after five days (b).

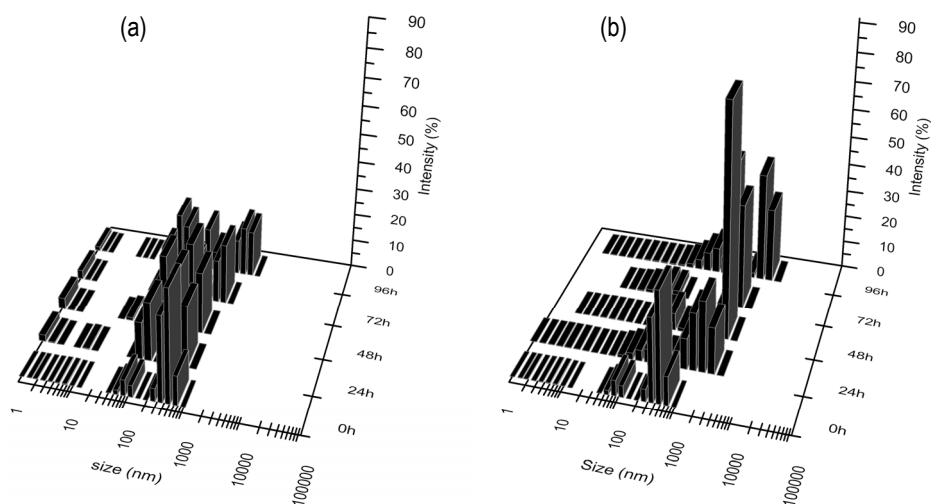


**Figure 8.6.** DLS measurements of PGLu<sub>60</sub>-*b*-PALa<sub>30</sub>-*b*-PGLu<sub>60</sub>, blank (a) and in the presence of elastase (b).

### 8.3.3 Functionalities for cell-membrane recognition

To enable selective cell recognition for PGLu-*b*-PALa vesicles, the propargyl chain end was functionalized. 1-Azide- $\beta$ -galactose was used in an azide-alkyne Huisgen cycloaddition with propargylamine-initiated PGLu<sub>60</sub>-*b*-PALa<sub>30</sub> in NMP. The CuBr / PMDETA catalyst and the excess of galactose reactant were removed by dialysis in water or PBS. <sup>1</sup>H-NMR showed the presence of galactose on the polymer chain end (Figure 8.7). DLS confirmed the presence of suprastructures with a similar size and size distribution as compared to the unfunctionalized PGLu<sub>60</sub>-*b*-PALa<sub>30</sub> (Table 8.1).

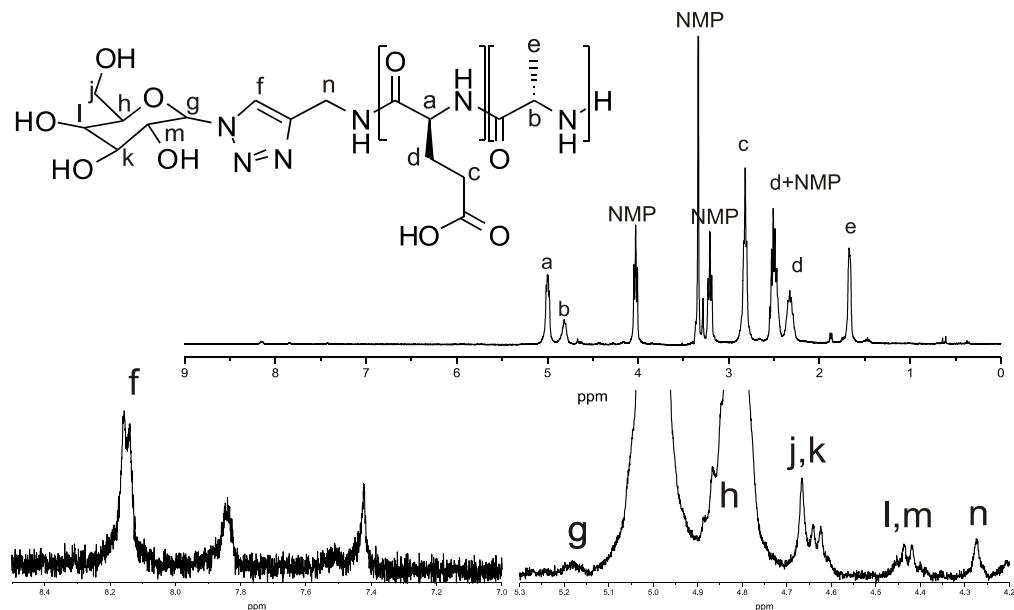


**Figure 8.7.**  $^1\text{H-NMR}$  of  $\beta$ -galactose-functionalized of  $\text{PGLu}_{60}\text{-}b\text{-PAla}_{30}$  in  $d\text{-TFA}$ .

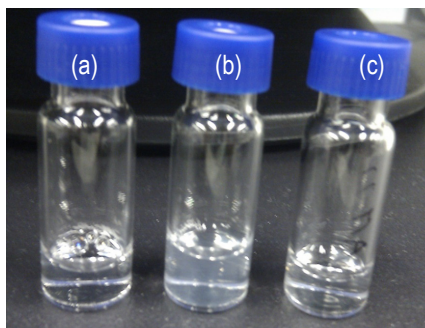


**Figure 8.8.** Lectin ( $30\ \mu\text{l}$ ,  $2\ \text{mg/ml}$ ) turbidity test of  $\text{PGLu}_{60}\text{-}b\text{-PAla}_{30}$  vesicle particles ( $300\ \mu\text{l}$ ,  $1\ \text{mg/ml}$ ). Unfunctionalized  $\text{PGLu}_{60}\text{-}b\text{-PAla}_{30}$  with lectin RCA 120 showed no response (a).  $\beta$ -Galactose-functionalized  $\text{PGLu}_{60}\text{-}b\text{-PAla}_{30}$  with lectin RCA 120 showed increased turbidity (b).  $\beta$ -Galactose-functionalized  $\text{PGLu}_{60}\text{-}b\text{-PAla}_{30}$  with lectin Con A showed no response (c).

To test the selectivity of the  $\beta$ -galactose suprastructures, a PBS solution of  $\beta$ -galactose- $\text{PGLu}_{60}\text{-}b\text{-PAla}_{30}$  was tested for different lectins (Figure 8.8).  $\beta$ -Galactose is known to bind selectively to the lectin RCA 120 from castor beans.<sup>12</sup> A different lectin, Con A, should not show any response, since it binds selectively to glucosyl and mannosyl residues. Since the binding between lectins and carbohydrates is a multivalent event, positive binding can be identified by solution turbidity due to lectin/polymer aggregation.<sup>14</sup> Qualitative turbidity experiments carried out by mixing a solution of  $\beta$ -galactose-functionalized block copolypeptide with RCA 120 lectin showed a positive result. For the Con A lectin,

on the other hand, no increased turbidity was observed, not even with a tenfold increase and decrease of the concentration of  $\beta$ -galactose-PGlu<sub>60</sub>-*b*-PAla<sub>30</sub>. These simple experiments show that the functionalized polypeptide material interacts with lectins, and opens possibilities for selective delivery with chain end functionalized poly(L-glutamic acid) block copolypeptide vesicles.

#### 8.4 Conclusions

The preparation of vesicles consisting of PGlu-*b*-PAla was proven to be successful both in demineralized water and in 0.10 M phosphate buffered solution. When compared, smaller particle sizes were obtained in the PBS buffer. During the enzymatic degradation of the superstructures the particle size increased depending on the block chain length. Precipitation as a result of the enzymatic degradation was also observed in most cases. This is an unwanted side-effect for drug-delivery, because it could lead to accumulation of precipitated polypeptide. The precipitation was overcome by altering the composition of the L-alanine block by copolymerizing a small amount of L-glutamic acid, which increased the solubility of the degradation products. The effect of the enzyme on the PGlu-*b*-PAla was relatively complex and more tests should be done on the precise effect of the oligomer degradation products on the superstructures. Moreover, release studies should be done with loaded vesicles.

Preliminary experiments were carried out with propargyl-PGlu-*b*-PAla functionalized by a Huisgen click reaction with 1-azide- $\beta$ -galactose. Particles with the  $\beta$ -galactose showed a selective response with lectin RCA 120. Further experiments with other azide-functionalized carbohydrates and more sensitive methods of lectin testing should be the next step to further investigate the full potential of this system.



## References

- <sup>1</sup> C. LoPresti, H. Lomas, M. Massignani, T. Smart and G. Battaglia, *J. Mater. Chem.* **2009**, 19, 3576-3590
- <sup>2</sup> A. Blanz, S.P. Armes, A.J. Ryan, *Macromol. Rapid Commun.* **2009**, 30, 267-277
- <sup>3</sup> A. Carlsen and S. Lecommandoux, *Curr. Opin. Colloid In.* **2009**, 14, 329-339
- <sup>4</sup> H. Schlaad, *Adv. Polym. Sci.* **2006**, 202, 53-73
- <sup>5</sup> E.P. Holowka, D.J. Pochan, and T.J. Deming, *J. Am. Chem. Soc.* **2005**, 127, 12423-12428
- <sup>6</sup> J. Sun, X. Chen, C. Deng, H. Yu, Z. Xie and X. Jing, *Langmuir* **2007**, 23, 8308-8315
- <sup>7</sup> H. Iatrou, H. Frielinghaus, S. Hanski, N. Ferderigos, J. Ruokolainen, O. Ikkala, D. Richter, J. Mays and N. Hadjichristidis, *Biomacromolecules* **2007**, 8, 2173-2181
- <sup>8</sup> E.P. Holowka and T.J. Deming, *Macromol. Biosci.* **2010**, 10, 496-502
- <sup>9</sup> E.P. Holowka, V.Z. Sun, D.T. Kamei and T.J. Deming, *Nature Mat.* **2007**, 6, 52-57
- <sup>10</sup> V.Z. Sun, Z. Li, T.J. Deming and D.T. Kamei, *Biomacromolecules* **2011**, 12, 10-13
- <sup>11</sup> C. Schatz, S. Louguet, J.-F. Le Meins and S. Lecommandoux, *Angew. Chem. Int. Ed.* **2009**, 48, 2572-2575
- <sup>12</sup> H.-J. Gabius, H.-C. Siebert, S. Andry, J. Jimenez-Barbero and H. Rüdiger, *ChemBioChem* **2004**, 5, 740-764
- <sup>13</sup> U. Talas, J. Dunlop, S. Khalaf, I.M. Leigh and D.P. Kelsell, *J. Invest. Dermatol.* **2000**, 114, 165-170
- <sup>14</sup> J. Huang, G.J.M. Habraken, F. Audouin and A. Heise, *Macromolecules* **2010**, 43, 6050-6057
- <sup>15</sup> C. Sanson, C. Schatz, J.-F. Le Meins, A. Brûlet, A. Soum and S. Lecommandoux, *Langmuir* **2010**, 26, 2751-2760
- <sup>16</sup> M. Le Hellaye, N. Fortin, J. Guilloteau, A. Soum, S. Lecommandoux and S.M. Guillaume, *Biomacromolecules* **2008**, 9, 1924-1933
- <sup>17</sup> C. Wu and Z. Gan, *Polymer* **1998**, 39, 4429-4431

# Curriculum Vitae

Gijs Habraken was born on 19<sup>th</sup> July 1983 in Boxtel, the Netherlands. After completing his secondary education in 2001 at 'het Elde College' in Schijndel, he studied Chemical Engineering and Chemistry at Eindhoven University of Technology. In 2007 he graduated within the polymer chemistry group of prof. dr. Cor Koning in the field of N-carboxyanhydride ring opening polymerization in combination with the combination of controlled radical polymerization. In 2007 he started a PhD project under the supervision of prof. dr. Cor Koning and Dr. Andreas Heise. The results of his PhD research are presented in this thesis. From June 2011 he will be employed at BASF SE in Ludwigshafen, Germany.

## List of Publications:

Ziwei Deng, Gijs. J.M. Habraken, Marloes Peeters, Andreas Heise, Gijsbertus de With and Nico A. J. M. Sommerdijk, *Biomimetic Synthesis of Luminescent CaCO<sub>3</sub> Directed by Fluorescein Functionalized Polypeptides*, Soft Matter, submitted

G.J.M. Habraken, M. Peeters, C.E. Koning and A. Heise, *Selective Enzymatic Degradation of Biohybrid Block Copolymers Particles*, in preparation

Gijs J.M. Habraken, Karel H.R.M. Wilsens, Cor E. Koning and Andreas Heise, *Optimization of N-carboxyanhydride (NCA) polymerization by variation of reaction temperature and pressure*, Polymer Chemistry, accepted

Jin Huang, Gijs Habraken, Fabrice Audouin and Andreas Heise, *Hydrolytically Stable Bioactive Synthetic Glycopeptide Homo- and Copolymers by Combination of NCA Polymerization and Click Reaction*, Macromolecules 2010, 43, 6050-6057

Rutger J.I. Knoop, Matthijs de Geus, Gijs J.M. Habraken, Cor E. Koning, Henning Menzel and Andreas Heise, *Stimuli Responsive Peptide Conjugated Polymer Nanoparticles*, Macromolecules 2010, 43, 4126-4132

Gijs J.M. Habraken, Marloes Peeters, Carin H.J.T. Dietz, Cor E. Koning and Andreas Heise, *How controlled and Versatile is N-Carboxyanhydride (NCA) Polymerization at 0 °C? Effect of Temperature on Homo-, Block- and Graft (co)Polymerization*, Polymer Chemistry 2010, 1, 514-524

G.J.M. Habraken, C.E. Koning and A. Heise, *Peptide Block Copolymers by N-Carboxyanhydride Ring-Opening Polymerization and Atom Transfer Radical Polymerization: The Effect of Amide Macroinitiators*, Journal of Polymer Science, Part A: Polymer Chemistry 2009, 47, 6883-6893

G.J.M. Habraken, C.E. Koning, J.P.A. Heuts and A. Heise, *Thiol chemistry on well-defined synthetic polypeptides*, Chemical Communications 2009, 3612-3614

J.R.I. Knoop, G.J.M. Habraken, N. Gogibus, S. Steig, H. Menzel, C.E. Koning and A. Heise, *Synthesis of Poly( $\gamma$ -Benzyl-L-Glutamate-*b*-Styrene) Rod-Coil Block Copolymers by Dual Initiation in One Pot*, Journal of Polymer Science, Part A: Polymer Chemistry 2008, 46, 3068-3077

S. Steig, F. Cornelius, A. Heise, J.R.I. Knoop, G.J.M. Habraken, C.E. Koning and H. Menzel, *Synthesis of Rod-Coil Block Copolymers using Two Controlled Polymerization Techniques*, Macromolecular Symposia 2007, 248, 199-206

# Acknowledgements

First of all I would like to thank Cor and Andreas for their guidance over the last couple of years. Cor, thanks for the trust you had in me. Andreas thanks for being there as a daily coach. Although you moved far away in my second year, I don't think that was a problem, with all the skypeing, calling and emails I never had to wait long for advice or reassurance. DPI is greatly acknowledged for the funding of this PhD project and for giving the opportunity to interact with other DPI projects.

I would like to thank the reading committee, prof.dr. Harm-Anton Klok, prof.dr. Arend Jan Schouten and dr. Nico Sommerdijk for the time they spent reading the thesis and giving their comments.

Although my name is on front of the thesis it would not look like this if I did not have the help from students and cooperations with different groups and individuals. First of all, I would like to thank Marloes, Karel, Stephan and Jeroen for their contributions and the pleasant cooperations. I wish you all good luck in finishing your master degrees and PhDs. You guys made my time here so much more interesting, thanks!

Nico, Ziwei, Vladimir, Heiner and Pedro thank you for the cooperation on the biomimetic crystallizations. It was a really interesting and multi-disciplinary project to work on. Nico, thanks for giving me the opportunity of working in an interdisciplinary team and to get a taste of a different field. Ziwei, I have deep respect for the endless and laborious crystallizations you did. Good luck in your scientific future. Vladimir, good luck with your PhD. Combined efforts of Ziwei and me were only able to show what a limited combination of three amino acids can do, so there are enough exciting discoveries for you to do! Hans, thank you for the advice regarding radical polymerizations, thiol-related chemistry and amphiphilic block copolymers. It was very nice to pop into your office for a few questions once in a while and to walk out with a couple of experiments that should solve the problem.

I am very grateful for the contact and cooperation with the polymer chemistry group at DCU in Dublin. Specifically, I would like to thank Jin and Paul for the work on the NCA ROP, enzymes and glycopeptides. Your involvement really made my work more interesting! Paul, thanks for helping me with understanding the world of peptidases a little bit better. Jin, thank you for your help with Chapter 8 and the interesting work we did together on your projects. I wish you all the best with finishing your PhD. I am sure that your thesis will contain more depth and plots than most recognized literature works.

I would like to thank and recognize the work the analytical staff of SPC did over the years. In the beginning of my PhD Marion and Wieb were there to help out with any problems. Now, we have Carin, Hanneke, Rinske and Martin to help us out. Your combined efforts were the light in my chemical darkness. Thank you very much everybody!

I would like to thank my office buddies from the last couple of years for the well-needed scientific and cultural insights and social interactions that made working so much nicer: Inge, Wouter, Hector, Petra, Evgeniy, the Fluorinator, Shaneesh, Erik, Karel and Juliën. I would like to thank the colleagues that were involved in the Heise group (the Eindhoven chapter) over the years for their involvement in my project: Matthijs, Rutger, David, Yan, Gaëtan, Inge, Hemant and Bahar. Rutger, because of your work I had a nice head-start at the beginning of my project, thanks for that!

I hope this is also the right moment to apologize to my colleagues that I shared the laboratory space with. Sorry for the mess, the verbal abuse related to failed experiments, the (occasional) grumpiness, the first smelly thiol experiments, the horrible music, the continuous annoyance and the fact that I think that I am always right. I hope this apology is in time to save me from any embarrassing pictures during my defense party.

Of course I need to thank the rest of the people who were SPC members over the years for the lovely time as well. I must say it was a privilege to work with such fine and nice people as you (you all know your own name, so I do not need to mention that here). I do hope that contact will remain strong among us, even when we have all left the TU/e.

Aan al mijn vrienden en familie die de afgelopen jaren interesse hebben getoond voor mijn promotie: hartelijk dank. Natuurlijk wil ik mijn ouders bedanken voor de onvoorwaardelijke steun door de jaren heen. Gem, thank you for the help with correcting the thesis and for everything else.

Bedankt! Thank You! Danke!